

ISSN 1512-1127

საქართველოს გეოფიზიკური საზოგადოების
ჟურნალი

სერია ა. დედამიწის ფიზიკა

**JOURNAL
OF THE GEORGIAN GEOPHYSICAL SOCIETY**

Issue A. Physics of Solid Earth

ტომი 15ა 2011-2012

vol. 15A 2011-2012

ISSN 1512-1127

საქართველოს გეოფიზიკური საზოგადოების
ჟურნალი

სერია ა. დედამიწის ფიზიკა

**JOURNAL
OF THE GEORGIAN GEOPHYSICAL SOCIETY**

Issue A. Physics of Solid Earth

ტომი 15ა 2011-2012

vol. 15A 2011-2012

საქართველოს გეოფიზიკური საზოგადოების ჟურნალი

სერია ა. დედამიწის ფიზიკა

სარედაქციო კოლეგია

კ. ზ. კართველიშვილი (მთ. რედაქტორი), ვ. აბაშიძე, ბ. ბალავაძე, ა. გველესიანი (მთ. რედაქტორის მოადგილე), გ. გუგუნავა, კ. ეფტახიასი (საბერძნეთი), თ. ჭელიძე, ვ. ჭიჭინაძე, გ. ჯაში, ი. გუგენი (საფრანგეთი), ი. ჩაუ (გერმანია), თ. მაჭარაშვილი, ვ. სტაროსტენკო (უკრაინა), ჯ. ქირია, ლ. დარახველიძე (მდივანი)

მისამართი:

საქართველო, 0193, თბილისი, ალექსიძის ქ. 1,
მ. ნოდიას გეოფიზიკის ინსტიტუტი
ტელ.: 33-28-67; 94-35-91; Fax; (99532 332867); e-mail: root@geophy.acnet.ge

ჟურნალის შინაარსი:

ჟურნალი (ა) მოიცავს მყარი დედამიწის ფიზიკის ყველა მიმართულებას. გამოქვეყნებულ იქნება: კვლევითი წერილები, მიმოხილვები, მოკლე ინფორმაციები, დისკუსიები, წიგნების მიმოხილვები, განცხადებები.

გამოქვეყნების განრიგი და ხელმოწერა

სერია (ა) გამოიცემა წელიწადში ერთხელ.
ხელმოწერის ფასია (უცხოელი ხელმძღვრისათვის) 50 დოლარი, საქართველოში – 10 ლარი, ხელმოწერის მოთხოვნა უნდა გაიგზავნოს რედაქციის მისამართით.

ЖУРНАЛ ГРУЗИНСКОГО ГЕОФИЗИЧЕСКОГО ОБЩЕСТВА

серия А. Физика Твердой Земли

Редакционная коллегия:

К. З. Картвелишвили (гл. редактор), В.Г. Абашидзе, Б.К. Балавадзе, А.И. Гвелесиани (зам. гл. редактора), Г.Е. Гугунава, К. Эфтаксиас (Греция), Т.Л. Челидзе, В.К. Чичинадзе, Г.Г. Джаши, И. Геген (Франция), И. Чшау (Германия), Т. Мачарашвили, В. Старостенко (Украина), Дж. Кириа, Л. Дарахвелидзе

Адрес:

Грузия, 0171, Тбилиси, ул. Алексидзе, 1.
Институт геофизики им. М. З. Нодия
Тел: 33-28-67; 94-35-91; Fax: (99532) 332867; e-mail: root@geophy.acnet.ge

Содержание журнала:

Журнал (А) Грузинского геофизического общества охватывает все направления физики твердой Земли. В журнале будут опубликованы научные статьи, обзоры, краткие информации, дискуссии, обзоры книг, объявления.

Порядок издания и условия подписи:

Том серии (А) издается по одному номеру в год.
Подписная цена 50 долларов США, включая стоимость пересылки.
Заявка о подписке высылается в адрес редакции.

JOURNAL OF THE GEORGIAN GEOPHYSICAL SOCIETY

Issue A. Physics of Solid Earth

Editorial board:

K. Kartvelishvili (Editor-in-Chief), V. Abashidze, B. Balavadze, T. Chelidze, V. Chichinadze, K. Eftaxias (Greece), A. Gvelesiani (Vice-Editor-in-Chief), G. Gugunava, G. Jashi, Y. Gueguen (France), I. Zschau (Germany), T. Matcharashvili, V. Starostenko (Ukraine), J. Kiria, L. Darakhvelidze

Address:

M. Nodia Institute of Geophysics, 1 Alexidze Str., 0171 Tbilisi, Georgia
Tel.: 33-28-67; 94-35-91; Fax: (99532) 332867; e-mail: root@geophy.acnet.ge

Scope of the Journal:

The Journal (A) is devoted to all branches of the Physics of Solid Earth. Types of contributions are: research papers, reviews, short communications, discussions, book reviews, announcements.

Publication schedule and subscription information:

One volume issue (A) per year is scheduled to be published.
The subscription price is 50 \$, including postage.
Subscription orders should be sent to editor's address.

Pitfalls and Reality in Global and Regional Hazard and Disaster Risk Assessments

Tamaz Chelidze

M. Nodia Institute of Geophysics of I. Javakishvili Tbilisi State University; 1 Aleksidze str., Tbilisi, Georgia; e-mail: tamaz.chelidze@gmail.com

Abstract

Last years natural disasters brought enormous economical losses and caused hundreds of thousand deaths, which make the problem of disaster risk reduction (DRR) one of priorities for all countries and nations. The results of such investigations are very important as they distinguish the “hot spots”, i.e. the most vulnerable areas and the most dangerous phenomena, characteristic for specific areas. Unfortunately these efforts sometimes lead to erroneous conclusions, which can be explained by using imperfect or just erroneous local inventories on disasters. In the present paper authors try to analyze some of pitfalls in Global and National Disaster Risk Assessments and in particular those related to South Caucasus region and Georgia. Hazards and risks in Georgia are recalculated using representative local data.

1. Introduction

The problem of disaster risk assessment is quite complicated as it integrates many quantities, which are evaluated very approximately (ADRC, 2006; Beer, 2010; CAC DRMI, 2009; MunichRe, 2010; CRED, 1991; CRED, 1994; Dilley et al, 2005; Push, 2004; UNDP, 2004; ISDR/UNDP, 2004;)

The main issue is that in the many cases there is not corresponding well grounded physical and mathematical model/theory of disaster. As the methodology of hazard and risk assessment is essentially based on the statistical approach, the question of the uncertainties, both alleatory and epistemic, are decisive for obtaining reliable results.

The most vivid example demonstrating difficulties in disaster risk evaluation is the problem of seismic hazard and risk assessment. Even the approved methods of Seismic Hazard Assessment (SHA) such as SEISRISK III, EF RISK, Open SHA etc contain a lot of quite crude approximations. This is evident from comparison of predicted by Global Seismic Hazard Assessment Program, GSHAP (Giardini et al, 1999) and other standard programs with observed data on the Peak Ground Accelerations of recent strong earthquakes (Table 1):

Table 1.

Expected according to GSHAP (with probability of exceedance of 10% in 50 years) and observed PGA (g) for recent strong earthquakes			
EQ location	Date	PGA expected	PGA observed
Kobe	17.01. 1995	0.40-0.48	0.7-0.8
Gujarat	26.01. 2011	0.16- 0.24	0.5-0.6
Boumerdes	25.05.2003	0.08-0.16	0.3-0.4
Bam	26.12.2003	0.16-0.24	0.7-0.8
E-Sichuan	12.05.2008	0.16-0.24	0.6-0.8
Haiti	12.01. 2010	0.08-0.16	0.3-0.6
Japan	11.03. 2011	0.32-0.40	1.0-2.9

It is evident that the observed PGA values are much larger than predicted by the Probabilistic SHA (Cornell, 1968; Field, E.), which means larger number of deaths and larger economic losses than expected.

The sources of some of these errors can be epistemic: for example, another methodology, namely, Deterministic Seismic Hazard Assessment (DSHA) and especially so called new DSHA (Panza et al, 2008) predicts PGA values, which are closer to observed ones. Another source of errors can be the wrong choice of distribution function: Gutenberg-Richter magnitude-frequency distribution of earthquakes is the basis of accepted SHA technique, but it is quite possible that seismic process follows statistics of extremes (Gumbel distribution), which leads to different predictions of strong events. The problem of correct prediction of extreme events is especially important for critical structures (dams, NPP-s, large bridges and pipelines) for which the statistics of events with long recurrence time should be used.

On the other hand quite often the reason of big discrepancies between predictions and observations is not the wrong methodology, but just using incorrect input data.

In the present paper mainly the second source of pitfalls in natural hazards and risk assessment will be analyzed.

2. Pitfalls in the global level disaster risk assessment: discord in hazards' shares in losses.

The problem of disaster risk assessment is quite complicated as it integrates many quantities, which are evaluated very approximately; often it is necessary to use expert estimations, based on short observation periods and insufficient data.

Some discrepancies arouse from differences in the disasters lists. As a rule, the main disasters are included in all lists, but their classification by separate organizations differs significantly. For example, according to UNISDR terminology on disaster risk reduction (UNISDR, 2009) there are two classes of natural hazards, geological and hydrometeorological. Geological hazards include earthquakes, volcanic activity and mass movements: landslides, rockslides, surface collapses and debris and mud flows. Tsunamis are difficult to classify: although they are triggered by undersea earthquake, they are essentially oceanic processes. Hydrometeorological hazards include tropical cyclones, thunderstorms, hailstorms, tornadoes, avalanches, floods including flash floods, droughts, heatwaves and cold spells. Hydrometeorological factors also influence such geologic processes as mass movements.

The insurance company MunichRe gives the following classification: Climatological events (Extreme temperature, drought, forest fire), Hydrological events (Flood, mass movement), Meteorological events (Storm), Geophysical events (Earthquake, tsunami, volcanic eruption).

C. van Westen (2009) suggests the following classes: Meteorological (Drought, Dust storm, Flood, Lightning, Windstorm, Thunderstorm, Hailstorm, Tornado, Cyclone, Hurricane, Heat wave, Cold wave), Geomorphological & Geological (Earthquake, Tsunami, Volcanic eruption, Landslide, Snow avalanche, Glacial lake outburst, Subsidence, Coal fires, Coastal erosion). This classification also singles out Ecological, Technological, Global environmental and Extraterrestrial hazards.

Naturally, all this leads to a big scatter in risk assessments. For example:

i. German Committee for Disaster Reduction presents the following distribution of economic damage from natural disasters worldwide 1980-2003 (total – 1,260 billion US\$): 28% - floods, 32% - storms; 22% - earthquakes, 15% - heat waves, droughts, wildfires.

ii. UN report- Living with Risk: A global review of disaster reduction initiatives , (2002, Geneva) gives distribution of losses due to natural hazards occurred in XX century; according to this UN report 51% of losses come from EQ-s.

iii. According to disasters data for 1975-2006 from CRED-EM DAT: two thirds of losses are due to meteorological disasters (wind storms and floods) and around 30% of losses are caused by earthquakes.

iv. World Meteorological Organization (<http://www.wmo.int>) in one of brochures gives following economic loss assessments: Floods – 37 %, Windstorms – 28%, Droughts and famines – 9 %, Earthquakes – 8 %, Forest fires – 5 %, Avalanches and landslides – 6 %, Extreme temperatures – 5 %, Volcanic eruptions - 2 %.

v. MunichRe gives the following numbers for great natural catastrophes in 1950-2009: 7% -

Climatological events (Extreme temperature, drought, forest fire), 23% - Hydrological events (Flood, mass movement), 38 % - Meteorological events (Storm), 32% - Geophysical events (Earthquake, tsunami, volcanic eruption).

It is evident that different sources present quite different assessments of disaster consequences (economic losses and mortality) on the global scale. For example, the contribution of earthquakes in total losses according to different sources varies from 8% (WMO) to 51% (UN report- Living with risk, 2002, Geneva). The reasons of these discrepancies are plenty. If the assessments are done for a short time interval (of order of years) the more frequent disasters, such as storms, floods and other hydrometeorological events, which occur every year or even several times per year will dominate in economic losses/mortality

calculations. On the other hand, if the rear event, such as strong earthquake, occurs in the chosen short interval, the analyzed area will appear as the utmost vulnerable one. For example, in World Bank publication "Central Asia and Caucasus Disaster Risk Management Initiative (CAC DRMI, 2009)" the vulnerability of Armenia appears extremely high, because just in the 20-years interval, chosen by authors for loss analysis, the disastrous Spitak earthquake (M=6.9) stroke. It caused 25 000 deaths and around 12 billion economic losses. At the same time it should be taken into account that such strong evens in Armenia occur once in thousand(s) years. The normalization of losses and mortality to the recurrence period seems to be a correct procedure, but for earthquakes the recurrence period is greatly irregular; even in regions with large recurrence period nobody will risk to abandon seismic code demands after a strong earthquake hoping that it will not occur for thousand years (by the way many seismologists were sure that after Spitak EQ the seismic potential of Caucasus is depleted for centuries, but the strongest Racha EQ (M=6.9-7) occur in less than three years after Spitak), which can be explained by additional impact of Spitak event to Coulomb stress distribution in the region .

Thus the problem of risk assessment for rare extreme events seems to be far from solution.

We conclude that the procedure of natural disaster risk classification, assessment and ranging should be standardized/adjusted taking into account the complexity of catastrophic processes. To us the classification suggested by MunichRe seems to be most rational: by introducing the term geophysical hazards the problem of tsunami classification, which is neither purely geological nor purely hydrometeorological is solved.

3. Pitfalls in global databases at the country level: PreventionWeb.net information

The sources of information used by global databases are quite often unreliable. For example, Fig. 1 presents risk profile of Georgia according to PreventionWeb (citation for August 2011).

Again, the information placed on the PreventionWeb is wrong: i. population exposed to landslides is much more numerous than 942 and according to (Javakhadze, Tsereteli, 2010) amounts to 200000; ii. population exposed to earthquakes is much more numerous than 203,350 – only the population of Tbilisi, which is in the zone of intensity 8 and really suffered from the Tbilisi EQ of 2002 exceeds 1.5 million.

The rating of the economic exposure is more or less close to truth, though the absolute values can be different: for example only the Racha 1991 earthquake invokes losses of the order of annual GDP (approximately 5 billion USD). This question will be analyzed in more detail later on.

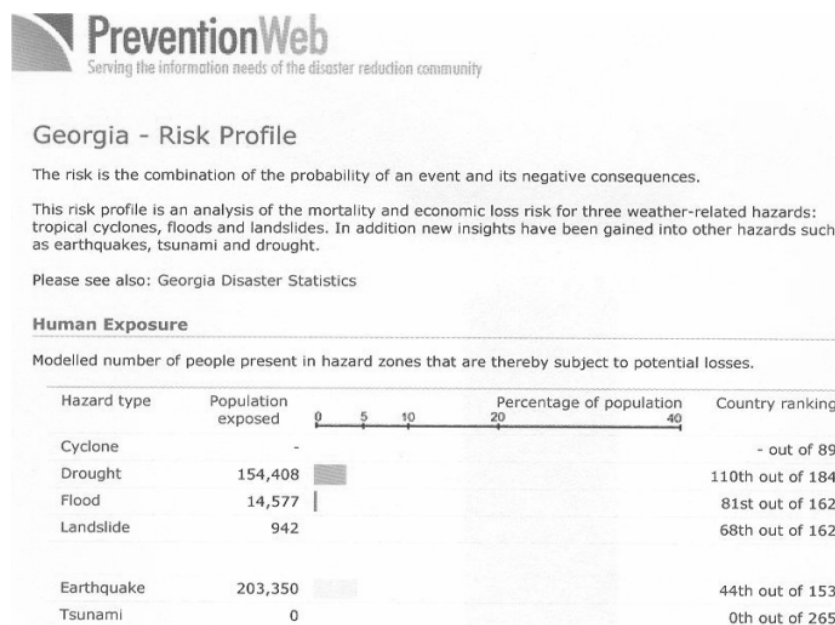


Fig.1

4. Pitfalls in global databases at the country level: 2005 Natural Disaster Hotspot Map

In 2005 International Bank of Reconstruction, World Bank and Columbia University compiled the set of global disaster risk maps for several types of hazards called Natural Disaster Hotspot Map – Fig. 2 (<http://www.ldeo.columbia.edu/chrr/research/hotspots/>).



Fig 2. Natural Disaster Hotspot Map (www.ciesin.columbia.edu/documents/globalhotspots.pdf)

The World Bank and the team of distinguished scientists (Dilley et al, 2005), which were involved in compilation of this pioneer map have carried out very important job. Unfortunately, this work contains some errors, which somehow discredits obtained results. This remark is in particular related to the economic and mortality assessments in the region of South Caucasus (Chelidze, 2006). According to the Hotspot Map, the Southern Caucasus (SC) is prone only to hydro-meteorological hazards, whereas the Northern Caucasus (NC) is subject to both Geophysical and Hydro-disasters. Geophysical hazards include earthquakes (EQ), volcanoes and landslides. The landslide risk for the both parts of Caucasus is approximately the same and the seismic activity of Southern Caucasus is larger than in the North. The sources of Hotspot Map assessments were GSHAP maps for PGA (Giardini, D et al. 1999) and database of EQ of $M > 4.5$ occurred in 1976-2002 from the Advanced National System EQ Catalog. It is easy to see that GSHAP map gives for the PGA in the North mainly in the range 0.2-0.3 g and for the South – in the range 0.2-0.4 g. Besides, the number of EQ of $M > 4.5$ is three times larger in Southern compared to Northern Caucasus. The infrastructure exposure, population density and vulnerability in Southern Caucasus are larger or at least equal to that in the North, so the difference cannot be prescribed to these components of risk either.

The mortality assessment for Southern Caucasus by Hotspot map is entirely wrong: only the Spitak EQ of $M=6.9$ (1988) victims' number (25 000) exceed many times the human losses of all other kinds of disasters in the North Caucasus for centuries. The direct economic losses from Spitak and Racha ($M=6.9$, 1991, Georgia) earthquakes amount to 18 billion USD, which is much larger than losses from hydro-meteorological hazards in the country for many years.

Unfortunately, the error is not corrected up to now, despite many attempts of one of the authors. For example, at present the Hotspot map is placed on the home page of GRIP (<http://www.gripweb.org>) and is included in many other publications. The last publication, which reproduced the uncorrected Hotspot map is the monograph "Geophysical Hazards" (Beer, 2010), issued in 2010. In the map of mortality from EQ-s, published by UN in (2009 "Global Assessment Report on Disaster Risk") the error is partially corrected and Armenia is marked as relatively high risk area, but even in this report on the global map the disastrous Ashgabat EQ (Turkmenistan) with 100 000 victims is neglected as well as Shemakha EQ in Azerbaijan with 80 000 victims.

Thus we conclude that during compilation of the Hotspot map the local input data were not analyzed correctly and the map needs serious revision in Caucasus as well as in other regions. Evidently, the new projects related to seismic risk re-assessment (Global Earthquake Model - www.globalquakemodel.org, Earthquake Model of Middle East - www.emme-gem.org) will improve the situation.

In addition we can mention the information published by the WHO Collaborating Centre for Research on the Epidemiology of Disasters or CRED (www.emdat.be, www.cred.be), which quite correctly tells us that economic losses in Georgia and Armenia are caused mainly by EQ-s, though the number of floods and droughts exceeds number of EQ-s and which is in agreement with the data presented by C. Push (2004), according to which average annual economic loss in Georgia is mainly due to EQ-s (Fig.3).

Average Annual Economic Loss

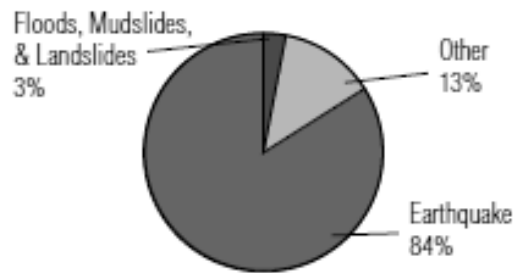


Fig.3. Average annual economic losses in Georgia: 84% of economic losses come from EQ-s (Push, 2004)

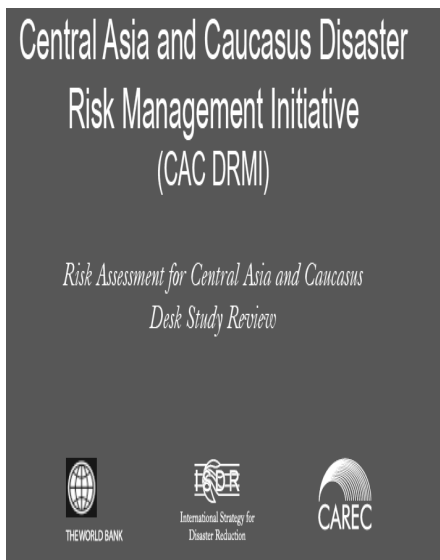
5. Pitfalls in Racha Earthquake's (M=6.9, 1991) loss evaluation and its role in national/regional economic assessments

The unfortunate tradition of mistakes in Global Disaster Hotspot Map (2005) is continued in the recent publication: "Central Asia and Caucasus Disaster Risk Management Initiative (CAC DRMI)", published in 2009 by World Bank, ISDR and CAREC (Fig.4a): this publication contains an error, related to direct economic loss from the major Racha earthquake 1991 in Georgia. On the page 33 is written: "magnitude 7 earthquake in the Racha-Imereti region on 29 April 1991 killed 100 people, left 100,000 homeless and caused an economic loss of \$10 million", which is borrowed from the UNDP information on Georgia (UNDP Georgia, Disaster Management, Risk Reduction, and Recovery, see website: <http://www.undp.org/cpr/disred/documents/publications/corporatereport/europe/georgia.pdf> and which is wrong in assessment of economic loss.

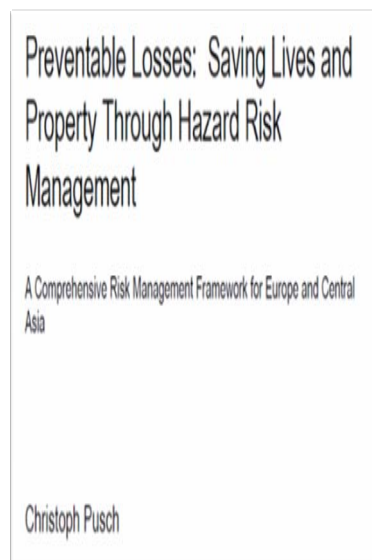
The original local data presented in "Engineering Analysis of Consequences of Racha Earthquake 1991 in Georgia" (Gabrichidze, Ed. 1996) issued in Tbilisi in 1996 (Fig.4c) tell us that the direct economic losses were evaluated as approximately 10 billion roubles (see pages 131-132 in Gabrichidze, 1996). 24 April 1991 the National Bank of Georgia established official course of 100 \$ USA to Russian rubles was 59.55 and commercial course – 178.65. So the economic losses from the Racha EQ are around 5.5 billion USD by commercial course and 16 USD billion by official course. This was of the order of annual GDP of Georgia in these years.

Besides, another publication of the same World Bank (C. Push, Preventable losses: saving lives and property through hazard risk management, 2004) gives correct assessment of EQ losses in Georgia as 84% of total losses (Figs. 3, 4b). Evidently, here the Racha EQ losses were counted correctly.

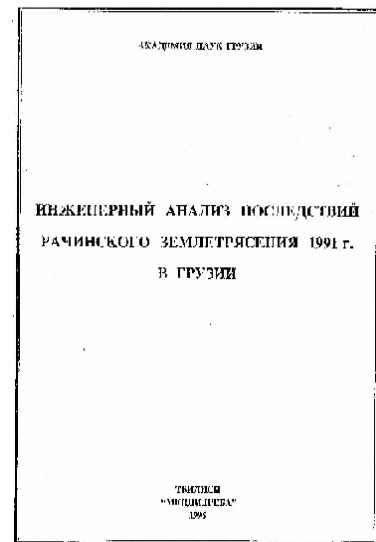
Munich Re Group (Globe of Natural Hazards, 2009) gives a lower number for Racha EQ losses than fixed by Georgian engineering seismologists, namely 1700 million USD, which, of course is much more realistic than UNDP and CAC DRMI assessments.



a.



b.



c.

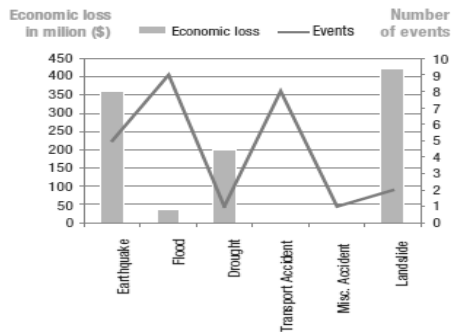
Figure.4. a,b,c. The recent publications on disaster risks, containing assessments for Georgia; a. Central Asia and Caucasus Disaster Risk Management Initiative (CAC DRMI), 2009.; b. Push, 2004; c. Monograph “Engineering Analysis of Consequences of Racha Earthquake 1991 in Georgia“, Tbilisi, 1996, Publishing House “Metsniereba”

According to Fig. 5 from CAC DRMI the economic losses from EQ-s in Georgia amounts to 30% of total disasters losses, when C. Push (2004) gives 2.5 times larger number – 84 %. Fig. 13c from CAC DRMI (2009) tells us that the EQ losses are around 250 million; but this is the loss from Tbilisi 2002 EQ only! Racha EQ, which causes an order larger loss, is practically ignored.

Unfortunately, the Racha EQ occurs in the very complicated period of the country, when Georgia declared its independence from USSR so the statistics of total losses were not investigated in detail. Nevertheless, the data published in (Gabrichidze, 1996) are reliable, because this report is the result of serious investigations carried out in the epicentral area immediately after EQ by experienced local earthquake engineers. It is possible to re-calculate losses from the data on damage, presented in the report (Gabrichidze, 1996, p. 132): according to it, 46 000 residential houses were destroyed or very heavily damaged. Exactly, 41% of dwellings have damage of category I, 31% - of category II and 28% - of category III. The total area of damaged dwellings is 6.4 mln sq.meters. Thus, accordingly, total damaged area for I, II and III categories are 2 624 000, 1 984 000 and 1 792 000 m². The reconstruction of 1 sq.m of I, II and III category dwellings was estimated by State Statistic Committee of Georgia as 300, 700 and 1500 roubles accordingly in course of 1991. These data allow calculation of direct losses due to damage of residential buildings, which amounts to 4 863 000 000 roubles. Thus, only direct losses due to damage of dwellings amounts to 4 863 000 000 roubles. But, besides dwellings, 1000 public buildings, lifelines, railway and highways were also damaged, which roughly amount to additional 100% or more of direct losses. Thus, only direct losses from residential houses and infrastructure damage are of order of 10 billion roubles (or around 5.5 billion USD by commercial course and 16 billion by official course of the National Bank of Georgia for 24 April 1991) as it is correctly given in (Gabrichidze, 1996).

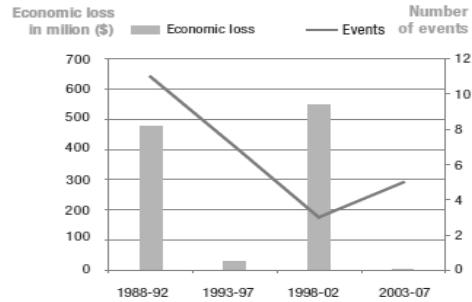
From above remarks it follows that the Fig. 5 a, b (Fig. 13c from CAC DRMI, 2009) should be corrected as is shown in Fig. 5 c, d: the difference is striking.

13c Disaster events and economic loss

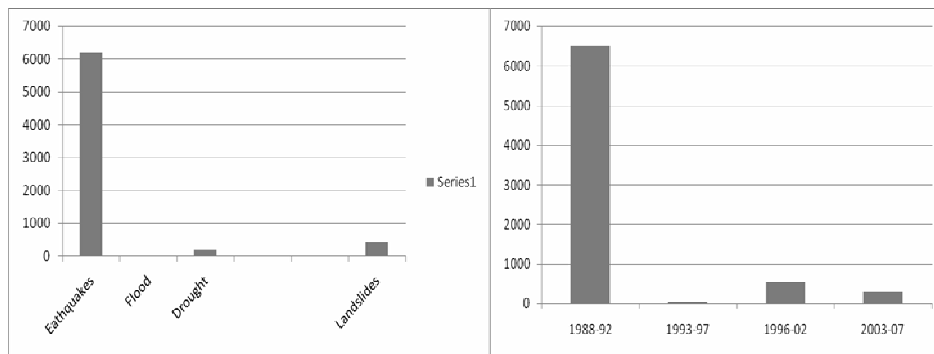


a

14c Disaster events and economic loss



c



b

d

Fig. 5 a, b, c, d. Disaster events and economic losses in Georgia according to Central Asia and Caucasus Disaster Risk Management Initiative (CAC DRMI, 2009), for disaster classes (a) and time intervals (b), note that according to CAC DRMI in Georgia EQ-s invoke only 30% of losses (due to error related to Racha EQ); corrected diagrams of disaster events and economic losses for classes (c) and time intervals (b), taking into account of local engineering observation data after major Racha earthquake (Gabrichidze, 1996); note that corrected values of EQ losses account for 75-80% of economic losses, which coincides with data of Push (2004).

This gross error affects also all regional and national assessments of relative economic losses given by (CAC DRMI, 2009) – instead of 200 million USD losses from EQ-s there should be at least 5.5 billion USD (Fig 5 a, b, c, d).

The source of error in the CAC DMI seem to be the information placed on the web-page of UNDP, which was cited above, as no independent additional studies were done to estimate real losses from Racha EQ after investigation, presented in (Gabrichidze, 1996). It seems that the value of total damage of 10 million USD in the UNDP text cited above and which was automatically replicated by CAC DMI appeared as a result of inaccurate translation of the number (10 billion was translated as 10 million) or just mechanical erratum.

6. Recalculation of hazards and risks in Georgia/South Caucasus

The confusion in risk assessment of Georgia/South Caucasus calls for reassessment of hazards and risk in above region using local inventories on disasters and the methodology used by authors of Hotspot Map (2005). The task was quite complicated as the data were mainly on the paper and some documents were destroyed or lost. Besides, some data necessary for accurate risk calculation (say GDP of separate administrative units) just do not exist as the state does not request them. That is why the indirect data were used to assess economical losses.

For assessment of economic risk the data of GDP (Gross Domestic Product) per unit area is needed. At the national level GDP measures the annual market value of final goods and services produced by a country. The national macro-economic parameters were calculated by the Ministry of Economical Development of Georgia in 2005. For unit areas (grid cells) of Georgia the GDP is not available: the data are only for sub-

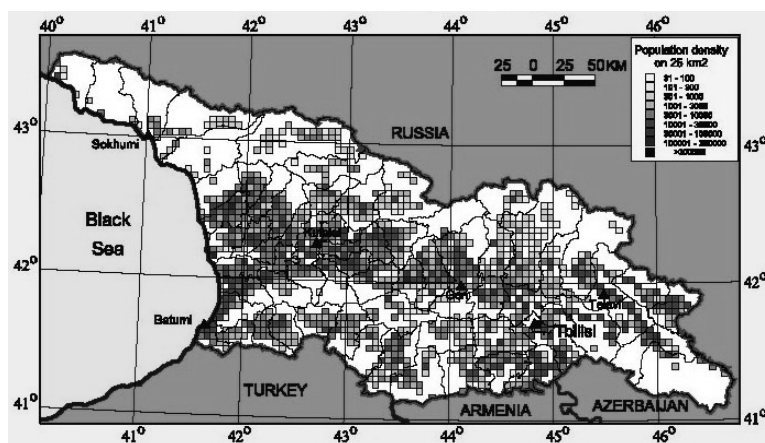
national units and territorial entities. That is why for indirect GDP calculation in cells the poverty mapping data were used. The poverty headcounts (*PH*) in districts was estimated by UNDP in Georgia (Labbate et al, 2003). *PH* measures the share of the population for which consumption or income is less than the poverty line. As GDP for Georgia is applied to the territorial entities, we decided to take into account the *PH* for districts multiplied by the GDP of territorial entities by the parameter $(1 - PH_n)$, where 'n' denotes the districts. This allowed the estimation of GDP for district centre units.

Population density map was compiled using the description of population in 2004.

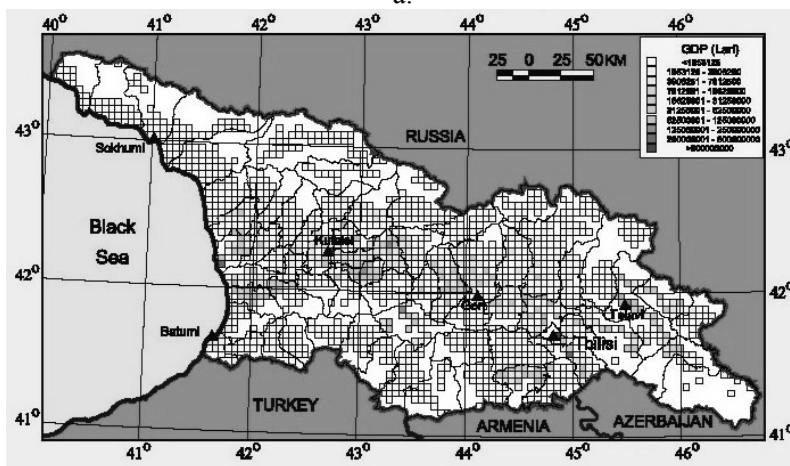
As a result, the following maps of GDP and population density were obtained (Fig. 6 a, b).

For each hazard the magnitude frequency relationship was estimated. So for each cell we have both the frequency and exposed area, admit economic loses the same for each hazardous event and consider the rate of economic loses the same for each even on the bases of GDP map and frequency the economic loss deciles were estimated for each hazard (Varazanashvili et al.2011, Varazanashvili et al., in press).

Economic losses were estimated for six natural hazards. They are: Earthquake (for 19 events, totally 147 events with intensity $I > 6$ at MSK-64 scale); flash flood (for 43 events, totally 302 events); drought (for 42 events, totally 269 events), hail (for all events from 1973 to 2007, totally 217 events), hurricane (for 75 events, totally 1760 events); frost (for 41 events, totally 1388 events). Standard statistic analysis was used to calculate the main statistical parameters such as: multiple linear correlation coefficient *R*, level of significance α , standard error. The period of time for calculating losses was 1961-2007. Details of calculations are presented in (Varazanashvili et al.2011, Varazanashvili et al., in press).



a.



b.

Fig. 6 a, b. Maps of Population Density (a) and GDP (b) in Georgia.

8. Economic loss risk and multiple risk calculation for six natural hazards in Georgia

For economic loss risk (ELR) calculation the technique developed by the Columbia University group (Dilley et al. 2005) during compilation of the Map of Global Natural Disaster Risk Hotspots was used.

The ELR for these six hazards are expressed in USD. Average value of GDP by grid was calculated. The values of economic losses exceeding 70 percent of this average value were chosen for calculation of the summary multi-hazard risk (Fig.7). The economic loss risk was not estimated for some regions of Georgia such as Abkhazeti and South Ossetia.

It is evident from re-calculation that the most economic losses come from geological hazard, though the occurrence rate of meteorological and hydro hazard is much higher (Fig. 7). There is practically a single cell on the map, where the dominant losses come from hydro-meteorological hazards only and such hazards are always accompanied by geological hazards.

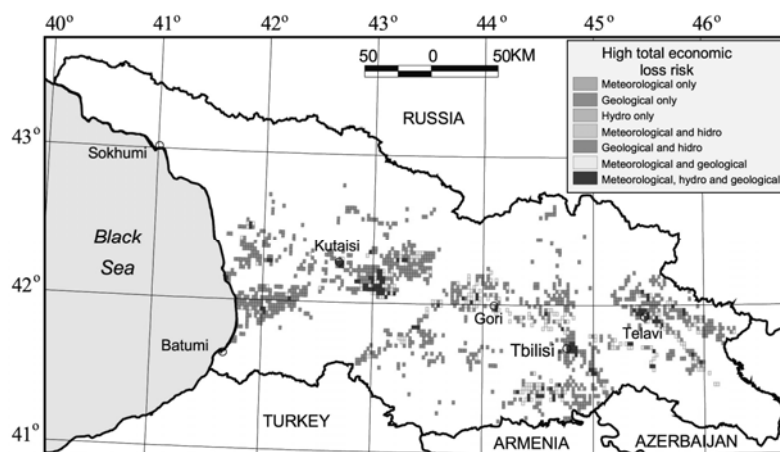


Fig.7. Economic loss risk for different natural hazards in Georgia. Note that in contrast with the Natural Disasters Hotspots map (Dilley et al, 2005), geological hazards are dominant in the country (Varazanashvili et al.2011).

This quantitative recalculation confirms the common sense assessments, given in section 4, namely that the statement of Natural Disasters Hotspots map (Dilley et al, 2005) that the Southern Caucasus (SC) and Georgia in particular is prone only to hydro-meteorological hazards is wrong and should be corrected in future (Varazanashvili et al.2011, Varazanashvili et al., in press). This conclusion is confirmed by the recently compiled “Atlas of Natural Hazards and Risks in Georgia” (2012).

9. Conclusions

- Different Global Hazard Maps give different assessments of hazards and risks for the same region. It is necessary to develop a standardized accounting of hazard events and losses for the nation.

- Information on economic losses and mortality global and regional hazard/risk maps is often misleading due to erroneous input information, used for compilation of such maps. One example of such discrepancies is Caucasus, where the World Hotspot Map predicts mainly hydrogeological risks, which is wrong. That means that information on local losses and mortality should be thoroughly checked by realizing close (direct) contact with local scientists, involved in hazard/risk estimation.

- A vivid example of significant errors in regional/national risk assessments is underestimation of losses caused by a strongest in Caucasus Racha earthquake (M 6.9-7) due to ignoring of local information, collected by local seismologists and earthquake engineers immediately after event and wrong information of UNDP on losses placed on internet, which become widespread in the world.

- Re-assessment of economic losses has been done for Georgia using well grounded local data. These recalculations show that the largest economic losses come from geological hazard, despite the fact that the frequency of meteorological and hydro hazards is much higher.

Acknowledgements

Authors acknowledge financial support of Georgian-European Center “Geodynamical Hazards of High Dams” (GHHD), Georgian National Scientific Foundation (GNSF) as well as fruitful cooperation with UNDP Center of Reduction of Catastrophes Risks in Georgia.

References

- [1] ADRC. 2006. Natural Disasters Data Book.
- [2] Atlas of Natural Hazards and Risks in Georgia.(2012), <http://drm.cenn.org/index.php/en/background-information/paper-atlas>
- [3] Beer, T. The hazard theme of the International Year of Planet Earth. In: Geophysical Hazards. T. Beer (Ed.), 2010, 3-16.
- [4] Benson C, Clay E. (2000) Developing countries and the economic impacts of catastrophes. In: Kreimer A, Arnold M (eds) Managing disaster risk in emerging economies, Washington DC, World Bank, pp 11-21
- [5] Central Asia and Caucasus Disaster Risk Management Initiative (CAC DRMI)”. (2009). World Bank, ISDR, CAREC.
- [6] Chelidze, T. (Ed). 2006. Atlas of GIS-based maps of natural disaster hazards for the South Caucasus, Tbilisi.
- [7] Chelidze T, Tsereteli N, Tsereteli E et al (2009) Multiple Risk assessment for various natural hazards for Georgia. In: Apostol I, Barry DL, Coldewey WG, Reimer DWG (eds) Optimization of disaster forecasting and prevention measures in the context of human and social dynamics. IOS Press, Netherlands, pp.11-32.
- [8] Cornell, C.A. 1968. Engineering seismic risk analysis. Bull. Seism. Soc. Am., 58, 1583-1606. CRED. Statistical Update from CRED Disaster Events Database in: CRED Disasters in the World. November 1991.
- [9] CRED. Profiles in the World: Summary of Disaster Statistics by Continent. CRED Statistical Bulletin, May 1994
- [10] Dille M, Robert SCh, Deichmann U et al (2005) Natural disaster hotspots: a global risk analysis. Washington DC, World Bank, Synthesis Report.
Field, E. Probabilistic Seismic Hazard Analysis (PSHA) A Primer.
http://www.opensha.org/sites/opensha.org/files/PSHA_Primer_v2_0.pdf
German Committee for Disaster Reduction <http://www.dkkv.org>
- [11] Giardini, D.,Grunthal, G., Shedlock, K.M.,Zhang, P. The GSHAP Global Seismic Map. (1999). Annali di Geofisica, 42, 1225-1228.
- [12] Ghesquiere F, Mahul O (2010) Financial protection of the state against natural disasters: a primer. Policy research working paper series 5429, World Bank, http://www.gfdrr.org/gfdrr/sites/gfdrr.org/files/documents/DRF_Financial_Protection_of_the_State_ND.pdf
- [13] Gabrichidze, G. (ed), Engineering analysis of consequences of Racha earthquake 1991 in Georgia, Metsniereba, Tbilisi, pp 131-136 (in Russian) ISDR/UNDP, Vision of Risk, A Review Geneva, December 2004.
(<http://www.undp.org/bcpr/disred/documents/publications/visionsofrisk.pdf#search='Hotspots%20indexing%20project'>)
- [14] Javakhadze, Sh., Tsereteli, E., Gaprindashvili, M. (2010). Catastrophic geological processes in Georgia in 2010: results and prognosis for 2011. Information Bulletin of Ministry of Environment protection of Georgia, (in Georgian).
- [15] Labbate G, Jamburia L, Mirzashvili G (2003) Improving targeting of poor and extremally poor families in Georgia: the construction of poverty maps at the district level. UNDP Country Office, Georgia (in Russian)
- [16] Munich-Re (2010) Topics GEO, natural catastrophes, analyses, assessments, positions. Munich, Germany. http://www.munichreamerica.com/pdf/topicsgeo_2010_us.pdf.
- [17] Panza, G. F., Kouteva, M., Vaccari, F., Peresan, A., Cioflan, C. O., Romanelli, F., Paskaleva, I., Radulian, M., Gribovszki, K., Herak, M., Zaichenco, A., Marmureanu, G., Varga, P., Zivcic, M., (2008). Recent achievements of the neo-deterministic seismic hazard assessment in the CEI region, In: Seismic Engineering Conference Commemorating the 1908 Messina and Reggio Calabria Earthquake (editors A. Santini and N. Moraci), AIP, 1020, 402-409.
- [18] Push, C. (2004) Preventable losses: saving lives and property through hazard risk management., World Bank.
- [19] Qaldani L, Saluqvadze M (2007) Avalanche zoning of South Caucasus. In: Chelidze, T. (ed). Atlas of GIS-based maps of natural disaster hazards for the Southern Caucasus, Tbilisi, pp 16-19.

- [20] Tsereteli E (2007) Mapping of mass-movement potential on the territory of Georgia: criteria of destabilization. In: Chelidze, T. (ed). Atlas of GIS-based maps of natural disaster hazards for the Southern Caucasus, Tbilisi, pp 13-15.
- [21] UN – (2002) Living with risk. Geneva UNDP (2004) Reducing Disaster Risk: a Challenge for Development. Global report, UNDP/Bureau for Crisis Prevention and Recovery, New York. <http://www.undp.org/bcpr/disred/rdr.htm/> UNISDR. (2009) Global assessment report on disaster risk reduction. van Westen C.J. (2010) Multi - hazard risk assessment: distance education. ITC, Enschede, Netherlands.
- [22] Varazanashvili , O., Tsereteli, N., Amiranashvili, A., Tsereteli, E., Elizbarashvili, E., Dolidze, J., Qaldani, V., Adamia, Sh., Arevadze, N., Chelidze, T., Gvencadze, A. Vulnerability, Hazards and Multiple risk assessment for Georgia (submitted to Natural Hazards).
- [23] Varazanashvili , O., Tsereteli, N., Butikashvili, N., Goguadze, N., Vepkhvadze, S., Khvedelidze, I., Gvenctsadze, A., Kupradze, M. 2011. Scientific Annual Report of M. Nodia Institute of Geophysics at I. Javakhishvili Tbilisi State University for 2011. (in Georgian)

(Received in final form 20 December 2011)

Просчеты и реальность в глобальных и региональных оценках риска катастроф

Тамаз Челидзе

Резюме

В последние годы природные катастрофы привели к огромным экономическим потерям и сотням тысяч человеческих жертв. Поэтому правильная оценка риска природных катастроф очень важна для выявления «горячих точек», т.е. наиболее уязвимых областей для той или иной опасности. К сожалению, часто имеют место ошибочные выводы из-ва использования неполных или неправильных локальных данных о происшедших катастрофах. В настоящей статье автор попытался проанализировать некоторые просчеты в глобальных и региональных оценках риска катастроф в особенности относящихся к Южному Кавказу и Грузии. Опасности и риски для Грузии пересчитаны с использованием представительных локальных данных.

შეცდომები და სინამდვილე კატასტროფების რისკების გლობალურ და რეგიონულ შეფასებებში

თამაზ ჭელიძე

რეზიუმე

ბოლო წლებში ბუნებრივი კატასტროფების გამო მსოფლიოში უზარმაზარი ეკონომიკური ზარალი და ასიათასობით მსხვერპლი დაფიქსირდა. ამიტომ ძალზე მნიშვნელოვანია ბუნებრივი კატასტროფების რისკების სწორი შეფასება, რათა გამოვლინდეს „ცხელი წერტილები“, ანუ ამა თუ იმ საშიშროებისათვის ყველაზე მოწყვლადი უბნები. სამწუხაროდ, ხშირად ავტორები მცდარ შეფასებებს აკეთებენ, რაც აიხსნება მომხდარი კატასტროფების შესახებ არასრული ან არასწორი ლოკალური ინფორმაციის გამოყენებით. წინამდებარე სტატიაში ავტორი შეეცადა გაეანალიზებინა ზოგიერთი შეცდომა, რომელიც დაშვებულ იქნა კატასტროფების რისკების გლობალურ და რეგიონულ შეფასებებში, განსაკუთრებით სამხრეთ კავკასიასა და საქართველოში. საშიშროებები და რისკები საქართველოსთვის დათვლილია ხელახლა წარმომადგენლობითი ლოკალური მონაცემების გამოყენებით.

Problems of natural and anthropogenic disasters in Georgia

**Tsereteli E.^{1,2}, Gaprindashvili M.¹, Gaprindashvili G.¹,
Chelidze T.^{2,3}, Varazanashvili O.³, Tsereteli N.³**

1. *National Environmental Agency, Ministry of Environment Protection of Georgia*
2. *Georgian National Committee on Disaster Risk Reduction*
3. *M. Nodia Institute of Geophysics of I. Javakhishvili Tbilisi State University*

Abstract

In the paper the problems, related to geological catastrophes in Georgia are considered. The main factors responsible for activating of these processes, their scale and negative consequences as well as objectives in disaster risk reduction activity.

International and national state of art in respect of natural disasters

In the last decades of the XX century, protection of the most of the planet population against the natural disasters, ensuring safe functioning of economic and engineering objects and stable state of nature have become an important social-economic, political and environmental problem. This problem has become even acuter at the turn of the XXI century when the natural cataclysms in terms of a wide-scale human pressing, increased urbanization and use of technologies have acquired even larger scales. This has caused a dramatic disturbance of the environment balance and has made the activation of the natural-anthropogenic disasters even more irreversible. This leads to an inconceivable economic and human losses. This is why the decisions to reduce the natural disasters and mitigate their results made at the World Summit of Johannesburg (South Africa) held under the aegis of the United Nations Organization in 2002 and International Conference of Hyogo (Japan) of 2005 were recognized as a basic guidelines.

It was because the activation of the natural disasters, that a number of countries have developed their national programs of management of natural effects.

Natural hazardous processes are divided in two different events: (1) hazardous meteorological events taking place in the atmosphere and (2) hazardous geological processes taking place on the Earth surface and crust. Nevertheless, some hazards such as landslides and debris-flows are caused by simultaneous activation of meteorological and geological factors. Therefore proper specialists and institutions are engaged in the management of the given problems. However, the study of regularities of the natural disasters, their permanent monitoring, forecasting their spatial and time developmental trends and drafting the managerial measures in any country should be at the expense of the state budget.

Particularly grave situation has been created as a result of the negative results of the hazardous geological processes.

Catastrophic development of natural processes has necessitated the creation of a single information bank of the management measures undertaken in different countries of the world and development of the strategy. The coordination of the study, forecasting and management of these very complex events was undertaken by the UNO institute of environmental protection, and the decade starting from 1990 was declared by the UNO as the decade to study the natural disasters and mitigate natural disasters, and the year of 2002 was declared an International Mountain Year. A number of countries have developed the national programs for the mountain development and preventing the catastrophic events, and a number of European states have been united under the aegis of "The Alpine Convention".

Georgia joined the mentioned decisions and under the Presidential Decree No. 36 of 1995, a national committee to carry out the international decade of mitigation of hazardous disasters was established. Earlier, in 1993, a special governmental decree No. 967 "About creating a single

protection system of environmental monitoring” was adopted, whose international coordination was the function of the Ministry of Environmental Protection and Natural Resources. In 1997, a special Presidential Decree No. 66 “About the development of hazardous geological processes on the territory of Georgia and measures to protect the ground and underground hydrosphere against them” was published. The Department of Geology, aiming at operating at the level consistent to the geo-monitoring studies, together with the Institute of Geography developed a state target program, which was considered and approved by the government and was handed to the Ministry of Economic Development to be included in the indicative plan of social-economic development. Besides, in 1999, the Parliament of Georgia adopted the law “About the social-economic and cultural development of the mountainous regions of Georgia”. In addition, the laws “About the protection of environment and soils” underlining the negative role of hazardous processes were adopted. Later, in 2007, the President of the country issued a special decree No. 542 “About the protection of the population and territories against some natural and anthropogenic hazards”.

Despite the fact that more and more territories, population and economic and engineering objects of Georgia are prone to risk of the natural catastrophes, the priority trends of the National Environment Action Plan (NEAP) of Georgia adopted in 2000 do not incorporate the problems of management of natural hazardous catastrophes and therefore, they were not considered within the state or international organizations targeting financial plans.

Therefore, in the field of improving the system of evaluation and safety of the risks of natural disasters there are still serious problems.

Risk of geological hazards in Georgia and relevant problems

Georgia, with its scales of origination of the natural-catastrophic processes, their reoccurrence and with the negative results inflicted by these processes to the population, agricultural lands and engineering objects, is one a most complex mountainous region of the world (See the Hazard risk map of the population of Georgia, Fig.1).



Fig. 1. Risk areas prone to hazardous geological processes on the territory of Georgia.

A strong influence of geological natural processes (frequently ending with the catastrophic results) is experienced by thousands of populated areas, plots of field, roads, oil and gas pipes, high-voltage electric power transmission towers, hydraulic structures and reclamation constructions, mountain and tourist complexes, etc.

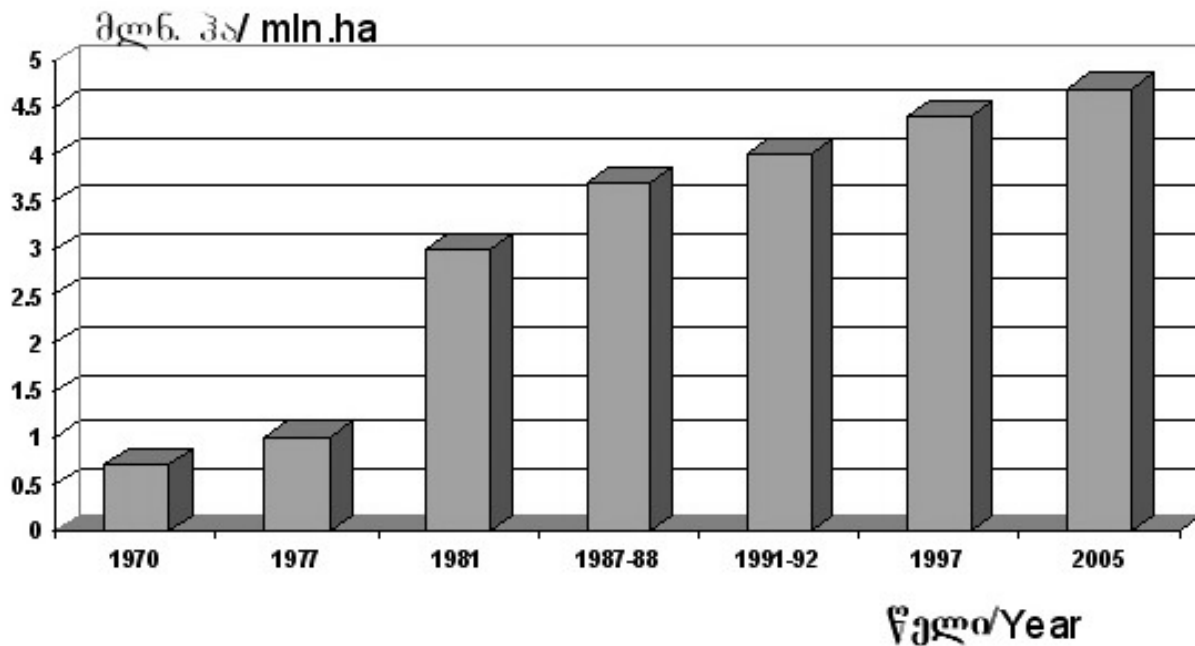


Fig. 2. The territory of Georgia within the zone damaged by hazardous geological processes.

Particularly grave is the situation in the mountainous regions, where due to the extreme activation of the processes, the local population is forced to abandon their historical places of residence, and sometimes to leave for other regions. This has resulted in tens of emptied mountain villages in the second half of the XX century. The most alarming thing is that these processes often cause human loss.

Below is an incomplete list of the negative results of the geological disasters since 1968:

- The hazardous area covered over 70% of the territory;
- 3000 populated areas (63%) fell within the risk area of the geological disasters;
- The human loss due to the geological disasters exceeded 1000;
- Over 400 000 residential houses and premises were damaged with different degrees or were ruined;
- 1.5 million ha of land was damaged and taken out of exploitation;
- 560 km of motorways were damaged and were to be rehabilitated.

Incomplete data of the economic loss occurring due to geological catastrophe in different years:

- In 1967-1968 – 500 million US Dollars;
- In 1973-1975 – 650 million US Dollars;
- In 1987-1990 - 1 million US Dollars;
- In 1991-1992 - 10 billion US Dollars;
- In 1995-2008 - 1. 241 billion US Dollars.

Note: The cost of realization of anti-erosive measures in Georgia drafted in 1981-2000 was fixed at 1.300 million US Dollars. At present, the urgency of anti-erosive measures has doubled.

Specialized studies prove that the origination and activation of landslide-gravitational and mudflow processes increases by a geometric progression year after year. This is evidenced by the graphs of landslide-gravitational and mudflow events (Figs. 4, 5).

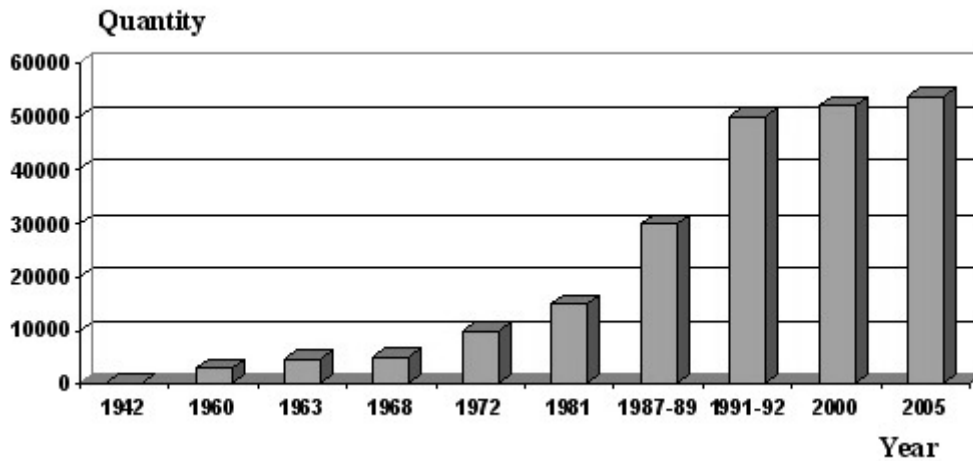


Fig. 3. Landslide-gravitational events on the territory of Georgia mapped for different years.

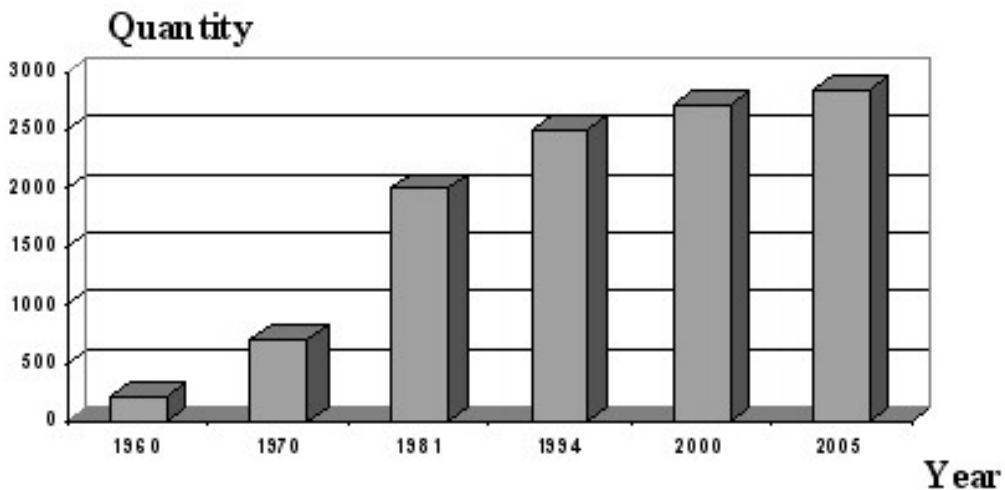


Fig. 4. Mudflow-transforming river gorges on the territory of Georgia mapped for different years.

If in the last decade of the XX century, the extremums of activation of the mudflow-gravitational processes were mostly subject to a certain cyclicity and following the geological-climatic conditions of the given area, occurred once in every 2-5 years on average, since the 1990s, the activation of the processes in excess of their mean value takes place almost every year, and the intervals of their extreme occurrences are significantly reduced. As a result, more and more new territories, populated areas and engineering-economic objects are subject to the negative impact of the processes.

Intensity of landslide and mudflow processes on the urbanized area fixed during the regional geo-monitoring in different years and damage caused by them

Table 1

Year	Landslide			Mudflow		
	Intensity (in dynamics)	Approximate direct damage (in million lari)	Victims	Intensity (transformable mudflows)	Approximate direct damage (in million lari)	Victims
1995	666	132	6	693	96	1
1996	404	80.3	4	198	27	5
1997	510	102	3	318	44	-
1998	333	67	2	147	20	6
1999	56	12	1	27	4.5	-
2000	65	13	1	23	3	-
2001	75	15	-	26	4	-
2002	69	13.8	1	23	2.5	2
2003	71	14.4	3	28	4	-
2004	736	147	1	192	28	-
2005	480	96	-	68	9	4
2006	316	70.5	1	73	40	-
2007	236	54	-	88	28	-
2008	407	78	10	100	36	8
Total	4424	895	33	2004	346	26

Recent development and reactivation of hazardous geological events in an unimaginable scale and severe geological complications of the engineering-geodynamic situation taking place in a non-stationary mode in the geological environment in Georgia, together with the extremely sensitive geological conditions, were conditioned by:

1. Activation by strong earthquakes, occurred in the last decades;
2. Drastic activation of the negative meteorological events provoking the geological processes on the background of global climatic changes and their abnormally frequent occurrence (mostly increased atmospheric precipitations, temperature and humidity);
3. Large-scale human impact on the environment and severe disturbance of the environmental balance, in particular, settlement of the population and unorganized land reclamation, often without any assessment, building and restructuring of new transport objects, intensive cutting down of forests, etc.

One of the most important reasons for poor protection of the population against the geological catastrophes, unsafe functioning of the engineering-economic objects and damage inflicted to the economy of the country is the low level of the society readiness to the above-described events, meaning not sufficient awareness of the population and responsible people of the expected disasters, their possible localization and accomplishment of measures to mitigate their hazards.

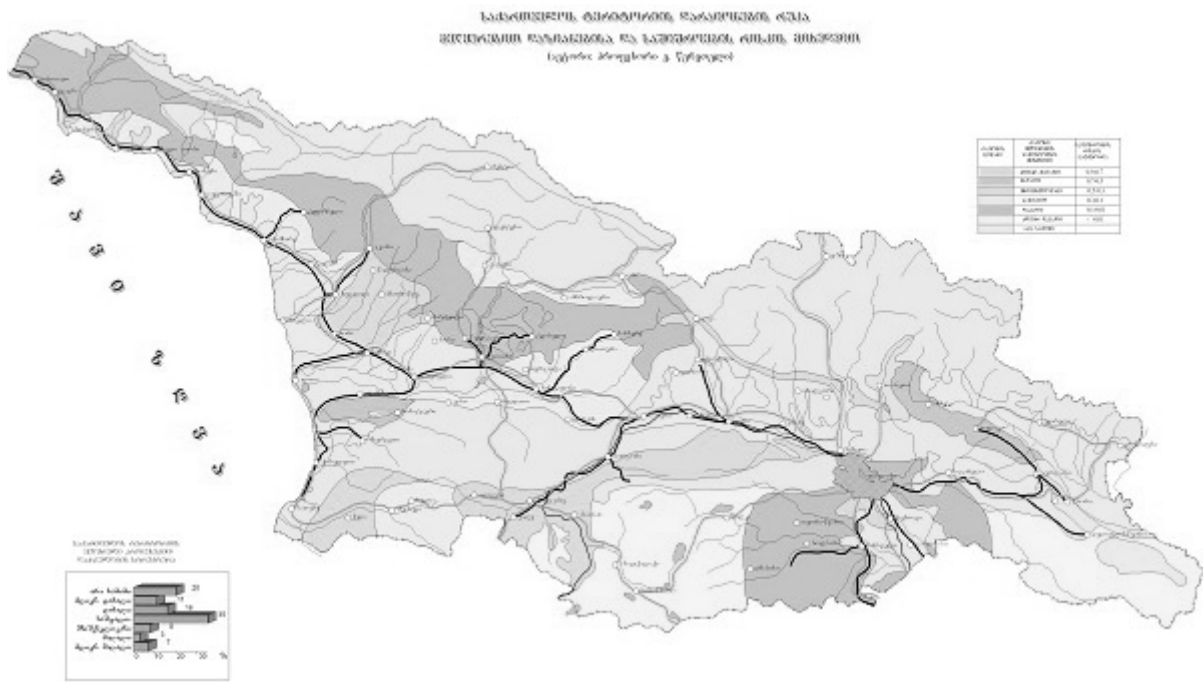


Fig. 5. Map of zoning of the territory of Georgia according to the landslide damage and risk of hazard (Author E. Tsereteli).



Fig. 6. Map of zoning of the territory of Georgia according to the damage caused by mudflow processes and risk of hazard (Author E. Tsereteli).

Actions and results associated with the natural hazardous processes in Georgia

Large-scale development of the hazardous geological processes in Georgia and great damage inflicted to the economy of the country since the second half of the XX century have forced the management of the country to pass more than one document about the mitigation and reduction of the risk of the geological hazards and optimization of the managerial measures.

Following the problem urgency, a number of departmental and research institutions have made their operations more intense in the given direction within the limits of their competence. First of all, the activity of the Department of Geology of Georgia (which is at present included in the National Environmental Agency of the Ministry of Environmental Protection and Natural Resources of Georgia), which identified, mapped and cataloged the hazardous geological processes on the territory of the country and identified the spatial limits and developmental regularities of these processes for tens of years. It has been establishing the risks of hazard posed by the geological processes to the population and engineering-economic objects, developing special engineering-geodynamic basic maps of the scale 1:200000, 1:50000, 1:25000 of different content:

- Specialized engineering-geological studies of agricultural lands was undertaken scaled 1:10000 with the purpose of zoning the risk of hazardous processes, accomplishing the protection and restoration measures and community land management. The processed materials were handed to the Ministry of Agriculture;
- The risk of hazard and damage of landslides, mudflows and erosive processes on the territory of Georgia, of the scale 1:500000 was assessed;
- The detailed studies (1:2000) of over 200 objects within the zone of high risk of landslides, mudflows and erosive processes with the purpose of protecting the population were undertaken, and proper preventive measures were accomplished;
- On the instruction of the government, a monograph "General anti-erosion plan on the territory of Georgia for 1981-2000" was drafted and published, which discussed all geological processes developed in Georgia and different measures to be accomplished;
- Special engineering-geological studies scaled 1:50000-1:25000 were undertaken in the coastal region of the Black Sea of Georgia, serving as the basis for drafting the scheme of integrated management and protection of the coastal area;
- A long-term prognosis of landslides, mudflows and sea coast washout (abrasion) for 1981-2000 was developed.

The basic scientific results of the studies carried out for tens of years have been analyzed in more than 300 monographs and publications, with most of them published in the international press, including the methodological publication under the UNESCO and UNEP projects.

In respect of natural hazardous events, in addition to the Department of Geology, the former research institutes of the National Academy of Geophysics, Geography, Water Economy and Hydrogeology and Engineering Geology (at present, Ministry of Education and Science) have accomplished significant studies, in particular.

Wide-scale studies are being accomplished at the Institute of Geophysics on the lithosphere structure, its dynamics and evolution, seismicity and physics of the atmosphere and ocean. Institute carried out the detailed studies of the generation of earthquakes in Caucasia and Georgia, in particular, their physical parameters and performed macro-seismic zoning of the earthquake hazard. Particular attention was paid to gravitational events provoked by earthquakes. Geophysical prospecting methods have been successfully applied to study in detail the structure of landslides in different regions of Georgia.

The complex geographical study of the mountainous regions has been prioritized at the Vakhushti Institute of Geography since the 1970s. One of the most important trends was the study of modern geomorphologic processes in the mountainous areas, and the study of mudflows and landslide events was undertaken at the laboratory created specially for this purpose. On the other hand, the well-organized studies of mass-movements gradually covered the whole of the Caucasus. The gained materials served as the basis for the monographs "Karst of Georgia", "Karst caves of Georgia".

There is also a laboratory of the sea coastal zone at the Institute of Geography. The laboratory undertook the detail study of the Black Sea coastal zone of Georgia, and the impact of the streams along the coast on the stability of the coast, deficit of the alluvium, formation of underwater canyons and their role and place in respect of the coast stability were defined.

Significant studies of the dynamics of the Black Sea coast and offshore zone of Georgia have been undertaken by the Institute of Engineering Geology and Hydrogeology, whose scientific studies are given in the monographs “Engineering geography of the Black Sea offshore zone and coast within the limits of Caucasus” (Janjgava, 1979); “Engineering geology of the Black Sea and protection of environment” (Khachapuridze, 1990).

So, at present, the basic foundation of information at the national and regional levels for the priority trends of action for the territory of Georgia in respect of the risk of geological hazard has been developed. The efficient management of the identification, evaluation, early notification and reaction to the geological risks should be included in the organizational, legal and political frames, what is first of all, envisaged by the Decree No. 967 of the government of Georgia of 1993 about functioning of the geo-monitoring studies system, Presidential Decree No. 66 of 1997 and Hyogo action frame plan of the 2005 on the disaster risk reduction by 2005-2015.

The practice has proved that there is no country with developed economy undertaking preventive capital measures for every existing or newly evoked geological event. Moreover quite often the measures against aggravated landslide processes with even great capital expenses do not produce the desirable effect. Therefore, the principal thing is to establish the place, kind and scale of the expected geological event and the risk of expected hazard to the population and economic-engineering objects. Realization of the scenario of reduction of the disaster risk posed to the population and strategic objects during the emergency is the principal and decisive task. Most importantly, the population should be informed timely about the hazardous situation and the recommendations should be given about simple mitigating measures, which can be undertaken easily by the local population, communities and municipalities. Consequently, one of the main directions in prevention or mitigation of geological risk is functioning of well-organized geo-monitoring studies at the regional, as well as secondary and tertiary levels.

It should be noted that the geo-monitoring studies in Georgia, due to insufficient financing, were undertaken with a minimum funding and with interruptions, only on the particularly dangerous and geo-ecologically stressed urbanized areas. The high mountainous regions, where there are catastrophic events (landslides, rockfalls, mudflows, snow avalanches) formed were not subject to regular observations. These disastrous events often reach the populated areas and engineering objects and quite often end up with tragic outcomes. There are many examples of such disasters, especially in Kazbegi, Dusheti, Svaneti, Ajara and Racha regions.

Strategic aims

The principal strategic aims in mass-movement related disaster risk reduction are as follows:

- Basic evaluation of the existing level of the natural catastrophes and identification of events;
- Establishing the spatial limits and their causal effect;
- Assessment of risk;
- Establishing a reliable early warning system for forecasting natural disasters;
- Identifying the possible damage of the geological catastrophes and identifying concrete preventive measures;
- Registering the development of the hazardous processes on the territory of Georgia in a long-term perspective, cataloguing, processing, analyzing and generalizing the statistical information about the damage caused by these processes and creating the electronic database;
- Scientific long-term prognosis of the trends in development of natural disasters and changes of the geological environment due to the anthropogenic impact (for a 20-25-year-long period);
- Drafting the basic maps of risk zoning for erosive, landslide-gravitational and mudflow processes on the territory of Georgia in GIS system;

- Extending the geo-monitoring studies to every hierarchical level on the whole territory of Georgia and their permanent implementation starting from observation, control and assessment through prognosis and management, by using ground and space technologies;
- Organization of the observation test areas of the geological catastrophes for the second and third geo-monitoring levels and their operating to study thoroughly the regularities of origination of a concrete event and develop optimal contra measures;
- Urgent situation assessment in force-majeure circumstances during the extreme activation of geological elements, fixing the risk of hazard, giving geological recommendations to the population and offices in extraordinary situations in the high risk areas; developing detail conclusions about the established situation by specifying the preventive measures for the local administration and government;
- Drafting annual information bulletins of prognosis of geological catastrophes and expected hazard, developing proper mitigation and preventive measures and their urgent delivery to the relevant institutions at the regional and central levels.

Geo-monitoring studies of the natural disasters must be considered a priority at the state level and must be financed within the limits of the state target program.

Legal basis of strategic aims

The Constitution of Georgia; Georgian Laws about the “Environmental protection” and “Soil protection”; the 2005 UN Hyogo action frame plan on disaster risk reduction strategy in 2005-2015; Decree No. 542 of the President of Georgia of 2007 “About the protection of the population and territory against natural and anthropogenic situations”; Environmental safety concept of Georgia; the National reaction plan for the natural-anthropogenic extremal situations; Provision of the Ministry of Environmental Protection and Natural Resources of Georgia and activity of the national agency of the same Ministry.

(Received in final form 27 December 2011)

Проблемы природно-антропогенных катастроф в Грузии

**Церетели Э. Д. , Гаприндашвили М. В. , Гаприндашвили Г. М. ,
Челидзе Т. Л. , Варазанашвили О. Ш. , Церетели Н. С.**

Резюме

В статье рассмотрены проблемы, связанные с геологическими катастрофами в Грузии, оценены основные факторы, обуславливающие возникновение этих процессов, масштабы их развития и негативные последствия, даны цели и задачи уменьшения риска катастроф.

ბუნებრივ-ანთროპოგენური კატასტროფების მდგომარეობის პრობლემა საქართველოში

ემილ წერეთელი, მერაბ გაფრინდაშვილი, გიორგი გაფრინდაშვილი,
თამაზ ჭელიძე, ოთარ ვარაზანაშვილი, ნინო წერეთელი

რეზიუმე

სტატიაში განხილულია საქართველოში სტიქიურ-გეოლოგიურ პროცესებთან დაკავშირებული პრობლემები, შეფასებულია მათი გამომწვევი მთავარი ფაქტორები, განვითარების მასშტაბები და მათგან მიყენებული ნეგატიური შედეგები, მოცემულია სტიქიის საშიშროების რისკის შემცირების სტრატეგიული მიზნები და ამოცანები.

Archaeogeophysics in Georgia – New Results, New Prospects

T. Chelidze¹, D. Odilavadze¹, K. Pitskhelauri², J. Kiria¹, R. Gogua¹

1. Institute of Geophysics of Ivane Javakhishvili Tbilisi State University

2. Ilia State University

Abstract

The basics of archaeogeophysics is a difference in physical properties (electrical conductivity, dielectric constant, magnetic susceptibility) of a buried archaeological object and surrounding geological media: as a result the physical field measured on the surface creates anomaly. Modern precise devices and special computer programs allow fast and accurate location of buried archaeological object and determination of its size and burial depth. A short review of archaeogeophysical research in Georgia is given. Fundamentals of main archaeogeophysical methods: georadar, magnetic and electrical prospecting are set forth. The results of archaeogeophysical investigations in areas of Shiraki (georadar) and Armaztsikhe-Bagineti (electrical prospecting) are analyzed,

1. Introduction

Geophysical methods have intensively been used in archaeology during the recent years. The first tests were carried out in 1946 and they are increasingly popular nowadays (Clark, 1996; Gaffney and Gater, 2003; Witten, 2006; Schmidt, 2001). Among them most frequently are used georadar, electric resistance and magnetic methods and more rarely – the methods of natural electric fields, microgravimetry, radiometry, thermal infrared and acoustics or seismicity.

“Archaeogeophysics” or “archaeogeophysical exploration” is based upon contrast of physical properties between component materials of an archaeological monument and its surroundings. If a structure with certain physical properties (electric resistance, magnetism) is covered with a layer of soil with different properties, this causes changes in the measured field of day surface, i.e. a geophysical anomaly. Processing of an anomalous field by means of specific software enables to determine precisely the location of a monument covered with soil, the depth of its location, its size and other details.

As a rule, archeological monuments are strogly localized, i.e. their horizontal and vertical measures are limited. Besides, localization depth of any archaeological monument rarely exceeds 5 meters. Therefore, one of the demands of archaeogeophysical exploration is detail approach to field data, which means that the distance between observation points must be short and observation network should be dense.

The last years’ achievements in geophysical instrumentation and data processing substantially increased exploratory potential of so called “emergency archaeology”, while in areas of big industrial objects it is necessary to map buried cultural heritage monuments localized in a short time and without damaging the environment.

The above statements do not at all contravene purely archaeological methods. Sooner or later archaeologists will reach their goal. We would just like to note that by means of archaeogeophysics archaeologists are able to study the area under exploration more quickly, with less expenditure and

more thoroughly. Importance of archaeogeophysical exploration for such a historical heritage country as Georgia is evident.

2. Archaeogeophysical explorations in Georgia

The territory of Georgia is known for the world civilization since the ancient times. It is proved by the existence of old Greek myths about Prometheus and the Argonauts. Consequently, it is natural that there are numerous archaeological monuments of different periods in our country. Many of them are covered with Quaternary sediments and it is very difficult and quite expensive to discover them without the help of geophysical methods.

In Georgia archaeogeophysical explorations began in 1964-1968 on the territory of ancient town Bichvinta (Tsitsishvili, Tabagua, Khvitia, 1968). The exploration was carried out in different ways by electric, magnetic, gravimetric and radiometric methods, which enabled its completion with satisfactory results: the location of the ancient buried walls was determined on the basis of the discovery of clear geophysical anomalies.

Since then similar explorations have been carried out for many objects (Tsitsishvili, Tabagua, Khvitia, 1968; Tsitsishvili, Tabagua, 1975; Chanturishvili, Jakhutashvili, Kutelia, 1993): for the ancient city of Vani, the surroundings of Tbilisi, the old irrigation system of Tetrtskaro, Bichvinta (1983), the David-Garedja complex, Monastery of Bagrat, the Queen's Palace in Atskuri (1991), a former town in Kakheti (1985-88), the monastery in Ninotsminda (1997-98), the territory of Armaztsikhe-Bagineti (2000-2001).

Since M. Nodia Institute of Geophysics has obtained new up-to-date equipments like GEORADAR ZOND 12, electrical prospecting station SARIS and magnetometer GEOMETRICS, its potential for archaeogeophysical prospecting has greatly increased. The GEORADAR method is especially efficient for its high precision, detailing and reliability as well as for short time, needed for measurements and interpretations.

3. GEORADAR

The georadiolocation or GEORADAR method (Neal, 2004; Witten, 2006) has become very popular in archaeogeophysical explorations during the last years. This method, like the usual radar method, uses the radiation of high frequency electromagnetic waves and their property of reflecting from objects with different properties; the difference is that in the case of georadar method the radiation is directed to the Earth's crust. Both the radar and GEORADAR methods enable to determine the distance of reflect surface by means of measuring the travel time of a direct and reflected ray: travel time divided by wave velocity makes distance. The difference between these two methods is that a radar ray directed to the atmosphere spreads over a quite long distance; while due to high conductivity of the Earth's composite rocks the geo-radar radiation is strongly absorbed and in optimal cases it propagates down to several dozen meters into depth. As georadar ray is reflected from objects with different dielectric properties, by this method structures are distinguished according to a dielectric constant.

The georadar method gives possibility not only to cut expenses but also use funds more effectively as scanning a soil by georadar method enables to explore more area of the desirable territory in considerably little span of time.

If an explored object is placed in 10-20 m depth from the surface there is no alternative to the GEORADAR method in the contemporary archaeology.

Aerophotography and visual signs do not enable archaeology to determine in detail depth/location of objects that lack adequate features: e.g. graves and traces of settlements underneath soil, remains of foundations (Odilavadze, Chelidze, 2010).

Soil scanning by means of georadar method makes it possible to discover even objects with different density (as dielectric conductivity depends on porosity). Subjects discovered by GEORADAR can be a geological formation, void, a stone coffin, a crypt, a wine-jar etc. In certain cases it is possible to process and interpret obtained results in real time in field conditions. When scanning a soil in order to investigate barrows it is quite possible to reveal such structural elements as debris layer, central constructions, stone cover, etc. It is also possible to explore soil-filled graves (i.e. filled and covered with different dielectric materials) by GEORADAR despite there are no distinguishable signs on the surface.

GEORADAR enables to obtain information about bedrock underneath the surface. According to contrast range of dielectric conductivity of layers we distinguish a soil type (clay, clay soil, sand soil, rocky soil), its structure (consolidates soil and destructed one, i.e. cultural layer), soil condition (dry, humid or saturated by water) and segments with different physical properties, among them different kinds of archaeological objects (walls, basements, graves, voids, different size objects).

Soil scanning by GEORADAR results in determining the depth, section of soil and cultural layers. This method enables to map their borders as well. It completes and enriches information for classical method of archaeological stratigraphy.

A section obtained by GEORADAR, unlike the classical stratigraphy method of archaeology, is constructed in a shorter time as it is presented on a PC screen immediately during profiling. The advantage of georadar stratigraphy compared to the classical one is that in this case the environment of the investigated object is not damaged after carrying out works on it. It is important also for archaeologists as an investigated object remains undamaged as well.

The conducted works and obtained experience makes possible to distinguish four main trends of GEORADAR investigations in archaeology. Each of them is significant as they can solve relevant archaeological tasks, the final main instrument of which is excavations.

The first one out of the above mentioned trends in archaeology is geological survey of future exploration area. Large profiles (1-2 km) are constructed by GEORADAR on a probable archaeological excavations territory. GEORADAR exploration makes it possible to make a general geological image, observe possible geological evolution of a relief and determine borders of the cultural layer, buried fields, buried riverbeds, etc. Analysis of a geological survey image obtained by GEORADAR investigation assists in planning of archaeological excavations works as it is able to precisely determine borders of locations of ancient towns and settlements.

The second trend of GEORADAR investigation in archaeology is detailed GEORADAR survey (georadar stratigraphy) of a cultural layer in order to verify location of a soil for processing (for excavations). It enables to reveal locations of foundations of certain constructions.

The third trend of georadiolocation investigation in archaeology is search, discovery and in certain cases identification of medium sized (of meter order) archaeological objects without processing the soil. Archaeological objects have radio image that is characteristic for them. This makes possible to define the object (size, shape, features) without destruction the integrity of the soil.

The fourth trend of GEORADAR investigation in archaeology is more detailed subsurface survey and search for relatively small sized (dozen cm) archaeological objects. According to the thumb rule GEORADAR is able to identify objects with size of the order of one tenth of bedding depth (for example the objects with size of 10 cm buried on the depth 1 m). Generally, discovery of relatively small buried objects by GEORADAR depends on several factors. One of them is frequency: high frequency is needed to find small sized objects. At the same time the propagation depth of such frequencies is small. Revealing objects located relatively deeper require lower frequencies. As a rule, archaeological monuments are situated in 1-5 m depth. Consequently, the central frequency is to be 100-1000 MHz. Discoverability of objects also depends on distance d between observation points: results are good if separation of the observation points is less than the one fourth of the wave length in

the soil, more precisely, when d is less than approximately $[75/f(\epsilon)^{1/2}]$ where f is a frequency in MHz and ϵ is a dielectric relativity constant of the embedding media. For detailed investigation the 1/5 of this value is recommended.

Below are the preliminary results of the 2011 Shiraki joint archaeological and archaeogeophysical expedition. The interperpendicular radiograms of barrows (not excavated) that were obtained by georadar method show the depth in meters on the y -axis and the distance in meters along the profile—on the x -axis. This preliminary study proves that the georadar method enables to vividly distinguish the borders of the barrow, its inner structure, zones of possible voids and water intrusion (fig. 1-4). Unfortunately, the black-and-white versions of the diagrams presented here have less resolution; the colour diagrams are more informative.

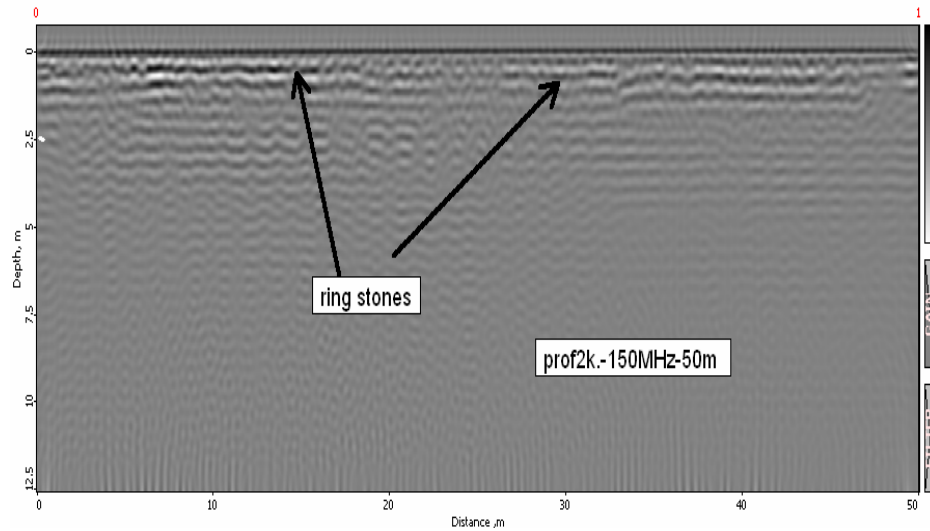


Figure 1. The diagram shows large stones of a barrow (probably) placed in circular shape (in the section). The radar signal distribution depth – 10 m shown in the figures 1-6: on the y -axis – depth in meters, on the x -axis – the distance in meters along the profile.

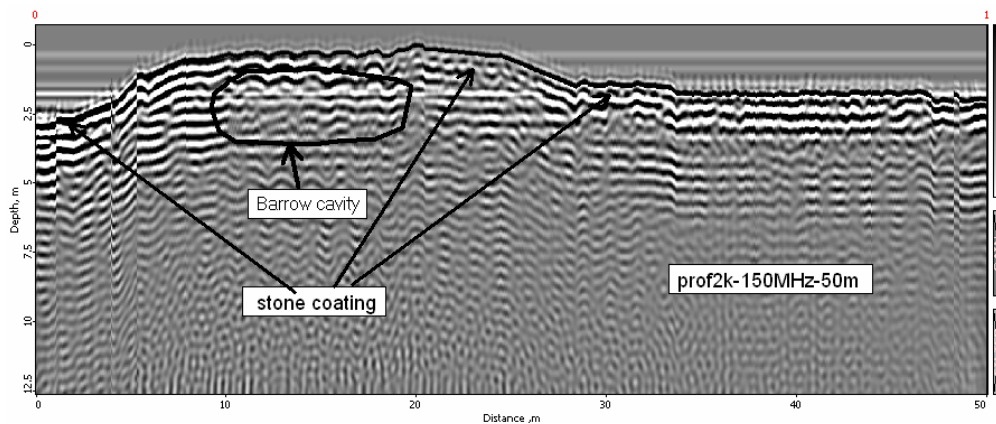


Figure 2. The same radiogram with corrections in the relief. The wide arrow shows the location of the probable cavity (contoured). The long arrows distinguish locations (coverage) of the large stones.

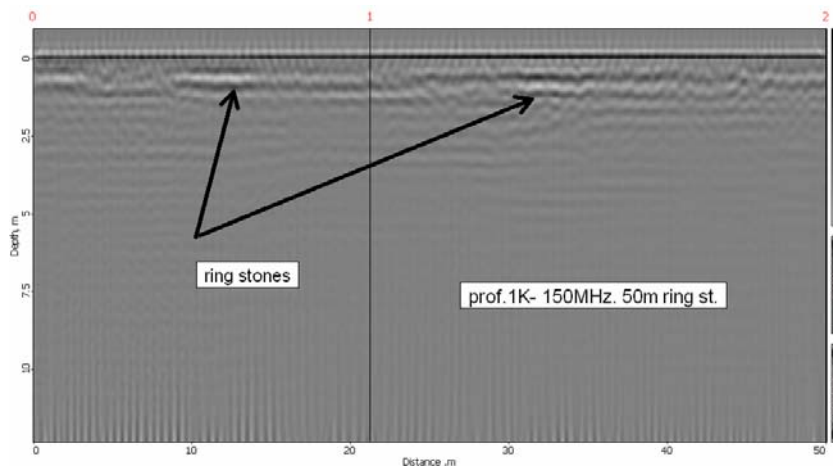


Figure 3. Radiogram constructed on the perpendicular profile of the radiogram in the figure 1-2. The arrows show the barrow stones situated in a circular shape.

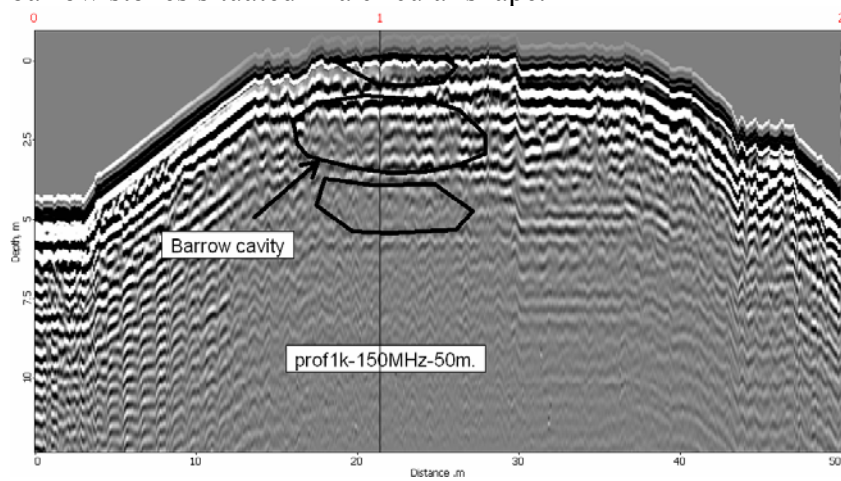


Figure 4. The same radiogram as in the fig. 3 after corrections in the relief. The arrows show and the lines contour the (probable) cavities in the barrow.

Figures 5-6 present Radiograms constructed for the former town in Shiraki. A section of 10 m depth was determined; water intrusion zones and (probably) pavement stones are distinguished.

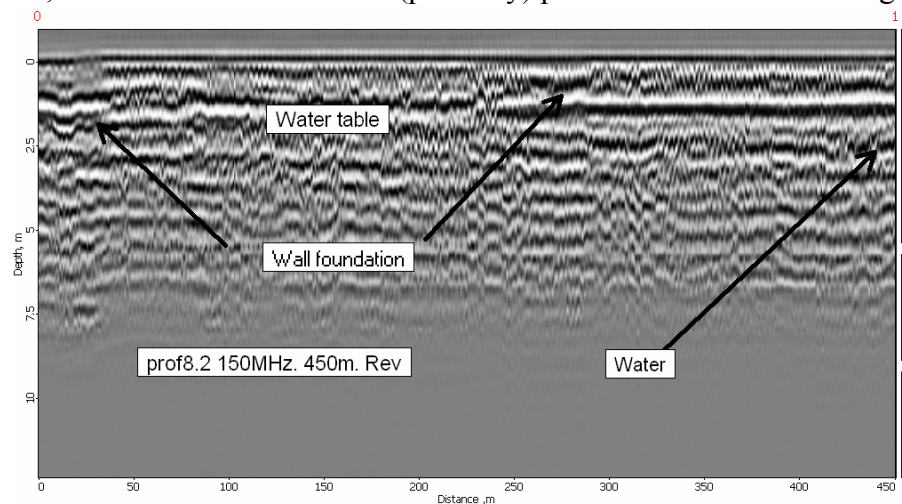


Figure 5. Georadar section of the 450 m length plot of the former town in Shiraki. Georadar layers were distinguished: the first layer is situated in 1-1.5 m and the second layer – in 2-1.5 m depths.

Along the section the ground water level in 1-1.5 m depth (black line) and the water intrusion area at the end of the radiogram were distinguished. The places indicated by the arrows near the surface (probably) are remains of the foundation.

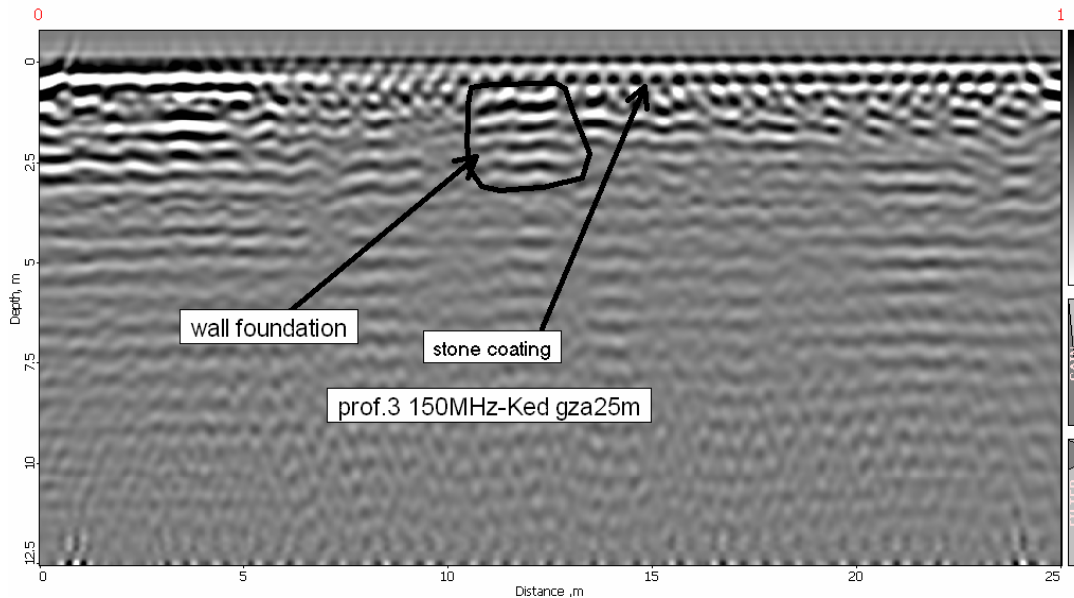


Figure 6. The radiogram (length – 25m) shows objects, possibly stones used for covering the road (approximately 3—35 cm size), regularly situated near the subsurface (0.8-1 m depth). It is supposed that the road crosses the remains of some old foundation.

The works were carried out by means of certified GEORADAR “ZOND-12” with supporting 2GHz, 150MHz and 75MHz antennas possessed by Institute of Geophysics. The results were processed by certified software PRIZM-2.5.

4. The archaeomagnetic method

The magnetic method, as a quick and high resolution method, is often used in archaeology. Nowadays it is one of the main methods in archaeological search. It is used for revealing objects with magnetic properties different from the environment such as covered metal (iron) segments, stone walls and foundations, kilns and stoves. Institute of Geophysics has a modern magnetometer GEOMETRICS G-856, which can be successfully used in archaeological survey (Fig. 7).



Figure 7. Magnetometer GEOMETRICS G-856

Below (Fig.8) are the results obtained by surveying an ancient kiln in Germany. The red colour indicates anomalous areas corresponding to the locations of the kilns.

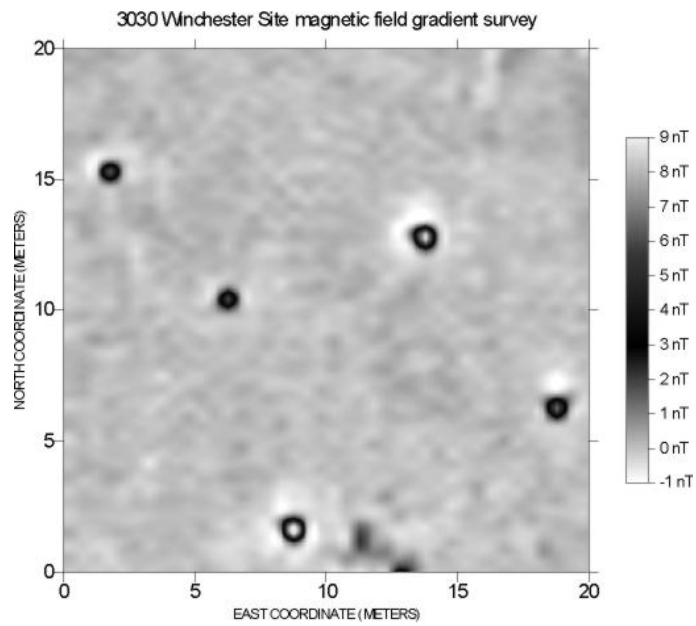


Figure 8. Ancient kilns (dark rings) surveyed by magnetic method (Germany).

Institute of Geophysics carried out field magnetic survey at Shiraki plain, where Google map reveals buried archaeological monument (Fig. 9).



Fig.9. Map of the test area Shiraki 1

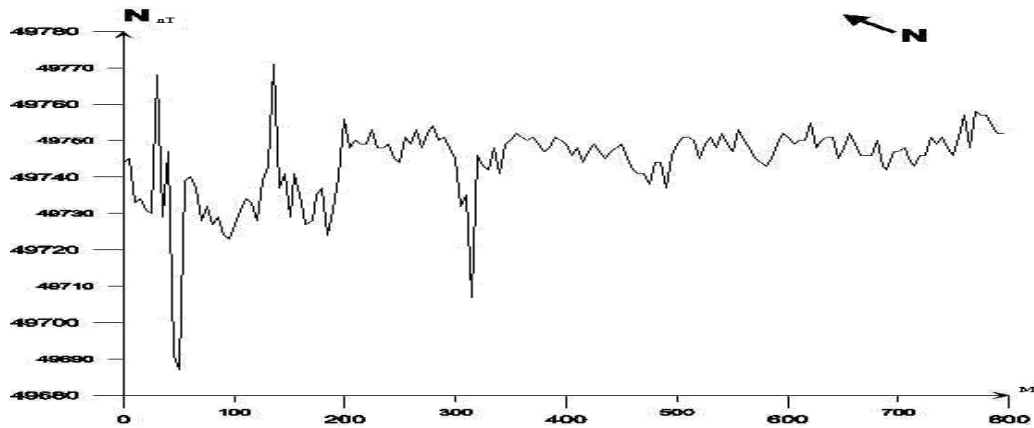


Fig. 10. Magnetic field profile 1 (test area Shiraki1)

The T-component of the geomagnetic field was mapped using proton magnetometer G-856 (precision 0.1 nT). Two parallel profiles were done along highway; the first one on the distance 15-20 m and the second one on the distance 30-40 m from the highway. The magnetic field along profiles is presented on the Figs. 10, 11). The relatively low mean field and significant localized anomalies at the left section of the first profile are absent on the parallel profile, which is separated by only 10-15 m), though the mean values of the field are close for both profiles. Comparison of profiles allows drawing conclusion that the intensive local anomalies on the first profile are probably caused by archaeological objects.

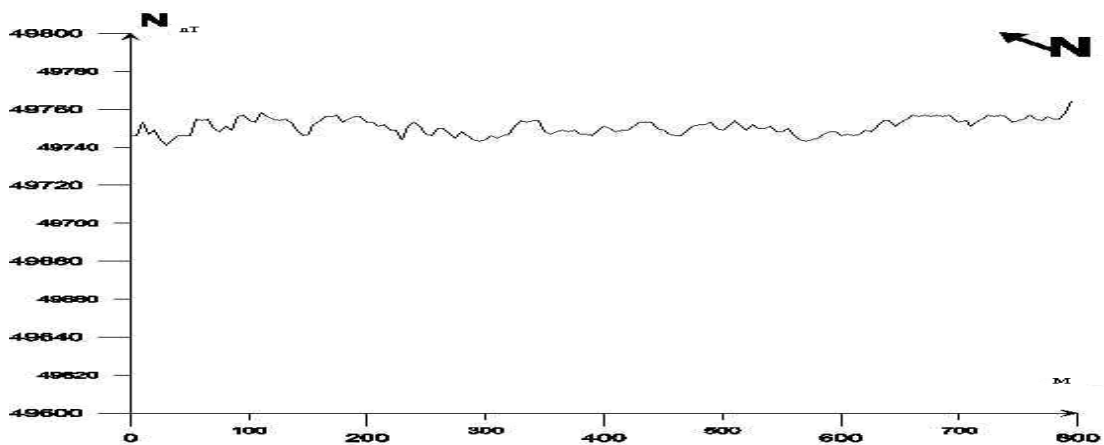


Fig. 11. Magnetic field profile 2 (test area Shiraki1)

Another example is a magnetic survey on the barrow (also in Shiraki plain). The magnetic field on the profile crossing the barrow is shown in Fig. 12. It is evident that absolute values of magnetic field above barrow is significantly less than in surrounding area and the field minimum coincides with the top of the barrow, which confirms results obtained by GEORADAR (compare Figs. 1-4 and 12).

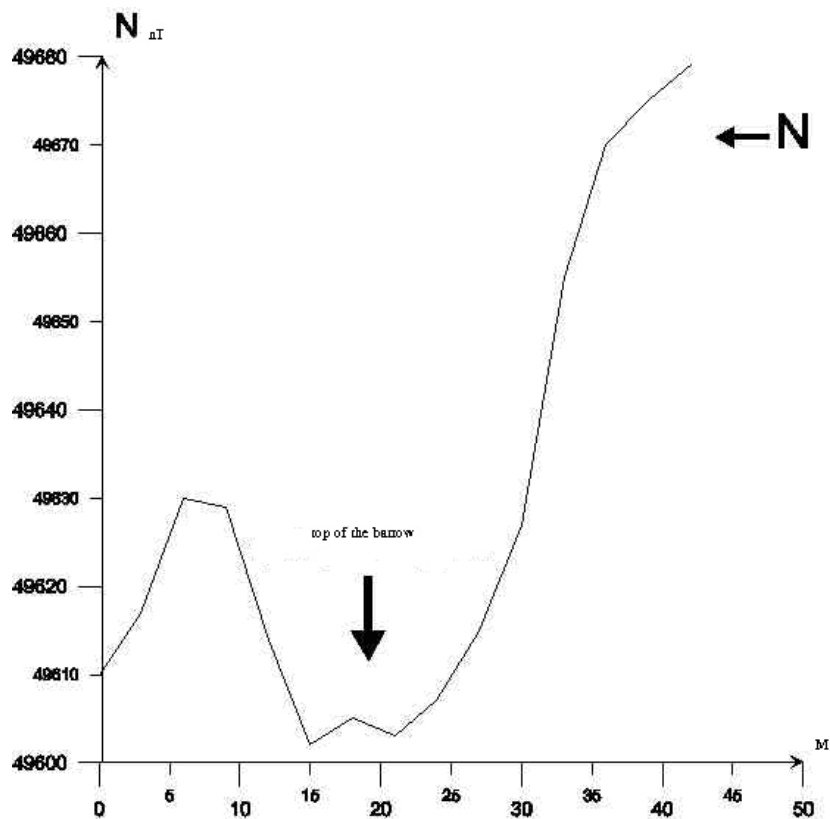


Fig. 12. Magnetic field profile across barrow (test area Shiraki2).

Above results show that precise magnetic survey (in the range of several nT) is very efficient method for revealing buried archaeological objects.

5. The electrical prospecting method

A method of electrical prospecting enables to distinguish objects with different conductivity in dozens of meters' depth (walls, foundations, graves, voids, etc). Institute of Geophysics own an up-to-date equipment SAR and many years' experience in using this method.

The fig.6 below shows the results of electrical prospecting fulfilled by institute of Geophysics on the Armaztsikhe-Bagineti complex (near Mtskheta) (Apakidze, Tabagua et al, 2001; Chanturishvili, Chelidze, Tabagua et al, 2001). The results obviously show that use of geophysical methods makes archaeological investigations easier.

In the figure the black rectangles indicate soil processing areas carried out earlier without using geophysical methods. The so called anomalous areas distinguished by geophysical electrical prospecting method are marked with figures 1, 2, 3, 4. The rectangles in these areas stand for the bore holes made on the basis of the geophysical results. It turned out that making bore holes without the use of geophysical methods ended with no results, i.e. they could not reveal the covered archaeological objects. Meanwhile, the efficiency of the bore holes made on the basis of geophysical methods is high: some certain cultural layers (a wall, a floor, etc) were discovered during all test excavations of the anomalous areas. Finally, as a result of two seasons' geophysical expeditions some unknown archaeological objects of 1700 m² area were discovered with minimal expenses (1400 GEL) on the territory of Armaztsikhe.

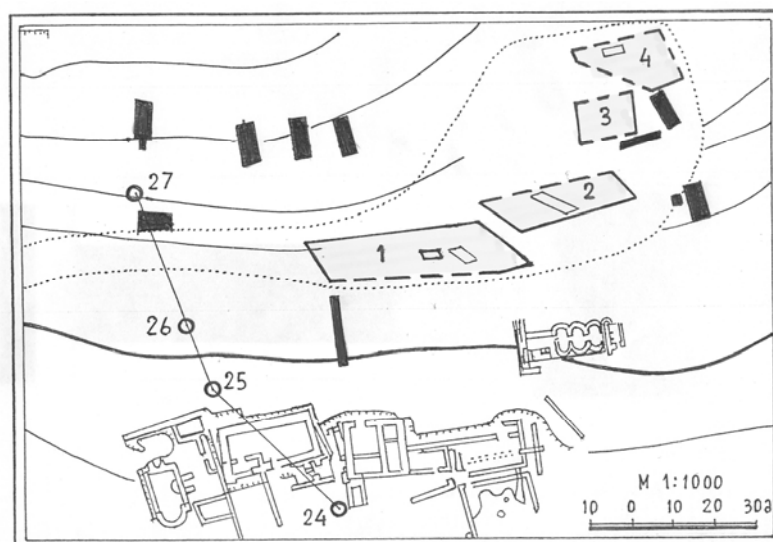


Figure 9. The results of the electrical prospecting carried out on Armaztsikhe-Bagineti complex. The black rectangles indicate excavation areas without the use of geophysical methods. In fact nearly all the works ended with no results. In the areas 1, 2, 3, 4 electrical prospecting by direct current method was conducted. The anomalies in these areas are marked with rectangles. Excavations made obvious that there were covered archaeological object such as walls, foundations and cultural layers in all the anomalous areas.

References

- [1] Apakidze, A., Tabagua, G., Chanturishvili, L., Chelidze, T., Kipiani, G., Jakhutashvili, M (2001). Some Results of Archaeogeophysical Studies on the Territory of Ancient Urban Area Armaztsikhe-Bagineti. *Bulletin of the Georgian Academy of Sciences*. V. 163, 470-472.
- [2] Chanturishvili, L., Chelidze, Tabagua, G., Jakhutashvili, M., Tarkhnishvili, A., Zardiashvili, T., Odilavadze D. (2001). New results of archaeogeophysical investigations of Armaztsikhe-Bagineti ancient urban area. *Journal of the Georgian geophysical Society*. Issue A. Physics of Solid Earth. V.6, 112-117.
- [3] Clark, A. J. (1996). *Seeing beneath the Soil. Prospecting Methods in Archaeology*. London, United Kingdom: B.T. Batsford Ltd.
- [4] Gater J. and Gaffney C.F. (2003). *Revealing the Buried Past: Geophysics for Archaeologists*. Taylor&Francis.
- [5] Neal, A. (2004) Groundpenetrating radar and its use in sedimentology: principles, problems and progress. *Earth-Science Reviews*, 66, 261-330.
- [6] Odilavadze D.T., Chelidze, T.L. (2010). A Preliminary GPR investigation of Metekhi Cathedral and the surrounding area. *Journal of the Georgian geophysical Society*. 14 A.32-38.
- [7] Schmidt, A. (2010). *Geophysical Data in Archaeology: A Guide to Good Practice (AHDS Guides to Good Practice)*.
- [8] Tsitsishvili D., Tabagua, G., Khvitia, G. (1968). Electrical prospecting in archaeological research: Bichvinta case history. *Bulletins of Academy of Sciences of Georgian SSR*, v.4., N 3 (in Russian).
- [9] Tsitsishvili D., Tabagua, G. (1975). Results of investigation of Pitsunda ruins by geophysical methods. *Proceedings of Institute of Geophysics*, v.34, (in Russian).

[10] Witten, A. (2006). Handbook of Geophysics and Archaeology. London, United Kingdom: Equinox Publishing Ltd.

[11] Chanturishvili, L., Jakhutashvili, M., Kutelia, G. (1993). Search for archaeological monuments by geophysical methods in deserts. Edition of Tbilisi State University, scientific conference III.

(Received in final form 20 December 2012)

Археогеофизика – новые перспективы

Т.Челидзе, Д. Одилавадзе, К. Пицхелаური, Дж. Кириа, Р. Гოგუა

Резюме

Основу археогеофизики составляет контраст физических свойств (электропроводности, диэлектрической или магнитной проницаемости) погребенного археологического объекта и вмещающей геологической среды, в результате чего физическое поле, измеренное на поверхности, проявляет аномалию. Современные точные приборы и специальные программы обработки позволяют быстро и достаточно точно установить местоположение, размеры и глубину залегания погребенного археологического объекта. Приводится краткий обзор современного состояния археогеофизики в мире и в Грузии. Изложены базовые положения основных археогеофизических методов: георадиолокационного (георадара), магнитного и электроразведочного. Проанализированы результаты археогеофизических исследований в районе Шираки (георадар) и Армазцихе-Багинети (электроразведка).

არქეოგეოფიზიკა – ახალი პერსპექტივები

თ. ჭელიძე, დ. ოდილავაძე, კ. ფიცხელაური ჯ. ქირია, რ. გოგუა

რეზიუმე

არქეოგეოფიზიკის ფუნდამენტურ საფუძველს წარმოადგენს ფიზიკური თვისებების კონტრასტი არქეოლოგიური ძეგლის შემადგენელი მასალისა და მის ირგვლივ არსებული გარემოს შორის. თუ რაღაც განსხვავებული ფიზიკური თვისებების (ელექტროწინალობის, დამაგნიტების) მქონე სტრუქტურა დაფარულია ნიადაგის ფენით, ის იწვევს დღის ზედაპირზე გაზომილი ველის შეცვლას, ე.წ. გეოფიზიკურ ანომალიას. თანამედროვე ზუსტი ხელსაწყოები და მონაცემთა დამუშავების სპეციალური პროგრამები შესაძლებლობას იძლევა საკმაოდ ზუსტად დადგინდეს დაფარული ძეგლის ადგილმდებარეობა, მისი ჩაწოლის სიღრმე, ზომები და სხვა დეტალები. მოყვანილია არქეოგეოფიზიკის თანამედროვე მდგომარეობის მიმ ოხილვა მსოფლიოსა და საქართველოში. მოყვანილია ძიების ძირითადი მეთოდების: გეორადარის, მაგნიტური და ელექტრული საბაზისო აღწერა. გაანალიზებულია არქეოგეოფიზიკური კვლევის შედეგები შირაქისა და არმაზციხე-ბაგინეთის რაიონებში.

Acoustic early warning telemetric system of catastrophic debris flows in mountainous areas

T. Chelidze ^{1,2}, N. Varamashvili ¹, Z. Chelidze ¹

1. M. Nodia Institute of Geophysics at the I. Javakhishvili Tbilisi State University
2. European Centre "Geodynamical Hazards of High Dams" of Council of Europe

Abstract

The paper is devoted to creation of Acoustic Early Warning Telemetric System of catastrophic debris flows in mountainous areas, namely, for Durudji valley (East Georgia). The field test of the system shows that it is capable to register acoustic pulses in the range 10-1000 Hz and transmit the signal on the distance of 10-15 km.

Introduction

Each year debris-flows (mud-flows, earth-flows) cause a lot of disasters in mountainous areas all over the world (see special issue of Journal of Physics and Chemistry of Earth, vol.25, No.9, pp. 705-797, 2000). Periodically thousands of populated areas, roads, oil and natural gas pipeline routes, high voltage electric lines and agricultural lands are under the heavy influence, sometimes with catastrophic impact of hazardous geological processes. Catastrophic mass-movements not only periodically strongly damage the environment but they also are followed by human losses. Thus it is of great importance to create reliable and cost-effective early warning systems for monitoring mass-movements in potentially dangerous areas.

The territory of Caucasus due to the development of large-scale hazardous geological processes, their frequent reoccurrence, growth of population and land use as well as of large engineering constructions belongs to the hardest hit mountainous regions in the world. The annual economical losses due to geomorphological hazards in Georgia are of order of 100 million USD.

Basin of r. Duruji in Eastern Georgia (Fig. 1) is the classical example, illustrating the intensity and power of debris flows and their catastrophic consequences, directly threatening the town of Kvareli located on the eastern part of the accumulation zone of the mass flow as well as the objects of agricultural designation. In the last 115 years there were 31 cases of large debris-flows; the associated human losses reach 200 mln USD. The preventive activity in the last years, due to difficulties in economy, was practically abandoned. Thus creation of effective early warning/ monitoring system (EWS/MS) for the region is of vital importance.

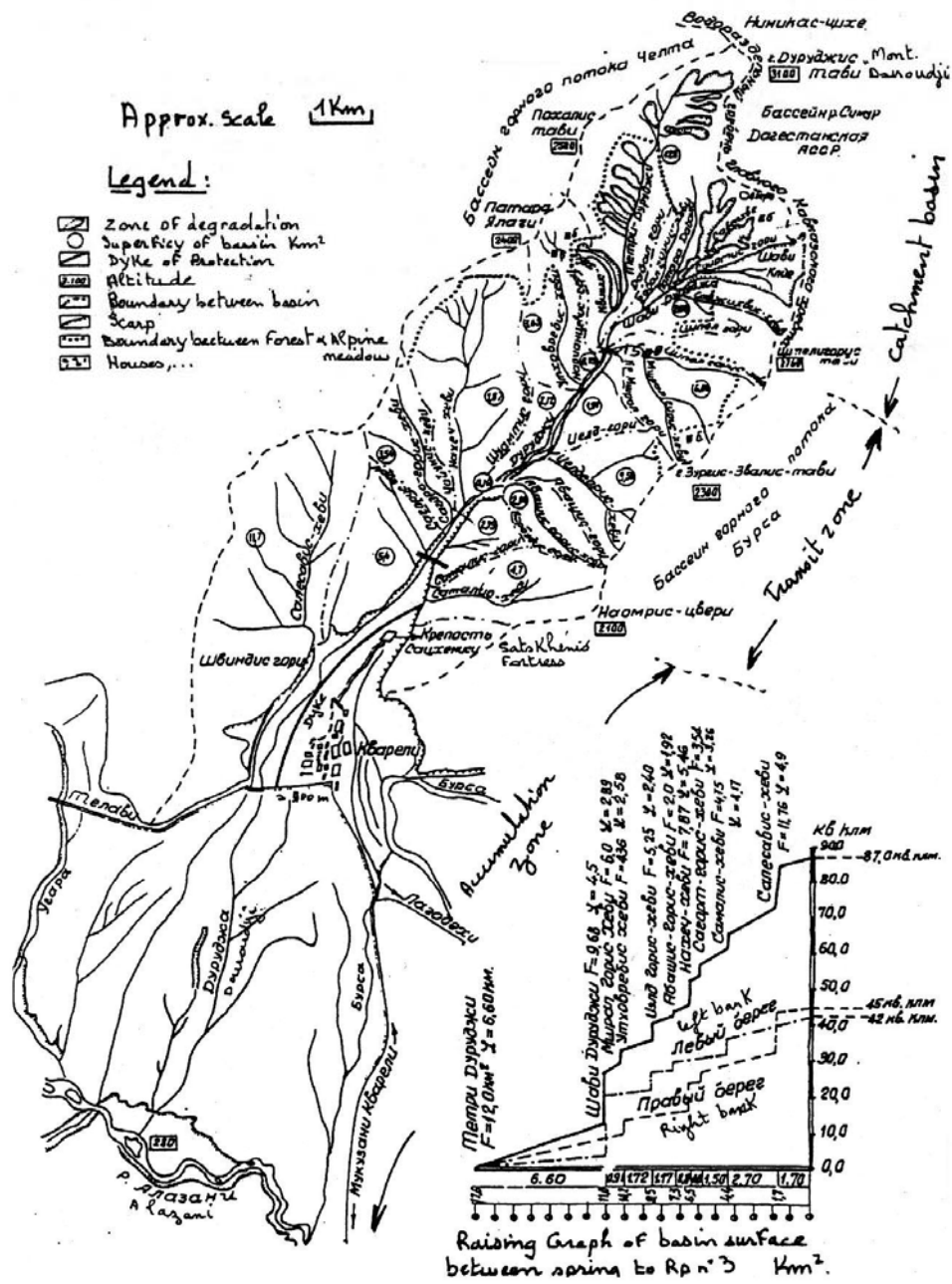


Fig1. Douroudji debris basin (Eastern Georgia).

Equipment

There are a lot of methods in monitoring mass-movements: geodesy, extensometry, Global Positioning Systems, laser and radar interferometry, etc (Malet, Maquaire and Calais, 2001, Savvaidis, 2003; Tonnellier and Malet, 2010). The accuracy of most precise techniques approaches 0.1 mm. The cost of such systems is high enough. Besides direct measurements of displacements, it is possible to register the accompanying effects, for example, acoustic emission, generated by the mass-movement; these methods are less expensive. Recently

several such systems for registration of dynamical geomorphological processes have been developed, namely, seismometers, piezoelectric or magnetoelectric sensors and acoustic microphone sensors. The best signal (S) to noise (D) ratio (S/D) was obtained for acoustic sensors.

It is established that the debris-flows generate soil vibration in the low-frequency range (0-100 Hz); according to (Itakura et al., 2000) the maximum in the power spectrum is obtained in the vicinity of 40 Hz.

Taking into account the results of field observations of acoustic emission (AE) during catastrophic debris-flows (Itakura et al., 2000; Lavigne et al., 2000; Betri et al., 2000; The sound of the underground, 2010) Institute of Geophysics and European Centre of Geodynamical Hazards of High Dams carried out analysis of existing systems and the debris-generated AE monitoring equipment, consisting of acoustic sensors, special filters and low-noise amplifiers (LNA) and a notebook, has been assembled. The principal scheme of electronic block is shown in Fig 2.

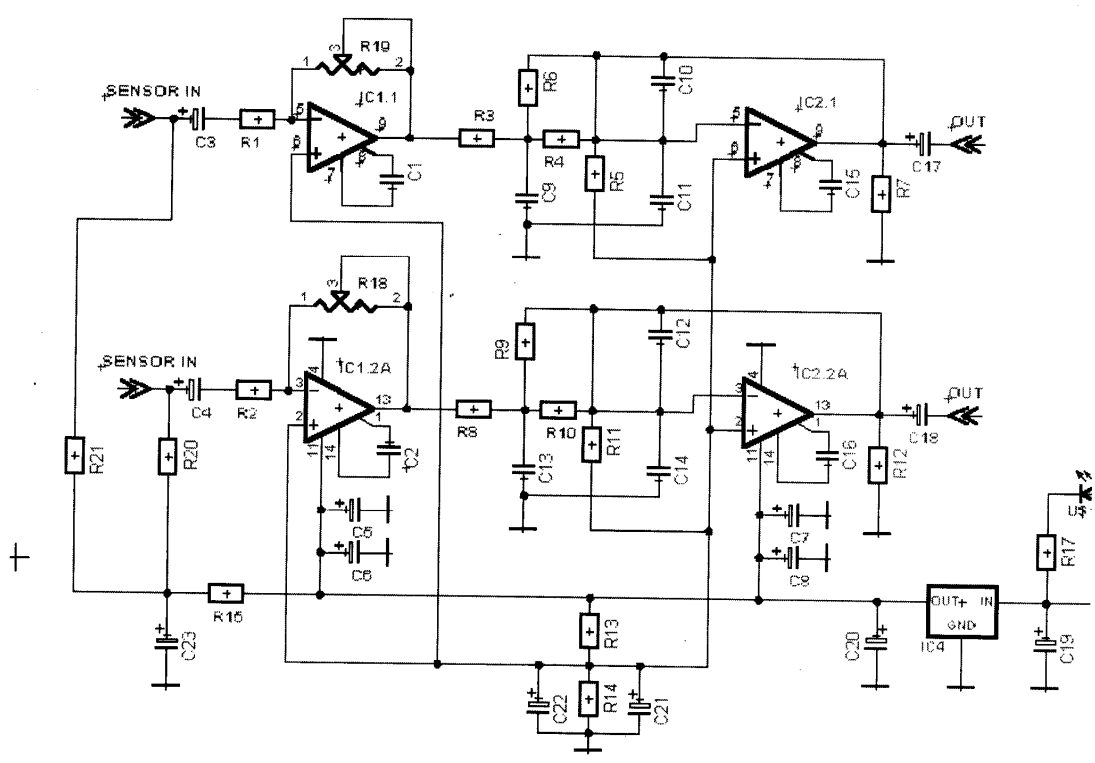


Fig.2. The principal electronic scheme of electronic block for recording acoustic emission during catastrophic debris-flows with special filters and low-noise amplifiers.

The main requirements to the system were: minimal energy consumption, autonomous functioning, maximal linearity of amplitude-frequency characteristics (AFC) of sensors and amplifiers in the used frequency range, maximal signal to noise ratio. To fulfill these requirements the capacity microphones were used as sensors, due to the linearity of their AFC in the range 10-1000 Hz. Microphone heads were installed directly on the card of the primary low-noise amplifier in the waterproof casing of the sensor (metal casing of a length 60-70 cm and external diameter 3.5-4 cm). The power (stabilized voltage 9 V) is supplied to LNA through waterproof connector by the signal coaxial cable. The current consumption by two sensors does not exceed 10 mA). Location of LNA in the close vicinity to sensors allows using long signal cables without risk of spoiling signal to noise ratio; in turn this makes it possible to place sensors relatively far from each other (at the distance 150-200 m). Two-sensor system of registration is much more reliable for recognition of mass-movement initiation.

Filters are necessary for debris-induced signal bandwidth assignment and reduction of possible noise from the long signal cable. After processing of the signal by input LNA and filters the signal is amplified by scale amplifier in order to match the system output to the recorder characteristics.

The whole system (Fig.3) is powered by 12 V battery and consumes no more than 40-45 mA.



Fig. 3. The field acoustic system for debris-flow EWS, including the electronic unit with amplifiers and filters, two sensors and notebook

Field test of sensors

During field tests the microphone sensors were installed inclined in pits at the depth of 0.7 m; they were separated by the distance of 5 m. Acoustic signal was initiated by dropping of the weight (mass 7 kg) from the 1.2 m high approximately in the middle point between sensors. During the experiment microphone sensors were installed in two pits at the depth of 0.7 m. The distance between sensors was 1 or 5 m. The acoustic signal was generated by dropping the weight (with a mass 7 kg) from the 1.2 high at various separations from the sensors along the normal to the line, connecting sensors. The normal was located approximately at the middle point between sensors. Fig. 4 presents recordings of the sensors and the moments of acoustic signal initiation. The records correspond to following separations of the source and sensors

- 1) record take 001 – 2,5 m
- 2) record take 002 – 0,5 m
- 3) record take 003 – 4 m
- 4) record take 004 – 9 m

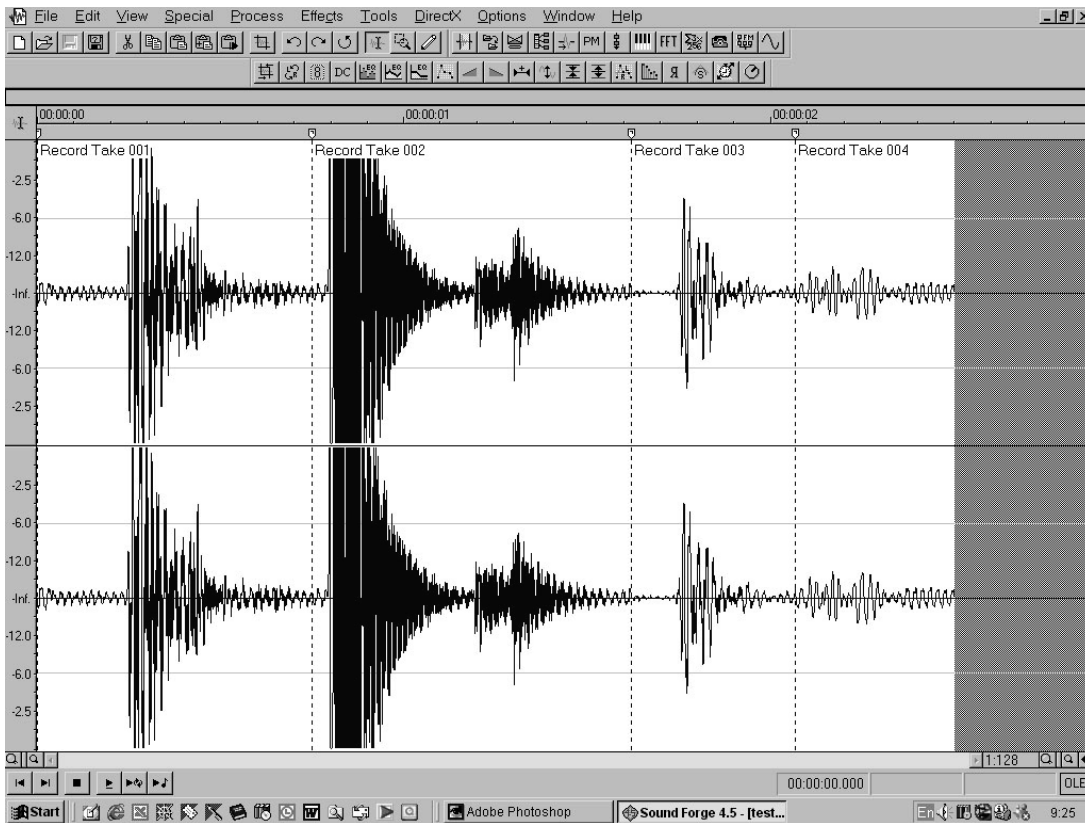


Fig. 4. The recordings of acoustic signals during field tests of EWS

Registration and processing of the acoustic signal was realized on the sound card of notebook using the program Sound Forge. Acoustic signal's amplitude substantially decreases with a distance: according to Itakura et al (2000) the decrease follows exponential law.

It seems that the sensitivity of the system suffice to register the initial stage of catastrophic debris flow.

The analysis of frequency content of the recorded signals shows that the maximal emission in the field tests corresponds to 70 Hz.

Developing EWS Communication System

During development of EWS system for Dourouji valley we used the experience obtained by the Ministry of Internal affairs, which for several seasons organized temporary observations at the source of debris flow. The special team was placed at the source and the communication with rescuer centre at the city of Kvareli was realized by radiotelephone. These observations prove that the frequency...157-170 MHz was good for communication between observation site and rescuer centre for special case of Dourouji valley orography. This frequency was approved as satisfactory for developing EWS system in the area.

The EWS Communication System should answer to following requests, taking into account the inaccessibility of observation site for regular visits:

- i. possibility of operative change of device parameters and warning tasks
- ii. necessity of permanent observation of natural process
- iii. autonomy of data transfer system and minimization of power consumption
- iv. high requirements to protection of sensors and transfer system from bad weather conditions

Accordingly, the flow block of the system looks like following:

- i. active shift sensors with phantom power supply (AD)
- ii. signal adder (Σ), phantom power supply scheme (E_+), codec modulator (C/M)

- iii. synthesiser-modulator of radio channel (SYN), HF power amplifier (PA HF) and filter (F HF) and antenna-feeder device (ANT)
- iv. system of self-contained power supply

Active mass-movement sensors with phantom power supply (AD)

For high reliability of system two active shift sensors are used. They are manufactured as water-proof devices – see Fig.3.

Signal adder (Σ), phantom power supply scheme (E₊), codec modulator (C/M)

Signal adder (Σ) adds signals from two active sensors which are placed at different locations. The phantom power supply scheme (E₊), provides the supply of power to sensors by the same coaxial cables, which connects signal adder with two sensors. The frequency range of wanted signal is 1-300 Hz. Translation of such LF signal by radiofrequency needs large energy consumption. Besides, it is hard to put this information into radio devices. It seems optimal to shift the spectra of data into standard modulation range of radio(-)telephony, namely, 350-3.5 Hz. Obtained narrow-range radio signal satisfies all conditions and norms of radio transfer of data and is also low consuming solution (narrower the range, less energy is consumed at the same transfer distance). The range shift is provided by codec-modulator; the demodulated signal can be recorded directly on the standard PC sound card.

Synthesiser-modulator of radio channel (SYN), HF power amplifier (PA HF) and filter (F HF) and antenna-feeder device (ANT)

Digital synthesiser of frequency provides forming of frequency of radiochannel for data transmission and frequency modulation by codec signal.

From the output of synthesiser-modulator the signal is sent to economic power amplifier of class “C” to minimize the power consumption. The amplified signal passes HF filter at the output of power amplifier and enters the antenna-feeder device (ANT).

Fider is of minimal length in order to decrease HF power losses. Antenna is chosen of limited amplification as the large number of directed elements increase the area of antenna, which may worsen the resistance of the system to the strong wind.

System of self-contained power supply

Data transfer system gets power from the battery 12V/50 AH. For charging of battery in the day time will be used solar panels of calculated power no less than 80 W. The large power of solar batteries is needed for normal functioning of the whole system in the night time.

For optimization of the battery charging the solar panels are connected to the syysem by DC/DC converter, which controls the charging current and voltage. This allows optimization of solar panels power consumption.

In the power system the battery protection scheme is foreseen; it switches off the appliance load when the battery voltage drops lower than 9.5 V. The scheme restores the power supply automatically when the voltage rises up to 12.6 V

Field test of transmission system

The test of transmission system has been carried out. The acoustic signal due to artificial source (weak shock, slipping) was successfully transmitted from settlement Napetvrebi to Tbilisi over the distance of 15 km. This equals the distance from the Duridji debris flow sources to settlement Kvareli (Fig.1), which means that the system is capable to issue the alarm in case of debris flow initiation. This gives around 10-15 min of time for action before the debris mass reaches Kvareli.

Acknowledgements

Authors acknowledge the support of Open Partial Agreement on the Major Disasters at the Council of Europe (EUR-OPA).

References

[1] M.Itakura, N.Fujii, T. Savada. Basic characteristics of ground vibration sensors for the detection of debris flow. Phys.Chem.Earth (B),25, 717-720, 2000

- [2] F.Lavigne et al. Instrumental lahbor monitoring at Merapi Volcano. Jour. at Volcanology and Geotherm. Res., 100, 457-478, 2000
- [3] M.Betri et al. Debris flow monitoring in the Acquabona Watershed on the Dolomites. Phys. Chem. Earth (B), 25, 707-715, 2000
- [4] Malet J.-P., Maquaire, O. and Calais E. The use of GPS techniques for the continuous monitoring of landslides. Geomorphology, 2001
- [5] L.Marchi, M.Arattano, A.Deganutti. Ten years of debris-flow monitoring in the Moscardo Torrent. Geomorphology, 46, 1-17, 2002.
- [6] Tonnellier A. and Malet J.-P.; 2010a: Acoustic and micro-seismic monitoring of landslides. State of the art. Michoud C., Abellán A., Derron M.-H., Jaboyedoff M. (Eds): Review of Techniques for Landslide Detection, Fast Characterisation, Rapid Mapping and Long-Term Monitoring. SafeLand European project, 4.1, 195-212.
- [7] The sound of the underground! New acoustic early warning system for landslide prediction. <http://www.epsrc.ac.uk/newsevents/news/2010/Pages/landslideprediction.aspx>, 2010
- [8] Savvaidis, P. D. Existing Landslide Monitoring Systems and Techniques. From Stars to Earth and Culture. In honor of the memory of Professor Alexandros Tsioumis pp. 242-258, 2003.
- Acoustic Early Warning Telemetric System of Catastrophic Debris Flows in Mountainous Areas.**

(Received in final form 20 December 2012)

Акустическая телеметрическая система раннего оповещения для катастрофических селей в горных районах

Тамаз Челидзе, Нодар Варамашвили, Зураб Челидзе

Резюме

Работа посвящена созданию акустической телеметрической системы раннего оповещения для катастрофических селей в горных районах, а именно для долины реки Дуруджи (Восточная Грузия). Полевые испытания системы показали, что она способна регистрировать акустические импульсы в диапазоне 10-1000 Гц и передавать сигнал на расстояние 10-15 км.

მთიან რეგიონებში კატასტროფული ღვარცოფების აკუსტიკური ტელემეტრული წინასწარი შეტყობინების სისტემა

თამაზ ჭელიძე, ნოდარ ვარამაშვილი, ზურაბ ჭელიძე

რეზიუმე

სამუშაო ეძღვნება მთიან რეგიონებში სახელდობრ მდინარე დურუჯის ხეობაში (აღმოსავლეთი საქართველო) აღძრული კატასტროფული ღვარცოფების აკუსტიკური წინასწარი შეტყობინების ტელემეტრული სისტემის შექმნას. სისტემის სავსე გამოცდა გვიჩვენებს, რომ მას შეუძლია 10-1000 ჰც დიაპაზონში აკუსტიკური სიგნალის რეგისტრირება და გადაცემა 10-15 კმ მანძილზე.

SEISMOTOOL – easy way to see, listen, analyze seismograms

T. Chelidze¹, N. Zhukova¹, T. Matcharashvili¹

M. Nodia Institute of Geophysics at the I. Javakhishvili Tbilisi State University, I Alexidze str, Tbilisi, 0171, Georgia

Corresponding author: Prof. Tamaz Chelidze, Chairman of the Scientific Council

M. Nodia Institute of Geophysics at the I. Javakhishvili Tbilisi State University, I Alexidze str, Tbilisi, 0171, Georgia

Ph: (995 32) 233 28 67; Fax: (995 32) 233 28 67

E-mail: tamaz.chelidze@gmail.com;

Mobile : + 995 577 79 07 45

Online material: Executive programs: SEISMOTOOLS.exe, seisfilt.exe, seisspectro.exe; sample data sets are presented in the folder examples.

In the 2012 March/April issue of SRL in the paper of D. Kilb et al (2012) the SeisSound package for listening, watching and learning seismic records using methods which allow “communicate effectively with diverse audiences who have a variety of learning styles and level” was presented.

SEISMOTOOL package presented in this paper is a convenient instrument to watch, listen and even analyze seismic records in easy way. Frequency content of seismic records (20 Hz-20 kHz) is too low to be taken by humans. The simplest way to listen seismic records is to compress time (accelerate audio playing by changing sampling rate), which was realized in the (Kilb et al, 2012, Peng et al, 2012).

Advantage of the program presented in our paper in comparison with the application running under MATLAB environment, such as in the SeisSound package (Kilb et al, 2012) is a possibility to process long data files, glue recordings, extract recording segments, change compression rate and filter records. In MATLAB environment used in SeisSound the data are loaded in the block of memory used by MATLAB, which has limited capacity. As a rule, digital seismic data files are long, for example, if the sampling rate of record is 100 Hz, 1 day seismogram includes 8 640000 samples and takes 67500 kilobytes in memory if the type of data is double or integer. SEISMOTOOL loads data into a computer memory directly, therefore it can process longer data sets.

SEISMOTOOL can “glue together “seismograms, for example, merge hourly seismograms into daily ones, etc. It converts seismograms to acoustic signals (16 bit wav files), which allow “listen to earthquakes”. As there are many programs for processing an acoustic signal, using this opportunity we can easy watch, listen and process long seismograms converted to acoustic signals. For example, it is possible to use different time scales (compression rates), which is impossible to do in the SeisSound.

There here are 2 options to process data: SEISMOTOOL package creates mono or stereo wav file. For example, we can create stereo wav file, where 1st and 2nd channels are original and filtered seismograms. Second example: stereo wav file can be composed from seismograms recorded at 2 different stations. 4th order Butterworth bandpass filter is implemented into SEISMOTOOL application. The filter was extracted from MATLAB signal toolbox and compiled as the standalone

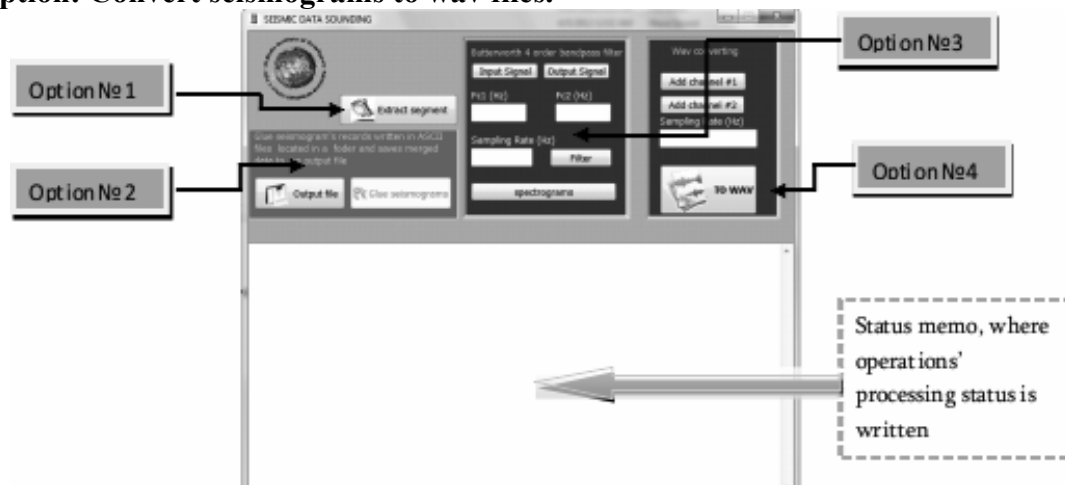
application. For the filtering and spectrogram running it is only necessary to install MATLAB Run Time Compiler if MATLAB is not installed on computer system. (This library can be downloaded free from <http://www.mathworks.com/products/compiler/>). Users have option to select the frequency range, which filter passes. Sony Sound Forge software was selected as an instrument to both process seismograms and listen to earthquakes vibrations. Sound Forge allows editing wav data, change time scale on time axis to see details of seismograms, analyzing segments of recording, etc. This tool is very useful for fast identification of triggered tremors generated by passing wave trains from remote strong earthquakes, which is now a hot topic in seismology (Hill, Prejean, 2009; Prejean, Hill, 2009).

The package includes examples' data (**input.dat** and folder **seism** with hourly seismogram files) which were used to demonstrate program capacity. MATLAB Run Time Compiler (**MCRInstaller**) also is provided in the package. Attention: seisfilt.exe and seis spectro.exe programs must be located in the same folder with SEISMO.exe

PROGRAM RUN

SEISMO application has 4 independent options (See picture bellow):

1. **Option: Extract segments from seismograms;**
2. **Option: Glue together seismograms;**
3. **Option: Filter seismograms by band-pass filter and plot spectrogram of original and filtered seismic series, spectrogram's plotting;**
4. **Option: Convert seismograms to wav files.**



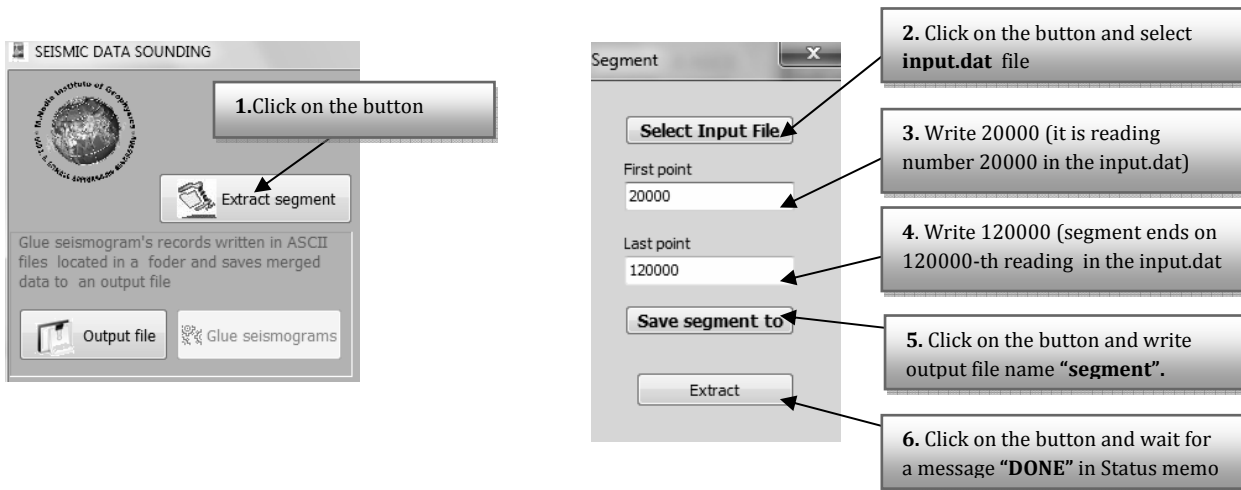
All options are independent. Each operation can be executed separately. If it's needed just to filter seismograms only the filter panel (Option №3) is to be called.

Option 1: Extract segment

This operation is used when we want to extract some segment from the whole seismograms.

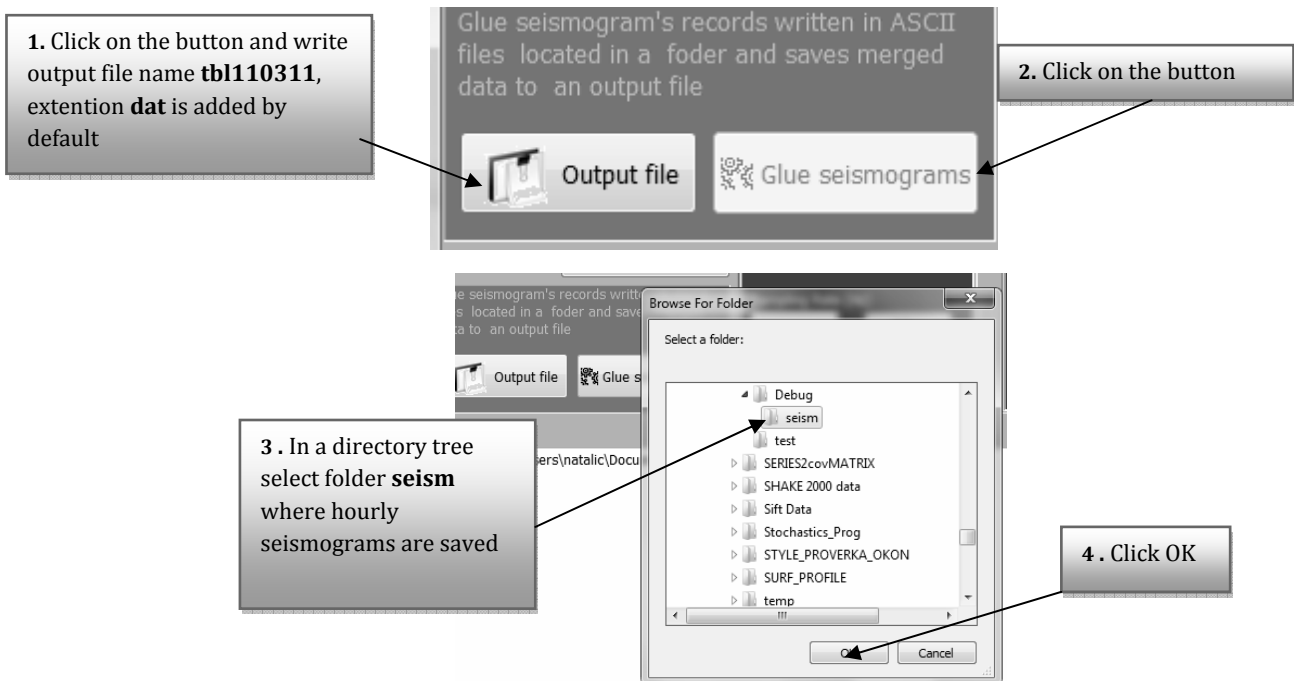
1. Click on button **Extract segment**;
2. In the appeared dialog window select an input file with seismogram;
3. Indicate in field **First point** the first position in a seismogram from which extract segment begins;
4. Indicate in the field **Last point** last extracting -position in an input seismogram;
5. Click on button **Save segment to** and write the output file name for a selected segment;
6. Click on button **Extract** and wait for a message **"DONE"** in the Status memo.

Example: from the file "input.dat" we need to extract segment (20000:120000) and save it to a file "segment.dat".



Option 2: Glue seismograms (If seismograms are split into several files there is an option to merge seismic records and process long seismograms).

1. Click on **Output File** button and indicate output file name. (Directory of output file and directory of input seismogram files must be different);
2. Click on the button **Glue seismograms** and indicate folder with the seismogram record files.
3. **Example.** We have directory “seism” with hourly recorded seismograms, we want to glue these seismograms and obtain one day seismogram saved to the output file “tbl110311.dat”. **Notation:** the output file **tbl110311.dat** will be written to different from “seism” directory
In **Status Memo** we will see a work execution process:



```

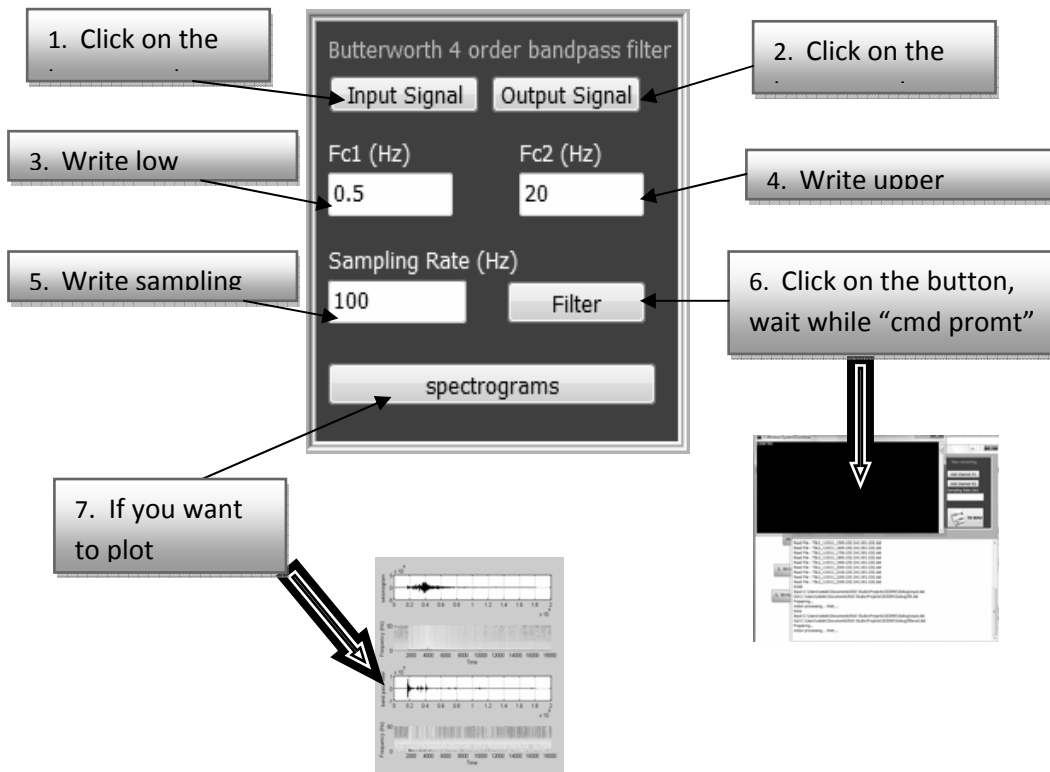
Output file C:\Users\natalic\Documents\RAD Studio\Projects\SEISMO\Debug\tbl110311.dat
Directory for reading: C:\Users\natalic\Documents\RAD Studio\Projects\SEISMO\Debug\seism
Sorting list of files....
File number for listing = 23
Read File : TBLG_110311_0100.GSE.SAC.002.GSE.dat
Read File : TBLG_110311_0200.GSE.SAC.001.GSE.dat
Read File : TBLG_110311_0300.GSE.SAC.001.GSE.dat
Read File : TBLG_110311_0402.GSE.SAC.001.GSE.dat
.....
Read File : TBLG_110311_2000.GSE.SAC.001.GSE.dat
Read File : TBLG_110311_2100.GSE.SAC.001.GSE.dat
Read File : TBLG_110311_2200.GSE.SAC.001.GSE.dat
Read File : TBLG_110311_2300.GSE.SAC.001.GSE.dat
DONE (←means that operation is finished)

```

Option 3: Band pass filter

1. Click on **Input Signal** and select a file with seismogram;
2. Click on **Output Signal** and indicate a file name for filtered seismogram;
3. In the fields **Fc1** and **Fc2** indicate bandpass frequency range (in Hz). Notation: **Fc1** and **Fc2** should be less than half of record sampling rate;
4. In the field **Sampling Rate** indicate sampling rate (in Hz) of a seismic signal;
5. Click on **Filter** button and wait for the end of the operation. If everything is OK, command window will appear and after its closing a file with filtered seismogram will be created;
6. Optionally. Plot spectrogram of original and filtered seismograms.

***Example:** We want to filter seismogram in the frequency range: (0.5-20Hz). The seismogram is recorded at the sampling rate 100 Hz and saved in the file "input.dat". Filtered seismogram will be saved to the file "filt.dat"*

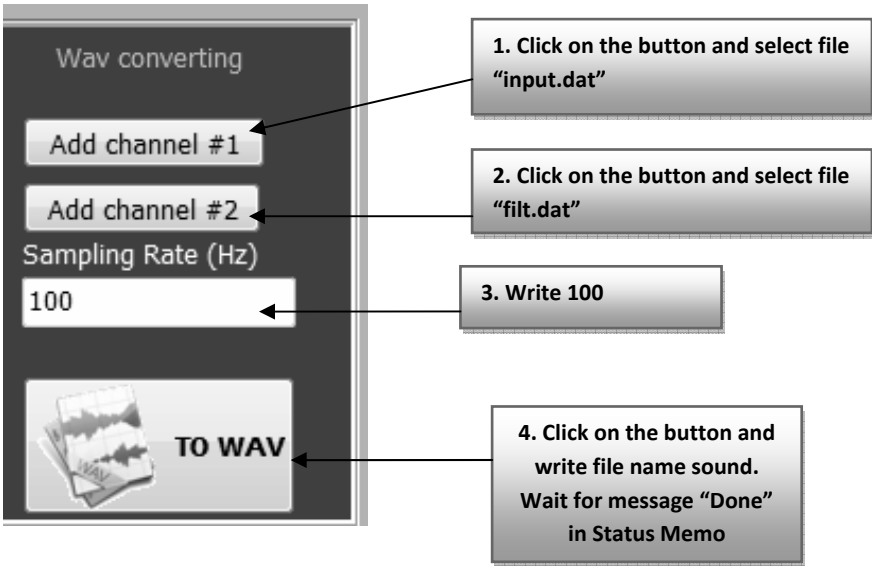


Option 4: Convert seismogram to a Wav file

1. Click on **Add channel #1** and select input file with a seismogram;
2. Click on **Add channel #2** and select input file with a filtered seismogram;
3. In the field **Sampling Rate** indicate sampling rate (in Hz) of a seismic signal;
4. Click on **To WAV** button and indicate output wav file name. Wait when operations will be finished.

If the channel #2 is not selected only mono file will be created.

Example: we want to convert original and filtered seismograms saved in file "input.dat" and "filt.dat" to stereo wav file with the name "sound.wav". 1st channel will represent original seismogram, 2nd channel – filtered one. Seismogram is recorded with sampling rate 100 Hz.



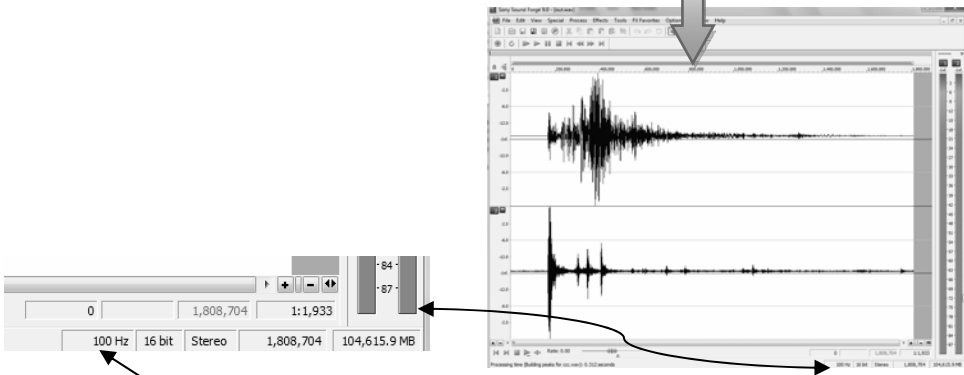
1. Click on the button and select file "input.dat"

2. Click on the button and select file "filt.dat"

3. Write 100

4. Click on the button and write file name sound. Wait for message "Done" in Status Memo

Watch and listen seismogram in Sound



100 Hz 16 bit Stereo 1,808,704 104,615.9 MB

Increase Sampling Rate 100, 200, 300, 400 or more times to hear seismic signal

We presume that presented package will render to wide public an easy way to understand earthquake recordings and will be an useful addition to package of Kilb et al. (2012).

Acknowledgments: Authors acknowledge financial support of European Centre “Geodynamical Hazards of High Dams” operating in the frame of Open Partial Agreement on Major Disasters at the Council of Europe.

(Received in final form 13 December 2012)

References:

- [1] Chelidze, T.,T. Matcharashvili, O. Lursmanashvili, N. Varamashvili and N. Zhukova, E. Meparidze. 2010. Triggering and Synchronization of Stick-Slip: Experiments on Spring-Slider System. In: *Geoplanet: Earth and Planetary Sciences, Volume 1*, 2010, DOI: 10.1007/978-3-642-12300-9; *Synchronization and Triggering: from Fracture to Earthquake Processes*. Eds.V.de Rubeis, Z. Czechowski and R. Teisseyre, pp.123-164
- [2] Kilb, D., Z. Peng, D. Simpson, A.Michael, M. Fisher, and D. Rohrlick. Listen, Watch, Learn: SeisSound Video Products. *Seismological Research Letters*, 83 (2), 2012, 281-286.
- [3] Peng, Z., C. Aiken, D. Kilb, D. R. Shelly, and B. Enescu (2012). Listening to the 2011 magnitude 9.0 Tohoku-Oki, Japan, earthquake. *Seismological Research Letters* 83(2), 287–293.
- [4] Hill, D. 2010. Surface wave potential for triggering tectonic (nonvolcanic) tremor. *Bull. Seismol. Soc. Am.* 100, 1859-1878, doi: 10.1785/0120090362.
- [5] Hill, D., Prejean, S. 2009. Dynamic triggering. In: *Earthquake Seismology*. Volume editor H. Kanamori. *Elsevier*. pp. 257-293.
- [6] Prejean S., Hill, D. 2009. Dynamic triggering of earthquakes. In: *Encyclopedia of Complexity and Systems Science*, R. A. Meyers (Ed.), Springer, pp. 2600-2621.

(Received in final form 20 December 2012)

СЕЙСМО-ТУЛ – метод для визуализации, прослушивания и анализа сейсмограмм.

Тамаз Челидзе, Наталия Жукова, Теймураз Мачарашвили

Резюме

Предлагается компьютерная программа для визуализации, прослушивания и анализа сейсмограмм, позволяющая с использованием пакета Sony Sound Forge и элементов МАТЛАБ-а (а именно МАТЛАБ Run Time Compiler) обрабатывать большие объемы данных, соединять или наоборот, вырезать различные участки записи, изменять ее временной масштаб и проводить фильтрацию. Программа может использоваться для популяризации и образования, например, она дает возможность «прослушивать» землетрясения путем перевода сейсмической записи в акустический диапазон.

სეისმო-ტული - ადვილი გზა სეისმოგრამების ვიზუალიზაციისათვის, მათი მოსმენისა და ანალიზისათვის

თ. ჭელიძე, ნ. ჟუკოვა, თ. მაჭარაშვილი

რეზიუმე

შედგენილია კომპიუტერული პროგრამა სეისმოგრამების ვიზუალიზაციისათვის, მათი მოსმენისა და ანალიზისათვის, რომელიც პაკეტის Sony Sound Forge და მატლაბ-ის ელემენტების (კერძოდ, MATLAB Run Time Compiler) გამოყენებით საშუალებას იძლევა დავამუშავოთ დიდი მოცულობის მქონე მონაცემთა მწკვრივები, შევაერთოთ ან პირიქით, ამოვჭრათ ჩანაწერის სხვადასხვა მონაკვეთები, შევცვალოთ ჩანაწერის დროითი მასშტაბი ან გავფილტროთ იგი. პროგრამა გამოიყენება როგორც პოპულარიზაციის, ისე საგანმანათლებლო მიზნებით, მაგალითად მისი საშუალებით შესაძლოა მიწისძვრის „მოსმენა“ თუ გადავიყვანოთ სეისმურ ჩანაწერს აკუსტიკურ დიაპაზონში.

Real time telemetric monitoring system of large dams and new methods for analysis of dam dynamics.

T. Chelidze^{1,2}, T. Matcharashvili^{1,2}, V. Abashidze^{1,2},
M. Kalabegishvili³, N. Zhukova¹, E. Meparidze¹

1. *M. Nodia Institute of Geophysics of i. Javakhishvili Tbilisi State University, 1, Alexidze str. 0171, Tbilisi, Georgia;*
2. *European Centre "Geodynamical Hazards of High Dams" of Council of Europe, str., 1, Alexidze str. 0171, Tbilisi, Georgia.*
3. *Georgian Technical University, 0171, Tbilisi, Georgia*

Abstract

Large dams are complex systems with nonlinear dynamic behavior. Engineers often are forced to assess dam safety based on just available imperfect data, which is extremely difficult. Solution of this principal problem comes from the modern theory of complex systems. It is the well known that it is, possible to derive characteristics of the whole unknown dynamics using few data sets of certain carefully selected parameter(s). By means of such continuously recorded high quality sets of dam geotechnical characteristic(s), modern methods of time series nonlinear analysis allows accomplishment of valuable reconstruction of the main dynamical features of the entire, unknown process (here - dam deformation).

We created the Early Warning Telemetric System for Dam Diagnostics (DAMWATCH), which consists of sensors (tiltmeters), terminal and central controllers connected by the GSM/GPRS Modem to the diagnostic center. The dam tilt data for varying reservoir load will be compared to (static) design model of dam deformation computed by finite element method (FEM). Besides, recently developed nonlinear data analysis and prediction schemes may help to quantify fine dynamical features of dam behavior. The corresponding software package DAMTOOL is developed.

The differences between characteristics of real (measured) and theoretically predicted data may signal either abnormal behavior of the object or some deficiencies in theoretical model. The data obtained already during exploitation of the system show interesting long-term and short-term patterns of tilts in the dam body, which can be used for dam diagnostics. Proposed complex of real-time telemetric monitoring (DAMWATCH) and nonlinear dynamical analysis system (DAMTOOL) has no analogues worldwide.

1. Intrudaction

Dams bring enormous benefits to mankind but they are also sources of high hazard. In large storage dams many different types of hazards are possible; here we focus on the technical hazard connected with the state of dam and its components.

We assume that generally the technical hazards, such as extreme strains in the body of dam, due to aging, damage or overloading can be monitored and in some cases even predicted by networks of special devices: strainmeters, tiltmeters, piezometers, plumblines etc.

Usually, the safety level of a dam is established at the design stage and depends on the extent of its stability. In its turn, the mechanical stability of construction depends on many factors (e.g. aging, quality of materials, exploitation regime, etc.) but it is mainly a function of stress state (Wieland, 2005). Thus, the essence of the mentioned dam-related threat is the risk of the loss of dam's stability under the influence of many load factors possibly leading to dam failure or damage.

As a rule, in the case of dam there are pre-defined operational load factors for which the structure has been designed, namely: primarily the horizontal force field caused by the stored water masses; the second main category includes the load of the geophysical environmental processes such as tectonically induced loading, pore pressure variations or fracture processes. Other categories could be abnormal water influx, flood waves generated by landslides or meteorological causes, thermo-elastic effects caused by air tempera-

ture variation, interaction of the foundation with the dam, the transfer of stresses between the various zones of the dam, etc.

The stability of dam structure can be tested by its long-term and short-term response to stress, here to water loading (Chelidze et al, 2011; Savich et al, 2006). The visco-elastic dam structure as a whole or its individual elements may respond to certain loading conditions through time-dependent inelastic deformations. For each kind of deformation there is a corresponding safe (theoretical) limit which must not be exceeded. At larger loading values or accumulation of critical value of damage extensive deformations may occur which are beyond the safe limit and which may compromise the dam's stability leading to damage and possibly to failure.

Full scale monitoring of dams must include permanent environmental, geotechnical, geophysical, geodetic etc. observations. These include pore pressure measurements using piezometers, measurements of seepage through the foundation and the abutments, and measurement of stresses, temperatures, seismic and ultrasound velocities, etc. within the selected locations in the dam and in the foundation, monitoring of dam and foundation tilts and displacements using tiltmeters, plumb-lines or inclinometers, strainmeters and leveling should be performed (Bartsh, 2011; Monitoring of Dams and their foundations, 1989; Automated Dam Monitoring Systems, 2000).

2. ENGURI DAM INTERNATIONAL TEST AREA (EDITA)

The 271 m high Enguri arch dam, still the highest (in its class) dam in the world, was built in the canyon of Enguri river (West Georgia) in the 1970s. It is located in a zone of high seismicity (MSK intensity IX) and close to the Ingirishi active fault system (Fig. 1).



Fig. 1. Space image of EDITA region.

The high seismic and geodynamical activities together with a high population density of the adjoining region made the Enguri dam a potential source of a major technological catastrophe in Georgia. That is why in 1996 the European Centre “Geodynamical Hazards of High Dams” with the International Enguri Dam Test Area (EDITA) was organized in Georgia by the Council of Europe.

From the very beginning in EDITA the unique geotechnical, geodynamical and geophysical monitoring system (Fig.2) was functioning (Abashidze, 2001). Several years before construction of dam geodynamical and seismological networks were created; so it is possible to compare the natural background state of seismicity and geodynamics with impacts of dam construction and reservoir filling/discharge processes (Fig.3). The database of observations (tilts, strains etc) contains information accumulated during more than 30 years.

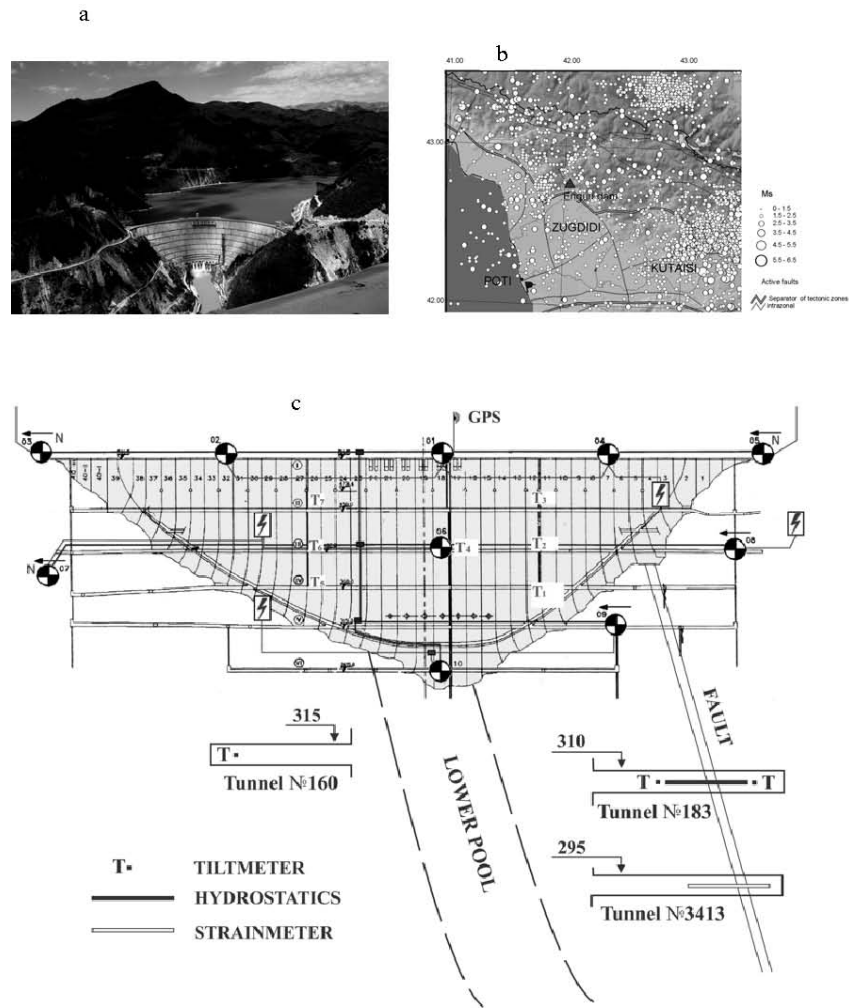


Fig. 2 a, b, c. Map showing location of EDITA and patterns of local seismicity; b) downstream view of Enguri Dam, c) Scheme of monitoring network at EDITA, numbers show location of accelerometers and T - location of tiltmeters (downstream view).

3. Long-term diagnostic tools

i. The simplest approach to dam safety problem is to compare response of real strain/tilt data with design values, which as a rule use Hook's rheology (static, linear elasticity approach). If measured characteristics, e.g. strains are close to or larger than theoretically predicted limit deformations, some preventive measures will be realized. However, the real engineering structures manifest deviations from this simple model, which can be used for diagnostics.

ii. From above it follows that a promising technique could be analysis of deviations from static elasticity model, namely, analysis of nonlinearity of stress-strain relation such as hysteretic behavior during load-unload cycle. Figure 3 (left) shows how two components of tilts of dam body, along (X) and normal (Y) to the dam crest at Enguri Dam respond to the seasonal recharge-discharge cycle of the reservoir; on the right the hysteresis in seismic velocities of foundation section for the same cycle is shown.

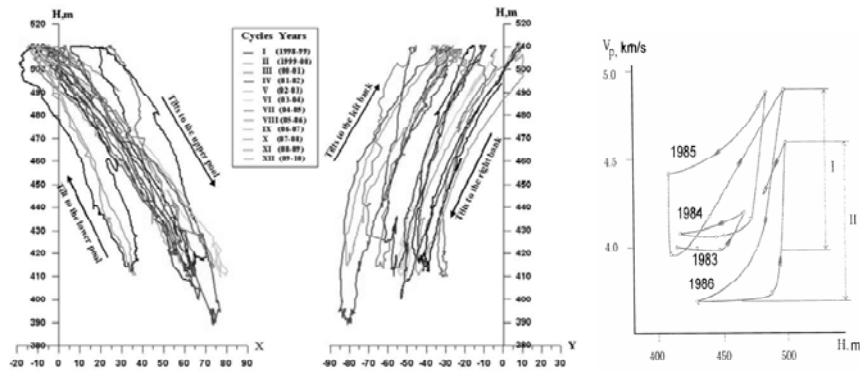


Figure 3. Left: Tilts in sec, registered in the body of Enguri High Dam, Georgia (section 12, mark 402) in two directions, along (X) and normal (Y) to the dam crest versus water level in the lake H in meters, during 12 seasonal cycles (1998-2009). Right: Variation of longitudinal seismic waves' velocity in the Enguri dam foundation versus water level in the lake. Note hysteresis in velocities at load-unload and different response to normal (I) and fast (II) discharge of water from the reservoir (Savich et al. 2002).

It is evident that tilts (and consequently, strains) increase with loading and return after discharge to the values close to initial ones following hysteresis path. The hysteresis in the cycle manifests presence of some non-linear components of strain, which can be used for diagnostics of dam state as the nonlinearity is related to the presence of fractures. The problem is that not only the dam body, but also the upper earth crust (dam foundation) also manifests hysteretic response to load/unload process. We believe that the configuration and shifts of hysteretic cycles after separation of foundation component can be used for dam state diagnostics.

iii. In the rigid enough structure the theoretically calculated tilts/strains behavior in the time domain should be close to uniform in the definite areas/sections of the dam (Wieland 2005); strong local deviation from the correlated behavior of tiltmeters in some sections of the dam points to serious disruption of the dam elastic structure.

iv. Other peculiarities of the load-unload process (time-lag between water load and strains in the dam, details of strain build up and relaxation) also can be used for long-term diagnostics.

v. Fast change of strains during slow change of load can be a sign of closeness to the critical state – failure, caused by intensive generation of defects (Chelidze et al., 2006).

Mentioned diagnostic tools need relatively long time series of observations from days to months.

4. Short-term diagnostic tools

Besides above indicators there are some short-term features, which can be used for operative/express dam state diagnostics, namely:

i. spectrum of natural frequencies of dam vibration (dam tremble), which are generated by various impacts such as water discharge, wind and waves, turbine rotation or ambient seismic noise.

ii. amplitudes of various components of spectrum. It is well known that dams have some characteristic natural frequencies, which depend on peculiarities of dam structure, water level in the lake and on the damage rate of dam material. The record of natural dam vibrations at Enguri dam shows that the dominant frequency on the crest of the dam is about 1 Hz; this is in a good accordance with results of analysis of accelerograms during the last Racha earthquake (2005, M=6) and linear elasticity theory, but our data show that the spectrum is much wider (Fig. 7c).

We believe that the spectrum (amplitudes) of natural frequencies will respond to change of the state of dam damage (some frequencies disappear; new harmonics appear, etc).

5. Real time telemetric monitoring systems of dams (damwatch)

The M. Nodia Institute of Geophysics (MNIG) and Georgian-European Centre "Geodynamical Hazards of High Dams" operating in the frame of Open Partial Agreement on Major Disasters at the Council of Europe (EUR_OPA) are developing the real time geotechnical telemetric monitoring system of large dams (DAM-

WATCH). This low-cost early warning system designed by MNIG and the company LTD “ALGO” (Tbilisi) consists of sensors (here - tiltmeters, APPLIED GEOMECHANICS Model 701-2) connected to terminal and central controllers and by the GSM/GPRS Modem - to the diagnostic center (Fig.4). The innovation in comparison with similar systems, say that at the Coolidge dam (Holzhausen, 1991) is implementation of new methodology (nonlinear dynamics) for processing geotechnical time series and assessment/prediction of the dam behavior.

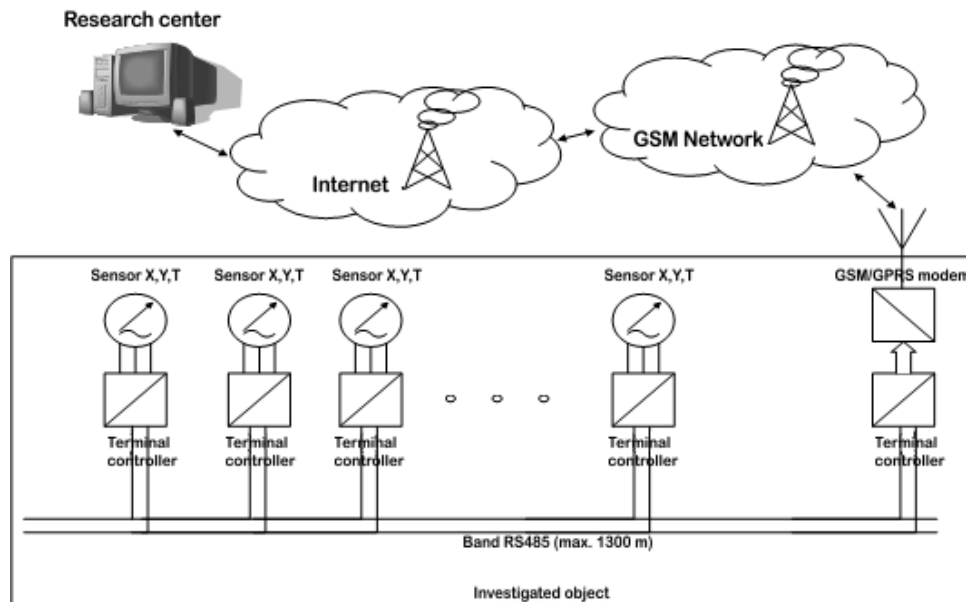


Fig. 4. The cost-effective early warning system designed by MNIG and “ALGO Ltd” (Tbilisi) consists of sensors (tiltmeters, APPLIED GEOMECHANICS Model 701-2), which are connected to terminals and central controllers and by a GSM/GPRS modem transmits the data to the diagnostic center.

6. Theoretical basis and methodology

The main idea of diagnostics is that as a result of dam material/structure damage elastic properties of the dam body diverges from the predictions of the simple linear elasticity. Elastic properties of such materials, which are called inhomogeneous (disordered, diluted) at small concentration of defects (cracks, pores, voids etc) can be calculated by the theory of effective media (Hill 1965) or at high density of defects - by the mechanical percolation theory (Chelidze et al., 2006).

Static (Linear Elasticity) Approach - Finite Element Model (FEM)

Standard static analysis of monitoring data will be performed using dam-foundation 3D model (Fig. 5a), which is represented by isoperimetric finite elements (Zienkiewicz, 2000), taking into account properties of foundation (by elasticity modulus) and geological fault in the right bank of canyon.

The weight of rock mass, including up to riverbed under-saturated surface, was taking into consideration by the uplift body force (1 t/m^3). The saturated surface was determined by model investigations. The seepage load on the grout curtain was determined as a difference of pressure between grout curtain and drainage. The hydrodynamic seepage force was taking into consideration in the nodes of foundation net by piezometric measurements.

Static FEM calculations were carried out with acting operating force, including weigh of dam; hydraulic pressure on the dam and canyon surface; seepage load in foundation in the reservoir operating level from 410 m to 510 m. Fig. 5 b presents dam's maximal horizontal displacements to lower pond according to plumb-lines data from 1999 to 2005 (Emukhvari, Bronshtein, 1991). The correlation between natural observations and theoretical calculation mainly at lower level of the dam is acceptable, but there are significant deviations in the upper dam levels (Table 1).

The most important is that the design model does not predict different (static) response to load and unload, i.e. existence of hysteresis phenomenon. The hysteresis in some works is explained by thermal effects (Engineering Guidelines..., 1999).

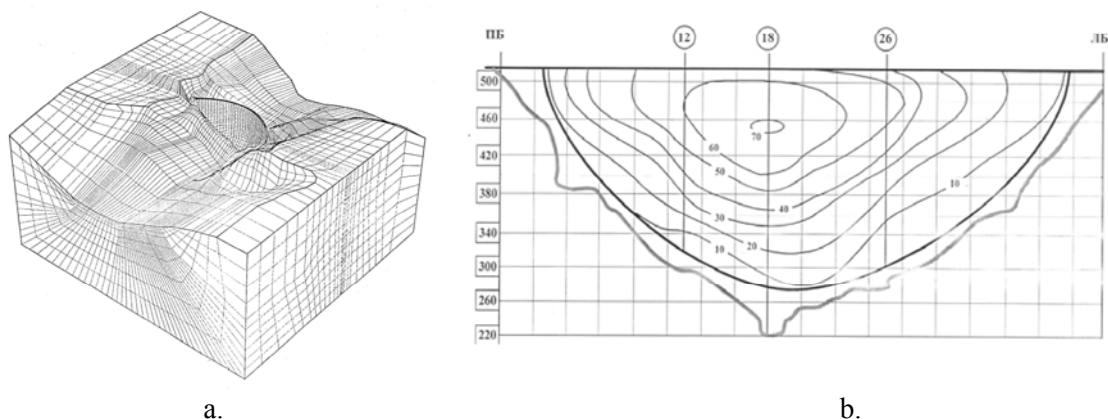


Fig. 5 a, b. a) 3D model of dam-foundation system; b) dam's maximal horizontal displacements to lower pond according to plumb lines data (1999-2005); compare with Table 1.

Time series analysis and forecasting methods: In order to ensure operative statistical and dynamical investigation of dam stability problem, modern methods of linear and nonlinear analysis of strain/tilt time series are appropriate to use (Press et al. 1996; Sprott, 2006; Kantz & Schreiber, 1997; Strogatz, 2000; Marwan, 2003; Sprott, 2006; Matcharashvili et al, 2010).

Linear methods besides traditional statistical (moments, distribution testing) include frequency (power spectrum, autocorrelation function), time-frequency (wavelet transformation) and eigenvalue (singular value decomposition) methods of analysis of data sets (Press et al, 1996; Sprott, 2006). Nonlinear methods of time series analysis include denoising of data sets (nonlinear noise reduction), testing of memory properties of targeted process (long range correlation testing, detrended fluctuation analysis (DFA), multifractal detrended fluctuation analysis; qualitative and quantitative evaluation of reconstructed from measured data sets phase space structures (correlation and information dimension calculation, Lyapunov exponents calculation, Recurrence Plots (RP) and Recurrence Quantitative Analysis (RQA), Shannon and Tsallis entropy (Kantz, & Schreiber, 1997; Strogatz, 2000; Marwan, 2003; Sprott, 2006; Matcharashvili et al, 2010). According to our experience assessment of stationarity (level of determinism) of investigated time series for different length moving windows is informative for tasks like targeted ones. The arguments for using suggested methods for dam safety analysis are: i. the strains/tilts and other geotechnical parameters of dams manifest as a rule quasi-periodic variations in time due to seasonal load-unload cycle; ii. this means that dynamics of strains/tilts time series should follow relatively stable orbits in the phase space or just manifest relatively high level of determinism; iii. the significant deviation from the stable orbit or strong decrease of determinism can be considered as a sign of instability.

The big merit of the above approach is that nonlinear analysis of complex system may be accomplished based on analysis of correctly selected and high quality few or even one component data set (Peinke et al, 2006; Matcharashvili et al, 2007).

For practical use special package DAMTOOL has been developed, which allows calculation of DFA and RQA parameters for selected monitoring time series.

The suggested linear and nonlinear analysis methods are able reveal changes in dynamics monitoring of time series, which can be connected to the mechanical state of construction.

Mesoelasticity (nonlinear elasticity) approach: The theoretical interpretation of experimental hysteretic stress-strain or tilt-stress dependences at present is mainly taking into account thermal effects, though in our opinion it can be accomplished also by the theory of mesoscopic elasticity (McCall & Guyer, 1994; Guyer & Johnson, 2009). The matter is that heterogeneous materials (concrete, rocks, etc) are nonlinear and their behavior is very different from this of its homogeneous components: for example, stress-strain (or tilt) of the system can manifest nonlinear hysteretic elastic behavior though its components have linear characteristics. Hysteresis is connected with specific response of so called mesoscopic structural features (mainly compliant

microcracks) to stress variation, namely, asymmetric response to load and unload. Real heterogeneous materials contain enormous number (10^9 - 10^{12}) of such defects in a square cm, which means that macroscopic elastic properties of material depend strongly on behavior of microcracks. Thus parameters of hysteretic cycle can be used for diagnostics of material: in the absence of cracks the brittle solid manifests linear elasticity, appearance of cracks leads to hysteresis and the opening of hysteresis curve increases with number of defects. If the hysteresis cycle is reversible (curve returns to initial position after reduction of stress) then the system is nonlinearly elastic, but if the hysteresis curve shifts in some direction it can be a sign of appearance of residual strain.

The formal approximation of experimental annual hysteresis data can be accomplished using Preisach-Mayergoyz (P-M) phenomenological model (Guyer& Johnson, 2009). In P-M model the system is represented by complex of hysteretic elastic units or hysterons; the unit can exist in one of two states, closed (having the length L_0 at pressure P_0) or open (having the length L_c at pressure P_c). We can assume that $P_c > P_0$ and accordingly $L_0 > L_c$, which corresponds to closing of existing cracks at rising pressure P from P_0 to P_c (Fig. 6, a). At decreasing pressure the hysteron opens at P_0 and remains in this state at even lesser pressures. Such approximation means that the change of state of hysteron (namely, of its length L) depends on the pressure history: transition from L_c to L_0 takes place at pressure P_c , but the backward transition from L_0 to L_c occur at pressure P_0 . The heterogeneous material can be modeled by a system of many hysterons with random distribution of parameters P_0 , P_c , L_0 and L_c . The P-M space consists of elements with different pairs of P_c and P_0 , thus P_c and P_0 can be considered as XY coordinates of P-M space (Fig.6b). The part of elements is located along the diagonal of P-M space, where $P_c = P_0$; these elements close and opens at the same pressure, which means that they are not hysteretic; the remaining hysterons with $P_c \neq P_0$ populate P- M space with varying density of states of open or closed hysterons; the points in P-M space are generated randomly according to some simple rule.

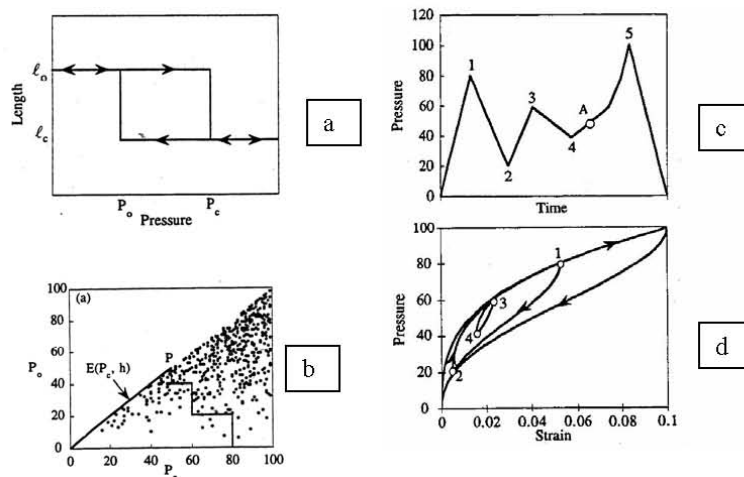


Figure 6 a,b,c,d. a) The P-M hysteron, characterized by a pair of pressures (P_0 and P_c) and corresponding lengths (L_c and L_0); b) The points, representing pairs (P_c , P_0) in the P-M space, generated by specific model equation; c) The history of pressure applied to a system, containing many hysterons (pressure protocol); d) The hysteretic stress-strain dependence corresponding to the above pressure protocol. Note the internal hysteresis loops, due to the pressure reversals at the points 1 and 3 (McCall& Guyer 1994).

The hysteresis in the stress-strain dependence stems from difference in the number of open/closed hysterons at increasing pressure from P_i to P_k , ($i > k$) and decreasing pressure from P_k to P_i . Thus at the same pressure P_i the state of the system and accordingly its elastic modulus is different and depends on the pressure pre-history (Figs. 6 c, d). Like in all hysteretic phenomena, this difference in load-unload response is due to irreversible energy losses during the process of crack growth (or generation) at loading from P_i to P_k , so that restoring the population of closed cracks at unloading from P_k to P_i demands application of additional pressure ΔP , which defines the extent of opening of hysteresis loop. On the other hand, the value of ΔP depends on content of defects (hysterons); thus the hysteresis loop opening reflects the level of material damage and can be used for diagnostics purposes

The hysteron described above corresponds to closure of (existing) open cracks at raising pressure, i.e. this is the case of relatively low pressures. At high pressures, close to material failure, the hysteron pattern is

reversed, namely, in this case at $P_c > P_0$ the length of hysteron increases from L_0 to L_c . The standard P-M model describes the case of reversible hysteresis, i.e. the hysteresis loop begins and ends at the same pressure, which means that the initial state of the system can be restored. In real systems besides elastic strain there is also often residual deformation, which means that at repeating load-unload cycles the shift of hysteresis loops will happen. The shift of hysteresis loops can be used as a measure of residual strain (damage rate) in a given material.

7. The first results of monitoring
Static approach.

Of course, predictions of the model have to be compared with monitoring data. The Table 1. presents data observed plumblines horizontal displacements (Bronshtein, 2008) and corresponding tiltmeters data (horizontal displacements in mm and tilts in seconds, with Root Mean Square) at maximal water level in the lake (510 m) for three sections of Enguri HPP (Abashidze et al. 2008) and theoretical (critical) admissible values of plumblines calculated by (Emukhvari, Bronshtein, 1991). The generally accepted approach is to compare the observed stress (strain) to calculated stresses, which correspond to some fraction of yield strength or of the ultimate strength of the material which the construction is made of.

Though high tensile stress in concrete are the most destructive factors (they generate cracks at 5-10% of uniaxial compressive strength of the concrete) the combined action of water load and dam dead load results in the dominating role of compressive stress under static load conditions; only under oscillating forcing tensile stress became equal to compressive one. As for static tensile stress, its maximal value is observed generally along the upstream heel of arch dams (Wieland, 2005). “The ultimate load-resisting capacity of an arch dam is limited by the compressive strength of the concrete (unless foundation or other mode of failures occur first), but severe and widespread joint opening and cracking might eventually exhaust the capacity of the concrete to carry compression due to subsequent load redistributions” (Engineering Guidelines, 1999). As regarding Enguri dam, according to (Emukhvari&Bronshtein, 1991) the diagnostics of dam safety considers three versions: diagnose 1 - normal state (N); diagnose 2 – maximal allowable strain (MAS); diagnose 3 – pre-failure strain (PFS). Diagnose MAS implies that deflection of dam response (strains) to acting loads exceeds theoretical values, which means that object needs detailed investigation by special program, though the exploitation of the dam can be continued as usual and diagnose PF means that after repeated investigation exploitation regime should be changed up to full shutoff.

Table 1. Comparison of observed plumblines horizontal displacements (Bronshtein, 2008) and corresponding tiltmeters data (horizontal displacements in mm and tilts in seconds, with Root Mean Square) at maximal water level in the lake (510 m) for three sections of Enguri HPP (Abashidze et al. 2008) with theoretical (critical) admissible values of plumblines calculated by (Emukhvari, Bronshtein, 1991).

Level	Section 12			Section 18			Section 26		
	Observed plumblines data	Observed tiltmeter data	Critical Admissible values	Observed plumblines data	Observed tiltmeter data	Critical Admissible values	Observed plumblines data	Observed tiltmeter data	Critical Admissible values
360 m	20 mm	11 mm (38±5.1)''	89 (122)''	35 mm			15 mm	14 mm (46±5.6)''	88 mm
402 m	40 mm	32 mm (63±4.5)''	59 (112)''	60 mm	55 mm (70±3.9)''	55 mm	30 mm	37 mm (74±4.1)''	58 mm
475 m	60 mm	48 mm (56±8.7)''	31 (182)''	65 mm			55 mm	42 mm (55±5.5)''	26 mm

The Table 1 presents observed plumblines horizontal displacements (Bronshtein, 2008) and corresponding tiltmeters' data (horizontal displacements in mm and tilts in seconds, with Root Mean Square) at

maximal water level in the lake (510 m) for three sections of Enguri HPP (Abashidze et al. 2008) with theoretical (critical) admissible values of plumbines calculated by (Emukhvari, Bronshtein, 1991). Values of theoretical (critical) admissible values of plumbines given by (Emukhvari, Bronshtein, 1991) are calculated based on the stress state and concrete strength and mark the border between normal and “faulty” state of the dam.

Analysis of the Table leads to following conclusions: 1. at the level 360 m all displacements are less than critical values; 11. at the level 402 m only in the central 18-th section the displacements are close to critical ones; iii. at the highest level (475 m) displacement of the side sections are larger than critical, i.e. at this level the state should be considered as diagnosis MAS or “faulty”. According to Emukhvari and Bronshtein (1991) in this case it is necessary to carry out repeated diagnostics of construction on the basis of re-examination of monitoring data and correction of theoretical predictions of response of the dam to loads. The displacement observation data obtained by two different methods are in satisfactory agreement. Besides, the dam performs normally and there are no visual signs of significant damage. This means that the theoretical model needs some corrections, possibly taking into account complexity of construction structure (lifts, joints, nonhomogeneity etc).

Uncertainty of static data and long time (year) needed for safety assessment calls for developing new more efficient and operative methods, which are considered in following sections.

Time-dependent methods.

Figure 7 b presents the results of monitoring of X and Y components tilts of the dam body on three levels of section12 of Enguri dam, at levels 475 m (X3, Y3), 402 m (X2, Y2), and 360 m (X1, Y1), see (Fig. 2 c). The first months the data were collected with the rate once per minute: this allows catching short transient effects, which can be useful in diagnostics.

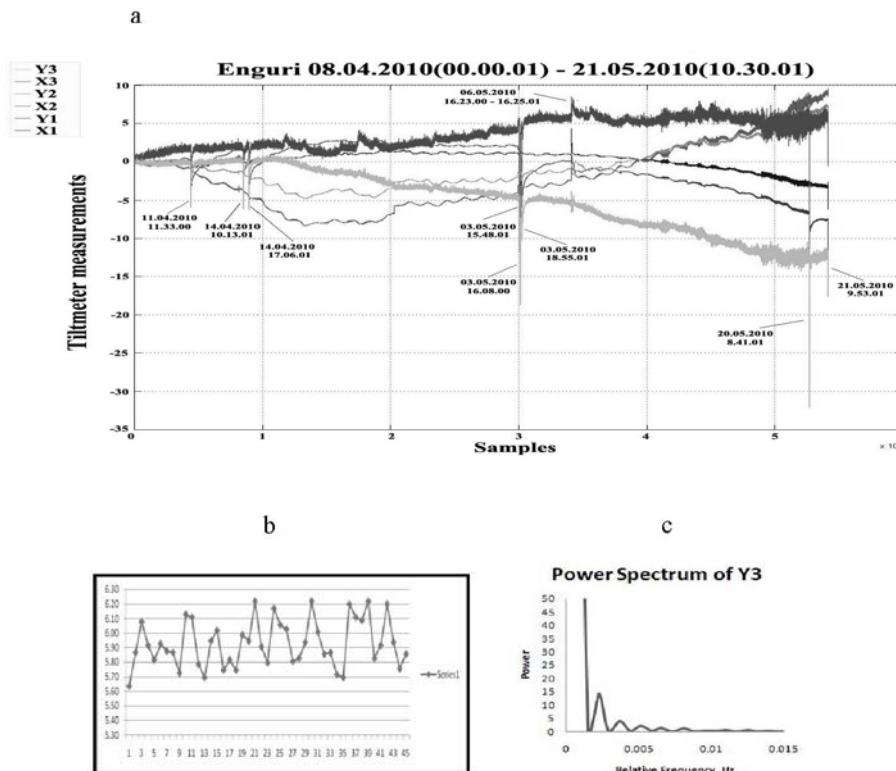


Figure. 7. a) Tilt records of dam tilts (in sec) at three sites versus time (in minutes) from April 4 to May 21, 2010. b) LF dam tremble – oscillations of Y3 component of tilt in sec versus time in minutes recorded by the tiltmeter in the section 12 at the level 475 m, part of record of 28.08.2010; note variations with a period of order of minutes; c) power spectrum of Y3 component - the first maximum is at 6-7 min.

Several effects were observed: tilt oscillations with a period of one to several minutes or “low frequency (LF) dam tremble”, sudden variations of dam tremble amplitudes, strong solitary peaks with relaxation period of several tens of minutes, stepwise change of tilts, daily variations and slow variations lasting months/years.

i. Analysis show that strong solitary peaks marked in Fig. 7 b by date and time are caused by power cuts, so these effects will be neglected as artifacts.

ii. LF dam tremble is most intensive for both components close to the dam crest (components X3, Y3), but is also visible on other levels also, especially at fast water discharge (Fig. 7 a). The tremble recording does not look as a white noise. It seems to be related to the state of construction, as its amplitude responds to the drastic increase of water discharge, realized through the body of dam at the level 330 m. In Fig. 7 b the arrows mark moments of water discharge exceeding 200 cubic meters per second. The origin of drastic increase of dam tremble on 17 May (marked by star) is unknown, as the discharge this day was not intensive.

iii. Stepwise change of tilt is evident for both components (X2,Y2) of tiltmeter installed in the middle of dam and is marked in Fig. 7 b by a thick arrow. The nature of this effect is not clear at present.

iv. Daily variations are well expressed on the recordings of both components (X2,Y2) of tiltmeter installed in the middle of dam and also with less intensity at the lowest level (X1,Y1) (Fig. 7 b, 8 b). As the amplitude of daily variation did not change after thermal isolation of device by foam plastic boxes, the direct effect of ambient temperature on the device (artifact) is excluded. These variations can be caused by daily water level variations, or thermoelastic response of the dam structure to ambient temperature, or earth tides. Further studies are needed to establish source of daily variations.

v. Middle-term (weeks, months) water level variations. It is evident that water level change (Fig.8, a) and medium-term tilt variations (Fig.8, b) are closely correlated and they can be used for diagnostics of dam response to lake load.

Note that this correlation is visible only on the level 402 m, which can be explained by relatively high response to a water load at the middle part of the dam, predicted by its design.

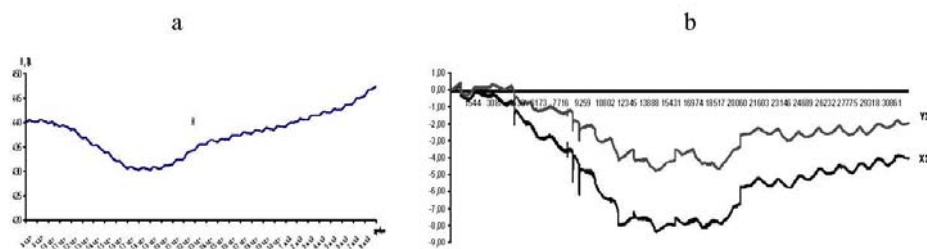


Figure 8 a, b. a) water level variations in Enguri reservoir, m (1-31 May 2010); b) variations of tilts in sec (components (X2, Y2) in the same period. Note daily variations of tilts and water level.

vi. Long-term/annual circles. Comparing outputs of Preisach-Mayergoyz model with annual hysteresis loops of Enguri dam tilts (Fig. 3 a) we can mark close similarity between model and observed data, i.e. P-M approach can be used in dam diagnostics. The successive annual Enguri tilt loops are shifted, which means that load-unload cycles involve appearance of some residual strain and this shift also can be a diagnostic sign (say, to assess aging effect). Of course, nonlinear contributions to stress-strain dependences are not very significant. That is why the dam design funded on linear approach works quite well, but analysis of nonlinear effects can produce promising methods of dam safety diagnostics.

Other experimental data:

Earthquakes (EQs): The relatively high frequency (HF) vibrations of dam in the range of 1-5 Hz due to earthquakes are extensively recorded by accelerometers and used for stability analysis. Record of the October 06, 2005 Racha event $M=6$ occurred at the distance 100 km was obtained at Enguri dam. The seismograph recordings were made at several places near the center of the crest (Fig. 9). One of the horizontal components was oriented perpendicularly to the crest. Several recordings with duration up to 30 minutes have been done on the crest of the dam. The records were analyzed, amplitude and power spectra have been calculated using software package PITSA and MATLAB. Analysis of records shows that two mean frequencies can be identified $\sim 1.6-1.7$ and $\sim 2.1-2.2$ Hz. This result is in good agreement with theoretical studies and is close to results, obtained on other dams with similar characteristics. That means that for relatively high frequencies the dam response is elastic, unlike its response to slow strains.

Besides, for the rough estimation of natural frequency of the dam special experiment was carried out using sensitive seismographs. It is well known that dams have some characteristic natural frequencies, which depend on peculiarities of dam structure, water level in the lake and on the damage rate of dam material. This last feature can be singled out from observations if other characteristics are kept constant. Installing sensor on the crest of the dam, we can estimate quite precisely the main mode (and in some cases first modes as well) of dam natural frequency. The Lenarts short period seismograph has been used. The structure subjected to a near white-noise ambient excitation responds primarily in the vicinity of its resonant frequencies. These frequencies can be identified from the peaks in power spectral densities (PDW) computed from the individual time histories.

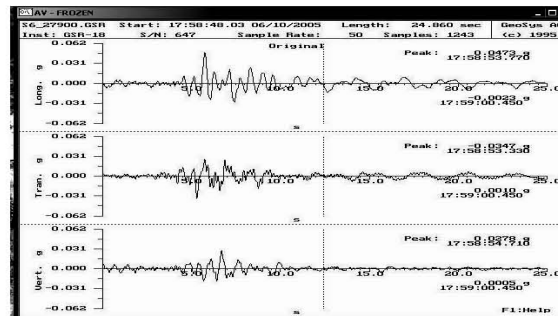


Fig. 9. Records of the October 06, 2005 Racha event $M=6$ (distance 100 km) obtained at Enguri dam.

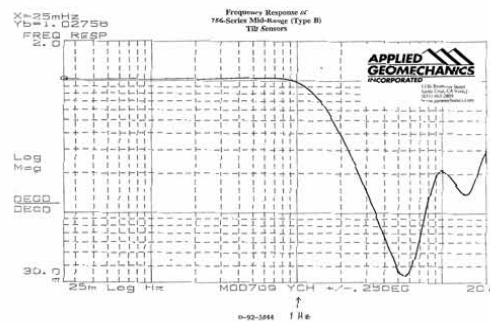


Fig. 10. The frequency response spectra of platform 701 tiltmeter. (Applied Geomechanics)

The record of natural dam vibrations at Enguri dam shows that dominant frequency (main mode) on the crest of the dam is about 1 Hz, this is in a good accordance with results of analysis of accelerograms during the last 2005 Racha earthquake (Fig. 9).

Usually the main short-term diagnostic tool is the analysis of the eigenfrequencies of the dam based on the power spectra of dam vibrations caused by water discharge, turbine operation or ambient seismic noise. Note that the turbines of Enguri PP are located far from the dam and thus the vibrations are due only to dam exploitation and some environmental processes.

At the same time our data obtained by 701 platform tiltmeters (Applied Geomechanics) at high sampling rate (1per minute) show that EQs excite vibrations at the much lower frequencies also. The analysis of frequency response spectra of platform 701 tiltmeter shows (Fig. 10) that the network consisting of such tiltmeters and ambient seismic

noise recorders allow monitoring of dam vibrations in very wide range from 100 Hz to quasi static state, which extends significantly the frequency range of non-broadband seismic devices: this can give enormous additional information on the dam state. This is demonstrated by recordings of remote and local earthquakes obtained during our experiments. Figs. 11 present recording of tilts response to the moderate local EQ (Vani, M= 5.3, 19.01.2011), which occur at the distance 80 km from the dam and Fig. 12 presents expanded recording of the event. The EQ generated significant tilts, which differ for different sites of the dam and vary in the range from 10-15 sec (X7, Y7, X3) to 2-3 sec (Y2, X5, Y5). The event was fixed well due to the relatively high sampling rate (1/min); at the sampling rate 1/hour it could be missed.

It is interesting to note that 13 hours before Vani EQ there was a long tremor on all sensors – its duration was 30 min and period of order of minutes. There was no significant strong EQ in the world these days so contribution of long period seismic waves is excluded (may be this was local slow/silent precursory EQ?). The tremor generated tilts in the range from 2-3 sec (X7, Y7) to 1 sec (X5, Y5).

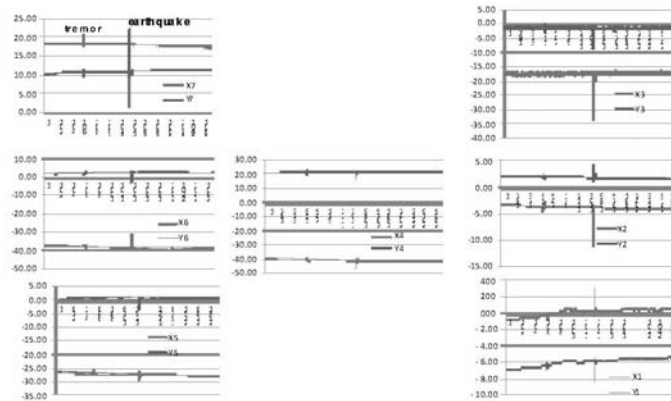


Fig. 11. Local EQ - Vani, M= 5.3, 19.01.2011 (distance to dam 80 km) and possible preliminary tremor (perturbation) 13 hours before the EQ. Here and in similar diagrams location of figures corresponds to their location in the dam body (see Fig. 2c). Sample rate 1/min.

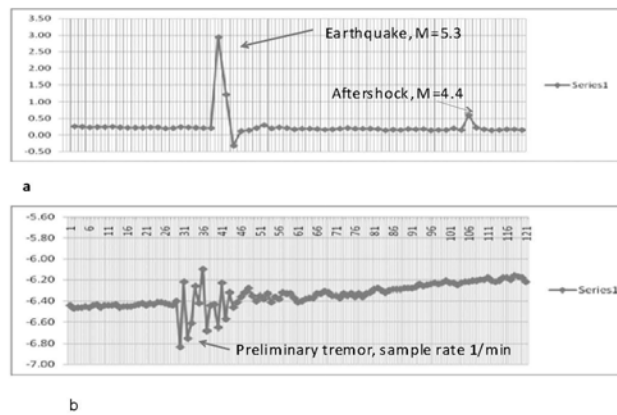


Fig.12 . Expanded recording of the Vani event: a. Local EQ - Vani, M= 5.3, 19.01.2011 (distance to dam 80 km) and aftershock M=4.4; b. preliminary LF tremor 13 hours before Vani EQ; sample rate - 1/minute. File: Engurgesimin-18.01.11(13.32.00)-20.01.11(12.00.00)

Besides local Vani EQ, strong remote EQs also cause very low frequency (VLF) vibration of dam. 11 March 2011 the great Tohoku M= 9 EQ stroke Japan. Tohoku earthquake epicentre is separated from Enguri by 7800 km. Nevertheless, the EQ was so strong that the Enguri dam experienced quite appreciable shaking (Fig. 13), just at the moment of arrival of seismic waves from Japan to Enguri, according to Georgian seismic network data. Unfortunately that time the sampling rate was only 1/10 min and the record of shaking show less details than record of Vani event. The wave trains of Tohoku EQ, presumably, slow surface (Love and Rayleigh) waves, induced on all levels of the dam observable tilts in the range 2-3 angular sec; maximal tilt was recorded at the X1 component – 4 sec. Duration of the tilt perturbation was of the order of 130 min.

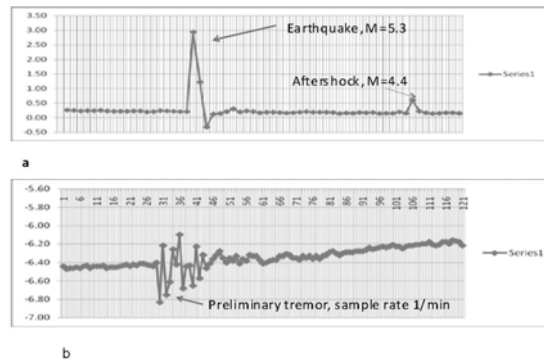


Fig. 13. Expanded record of tilts at Enguri dam to great Tohoku (Japan) EQ, M= 8.9 March 11, 2011, at 05:46:23 UTC on the stations 1 and 3, sample rate 1/10 min. Note maximal tilt (4 sec) recorded at the X1 component.

It seems that tiltmeter data at high sampling rates of the order of 1 per sec can give very useful information on the dam state, as the defects of dam structure affect mostly low frequency respond.

Seiches: It is well known that in an enclosed body of water (lakes, reservoirs, bays, harbors) a standing wave or seiches are generated by disturbances of water body by wind, earthquakes etc. These standing waves cause vibrations of dam body. Such effects were observed on the Enguri dam. The seiches-generated vibrations were recognized by their co-incidence with strong winds, recorded by meteorological station. As the amplitude of some tilt perturbation of duration from tens of min to hours strongly (almost to zero) decreases at lower levels of dam, the most probable source of perturbations (Fig. 14) are waves in the lake due to wind (seiches).

The clear example of wind-related perturbation in dam tilts is presented in Fig. 14: readings from 1 to 171 (arrow) correspond to calm weather (MeWV – 0.2m/s, MaxWV – 3.6 m/s, WD – ENE and readings from 171 to 292 – to stormy one (MeWV – 2-5 m/s, MaxWV – 15.2-16.5 m/s, WD – N-NW). Here MeWV is the mean wind velocity, MaxWV- maximal wind velocity, WD means wind direction, ENE means East-Nord-East and N-NW means Nord-Nord-West accordingly.

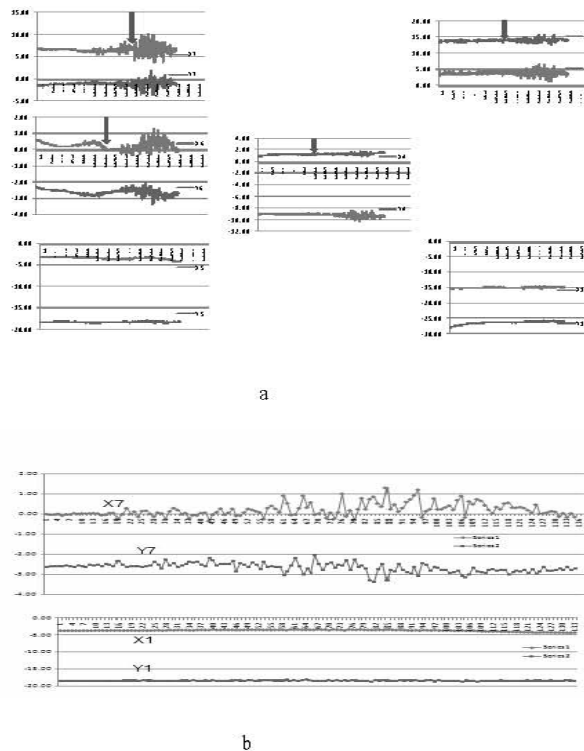


Fig. 14. a. Example of wind-related perturbation in dam tilts (seiches): readings from 1 to 171 (arrow) correspond to calm weather and readings from 171 to 292 – to stormy one (see text for abbreviations). b. Extended record of tremor caused by lake water perturbations by wind (seiches) – mean period of perturbations of order of 30-40 min! File - Engurhesi-22.11.2010 (13.40.00)-24.11.2010 14.00.00), sample rate – 1/10 min;

According to theory the longest natural period for a seiche in an enclosed rectangular body of water is usually represented by the formula: $T = 2L/\sqrt{gh}$ where L is the length, h the average depth of the body of water, and g the acceleration of gravity. Inserting data for Enguri lake $L = 25$ km, $h = 50$ m we get $T = 38$ min, which is close to observed values (Fig. 14 b). In principle the seiches-generated LF vibrations can be used in dam diagnostics, as their frequency should depend on dam state.

Besides “normal” seiches there were observed vibrations of much lower frequency –presumably, very slow seiches with period of order of several hours.

Intensive water discharge. Discharge of excess water also causes tremors in dam body: their signature is maximal intensity in the middle level of dam and smaller intensity at both upper and lower levels (Fig. 15). The characteristics of such tremors also can be used for diagnostics.

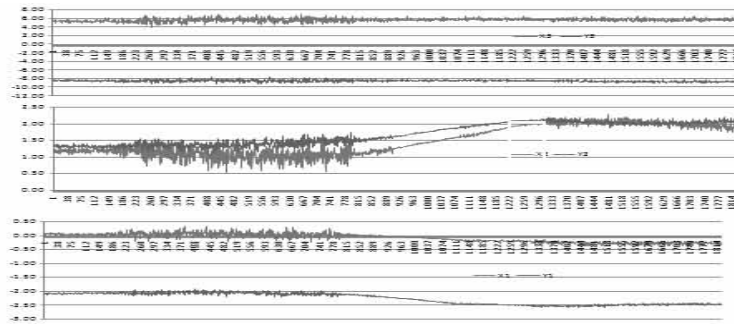


Fig. 15. Anomalous tilt tremors with deep penetration (probably water discharge done 11-12 May 2010) at readings between 120 and 780. File: Engurhesi 11-12 May, sampling rate 1/min.

9. Examples of application of nonlinear dynamics technique

In order to test sensitivity of selected methods and asses effects of external influences on Earth tilt dynamics in the dam foundation, we considered tilt data sets in the following 7 time windows for Enguri HPP: 1) long before reservoir filling, 2) immediately before and 3) just after beginning of filling, 4) after second, 5) third and 6) fourth stage of reservoir filling and 7) long after completion of reservoir filling, i.e during regular exploitation regime. Figs. 7, a, b, illustrate RQA determinism (RQA%DET) and Lempel-Ziv algorithmic complexity measure for mentioned 7 periods. It is evident that for different stages of dam construction and reservoir fill significant quantitative differences have been detected in the recurrence attributes of phase space structures reconstructed from tilt datasets. Note that nonlinear dynamical properties of tilt time series during regular (periodic) reservoir exploitation return to the patterns observed before the dam building and lake fill (see bars 1 and 7 in Fig. 16, a and b).

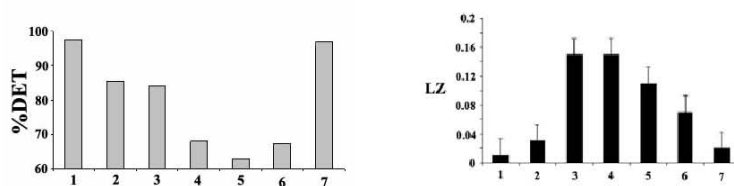


Fig. 16. Left: RQA determinism measure calculated for Earth tilt data series for different stages of observation. Right: Lempel Ziv complexity measure calculated for Earth tilt data series for different stages of observation. Numbers on abscissa correspond to periods of observation.

Thus our analysis confirms possibility of detection of man-made effects (i.e. diagnostics) in tilt time series. It is interesting that the local seismicity follows the similar pattern: the degree of determinism in seismic time series decreases in time windows 2-6 and returns to initial values long after filling.

Besides this long-term test the nonlinear dynamics software module DAMTOOL for short-term visual control, processing and nonlinear analysis of monitoring data (say, tilt time series) of engineering constructions has been developed.

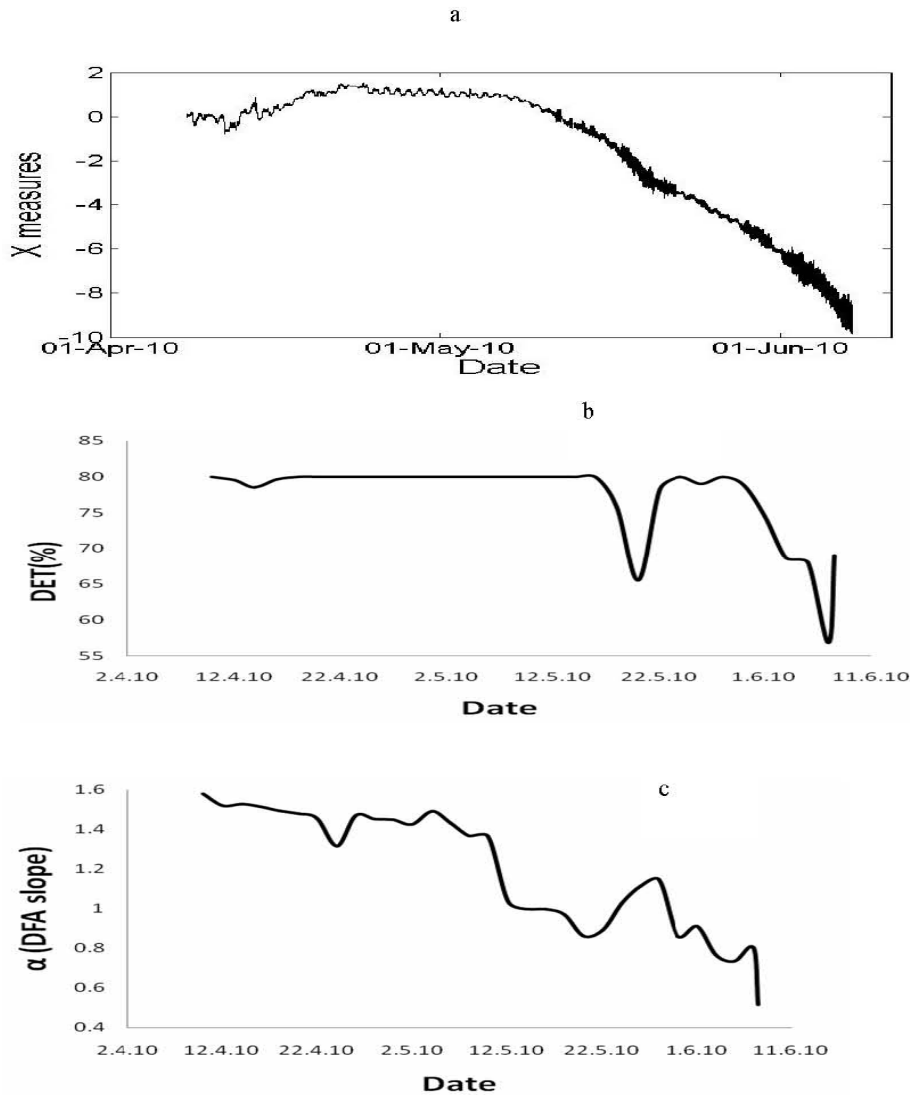


Fig. 17 a, b, c. Results of calculations by DAMTOOL of DFA and RQA (% of determinism) for the tilt time series from April 2010 to June 2010. a. Original tilt time series; b. RQA (% of determinism) ; c. DFA. Note high values of spectral slope (DFA) and DET during regular regime and strong deviations due to geotechnical impact – addition of high frequency component due to intensive discharge of water through dam outlet in 12.05-22.05.2010 and 01.06-11.06.2010 time intervals.

Thus, the disruptions in monitoring time series determinism can be caused both by construction damage and by usual geotechnical procedures, which means that results of analysis should take into consideration man-made impacts.

10. Conclusions

Automatic Real-Time Telemetric System for Dam Diagnostics (DAMWATCH) is installed at Enguri Dam International Test Area (EDITA). System consists of tilt sensors connected to terminal and central controllers and by GSM/GPRS Modem - to the diagnostic center. The important component of the system is the nonlinear dynamics module DAMTOOL for analysis of monitoring (say tilt) time series.

The tilt data for varying reservoir load were compared to (static) theoretical model of dam deformation computed by finite element method (FEM). The results for dam lower levels is satisfactory, but displacements for the crest area exceed theoretical assessments.

Besides static approach, the nonlinear analysis of low-frequency vibrations data can be used to detect changes in dynamics/stability in the dam tilts/strains time series. Corresponding package for nonlinear analysis of monitoring time series (DAMTOOL) has been developed. The arguments for using suggested methods

for dam safety analysis are: i. the strains/tilts and other geotechnical parameters of dams manifest as a rule quasiperiodic variations in time due to seasonal load-unload cycle; ii. this means that dynamics of strains/tilts time series should follow relatively stable orbits in the phase space or just manifest relatively high level of determinism; iii. significant deviation from the stable orbit or strong decrease of determinism can be considered as a sign of instability after excluding man-made effects.

The data obtained already show very interesting long-term and short-term patterns of tilts' dynamics in the dam body, including tilt hysteresis during annual loading-unloading cycle, low-frequency dam oscillations etc, which can be used for dam diagnostics. The possible interpretation of hysteresis phenomena in by mesoelasticity (nonlinear elasticity) approach is suggested. It is shown that the main contribution to annual tilts hysteresis comes from the dam body tilts, thus these data are appropriate for dam damage diagnostics. The tiltmeter recordings with one minute resolution reveal many interesting details of dam behavior, which expand the spectrum of dam vibrations to low frequencies and give new diagnostic tools. Analysis of retrospective tilt data show that used methods are appropriate to detect and quantify dynamical changes in dam body behavior caused by different external and internal causes, though mechanism of some observed effects still need to be studied in detail.

Acknowledgements

Authors acknowledge financial support of joint project (# 5016) of Georgian National Scientific Foundation (GNSF) and Science and Technology Center of Ukraine (STCU) and Open Partial Agreement on the Major Disasters at the Council of Europe (EUR-OPA).

References

- [1] Abashidze, V. 2001. *Geophysical Monitoring of Geodynamical Processes at Enguri Dam*. Tbilisi. Abashidze, V., Chelidze, T., Tsaguria, T., Kobakhidze, T.. Results of research, carried out on Enguri HPP by tiltmeters. Energy, N 1, 2008, Tbilisi (in Georgian).
- [2] Analysis and assessment of the state of Enguri HPP and its foundation, recommendations for improving reliability and safety of its exploitation.
- [3] Automated Dam Monitoring Systems. 2000. Bulletin of International Committee of Large Dams. N 118.
- [4] Bartsh M., Schiess Zamora, A., Steiger K.M. 2011. Continuous Dam Monitoring: an essential basis for reliable back-analysis. *Hydropower&Dams*. 18, 51-56
- [5] Analysis and assessment of the state of Enguri arch dam and its foundation, recommendations for strengthening reliability and safety of exploitation. Center of geodynamical surveys in energy domain. Hydroproject and Tbilhydroproject. Moscow-Tbilisi. 2008 (in Russian).
- [6] Chelidze, T., Kolesnikov, Yu., Matcharashvili, T. 2006. Seismological criticality concept and percolation model of fracture. *Geophysical Journal International*. 164, 125-136.
- [7] Chelidze, T., Matcharashvili, T., Abashidze, V., Kalabegashvili, M. 2011, Real time telemetric monitoring system of large dams. In: Proceedings of Int. Symposium "Dams and Reservoirs under changing challenges - CD-papers. (Eds. A. Shleiss, R. Boes), CD_01.
- [8] Engineering Guidelines for the evaluation of the Hydropower projects. 1999. Chapter 11- Arch dams. Federal Energy Regulatory Commission Division of Dam Safety and Inspections. Washington, DC 20426.
- [9] Emukhvari, N, Bronshtein, V. 1991. Inguri HPP – system of allowable and limiting parameters of arch dam state for operative control of its safety during exploitation. Ministry of Energy USSR. Moscow-Tbilisi.
- [10] Guyer, R & Johnson, P. 2009. *Nonlinear Mesoscopic Elasticity*. Wiley-VCH.
- [11] Hill, R. 1965. A self-consistent mechanics of composite materials. *J.Mech.Phys.Solids*, 13, 213-223.
- [12] Holzhausen, G. 1991. Low cost automated detection of precursors to dam failure: Coolidge dam, Arizona. 8th Annual Conference ASDSO, San Diego.
- [13] Press, W. et al. 1996. *Numerical Recipes*. Cambridge University Press.
- [14] Kantz, H&Schreiber, T., 1997. *Nonlinear time series analysis*. Cambridge University Press.
- [15] Marwan, M., 2003. Encounters with neighborhood, PhD Thesis.

- [16] Matcharashvili T., Chelidze, T., Peinke, J. 2007. Increase of order in seismic processes around large reservoir induced by water level periodic variation, *Nonlinear Dyn.* DOI 10.1007/s11071-007-9219-0.
- [17] Matcharashvili T., T. Chelidze, V. Abashidze, N. Zhukova and E. Meparidze. 2010. Changes in Dynamics of Seismic Processes Around Enguri High Dam Reservoir Induced by Periodic Variation of Water Level. in: *Geoplanet: Earth and Planetary Sciences, Volume 1, 2010*, DOI: 10.1007/978-3-642-12300-9; Synchronization and Triggering: from Fracture to Earthquake Processes. Eds. V. de Rubeis, Z. Czechowski and R. Teisseyre, pp.273-286.
- [18] McCall, K& Guyer, R. 1994. Equation of state and wave propagation in hysteretic nonlinear elastic materials. *J. of Geophys. Res.*, B99, 23 887-23897.
- [19] Mivenchi M.R., Ahmadi M.T., Hajmomeni A. 2003. Effective technique for Arch Dam Ambient Vibration Test. *JSEE*, 5, 23-34.
- [20] Monitoring of Dams and their foundations. 1989. Bulletin of Intern. Committee of Large Dams. N 68.
- [21] Peinke, J., Matcharashvili, T., Chelidze, T., et al. 2006. Influence of periodic variations in water level on regional seismic activity around a large reservoir. *Phys. Earth&Planetary Interiors*, 156, 130–142.
- [22] Savich, A. et al. 2002. Complex engineering-geophysical investigations at construction of hydropower objects. Moscow, Nedra, (in Russian).
- [23] Savich, A. et al. 2006. Safety of large dams in areas of high geodynamical risk. In “Geodynamical Studies of Large Dams” Tbilisi, (in Russian).
- [24] Sprott, J. S., 2006. *Chaos and Time Series Analysis*. Oxford University Press.
- [25] Strogatz, S., 2000. *Nonlinear Dynamics and Chaos*. Westview Press.
- [26] Wieland, M. 2005. Stress management. *International water power&dam construction*. March, 32-36.
- [27] Zienkiewicz, O. 2000. *The Finite Element Method*. Butterworth-Heinemann.

(Received in final form 20 December 2012)

Система телеметрического мониторинга больших плотин в реальном времени и новый метод анализа динамики плотин

**Тамаз Челидзе , Теймураз Мачарашвили , Вахтанг Абашидзе, Мириан
Калабегашвили , Наталия Жукова, Екатерина Мепаридзе**

Резюме

Большие плотины – это сложные системы с нелинейным динамическим поведением. Мы создали систему телеметрического мониторинга больших плотин в реальном времени (DAMWATCH) для диагностики плотин, состоящую из сенсоров (наклономеров), нескольких терминальных и одного центрального контролеров, соединенных GSM/GPRS модемом с диагностическим центром.

Для обработки данных как линейными методами, так и методами нелинейной динамики создан пакет DAMTOOL.

Отклонение измеренных статических и динамических характеристик от теоретически рассчитанных значений может свидетельствовать либо об аномальном состоянии объекта, либо о необходимости внесения коррекции в теоретическую модель.

Система введена в эксплуатацию и уже получены интересные долговременные и краткосрочные паттерны поведения наклонов плотины, которые могут быть использованы для диагностики. Комплекс DAMWATCH-DAMTOOL не имеет аналогов в мировой практике.

დიდი კაშხლების რეალურ დროში ტელემეტრული მონიტორინგის სისტემა და კაშხლების დინამიკის ანალიზის ახალი მეთოდი

თამაზ ჭელიძე, თეიმურაზ მაჭარაშვილი, ვახტანგ აბაშიძე ,
მირიან ყალაბეგაშვილი, ნატალია ჟუკოვა, ეკატერინე მეფარიძე

დიდი კაშხლები წარმოადგენენ რთულ სისტემებს არაწრფივი დინამიკით. ჩვენ შევქმენით დიდი კაშხლების რეალურ დროში ტელემეტრული მონიტორინგის სისტემა (DAMWATCH) კაშხლების დიაგნოსტიკისათვის, რომელიც შედგება სენსორებიდან (დახრისმზომებისაგან), რამდენიმე ტერმინალური და ერთი ცენტრალური კონტროლერისაგან, რომლებიც GSM/GPRS მოდემით დაკავშირებულია დიაგნოსტიკურ ცენტრთან. მონაცემთა წრფივი და არაწრფივი დინამიკის მეთოდებით დამუშავებისათვის შექმნილია პაკეტი DAMTOOL.

ობიექტის გაზომილი სტატიკური და დინამიკური მახასიათებლების გადახრა თეორიულად გათვლილი მნიშვნელობებისაგან შეიძლება მიუთითებდეს ან ობიექტის ანომალურ მდგომარეობაზე, ან თეორიული მოდელის შესწორების აუცილებლობაზე.

სისტემა შეყვანილია ექსპლუატაციაში და უკვე მიღებულია კაშხლის მდგომარეობის დამახასიათებელი დახრების გრძელ- და მოკლევადიანი პატერნები, რომლებიც შესაძლოა გამოყენებული იყოს დიაგნოსტიკისათვის.

კომპლექს DAMWATCH-DAMTOOL-ს არ გააჩნია ანალოგები მსოფლიო პრაქტიკაში.

Climate change in Georgia: Statistical and nonlinear dynamics predictions

A. Amiranashvili¹, T. Matcharashvili^{1,2}, T. Chelidze^{1,2}

1. M. Nodia Institute of Geophysics of I. Javakhishvili Tbilisi State University

2. European Centre "Geodynamical Hazard of High Dam", EUR-OPA

Abstract

The greenhouse effect (global warming) is one of the main hazards facing the whole planet. The climate forcing is due to rising concentration of greenhouse gases (CO₂, methane, water vapor): according to different assessments, the temperature will rise by 1.4-5.8⁰C at the end of 21-th century. This can cause a lot of devastating effects and many of them will be impossible to prevent, which means that the humankind should find some way to adapt itself to global warming.

Georgia as a whole Caucasus is prone to many negative effects, connected with climate change: the mountain glaciers can melt and partially disappear, the sea level can rise, the vast areas of land can become deserts, water resources can be seriously affected.

Despite some earlier efforts, devoted to assessment of climate change in Georgia, the results are still ambiguous. In particular, the research carried out shows that during last decades the mean temperature in the Eastern Georgia is rising and in Western Georgia it is decreasing. These conclusions are debated and there is a need to re-consider them using new data and new methods of mathematical analysis of meteorological time series. For reliable assessments new modern methods of obtaining and analysis of climate data in the past, present and future is necessary to use.

Another problem is to ascertain whether this warming is exclusively the man-made effect or it is the result of natural cyclicity in the earth climate.

Specific objective is assessment of persistence and memory characteristics of regional air temperature variation in Georgia in the light of global climate change. For this purpose longest available temperature time series of Tbilisi meteorological station (since 1890) are analyzed. Similar time series on shorter time scales of 11 stations in the West and East Georgia will also be used as well as monthly mean temperature time series of 11 stations (1907-2006) in the West and East Georgia. As far as most incorrect conclusions about dynamical properties of complex dynamics are related to "data bleaching" procedures, in order to avoid destruction of original dynamics caused by linear filtering in the present research special noise reduction procedure of time series as well as multi scaling analysis based on CWT are used. Both mono- and multivariate reconstruction procedures of climate change dynamics are implemented. Additionally, temporally and spatially averaged daily and monthly mean air temperature time series are analyzed. Extent of persistence in mentioned time series is evaluated.

1. Introduction: Global issues and South Caucasus

Most models of climate change are based on extrapolation of observed linear trends. At the same time, though global warming is well established, the question of persistence of trends on regional scales remains controversial. Indeed, climate change for specific region and specific time interval by definition includes more than the simple average of weather conditions. Either random events or long-term changes, or more often combinations of them, can bring about significant swings in a variety of climate indicators from one time period to the next. Therefore in order to achieve further understanding of dynamics of climate change and prevent related disasters, the character of stable peculiarities of analyzed dynamics should be investigated. Analysis of the character of long range correlations in climate time series or peculiarities of their inherent memory is motivated exactly by this goal. Such analysis carried out on different scales will help to understand and predict spatial and temporal features of regional climate change during general global warming.

According to Sylvén et al. (2008) “climate change has already started to have a significant impact on nature and people in the Southern Caucasus region – effects that will become even more severe in the future. This will create an extra burden on the development of societies in all the three countries of Armenia, Azerbaijan and Georgia, which still struggle to embark on a more sustainable path, including eradicating widespread poverty” (Table 1,2).

Table 1. The main environmental challenges related to climate change in Armenia, Azerbaijan and Georgia (Sylvén et al, 2008).

Country	Environmental challenges
Armenia	Deforestation & illegal logging, Desertification, Use of solid fuels, Access to safe drinking water in rural areas, Management of Lake Sevan
Azerbaijan	Deforestation, Desertification and land degradation, Deteriorating air quality, Water shortage & insufficient water sanitation
Georgia	Land degradation (overgrazing, soil pollution and erosion), Illegal logging, Regional water shortage (particularly in eastern regions), Lack of access to safe drinking water

Table 2. Summary of reported economic losses linked to climate change in Southern Caucasus 1978-2007. The list should merely indicate the scale of the costs related to climate change in the region (modified from Sylvén et al, 2008).

Country	Year	Events	Losses
Azerbaijan	July 1997	Floods/erosion	50 million USD
Azerbaijan	2000-2007	Floods and erosion (est. 70 mill/year)	490 million USD
Georgia	May 2005	Floods/erosion (low estimate)	3 million USD
Georgia	2000-2001	Drought	460 million USD
Armenia	2000-2005	Drought, frost, floods	107 million USD
Armenia	Sept 2006	Drought/forest fires	9 million USD

In (Harmeling, 2011) the climate risk index for 1990-2000 is presented for all countries of the world. Table 3 is a selection of data related to South Caucasus from above publication: according to it, Georgia has the largest values of losses per GDP in % and the highest rank (44), in comparison to Armenia and Azerbaijan.

Table 3. Climate Risk Index for 1990-2009 (Harmeling, S. GLOBAL CLIMATE RISK INDEX 2011) CRI = Climate Risk Index; GDP = gross domestic product; PPP = purchasing power parity; n/a = no data

Index	Country	Overall CRI score	Death toll		Death per 100,000 inhabitants		Losses in million US\$ PPP		Losses per GDP in %	
			Total	Rank	Total	Rank	Total	Rank	Total	Rank
136	Armenia	117.00	0	150	0.01	156	32.99	98	0.2	71
126	Azerbaijan	114.17	2	120	0.03	139	55.72	81	0.1	103

n/a	Ceo	n/a	4	112	0.08	103	0.00	n/a	0.38	44
a	rgia									

Still, despite grave assessments of Sylvén et al. (2008), according to numerous modeling results of Intergovernmental Panel on Climate Change (IPCC), Caucasus is the region of low or moderate magnitude of warming.

2. Climate change history in the Western Caucasus (Georgia).

The temperature measurements in Caucasus were first organized in Tbilisi (East Georgia) in 1844, namely, at the Tbilisi Geophysical Observatory. Thus we have here one of the longest temperature records; these data present average annual, as well as average seasonal temperature data. We tried linear, exponential, polynomial and 50 years average fittings to data. All of them reveal warming, which can be defined as $\Delta T = T_f - T_i$; here T_f is the final and T_i initial temperature. According to linear and exponential fits of ΔT data, the temperature during 156 years raised by 1.20°C . These two fits do not show the change in the rate of warming, that is why polynomial and many-year average approximations seem to be more representative: the graph in Figs. 1 reveals trends in this long-term temperature record of average annual data: according to polynomial fit the 156 years $\Delta T = 1.4^{\circ}\text{C}$ and for the last 50-years average $\Delta T = 1^{\circ}\text{C}$. Almost all this increment is obtained for the last 56 years, i.e. from 1950 to 2006.

The spatial distribution of ΔT in Georgia for 1906-1995 has been calculated in the frame of “Georgia’s initial national communication under the United Nations Framework Convention on Climate Change” (1999). This study reveals the striking difference in the climate change trend between West and East Georgia (Fig. 2):

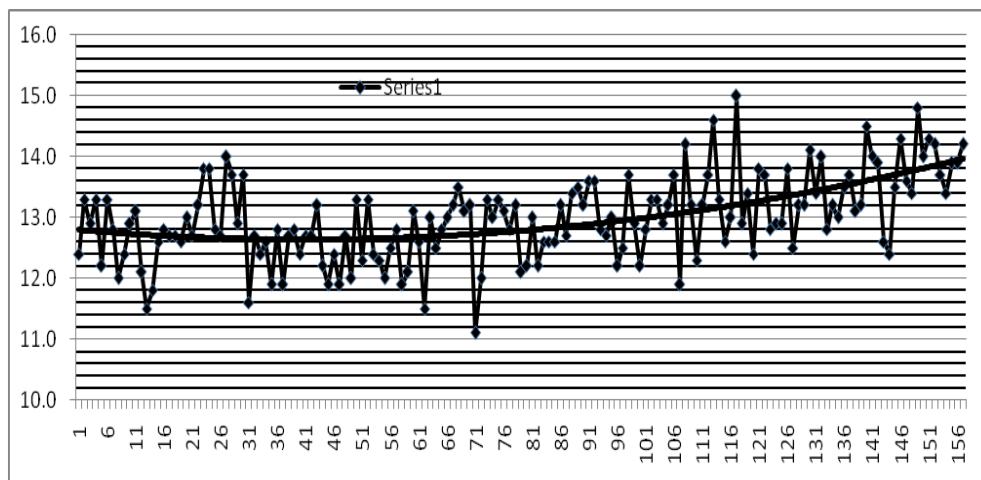


Fig. 1. Tbilisi temperature longest (156 years long) time series 1850-2006 (points) and the simplest fitting by second order polynomial (thick line)

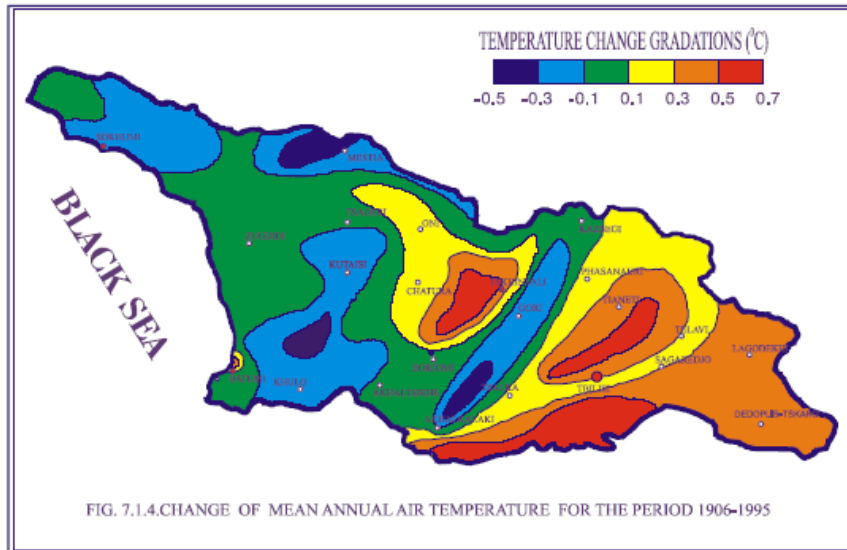


Fig. 2. Change of mean annual temperature in Georgia 1906-1995

More complicated statistical assessments were carried out using modern tools of statistics: autocorrelation, correlation fields, revealing periodicities, analysis of residuals etc. The estimation of difference between the investigated parameters was evaluated according to Student's criterion t with the level of significance not worse than 0.2. The results are shown below (Fig. 5, 6).

Analysis of air temperatures in the recent past in Tbilisi (Fig. 5) shows that after 1850-1906 period with cooling linear trend (section 1) there are permanent warming periods, 1907-1956 (section 2) and 1957-2006 (section 3). Temperature raised on average by 1°C during the last 100 years.

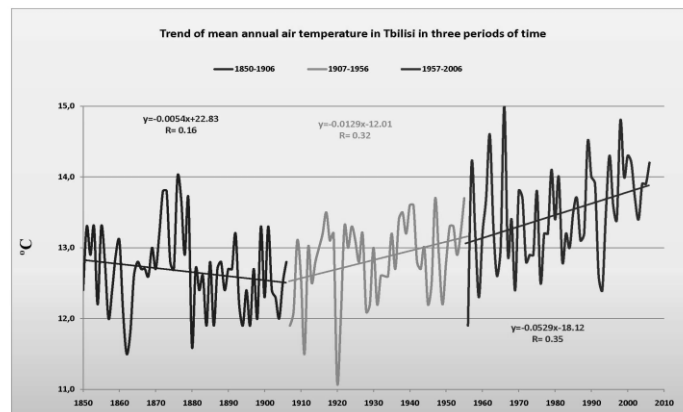


Fig. 5. Variability of mean annual air temperature in Tbilisi in 1850-1906 (section 1), 1907-1956 (section 2) and 1957-2006 (section 3) years with linear approximations

In Fig. 6 the difference between mean values of air temperature in Tbilisi in the period compared to 1907-1956 period. Significant differences (more than 0.1 degree C) are marked by dual shading (light and dark). It is evident that the largest differences, here - warming, are observed in cold months. The cold period months are in average twice warmer in the 1957-2006 compared to earlier 50 years.

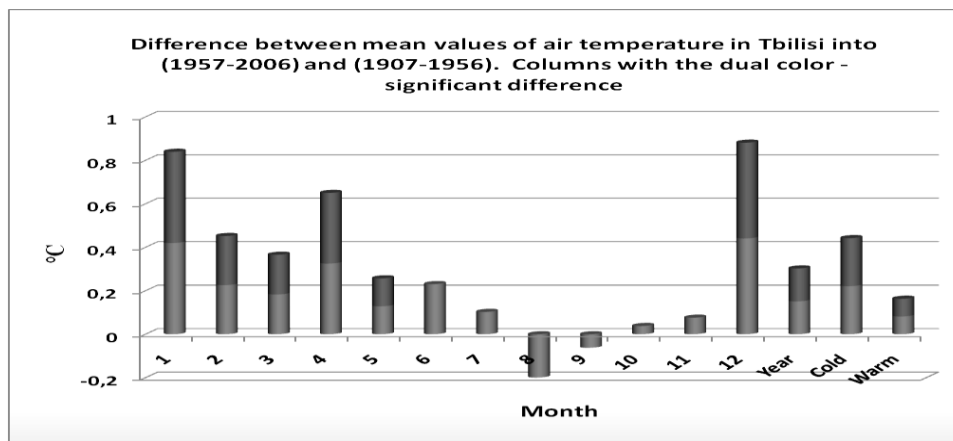


Fig. 6. Difference (dark parts) between mean values of air temperature in Tbilisi in (1957-2006) and (1907-1956). The last three columns – averages per year, per cold months and per warm months.

It is of fundamental importance to establish, is such warming the result of human industrial activity or there are some natural cycles of warming and cooling irrespective of man-made impact.

Last years in Georgia some proofs of earlier (pre-industrial) warm periods have been revealed. The monastery Betlemi dated to 10 cent. AD was cut in the rocks of the mountain Mkinvatsvery (Kazbek) at an altitude of 4200 m, where Christian priests lived at that time. Both pollen and non pollen palynomorphs were studied. The investigation showed that in 10th cent. AD, in the environs of the ancient monastery there grew alpine and sub-alpine meadows with rich taxonomic composition. The monks have had domestic cattle and were engaged in beekeeping, which was possible only in conditions of warm climate (Kvavadze et al, 2011). At present it is impossible to live at these altitudes because of the severe climatic conditions. Mean annual temperature here is at present

-6.1⁰. This points to existence of very warm periods in climate of Georgia even before industrial era.

The next substantial climate warming in the mountains of Georgia occurred from the end of the 13th century AD to 14-15 century AD. This is indicated by the pollen data of investigation of the settlement “Navenakhari” (Kvavadze et al, 2009).

Comparison of these conclusions with global proxy reconstructions, show that mentioned periods indeed were warm (Chapman and Davis, 2010) and are defined as a Medieval Optimum, which according to Archer (2007) “took place about 800-1200 AD. This was a period of generally warm stable climate in Europe, coincident with a prolonged drought in the American southwest of sufficient intensity to spell the end of the Mayan civilization”. In the same warm period Vikings settled in Greenland.

We can conclude that warm periods in South Caucasus/Georgia have been identified in earlier centuries, when anthropogenic impact was negligible.

In future for more reliable reconstruction of the past climate application of borehole geothermy method of reconstructing past temperatures up to 1000 year AD is necessary. Detailed variations of the surface temperature are evaluated from long-term highly resolved temperature measurements in boreholes: temperature variations slowly penetrate into the subground and can be measured hundreds or thousands of years after its occurrence. As the most part of heat comes from the Earth interior to the surface, the temperature profile would linearly increase with depth in case of constant temperature at the Earth surface, i.e for the stationary state. If the Earth surface is warming, than larger the warming, larger the deflection of temperature profile from the linear behavior; using mathematical inversion methods the past climate can be reconstructed up to 1000 years back. As a rule the linear trend is changed at the depth of the order of 150 m. Reduced temperatures are calculated by subtracting the background thermal regime from the measured temperatures. The deeper we measure temperature the more is the age of reconstructed surface temperature. There are good preconditions for application of geothermal method of reconstructing past temperatures up to 1000 year AD in Georgia and Caucasus. We have precise devices for temperature measurements in boreholes and good network of deep boreholes, which covers the whole region of Caucasus. Geothermal reconstruction of past temperatures seems to be a principal point for

making decision on the existence of very warm periods in Georgia in 10th and 13th centuries AD, before industrial era.

Of course, the present warming also can be partly of natural origin, but the man-made positive feedback could significantly fasten natural process.

3. Assessments of future climate change in the World and Regions

Prediction of the future climate change is an extremely complicated problem (Palmer, 1998; Johns T. et al. 2003 and references in them). There are mainly two approaches to solution: i. creation of mathematical model, using system of equations, which define contribution of different factors to the Earth climate, namely positive and negative feedbacks. There are more than 20 such models, which are too complicated for analytical solution and are solved by special computer programs; ii. statistical analysis of existing climate data, including indirect data and prediction of future changes using this information.

The mentioned models of future warming are calculated for different scenarios, which prescribe different weights to above listed feedbacks. Fig. 6 illustrates warming rates for different emission scenarios developed by the Intergovernmental Panel on Climate Change (IPCC) for the period from 1900 to 2100 (<http://www.ipcc.ch>) and Table 3 shows assessments of temperature increase for 8 different models. In total, there are forty emission scenarios, and they are grouped into six scenario "families": A1B, A1FI, A1T, A2, B1 and B2. The lowest growth is expected for scenarios B1 and B2 and the highest growth for the cases A1F1 and A2.

Table 3.3. Temperature Increase 2000 to 2100 (°C)

Model	Tot al	Lan d	Ocea n
CCSR/NIES	4.7	7.0	3.8
CCCma	4.0	5.0	3.6
CSIRO	3.8	4.9	3.4
Hadley Centre	3.7	5.5	3.0
GFDL	3.3	4.2	3.0
MPI-M	3.0	4.6	2.4
NCAR PCM	2.3	3.1	2.0
NCAR CSM	2.2	2.7	2.0

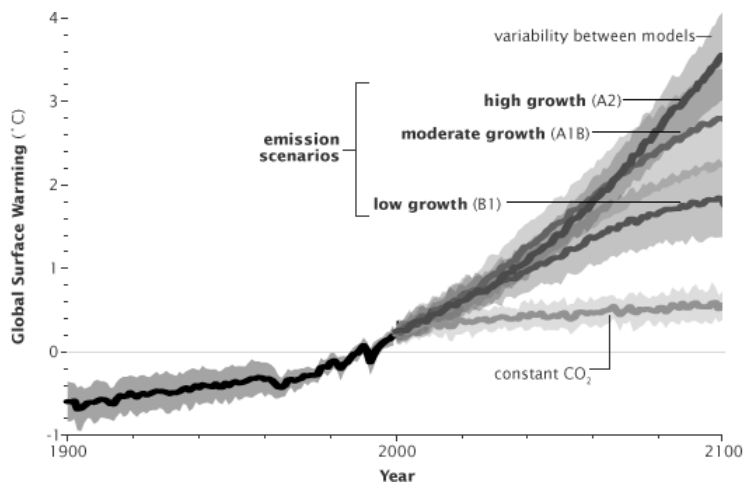


Fig. 3. Global warming simulations by the Intergovernmental Panel on Climate Change (IPCC). Earth will warm between two and six degrees Celsius over the next century, depending on how fast carbon dioxide emissions grow. Scenarios that assume that people will burn more and more fossil fuel provide

Both the climate and climate change vary from region to region. That is why besides global change (GCM) models covering scales of order of hundreds of km, development of regional climate change models (RCM) for processes covering scales from hundreds to several km is necessary (Brohanet al, 2006).

4. On the future climate change in Georgia - new statistical assessments:

In this part of work were used the data of the Hydrometeorological department of Georgia about the monthly average values of air temperature in 12 locations of Georgia (Table 1) for the period 1907-2006 (in Tbilisi 1850-2006 data are available). The data about monthly average values of Global Land, Global Land North Hemisphere and Zonal 24N-64N territories air temperature were used also for comparison [http://www.giss.nasa.gov].

The simplest prediction can be done by just extrapolation of time series: for example let us consider the extrapolation of 156 year Tbilisi temperature data (Fig. 4), which are best fitted by second order polynomial. The extrapolation display for the period 1850-2055 the increment $\Delta T = 2.4^{\circ}\text{C}$ with the most part of ΔT is in the last hundred years, from 1950 to 2050 and for the longer period 1850-2105, the increment $\Delta T = 4.4^{\circ}\text{C}$ with the most part of ΔT is in the last hundred fifty years, from 1950 to 2105.

It is interesting to note that this simplest extrapolation gives the assessment of temperature increment comparable with the predictions of the complicated mathematical models (Fig. 3).

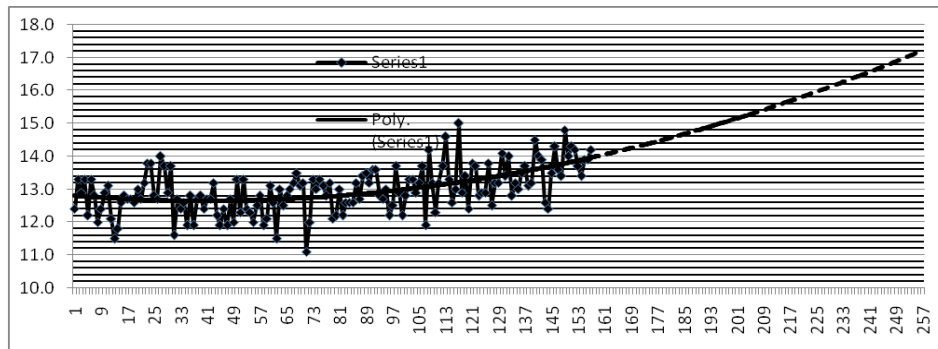


Fig. 4. Simple second order polynomial extrapolation of 156 year Tbilisi temperature data (see also Fig.3) to the year 2105.

Expected Temperature Change to 2055- statistical assessments

In this part we show results of (linear) statistical assessments of future trends in climate in Tbilisi (Fig. 7) and 12 locations in Georgia, marked on the map (Fig.2), using modern methods of statistical assessments: autocorrelation, correlation fields, revealing periodicities, analysis of residuals etc.

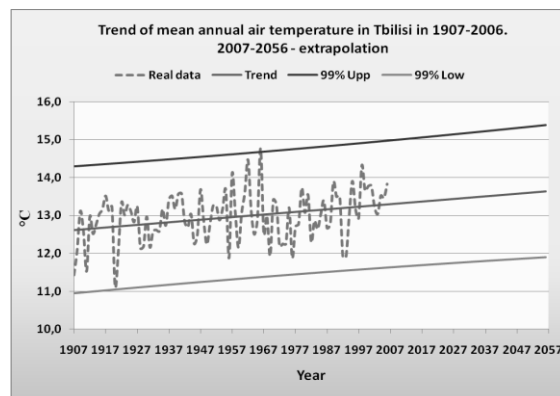


Fig 7. Trend and forecast of mean annual air temperature in Tbilisi using linear approximation. Upper and lower 99% limits are also shown.

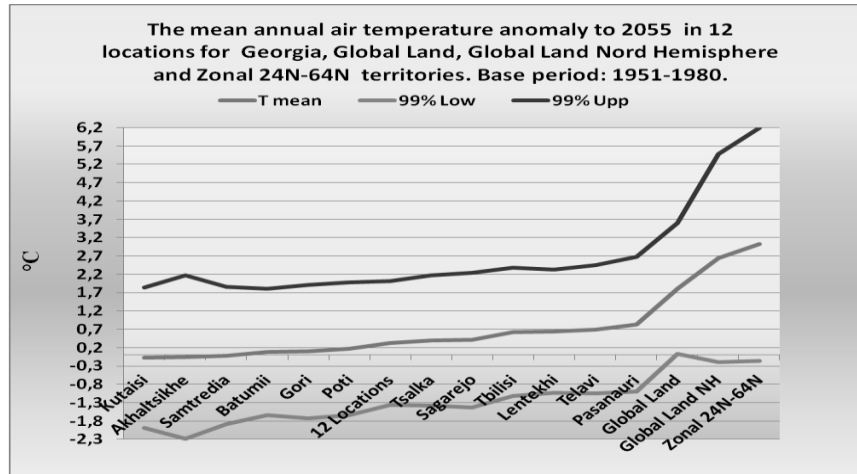


Fig. 8. The mean annual air temperature change prediction for 2055 in 12 locations for Georgia, Global Land, Global Land Nord Hemisphere and Zonal 24N-64N territories

In the correspondence with that indicated above to 2055 year the following values of the anomalies of mean air annual temperature (base period: 1951-1980) are expected for 12 Locations of Georgia (Fig. 8): Kutaisi: $-1.98 \leq -0.07 \leq 1.85$; Akhaltsikhe: $-2.29 \leq -0.06 \leq 2.17$; Samtredia: $-1.89 \leq -0.01 \leq 1.87$; Batumi: $-1.64 \leq 0.08 \leq 1.80$; Gori: $-1.72 \leq 0.10 \leq 1.92$; Poti: $-1.65 \leq 0.17 \leq 1.99$; : $-1.36 \leq 0.33 \leq 2.02$; Tsalka: $-1.38 \leq 0.39 \leq 2.17$; Sagarejo: $-1.43 \leq 0.41 \leq 2.25$; Tbilisi: $-1.11 \leq 0.63 \leq 2.38$; Lentekhi: $-1.04 \leq 0.65 \leq 2.33$; Telavi: $-1.05 \leq 0.70 \leq 2.45$; Pasanauri: $-0.99 \leq 0.84 \leq 2.67$. These values are less than predictions for the Global Land: $0.04 \leq 1.81 \leq 3.59$; Global Land NH: $-0.19 \leq 2.64 \leq 5.47$ and Zonal 24N-64N: $-0.15 \leq 3.02 \leq 6.20$, which is accordance with the IPCC assessments that Georgia is the zone of weak or moderate climate change.

Analysis reveals the existence of several periodic components in the air temperature time series.

As it follows from Fig. 9 periodic components, present in time series of mean annual air temperature for 12 stations of Georgia for real and residual data, are practically the same (20, 12.5, 9, 7.2 years etc.). Periodic components of mean annual global air temperature for real and residual data (Fig. 10) are similar for 20 years periodicity, but do not coincide (are shifted) for some ranges (11.5, 10 years etc.). We can only guess on the nature of these periodicities: as the temperature variations depend strongly on sun radiation, it seems reasonable to relate them to solar cycles, which are reflected in interplanetary magnetic field – IMF (Takalo, Mursula, 2002). For example, 20-22 years component can be related to 22-years long Hale cycle of solar magnetic field. There are also periodicities in IMF connected with well-known 10-12 year solar cycle and its first two harmonics, 5-6 and 2.5-3 years; some of temperature field periods are close to observed in the IMF: namely, 12.5, 5- 6.5 and 2.5-3 years periods in temperature field are close to 10-12, 5-6 and 2-3 years periodicities in IMF.

Multitude of periodic components in the spectra points to necessity of complexity (nonlinear dynamics) analysis of temperature time series, namely, analysis of scaling, fractal dimension etc, which will be presented in the final part of the paper.

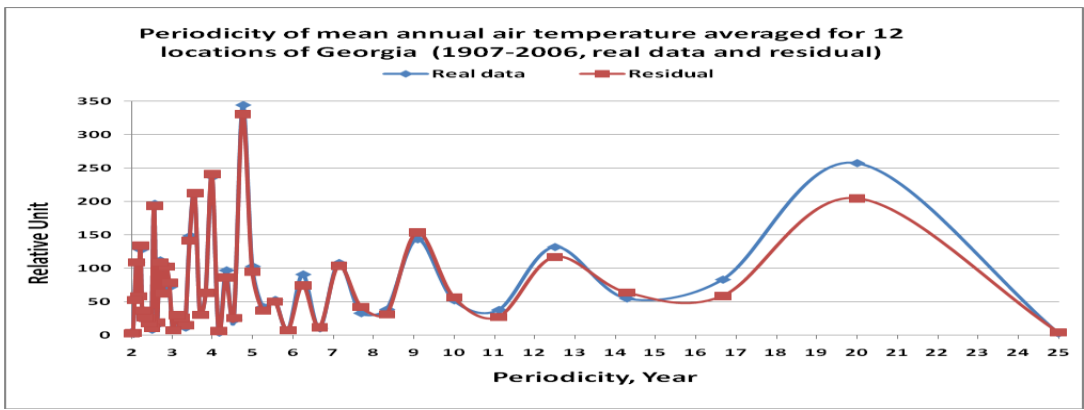


Fig. 9. Periodicities of mean annual air temperature averaged for 12 stations of Georgia (real data and residual)

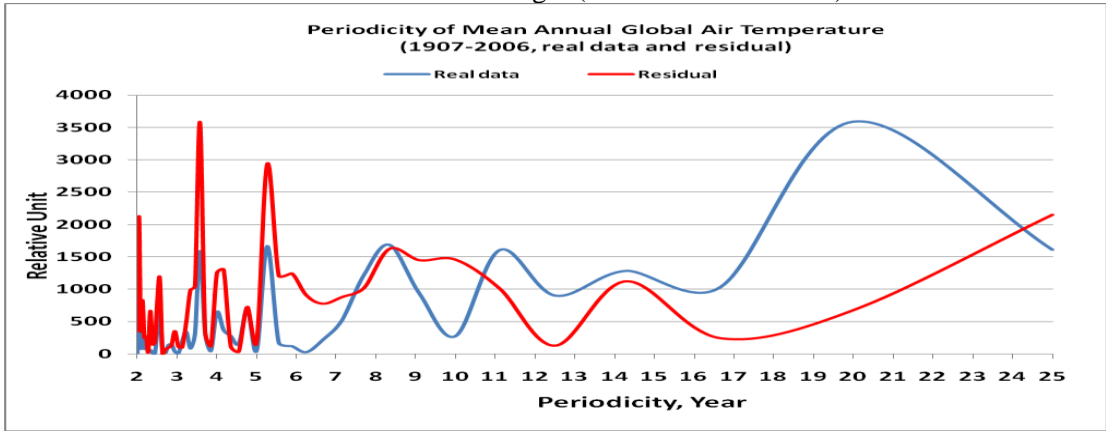


Fig. 10. Periodicities of mean annual global air temperature (real data and residual)

5. Past and Future Climate Change: nonlinear dynamics predictions, regional effects

Why is it necessary to use nonlinear dynamics tools for climate change studies? The matter is that atmospheric flows, an example of turbulent fluid flows exhibits signatures of nonlinear dynamics and chaos. They are characterized by self - similar fractal fluctuations of all space - time scales ranging from weather scale of days and month to climate scales tens and more years. Such types of dynamics of natural processes, when forming patterns have different character on different time and space scales, is too complex to be described by traditional (linear) statistical methods. Besides potential of scaling analysis, nonlinear dynamics reveals hidden nonlinear structures in sequences, which at the first glance seem to be random, in other words, reveal order in seemingly disordered data. As a rule such complex dynamics is difficult to be quantified. Fortunately in the last years new methods were developed, which allow to range quantitatively different levels of complexity allowing detection, identification and ordering from fully random (white noise) to more ordered types of systems behavior.

Thus used nonlinear dynamics tools give new important quantitative information on climate patterns – the degree of order in climatic time series, long-term correlations and their variation with space and time scales.

In this research in order to quantify scaling features in temperature data sets we used method of Detrended Fluctuation Analysis - DFA [Peng, et al. 1994, 1995] as well as Recurrence plots (RP) and Recurrence Quantitative Analysis (RQA).

According to DFA results presented as $F(n)$ vs. n relation (Fig. 11) and DFA exponent α (Fig.12), for 30-35 day length time scale, mean air temperature data of Tbilisi and Kutaisi from 1936 to 2006 (DFA

exponent $\alpha = 1.16$ and 1.04 accordingly) indicates different scaling features for different time scales. Fluctuations for Kutaisi ($\alpha = 1.04$) are $1/f$ noise ($\alpha = 1.0$) type process while for Tbilisi ($\alpha = 1.16$) dynamics of air temperature fluctuations is shifted to Brownian motion type ($\alpha = 1.5$). It is interesting that fluctuations on the larger time scales from month to one year reveal clear persistent, long-range power law correlations ($\alpha > 1.5$). Differences in dynamics of air temperature fluctuations is noticeable on one year time scale, where we see two crossovers on $F(n)$ vs. n relation. For Kutaisi process is not clearly flicker noise ($\alpha = 1.27$) but is far from to be regarded as close to Brownian motion as it is the case for air temperature fluctuations in Tbilisi ($\alpha = 1.42$).

It is worth to mention here, that for time scales larger than one year process always looks as strongly antipersistent, i.e. at this time scales stability of observed trends is questionable and inversion of observed trends is a typical feature of dynamical process. Results of DFA analysis are presented in Figs. 2-4. From these data it follows that such patterns as persistent over larger than 1.5-2 year time scale heat (droughts) periods as well as persistent cold regimes are less probable in Georgia.

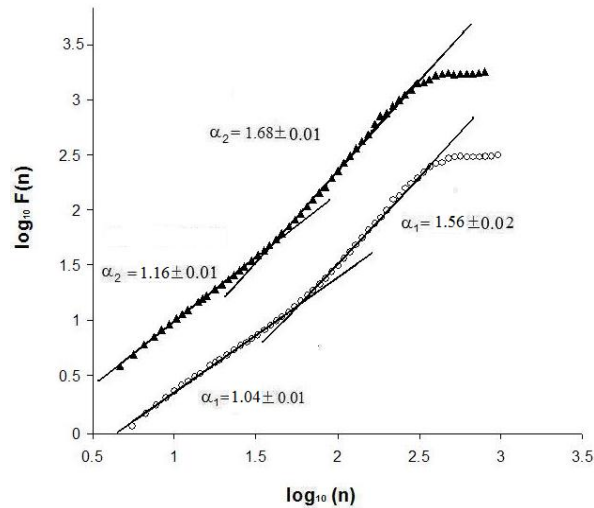


Fig.11. DFA analysis for daily mean temperature data Tbilisi 1936 -2006 (black triangles), Kutaisi 1936-2006 (white circles). 10 year windows one year step. Note crossovers at about 30-35 days and 350-370 days time scales.

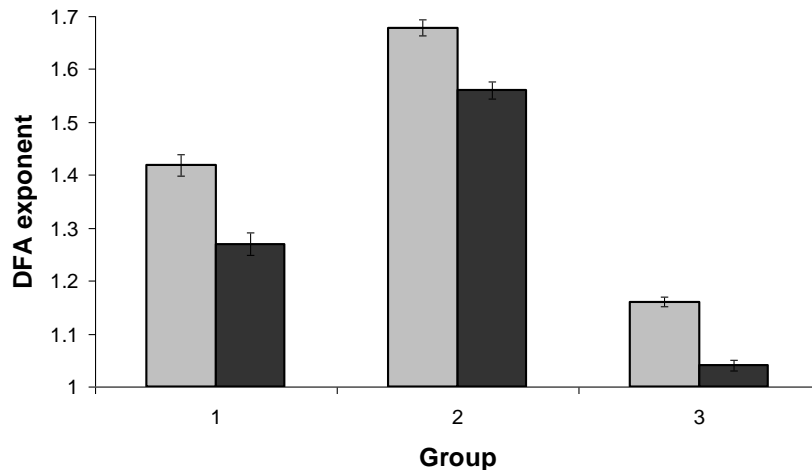


Fig. 12. Averaged DFA scaling exponents of daily mean temperature data Tbilisi 1936 -2006 (gray columns), Kutaisi 1936-2006 (dark columns). 3650 days windows 365 step. 1) one year time scale, 2) time scale from one month to one year, 3) one month time scale.

In Fig. 13 slopes of DFA vs. n relation are presented for daily mean temperature data from 1936 to 2006. Slopes are calculated for consecutive 10 year sliding windows with one year step. It follows from here that for both considered data sets scaling exponent is largest for time scales from one month to one year (upper pair of curves). Scaling exponent is smallest for one month time scale (lower pair of curves).

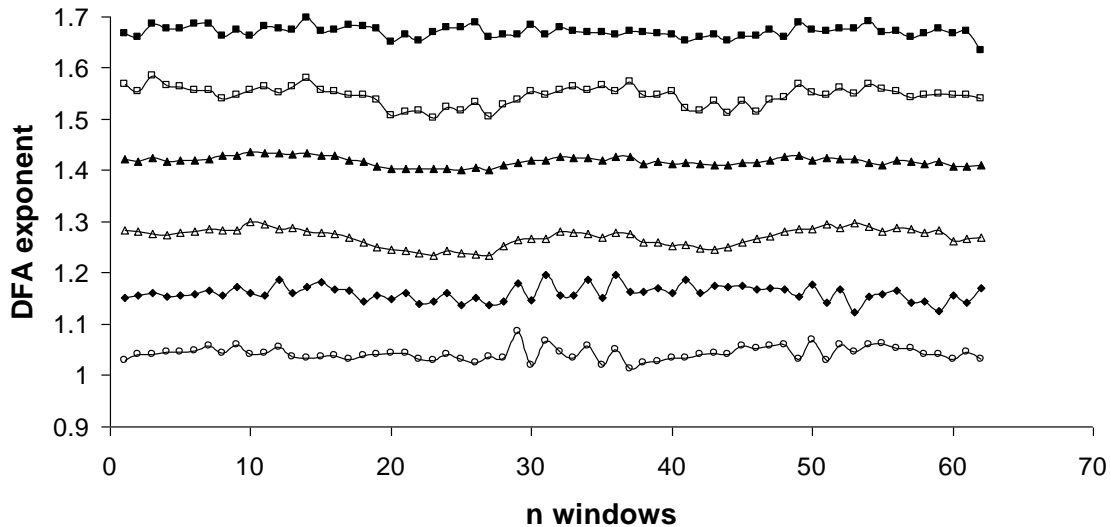


Fig. 13. Calculated for consecutive sliding windows (3650 days windows 365 step) DFA scaling exponents of daily mean temperature data Tbilisi 1936 -2006 (first, third, fifth curves from top), Kutaisi 1936-2006 (second, fourth, sixth curves from top). Dark and open squares, triangles and diamonds correspond to Tbilisi and Kutaisi data accordingly.

Taking into consideration that value of DFA exponent close to 1 means that investigated process is similar to white noise, it can be assumed, that daily temperature variation in Tbilisi is more regular comparing to Kutaisi for all considered time scales.

The variation of DFA exponents' values reveal some periodic features. In order to better visualize suggested quasi-periodicity in scaling features of analyzed data we used Savitzky Golay smoothing and filtering procedure for calculated DFA slope values for 3 different time scales – one year, one month to one year and one month (see e.g. Figs. 14,15,16).

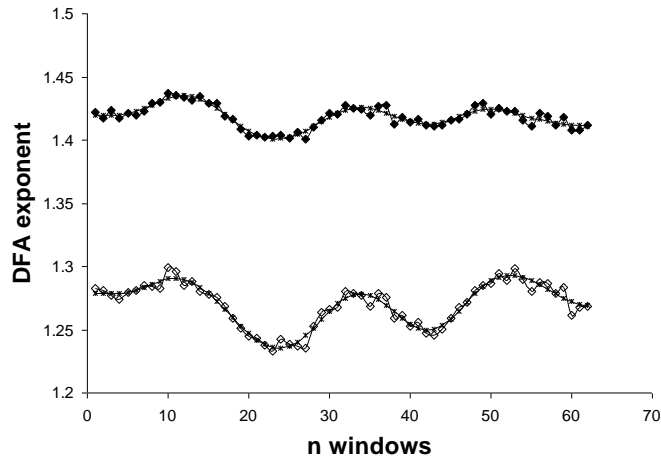


Fig. 14. Smoothed by Savitzky Golay filtering DFA scaling exponents for Tbilisi (top) and Kutaisi(bottom) mean daily temperature data, 1936-2006, One year time scale. Asterisks correspond to smoothed data.

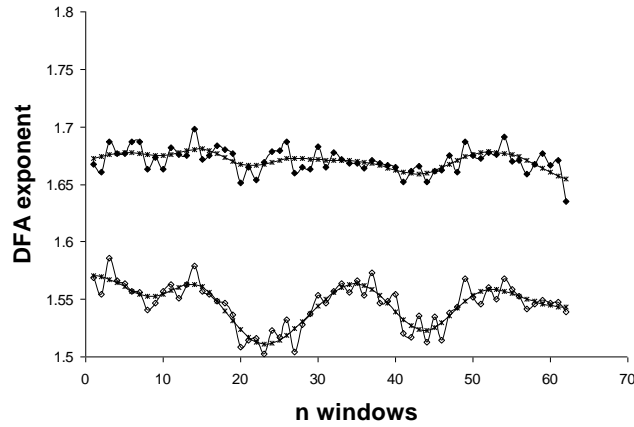


Fig. 15. Smoothed by Savitzky Golay filtering DFA scaling exponents for Tbilisi (top) and Kutaisi(bottom) mean daily temperature data, 1936-2006, Time scale from one month to one year. Asterisks correspond to smoothed data.

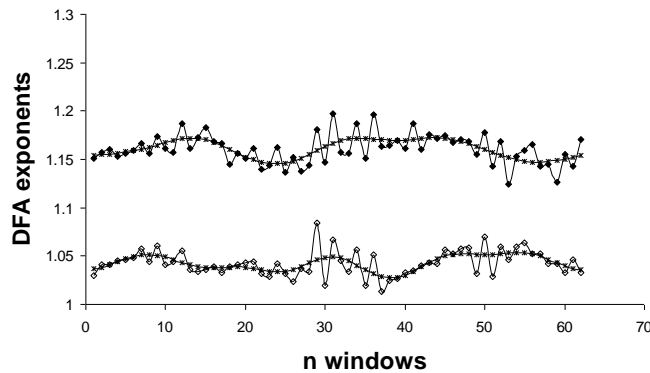


Fig. 16. Smoothed by Savitzky Golay filtering DFA scaling exponents for Tbilisi (top) and Kutaisi(bottom) mean daily temperature data, 1936-2006. One month time scale. Asterisks correspond to smoothed data.

We see from these results that scaling features of temperature data sets reveal periodic patterns but in different extent depending from time series and considered time scales. Namely about 24 year cycles are visible for longer (one year and one month to one year) time scales in DFA exponents of Kutaisi data sets while for one

month time scale such periodic patters are questionable (Fig.5, 6). For Tbilisi data sets about 24 year periodic cycle is visible only for longest one year time scale.

As far as in period 1936-2006 Tbilisi data reveal quasiperiodic patterns only on one year time scale, in Fig. 17 we show DFA scaling exponents calculated for consecutive 10 year windows by one year step of longest available data sets from 1881-2006. In this Figure by asterisks Savitzky Golay smoothing is shown. According to our results quasiperiodic patterns are more characteristic for the last several decades of observation period.

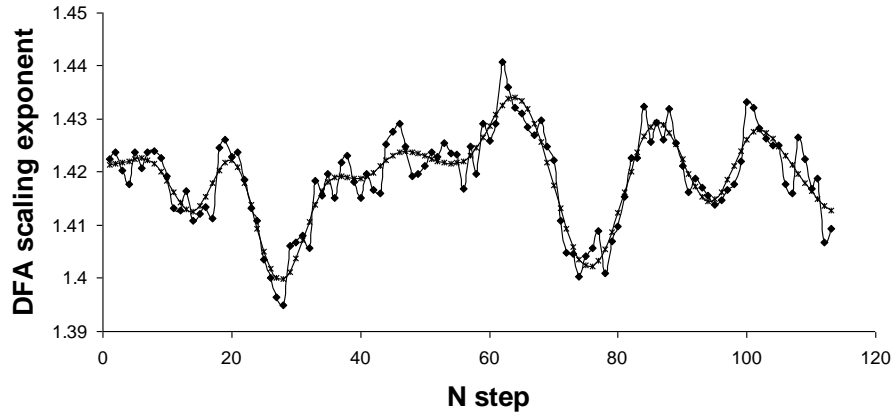


Fig. 17. DFA scaling exponents calculated for 1881-2006 Tbilisi daily temperature data, 10 year sliding windows one year step. Smoothed by Savitzky Golay filtering is shown by asterisks.

After documentation by DFA technique of differences in the scale depending long term correlation features of air temperature variation another methods: Recurrence plots (RP) and Recurrence Quantitative Analysis (RQA) were applied as a well recognized mean to detect and quantify recurring patterns (Marwan, 2003).

In addition to said above in methodology section RQA is a tool for qualitative and quantitative evaluation of nonlinear dynamical structure. It is sensitive and effective even for relatively short time series. Recurrence plots (Fig.18) shows much regular pattern for Tbilisi (East Georgia) in comparison to Kutaisi (West Georgia).

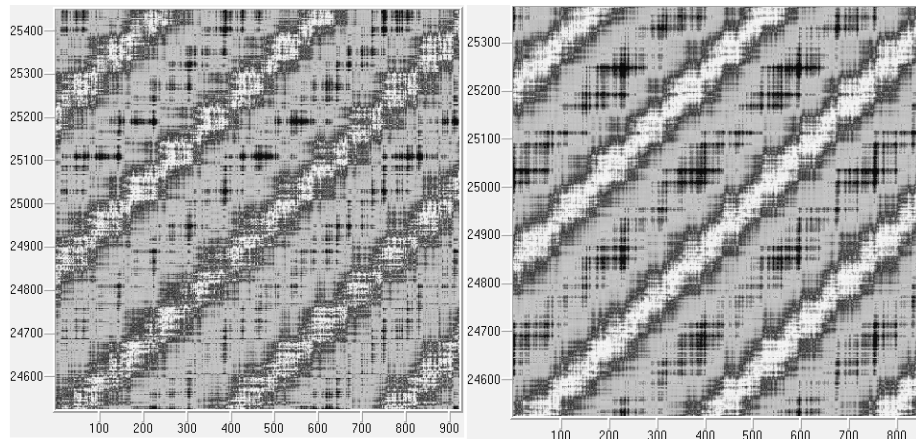


Fig. 18 . Recurrence plot of Kutaisi (left figure) and Tbilisi (right figure) daily mean temperatures data, 1936-2006.

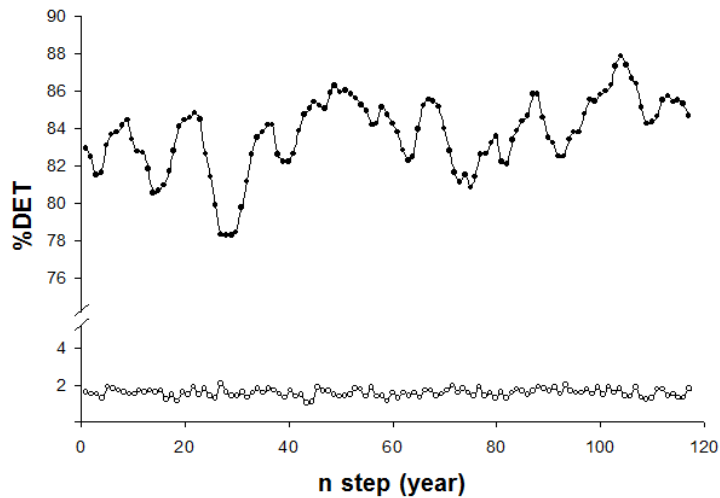


Fig. 5.19. Recurrence quantification analysis of daily mean temperature data Tbilisi 1981-2006, calculated for consecutive 5 year windows by one year step. Lower curve shows randomized time series.

We analyzed the longest available for Tbilisi data sets of daily mean temperatures (1881-2006) from the same point of view. Results presented in Fig. 5.19 show noticeable changes in the extent of regularity for analyzed period. We see prevalence of 10-20 year cycles in %DET variation except period about 1920 to 1950, when these cycles are questionable. Curve shown in the bottom of Fig. 5.19 corresponds to shuffled original data when internal dynamical structure was intentionally destroyed. Presented results indicate that the shuffled series lost all recurrence features manifested in original time series; no type of deterministic structure or extent of regularity is presented.

It is worth to mention that RQA%DET characteristic for all analyzed daily mean temperature data sets from several stations either in the West or East Georgia clearly show presence of increasing trend in the last decades. This points that in spite of differences found between East and West Georgian temperature variations generally the extent of regularity increased to the end of analyzed time period.

After analysis of existing past experimental (instrumental) data we proceed to assessment of possible future scenario of daily mean temperature variation based on concepts of nonlinear time series analysis. For this purpose we used local linear prediction scheme in the phase space. This procedure is inherently linear though is performed in the reconstructed phase space of nonlinear dynamical system and ensures acceptable compromise between quality of forecast and necessary computing resources for complex process.

Exactly we divided original measured time series in two parts to validate prediction model. In Fig. 5.20, we observe weak positive trend (0.11% of adjusted coefficient of multiple determination) in the second half of 1936-2006 Tbilisi daily mean temperature data. Forecasted from the first part of original data reveals almost the same weak trend (compare Figs. 5.20 and 5.21). As far as prediction results in principle coincide with existing data we calculate 10 year forecasting for Tbilisi based on longest available data (Fig. 5.22 14). We see from this Figure weak but still increasing trend in forecasted daily mean temperature values for the next 10 year.

It is also important to mention that forecasted data also reveal increase in extent of order in the temperature daily variation similar to the actual data sets (see e.g. Fig. 5.23 15).

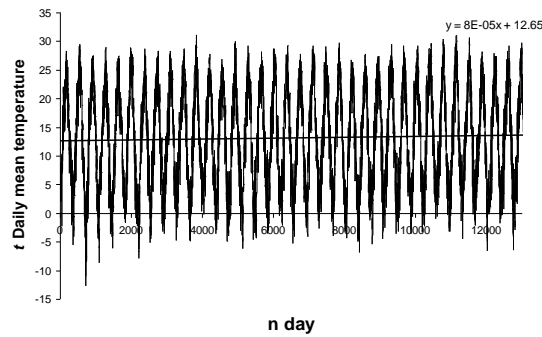


Fig. 5.20 12. Weak positive trend in the second half of Tbilisi mean daily temperature data from 1936 to 2006.

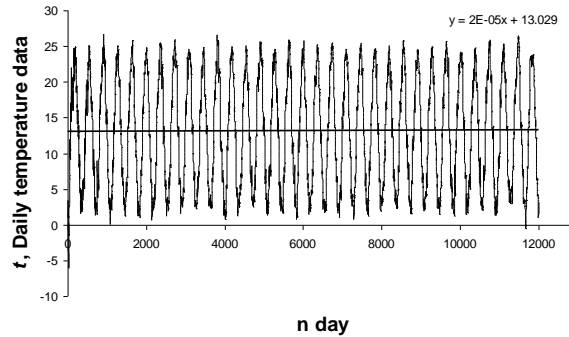


Fig. 5.21 13. Weak positive trend in the forecasted daily temperature (35 year forecast) from the first part of (70 year length data measured in Tbilisi from 1936 to 2006) of the whole time series.

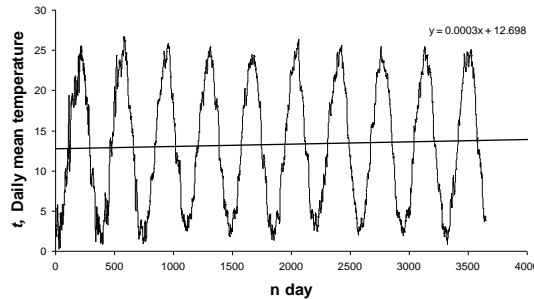


Fig. 5.22 14. Weak positive trend in the forecasted for 10 year Tbilisi daily mean temperatures data sets. Forecast was made based on Tbilisi mean daily temperature time series from 1881 to 2006.

According to our results forecasted data show different rates for different locations, but still all of them manifest increase in mean temperature values: e.g. for Tbilisi (predicted using 1936-2006 data) forecasted increase in the next 10 years is about 0.2% (from 13.10 to 13.12 degree, $\Delta T = 0.02^{\circ}\text{C}$), for Batumi forecasted increase is about 4% (14.50 to 15.15 degree, $\Delta T = 0.65^{\circ}\text{C}$), for Pasaunauri forecasted increase is about 4% (from 7.83 to 8.14 degree, $\Delta T = 0.31^{\circ}\text{C}$), for Poti - 4% (from 14.20 to 14.77 degree, $\Delta T = 0.57^{\circ}\text{C}$), for Samtredia - about 4% (from 14.50 to 15.06, $\Delta T = 0.56^{\circ}\text{C}$), for Kutaisi - about 7% (from 14.66 to 15.72 degree, $\Delta T = 1.06^{\circ}\text{C}$). Such differences may be caused by the quality of used data sets. Anyway for all locations increase in mean daily temperature values was forecasted.

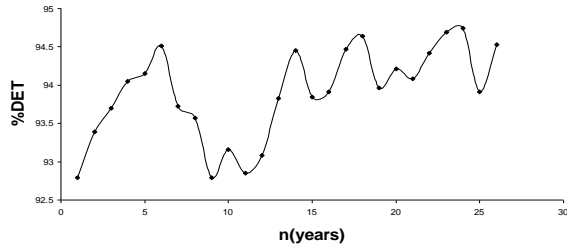


Fig. 5.23 15. RQA %DET values forecast for 1971-1998 calculated from the first part (1936-1970) of Tbilisi mean daily temperature data from 1936 to 2006 period.

Next in order to ensure that our results are not caused by influence of different noises we have carried out procedure, similar to above analysis on denoised original sets. We deliberately have avoided using of standard linear filtering procedures in order to preserve as possible closeness to original dynamical structure of temperature data sets. We performed nonlinear noise reduction procedure in reconstructed phase space of nonlinear dynamical system. As an example in Fig. 5.24 16. denoised and noise part of original data is presented.

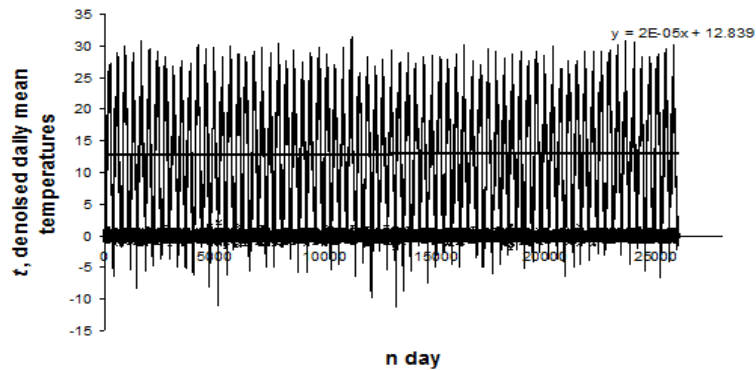


Fig. 5. 24 16. Denoised Tbilisi 1936-2006 daily mean temperature data sets, below is shown the reduced noise contribution to original data.

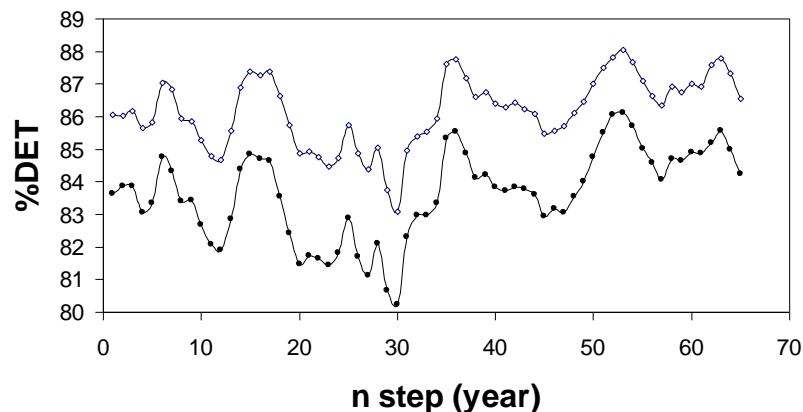


Fig. 5.25 17. RQA %DET of original (dark circles) and denoised (open circles) Tbilisi 1936-2006 daily mean temperature data sets.

As it follows from our results, denoising does not lead to qualitative changes in our results (Fig. 5.25 17). At the same time found variations in ordering are quantitatively more obvious in denoised time series, which is quite logical.

From our results it follows that dynamics of daily mean temperature variation is time and space scale depending process and this particular property can not be analyzed without application of modern tools of complexity theory. In the Eastern part of country dynamics of temperature variation is noticeably regular comparing to the West Georgia. These changes definitely are of local origin. At the same time there are large scale spatio-temporal influences, which cause similar patterns of variation in the extent of regularity in both parts of country.

We also conclude that increase of temperature can be predicted in both parts of Country and this process is not affected by different noises contained in existing data sets.

Conclusions

- There are many gaps in the climate change studies in Georgia, which call for action.
- Palaeo-biological investigations show that there were periods of very warm climate in Georgia (X-XI and XII-XIV centuries) before starting of strong anthropogenic impact.
- For quantitative reconstruction of the past climate the borehole geothermy should be applied.
- The existing instrumental temperature data are from 1850 in Tbilisi and from 1880 in 12 meteorological stations in Georgia. These data were used in analysis of trends and for climate forecast. The detail digital data bases covering the whole observation period (1850-2010) are absent.
- New statistical calculations of the climate regime in Georgia confirm earlier results on the difference in the climate patterns in the Western and Eastern parts of the country. The statistical calculations of temperatures for 2055 on the base of data for 1950-2006 period show that the maximal (local) increment of the average annual temperature is of the order of 0.7°C (settlement Pasaauri, East Georgia), when in the West Georgia the increment is close to zero or negative. This is less than global assessments for the land. It should be noted that the 99% confidence region for increment of the annual temperature in Georgia spans from approximately $+2^{\circ}\text{C}$ to -2°C .
- Common statistical analysis indicates to weak auto-correlation and at the same time reveals several periodicities both in original and detrended time series.
- Extrapolation of the observed temperature trends by statistical methods predict mainly continuation of warming in the East Georgia and cooling or negligible change in the West with predominant warming in the cool periods.
- Nonlinear analysis of temperature data, namely Detrended Fluctuation Analysis (DFA) shows that time series exhibit several time scales with different dynamical characteristics. The long-range correlation features of air temperature fluctuations in Tbilisi and Kutaisi are different. According to another method - Recurrence Quantitative Analysis (RQA) temperature time series are more ordered in the East compared to West Georgia. These differences in the degree of regularity are definitely of local origin.
- The ordering strength of temperature time series vary in time revealing existence in some periods of low-dimensional processes close enough to multi-scale quasi-periodicity, occurring simultaneously in West and East Georgia. We suppose that besides local peculiarities leading to different levels of ordering in both West and East Georgia, there are some global factors leading to similar type of time-dependent dynamics in the both parts of country. Physical mechanism of such regular time-dependence is not clear: our guess is that as the temperature variations depend strongly on sun radiation, it seems reasonable to relate them to solar cycles, which are reflected in interplanetary magnetic field cycles: 20-22 years component in temperature variations can be related to 22-years long Hale cycle of solar magnetic field. Besides, 12.5, 5- 6.5 and 2.5-3 years periods in temperature field are close to 10-12, 5-6 and 2-3 years periodicities in IMF.
- For time scales larger than one year process always looks as strongly antipersistent, i.e. at this time scales stability of observed trends is questionable and inversion of observed trends is a typical feature of dynamical process
- Using nonlinear methods small increase of temperature can be predicted in both parts of Georgia for the next 10 years and this process is not affected by different noises contained in existing data sets.

➤ Taking into account significant differences in climate patterns in the West and East Georgia, for reliable climate change prediction detail regional model should be developed.

Acknowledgements

Authors acknowledge financial support of Open Partial Agreement on Major Disasters at the Council of Europe (EUR-OPA)

References

- [1] Amiranashvili A., Amiranashvili V., Gzirishvili T., Kharchilava J., Tavartkiladze K. - Modern Climate Change in Georgia. Radiatively Active Small Atmospheric Admixtures, Institute of Geophysics, Monograph, Transactions of M.Nodia Institute of Geophysics of Georgian Academy of Sciences, ISSN 1512-1135, vol. LIX, 2005, pp.,1-128.
- [2] Amiranashvili A., Chikhladze V., Kartvelishvili L. – Expected Change of Average Semi-Annual and Annual Values of Air Temperature and Precipitation in Tbilisi, Journal of the Georgian Geophysical Society, Issue B, Physics of Atmosphere, Ocean and Space Plasma, ISSN 1512-1127, vol. 13B, Tbilisi, 2009, pp. 50 – 54.
- [3] Amiranashvili A., Kartvelishvili L., Khurodze T. – Application on Some Statistic Methods for the Prognostication of Long-Term Air Temperature Changes (Tbilisi Case), Basic Paradigms in Science and Technology Development for the 21st Century, Trans. of the Int. Conf Dedicated to the 90th Anniversary of Georgian Technical University, September 19-21, Tbilisi, 2012, vol. 2, pp. 331-338 (in Russian).
- [4] Amiranashvili A., Matcharashvili T., Melikadze G., Chelidze T. - On the Climate Change in Georgia in the Past, at Present and in the Future: What Should be Done for Filling the Gaps – Abstract of 7th Ann. Int. Conf. of REC Caucasus “Climate Change Adaptation – Challenge and Opportunity for Caucasus”, November 10-11, Tbilisi, 2011, pp. 29-30.
- [5] Archer, D. Global Warming. Blackwell. 2007.
- [6] Begalishvili N., Tavartkiladze K., Vachnadze J. - Modern Climate Change in Georgia. Century change of moisture content of atmosphere and its influence on moisture turn, Monograph, Institute of Hydrometeorology of Georgia, Tbilisi, ISBN 9928-885-9-8, 2007, 123 p., (in Russian).
- [7] Brohan, P., J. J. Kennedy, I. Harris, S. F. B. Tett and P. D. Jones (2006), Uncertainty estimates in regional and global observed temperature changes: A new data set from 1850, *J. Geophys.Res.*, *111*, D12106, doi:10.1029/2005JD006548.
- [8] Budagashvili T., Karchava J., Gunia G., Intskirveli L., Kuchava T., Gurgeniidze M., Amiranashvili A., Chikhladze T. - Inventory of Greenhouse Gas Emissions and Sinks. Georgia’s Initial National Communication on Under the United Nations Framework Convention on Climate Change, Project GEO/96/G31, Tbilisi, 1999,137 p.
- [9] Chapman, D. and Davis, M. 2010. Climate Change: Past, Present, and Future. *Eos Transactions*, AGU. Vol. 91, No. 37.
- [10] Dubrova T.A. - Statistical methods of forecasting in economy, the Moscow international institute of the econometrics, computer science, finance and right, M., 2003, 50 p., (in Russian).
- [11] Eckmann, J. P., Kamphorst, S. O., Ruelle, D., (1987). Recurrence Plots of Dynamical Systems, *Europhysics Letters*, *4*, 973-977.
- [12] First National Communication of the Republic of Armenia under the United Nations Framework Convention on Climate Change”, October 1998.
- [13] Forster E., Ronz B. - Methods of correlations and regressions analysis, M., “Finance and Statistics”, 1983, 304 p., (in Russian).
- [14] GINC - Georgia’s initial national communication under the United Nations Framework Convention on Climate Change, Tbilisi, 1999.
- [15] Gobejishvili, R . Glaciers of Georgia, Metsniereba Publ. House, Tbilisi. 1989 (in Russian).
- [16] Hansen, J., R. Ruedy, M. Sato, M. Imhoff, W. Lawrence, D. Easterling, T. Peterson, and T. Karl (2001), A closer look at United States and global surface temperature change, *J. Geophys. Res.*, *106*(D20), 23,947–23,963.

- [17] Harmeling, S. Global Climate Risk Index 2011. Germanwatch e.V. 2010.
- [18] “Human Development Report 2007/2008, Fighting climate change – human solidarity in a divided world”, UNDP 2007.
- [19] Initial Nation Communication of Azerbaijan Republic under the United Nations Framework Convention on Climate Change, Baku 2000.
- [20] Jacob, D. Regional Climate Models. In: Encyclopedia of Complexity and System Science. Springer, 2009, pp. 7591-7602
 Johns T. et al. 2003. Anthropogenic climate change for 1860 to 2100 simulated with the HadCM3 model under updated emissions scenarios. *Climate Dynamics*. 20: 583–612, DOI 10.1007/s00382-002-0296-y.
 Kantelhardt, J. W., S. A. Zschiegner, A. Bunde, S. Havlin, E. Koscielny-Bunde, and H. E. Stanley (2002),
- [21] Multifractal detrended fluctuation analysis of nonstationary time series, *Physica A*. 316, 87-114.
 Kendall M.G. - Time-series. Moscow, 1-200, 1981, (in Russian).
 Kobisheva N., Narovlianski G. - Climatological processing of the meteorological information, Leningrad, Gidrometeoizdat, 1978, 294 p., (in Russian).
- [22] Kvavadze, E., Licheli, V. 2009. The palaeocology and economics of Atskuri in Medieval period. *Bulletin of the Georgian National Museum, Natural Sciences and Prehistory Section # 1*, 68-76,
- [23] Kvavadze, E., Licheli, V., Margvelashvili, P. 2011. Climatic optima in the mountains of Georgia during Middle Age: results of palynological investigation of Navenakhari settlement and Betlemi monastery. INQUA 18-th Congress, Bern, Switzerland, <http://www.inqua2011.ch/>
- [24] Marwan, N., (2003). Encounters With Neighbours Current Developments Of Concepts Based On Recurrence Plots And Their Applications (PhD Thesis, University of Potsdam).
- [25] Maslin, M., Randalls, S. (Eds) 2011. *Future Climate Change*. Routledge.
- [26] National Aeronautics and Space Administration, <http://www.giss.nasa.gov/>
- [27] Palmer, T. N. Nonlinear Dynamics and Climate Change: Rossby’s Legacy. *Bulletin of the American Meteorological Society*, 1998, 1411-1423.
- [28] Peng, C.K., Buldyrev, S.V., Havlin, S., Simmons, M., Stanley, H.E., Goldberger, A.L., (1994). Mosaic organization of DNA nucleotides, *Phys. Rev. E* 49, 1685.
- [29] Peng, C.K., Havlin, S., Stanley, H.E., Goldberger, A.L., (1995). Quantification of scaling exponents and cross over phenomena in nonstationary heartbeat time series, *Chaos*, 5. 82–87.
- [30] Review of the World Climate Research Programme (WCRP). (2009). Paris, International Council for Science. 40 pp. Available at www.icsu.org
- [31] Riebeek, H. 2011. Global Warming. <http://earthobservatory.nasa.gov/Features/GlobalWarming/>
- [32] Rodriguez, E., J. C. Echeverria, and J. Alvarez-Ramirez (2007), Detrended fluctuation analysis of heart intrabeat dynamics, *Physica A: Statistical Mechanics and its Applications*. 384, 2, 429-438.
- [33] Shvangiradze M., Beritashvili B., Kutaladze N. – Revealed and predicted climate change in Georgia and its impact on economy and natural ecosystems. *Papers of the Int. Conference International Year of the Planet Earth “Climate, Natural Resources, Disasters in the South Caucasus”*, *Trans. of the Institute of Hydrometeorology*, vol. No 115, ISSN 1512-0902, Tbilisi, 18 – 19 November, 2008, pp. 76 – 80 (in Russian).
- [34] Sylvén, M., Reinvang, R., Andersone-Lilley, Ž. *Climate Change in Southern Caucasus: Impacts on nature, people and society*. WWF Norway- WWF Caucasus Programme. July, 2008
- [35] Stokes, C.R., Gurney, S.D., Shahgedanova, M. and Popovnin, V. Late 20th century changes in glacier extent in the Caucasus Mountains, Russia/Georgia », *Journal of Glaciology* (52): 99-109, 2006.
- [36] Taghieyeva, U. “Problems of forecasting: The key natural hydrometeorological phenomena affects ecological safety of the South Caucasus in the context of Azerbaijan”, National Hydrometeorological Department, Republic of Azerbaijan, 2006.
- [37] Takalo, J., Mursula, K. 2002. Annual and solar rotation periodicities in IMF components. *Geophys. Res. Letters*. 29, DOI 10.1029/2002GL014658
- [38] Tavartkiladze K., Elizbarashvili E., Mumladze D., Vachnadze J. – Empirical model of ground air temperature field change in Georgia, *Monograph*, Tbilisi, 1999, 128 p., (in Georgian).
- [39] Tavartkiladze K., Shengelia I. – Modern Climate Change in Georgia. Variability of radiation regime in Georgia, *Monograph*, “Metsniereba”, Tbilisi, 1999, 150 p., (in Georgian).

- [40] Tavartkiladze K., Begalishvili N., Kharchilava J., Mumladze D., Amiranashvili A., Vachnadze J., Shengelia I., Amiranashvili V. – Contemporary climate change in Georgia. Regime of some climate parameters and their variability, Monograph, Tbilisi, ISBN 99928-885-4-7, 2006, 177 p., (in Georgian).
- [41] Tavartkiladze K., Amiranashvili A. – Expected changes of air temperature in Tbilisi city, Papers of the Int. Conference International Year of the Planet Earth “Climate. Natural Resources. Disasters in the South Caucasus”, Trans. of the Institute of Hydrometeorology, vol. No 115, ISSN 1512-0902, Tbilisi, 18 – 19 November, 2008, pp. 57 – 65 (in Russian).
- [42] Webber, C. L., Zbilut, J. P., (1994). Dynamical assessment of physiological systems and states using recurrence plot strategies. Journal of Applied Physiology, 76, 965-973.

(Received in final form 20 December 2012)

Изменение климата в Грузии: статистическое и нелинейно-динамическое прогнозирование

А. Амиранашвили, Т.Мачарашвили, Т.Челидзе

Резюме

Парниковый эффект (глобальное потепление) - одна из главных опасностей, стоящей в целом перед планетой. Воздействие на климат происходит из-за роста концентрации парниковых газов (CO_2 , метан, водяной пар): согласно различным оценкам, в конце 21-го столетия температура повысится на 1.4-5.8 °C. Это может привести ко многим разрушительным эффектам, многие из которых невозможно будет предотвратить, что означает, что человечество должно найти способы адаптации к глобальному потеплению.

Грузия, как в целом и Кавказ, подвергается многим отрицательным эффектам, связанным с изменением климата: полное или частичное таяние горных ледников, повышение уровня моря, опустынивание обширных территорий, серьезное воздействие на водные ресурсы.

Несмотря на то, что многие предыдущие работы были посвящены оценке изменения климата в Грузии, результаты все еще неоднозначны. В частности, выполненные исследования показали, что в течение последних десятилетий температура воздуха в Восточной Грузии в среднем повышается, а в Западной Грузии - уменьшается. Эти выводы обсуждены и показано, что необходимо их переосмыслить с учетом использования новых данных и современных методов математического анализа рядов метеорологических наблюдений. Для более надежных оценок необходимо использовать современные методы получения и анализа данных о климате в прошлом, настоящем и будущем.

Другая проблема состоит в том, чтобы установить, является ли указанное потепление исключительно искусственным эффектом, или это результат естественной цикличности в климате Земли.

Особая цель - оценка постоянства и характеристик памяти регионального изменения температуры воздуха в Грузии на фоне глобального изменения климата. Для этой цели проанализирован имеющийся в наличии самый длинный температурный ряд для метеорологической станции Тбилиси (с 1890 г.). Подобные более короткие временные ряды годовых и месячных температур воздуха для 11 станций на Западе и Востоке Грузии также были использованы (1907-2006).

Так как наиболее ошибочные заключения относительно динамических свойств сложной динамики связаны с процедурой “отбеливания данных”, в целях предотвращения разрушения первоначальной динамики, вызванной линейным просачиванием, была использована существующая исследовательская специальная шумовая процедура сокращения ряда времен, так же, как и методика многомерного анализа масштабирования, основанного на SWT. Осуществлены как моно-, так и мультивариантные процедуры реконструкции динамики изменения климата. Проведен также анализ пространственно-временных характеристик средних дневных и месячных значений временных рядов температуры воздуха. Оценена степень постоянства в упомянутых временных рядах.

კლიმატის ცვლილება საქართველოში: სტატისტიკური და არაწრფივ-დინამიკური პროგნოზირება

ა. ამირანაშვილი, თ. მაჭარაშვილი, თ. ჭელიძე

რეზიუმე

სათბურის ეფექტი (გლობალური დათბობა) – ერთერთი იმ საშიშროებათაგანია, რომელიც დგას პლანეტის წინაშე. კლიმატზე ზემოქმედება ხდება სათბური გაზების (CO₂, მეთანი, წყლის ორთქლი) კონცენტრაციის ზრდის გამო: სხვადასხვა შეფასებებით 21-ე საუკუნის ბოლოს ტემპერატურა გაიზრდება 1.4-5.8 °C. ამან შეიძლება მიგვიყვანოს მრავალ დამანგრეველ ეფექტამდე, რომელთა შორის ბევრის თავიდან აცილება შეუძლებელი იქნება, რაც იმას ნიშნავს, რომ კაცობრიობამ უნდა მოძებნოს გლობალურ დათბობასთან ადაპტაციის საშუალებები.

საქართველო, როგორც მთლიანად კავკასია, ასევე განიცდის ისეთ მრავალ ეფექტის ზემოქმედებას, რომელიც დაკავშირებულია კლიმატის ცვლილებასთან: მთის მყინვარების სრული ან ნაწილობრივი დნობა, ზღვის დონის მომატება, დიდი ფართობების გაუდაბნობა, სერიოზული ზემოქმედება წყლის რესურსებზე.

იმის მიუხედავად, რომ არაერთი ადრინდელი ნაშრომი იყო მიძღვნილი კლიმატის ცვლილებასთან საქართველოში, შედეგები მაინც არაცალსახაა. კერძოდ, გამოკვლევებმა აჩვენა, რომ ბოლო რამდენიმე ათწლეულში ჰაერის ტემპერატურა აღმოსავლეთ საქართველოში საშუალოდ მატულობს, ხოლო დასავლეთ საქართველოში – კლებულობს. ეს დასკვნები განხილულია და ნაჩვენებია, რომ საჭიროა მათი ხელახალი გააზრება ახალი მონაცემებისა და მეტეოროლოგიური მონაცემების რიგების ანალიზის თანამედროვე მათემატიკური მეთოდების გამოყენების გათვალისწინებით. უფრო საიმედო შეფასებებისათვის საჭიროა გამოყენებული იქნას კლიმატზე წარსულში, ამჟამად და მომავალში მონაცემების მიღებისა და ანალიზის თანამედროვე მეთოდები.

სხვა პრობლემა იმაში მდგომარეობს, რომ საჭიროა დადგენილ იქნას, არის თუ არა აღნიშნული დათბობა მხოლოდ ხელოვნური ეფექტი, თუ ის შედეგია ბუნებრივი ციკლოზობისა დედამიწის კლიმატში.

განსაკუთრებული მიზანია – საქართველოში ჰაერის ტემპერატურის რეგიონალური ცვლილების მექანიზმების მუდმივობა და მახასიათებლები კლიმატის გლობალური ცვლილების ფონზე. ამისათვის გაანალიზებულია არსებული ყველაზე გრძელი ტემპერატურული მწკრივი თბილისის მეტეოროლოგიური სადგურისათვის (1890 წლიდან). ამგვარი შედარებით მოკლე დროითი მწკრივები წლიური და თვიური ჰაერის ტემპერატურისათვის აღმოსავლეთ და დასავლეთ საქართველოს 11 სადგურზე ასევე იქნა გამოყენებული (1907-2006 წწ.)

რადგან ყველაზე არასწორი დაკვნები რთული დინამიკის დინამიკური თვისებების მიმართ დაკავშირებულია “მონაცემების გათეთრების” პროცედურასთან, პირველადი დინამიკის დანგრევის თავიდან ასაცილებლად, რომელიც გამოწვეულია წრფივი გაუონვით, გამოყენებული იქნა არსებული დროითი რიგების შემოკლების სპეციალური კვლევითი ხმაურის პროცედურა ისევე, როგორც მასშტაბირების მრავალგანზომილებიანი ანალიზის მეთოდიკა, დაფუძნებული CWT –ზე. განხორციელებულია როგორც მონო, - ასევე კლიმატის ცვლილების დინამიკის მულტივარიანტული პროცედურები. ჩატარებულია აგრეთვე ჰაერის ტემპერატურის საშუალო დღიური და თვიური მნიშვნელობების დროითი რიგების მახასიათებლების სივრცულ-დროითი ანალიზი. შეფასებულია აღნიშნული დროითი რიგების მუდმივობის ხარისხი.

Dynamic triggering of local seismic activity in Georgia by the great 2011 Japan earthquake

T. Chelidze, N. Zhukova, A. Sborshchikov, D. Tepnadze
M. Nodia Institute of Geophysics of Iv. Javakhishvili State University

Abstract

Introduction of new sensitive broadband seismographs, new dense seismic networks and new methods of signal processing lead to the breakthrough in triggering and synchronization studies and formation of a new important domain of earthquake seismology, related to dynamic triggering of local seismicity by wave trains from remote strong earthquakes. In the paper are considered the peculiarities of triggered seismicity in Georgia on the example of 11.03.2011 great Tohoku earthquake in Japan. ($M=9$), and moderated earthquake in East Greece (09. 03.2011).

The study of seismic response of the lithosphere to a weak forcing is a fundamental problem for seismic source theory as it reveals the important detail of the tectonic system, namely, how close is it to the critical state. Last years introduction of new sensitive broadband seismographs, new dense seismic networks and new methods of signal processing lead to the breakthrough in triggering and synchronization studies and formation of a new important domain of earthquake seismology, related to dynamic triggering (DT) of local seismicity by wave trains from remote strong earthquakes (Hill, Prejean, 2009; Prejean, Hill, 2009; Hill, 2010). The trivial aftershocks' area is delineated mainly by static stress generated by earthquake and decay rapidly with distance d as d^{-3} , whereas the dynamically triggered stresses decay much slower (as $d^{-1.5}$ for surface waves). That means that dynamic stresses generated by seismic wave trains can induce local seismicity quite far from the epicenter; they can be defined as remote aftershocks. The first well documented DT episode is connected with 1992 Landers earthquake, when the sudden increase of seismicity above background value (calculated as β -statistic of Matthews and Reasenber, 1988) after the main event was observed by many seismic stations at distances up to 1250 km with delays ranged from seconds to days. Later on DT was observed in different remote areas after Denali Fault 2002, Hector Mine 1999, Kurile 2007, Sumatra, 2004 and many other EQ, though most clearly the effect is expressed in active extensional regime areas, as well as in volcanic and geothermal regions.

The main characteristic of DT events are peak dynamic values of stress (T_p) or strain (ε_p); for shear waves $T_p \approx G (u_p/v_s)$ and $\varepsilon_p \approx u_p/v_s$; here G is the shear modulus, u_p is particle' peak velocity and v_s is velocity of the shear wave. Calculated from the field data give values of T_p from 0.01MPa to 1MPa (ε_p from 0.03 to 3 microstrain). Such large scatter is due to the impact of another important factor, namely, the local (site) strength of earth material, which is highly heterogeneous. Thus what matters is not the absolute value of T_p or ε_p , but the difference between local stress and local strength (resistance to failure). This is why in some areas high T_p do not trigger local seismicity and, on contrary, some areas manifest DT even at low peak stresses. One of main factors reducing local strength is the pore pressure of fluids, which is the scope of relatively new direction, so called hydroseismology (Costain and Bollinger, 2010).

The stresses imparted by teleseismic wave trains according to assessments of D. Hill (2008) are 10^5 times smaller than confining stresses at the depth, where the tremors are generated. This is not

surprising as the synchronization theory predicts that even smallest forcing is able to adjust the rhythms of oscillating systems (Pikovsky et al, 2003)

In most cases triggering is observed during surface waves, especially during Rayleigh wave arrivals, i.e. long periods and large intensity of shaking are favorable for exciting remote triggered events. Periods in the range 20-30 sec are considered as most effective in producing triggered events for the same wave amplitude. In principle the optimal period of DT should depend on the earthquake preparation characteristic time and can change from dozens of seconds for microearthquakes to hours and days for moderate events. For tidal stresses with periods 12-24 h the threshold can be as low as 0.001 MPa.

Timing of triggered events is very variable: they can be excited immediately by the some phase of the wave train (say, Rayleigh) or delayed by quite a long time, hours or days. Duration of triggered activity period is also variable - from minutes to a month.

Magnitude of reported triggered events varies between $M = 0.2$ or less to $M = 5.6$. It is likely that most of triggered seismicity are just ignored due to their small intensity and are not included in seismic catalogs. Small (local) triggered events in a given area are revealed using very simple method: the original record of the strong (remote) earthquake are filtered in order to separate low-frequency component (0.01-1 Hz), i.e the dominant component of passing wave train, which can be considered as a forcing and high-frequency component (1-20 Hz), where local triggered events can be recognized.

The triggered events belong to one of two classes: regular earthquakes with sudden onset and so called non-volcanic tremors or tectonic tremors (TT) with emergent onset.

Tectonic tremors are considered as a new class of seismic events related to recently discovered phenomena of low frequency earthquakes and very low frequency earthquakes (Obara, 2003). As a rule individual tremor has dominant frequencies in the range 1-10 Hz, lasts for tens of minutes and propagates with shear wave velocity, which means that they are composed by S body waves. Spatially triggering is most frequently encountered in hydrothermal areas

At present a lot of instances of triggering and synchronization are documented using statistical approach, but the most informative technique is the above mentioned double-filtering method. As a rule, triggered events belong to the class of triggered tremors. Tremor's signatures are: emergent onset, lack of energy at frequencies higher than 10 Hz, long duration from dozens of seconds to several days, irregular time history of oscillations' amplitude, close correlation with large-amplitude surface waves.

Of course, different patterns can be observed also. For example great Tohoku $M= 9$ earthquake, Japan, triggered local seismic events (Figs. 1 a, b) in Georgia (Caucasus), which is continental collision area, separated from Japan by 7800 km. Recorded seismic waves were converted to WAV format with the corresponding sampling rate using tools provided in MATLAB application.

As the Caucasus is dominated by compression tectonics and the triggering examples from such areas are rare, presented data are significant for understanding trigger mechanisms. High pass (0.5-20 Hz) filtered records at two broadband seismic stations located in Oni (South slope of Greater Caucasus) and Tbilisi (valley of river Kura), separated by the distance 130 km show that in this case the strongest triggered event at both sites corresponds to arrival of p -wave instead of surface waves. The sequence of triggered events is quite similar at both stations. Tbilisi is a hydrothermal area and so it falls into general class of triggering-prone regions, but Oni is not a hydrothermal area. Here the fracture can be promoted just by pore fluid pressure.

The comparison of three components of records (N, E and Z) shows that (Fig.2, 3): i. on horizontal components (E and H) triggered events, besides p -arrival are also generated by Love and more intensively by Rayleigh waves; ii. vertical component (Z) generates tremors only at arrival of p - and Rayleigh waves, as it could be expected.

introduction of new sensitive broadband seismographs, new dense seismic networks and new methods of signal processing lead to the breakthrough in triggering and synchronization studies and

formation of a new important domain of earthquake seismology, related to dynamic triggering (DT) of local seismicity by wave trains from remote strong earthquakes.

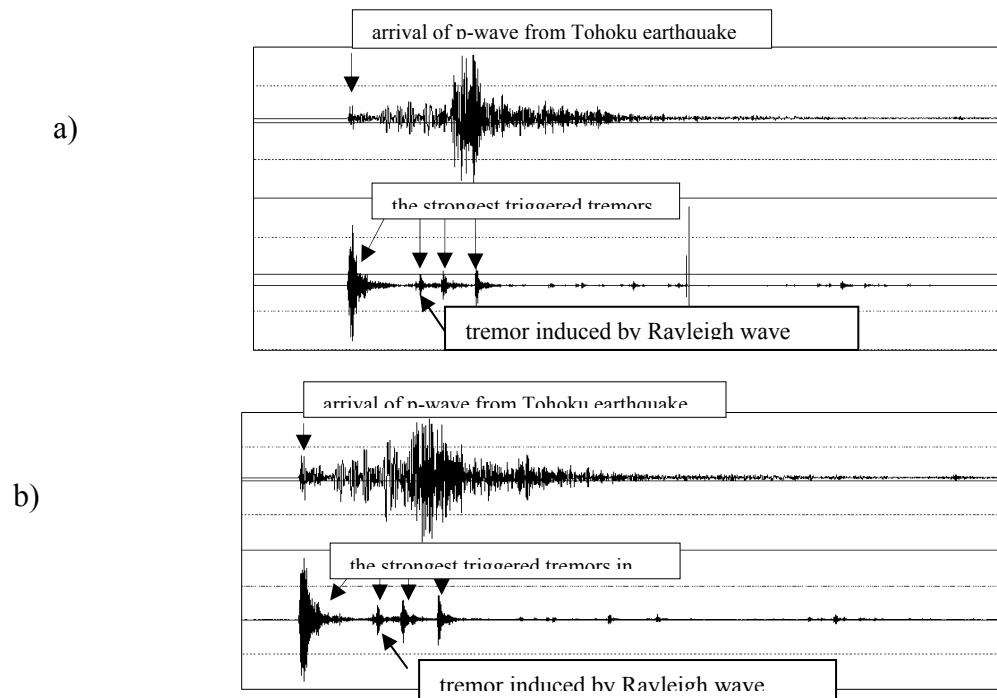


Fig. 1. Broadband record of M= 9 Tohoku EQ, Japan (11.03.2011) wave train z-component (upper channel) and the same high-pass band (0.5-20 Hz) filtered record (lower channel). Arrows mark p-wave arrival. The lower channel shows local triggered events; the strongest event corresponds to arrival of p-wave. a. Oni and b. Tbilisi seismic station.

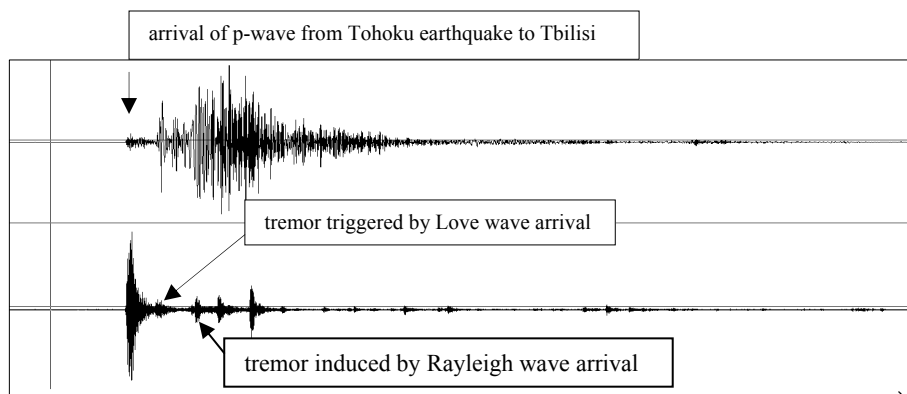


Fig. 2. Broadband record of M= 9 Tohoku EQ, Japan (11.03.2011) wave train N-component (upper channel) and the same high-pass band (0.5-20 Hz) filtered record (lower channel) in Tbilisi. Arrows mark p-wave arrival. The lower channel shows local triggered events; the strongest event corresponds to arrival of p-wave. Here the Love wave also generates relatively weak tremor.

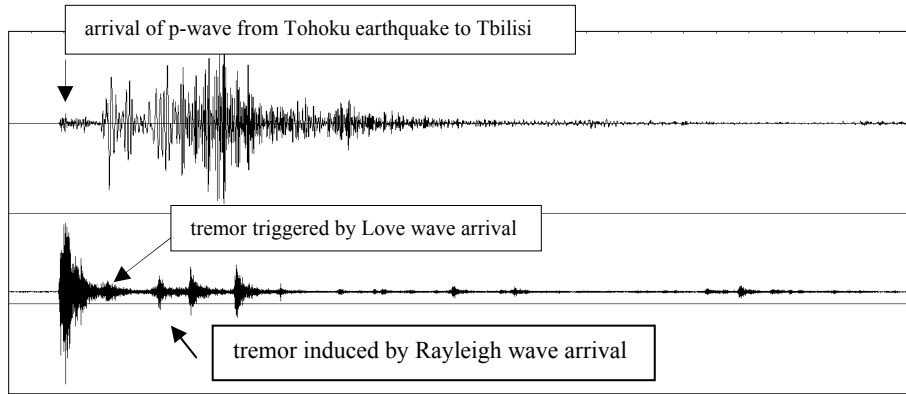


Fig. 3. Broadband record of M= 9 Tohoku EQ, Japan (11.03.2011) wave train E-component (upper channel) and the same high-pass band (0.5-20 Hz) filtered record (lower channel) in Tbilisi. Arrows mark *p*-wave arrival. The lower channel shows local triggered events; the strongest event corresponds to arrival of *p*-wave. Here the Love wave also generates relatively weak tremor.

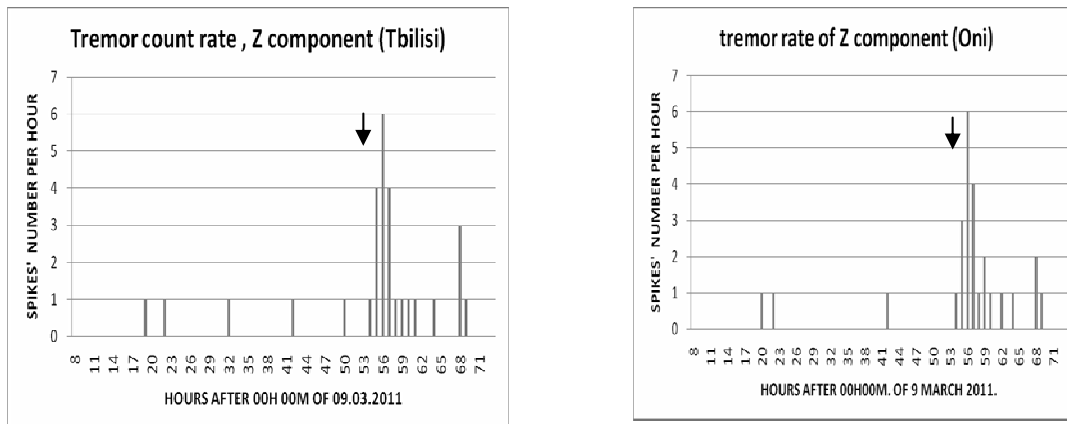


Fig. 4. Tremor rate (number of local events per hour) before, during and after Tohoku event in Tbilisi and Oni. Tohoku earthquake arrival time is marked by arrow.

The counting of tremors' rate (number of local events per hour) before, during and after Tohoku event both in Oni and Tbilisi reveals clear maximum just during the strong earthquake wave train passage, including coda (Fig. 4 a, b), which confirms the reality of triggering phenomenon. The duration of anomalously high tremor rate is of order of 6-8 hours.

Power spectrum of the triggered tremors shows that the maximal energy is released in the frequency range 0.4-0.8 Hz, i.e. these event are deficient at relatively high frequencies (Fig. 5 a). Tremor spectrum differs very much from the power spectrum of the broadband recording of Tohoku earthquake, which indicates that maximal power in Georgia was relieved at much lower frequencies, in the range 0.01-0.1 Hz (Fig.5 b). That means that very low-frequency forcing is necessary for triggering tremors. In other words, forcing of a period 100-10 sec is the time, necessary for tremor area activation.

It is interesting that not only strong earthquakes, but also middle size remote events also can trigger local earthquakes. For example, M=4.6 earthquake in East Greece (09. 03.2003) also triggered local seismicity in Georgia, separated from the epicenter by 1700 km, here again the strongest triggered event coincides with p-wave arrival (Fig. 6 a, b).

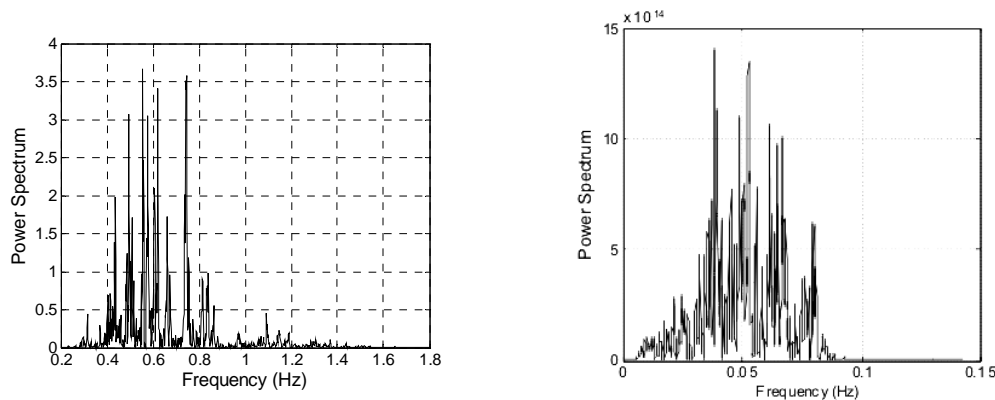
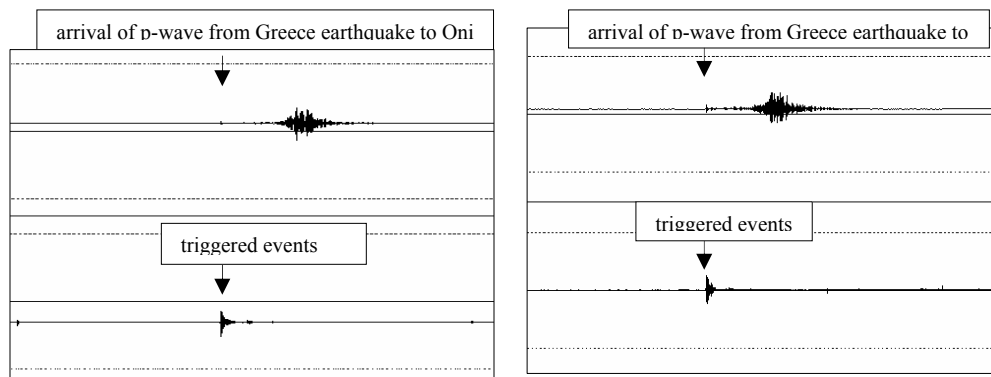


Fig. 5 a. Spectrum of the largest (first) triggered tremor in Tbilisi. Bandpass Butterworth filter was used to filter data in a range 0.5-20 Hz. b. spectrum of the broadband recording of Tohoku earthquake in Oni.



a. Oni

b. Tbilisi

Fig. 6 a, b. Broadband record of M=4.6 earthquake in East Greece (09. 03.2011) wave train z-component (upper channel) and the same high-pass band (0.5-20 Hz) filtered record (lower channel).

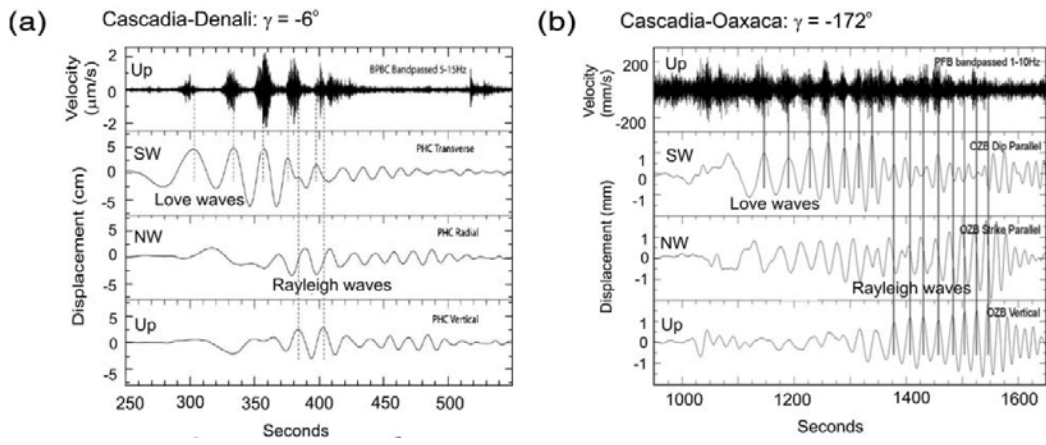


Fig.7. Examples of tremor triggered on the Cascadia megathrust beneath Vancouver Island, B.C., by surface waves from four Mw >7.5 earthquakes with incidence angles γ (Rubinstein et al. 2009; Hill, 2010). The top panel in each example shows broadband displacement waveforms for the incident surface waves (bottom three traces) and the high-frequency (5 to 15 Hz) traces for the triggered tremor (upper trace). (a) The Mw 7.9 Denali fault earthquake of 2002, tremor depth 15 km; (b) the Mw 7.5 Oaxaca earthquake of 1999, tremor depth 35 km

The lower channel shows local triggered events; the strongest event corresponds to arrival of p-wave. a. Oni and b. Tbilisi seismic station

Rubinstein et al. (2009) and Hill (2010) show clearly (Fig. 7a,b) that the weak forcing by wave train of remote strong earthquake can not only trigger, but also induce phase synchronization of induced events with surface waves.

The strong resemblance between our experimental results on electromagnetic (Fig. 8) or mechanical synchronization of stick-slip (Chelidze et al, 2006, 2007, 2010) and large scale natural events (Fig. 7) show that the phenomenon of synchronization has universal character and it can be successfully modeled in laboratory.

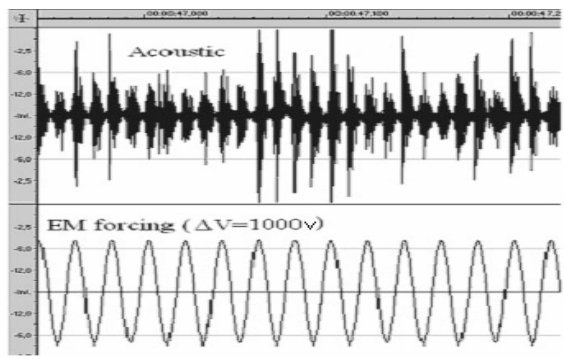


Fig.8. Acoustic emission (upper channel) during slip after application of 1000 V external periodical voltage (lower channel). Note complete phase synchronization between EM forcing and AE.

he physical mechanism of remote triggering is not clear. The mechanism should be different for triggered events closely correlated to wave train phase (direct triggering) and for delayed response.

Hill (2010) assessed (direct) triggering potential of wave trains from the fracture mechanics point of view, using Mohr and Coulomb-Griffiths failure criteria. In general, Love waves incident on vertical strike-slip faults have a greater potential than Rayleigh waves, but the potential of Rayleigh waves incident on dip-slip faults dominates over Love wave potential. At the same time, the fault geometry and frictional strength are variable. Such heterogeneity leads to deviations from the above simple rule.

For large delays frictional failure, subcritical crack growth and excitation of crustal fluids are suggested as appropriate models (Hill, Prejean, 2009; Prejean, Hill, 2009; Hill, 2010).

We can stress close resemblance of our laboratory stick-slip experiments with typical recordings of ETS (Fig. 9); it seems that different morphology of the ETS signals can be explained by the various conditions of frictional motion, in particular, by different stiffness of dynamical system.

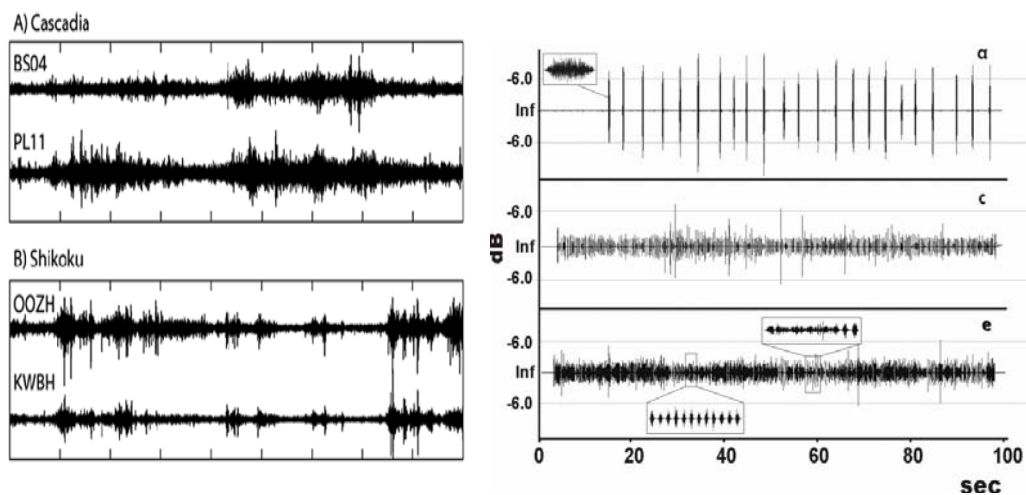


Fig. 9. Left side: recordings of non-volcanic tremor in the Cascadia subduction zone and the Nankai Trough. Records are bandpass filtered at 1–8 Hz. Right side: typical examples of AE recordings at different values of dragging spring stiffness: a) $K=78.4$ N/m, c) $K=1068$ N/m, e) $K=2000$ N/m, f) $K=2371.6$ N/m. Insets show AE wave train on extended time scales.

Obara (2002) and Rubinstein et al (2010) note that periods of tremor activity turn on and off by local or teleseismic earthquakes and remark that ‘no satisfactory model has been proposed to explain how teleseismic event might stop a period of active tremor’.

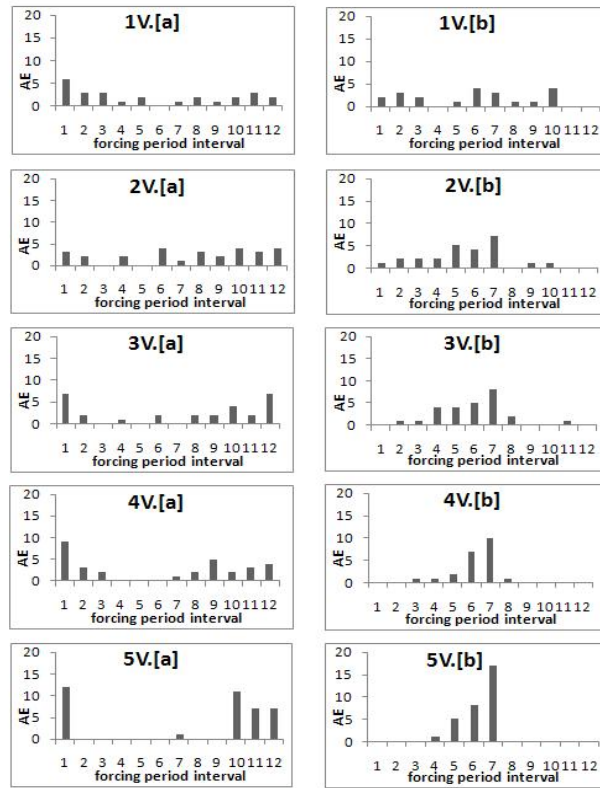


Fig. 10. Distribution of acoustic emission onsets (the left column) and terminations (the right column) relative to the (mechanical) forcing period phase (in twelfths of the forcing period) for different intensities of tangential forcing. Forcing frequency – 80 Hz.

The general explanation of how small-amplitude teleseismic wave can start or stop a period of tremor activity is the extremely high sensitivity of nonlinear systems to a weak forcing. The physical (laboratory) model of mentioned tremor arrest effect has been realized in our experiments with mechanical synchronization of stick-slip (Fig. 10). This remarkable result shows that very small mechanical forcing, 10^5 times smaller than the main driving force can affect both onsets and terminations of stick-slip generated acoustic wave train.

It seems that further development of sensitive devices, dense networks and processing methods will develop a new avenue in seismology, which can be defined as microseismology and which will study systematically small earthquakes and tremors, especially triggered and synchronized events. These events at present are ignored by routine seismological processing and are not included in traditional catalogues. At the same time, microseismic events contain very important information on geodynamics of processes and can give clues to understanding fine mechanism of nonlinear seismic process and may be, even contribute to the problem of earthquake prediction. Microseismicity can be compared by its importance to studies of elementary particles in physics.

References:

- [1] Chelidze, T., O. Lursmanashvili, T. Matcharashvili and M. Devidze. 2006. Triggering and synchronization of stick slip: waiting times and frequency-energy distribution *Tectonophysics*, 424, 139-155
- [2] Chelidze T., and T. Matcharashvili. 2007. Complexity of seismic process, measuring and applications – A review, *Tectonophysics*, 431, 49-61.
- [3] Chelidze, T., Matcharashvili, T., Lursmanashvili, O., Varamashvili N., Zhukova, N., Meparidze. E. 2010. Triggering and Synchronization of Stick-Slip: Experiments on Spring-Slider System. in: *Geoplanet: Earth and Planetary Sciences, Volume 1, 2010*, DOI: 10.1007/978-3-642-12300-9; *Synchronization and Triggering: from Fracture to Earthquake Processes*. Eds.V.de Rubeis, Z. Czechowski and R. Teisseyre, pp.123-164
- [4] Hill, D. Surface wave potential for triggering tectonic (nonvolcanic) tremor. 2010. *Bull. Seismol. Soc. Am.* 100, 1859-1878.
- [5] Hill, D., Prejean, S. 2009. Dynamic triggering. In: *Earthquake seismology*, Volume editor H. Kanamori. Elsevier. pp. 257-293.
- [6] Matthews, M. and Reasenber, P. 1988. Statistical methods for investigating quiescence and other temporal seismicity patterns. *Pure and Appl. Geophys.* 126, 357-372.
- [7] Obara, K. 2003. Time sequence of deep low-frequency tremors in the Southwest Japan Subduction Zone. *Chigaku Zasshi (J. Geogr.)* 112, 837-849.
- [8] Pikovsky, A., Rosenblum, M.G., Kurths. J. 2003. *Synchronization: Universal Concept in Nonlinear Science*. Cambridge University Press, Cambridge
- [9] Prejean S., Hill, D. 2009. Dynamic triggering of earthquakes. In: *Encyclopedia of Complexity and Systems Science*, R. A. Meyers (Ed.), Springer, pp. 2600-2621.
- [10] Rubinshtein et al. 2010, Non-volcanic tremors. In “*New Frontiers in Integrated Solid Earth Sciences*. S. Cloetingh, J. Negendank,(Eds), Springer, Berlin, doi 10.,1007/1007/978-90-481-2737-5. pp. 287-314.

(Received in final form 20 December 2012)

Динамическое триггерирование локальных землетрясений в Грузии сильнейшим землетрясением 2011 года в Японии

Т. Челидзе, Н. Жукова, А. Сборщиков, Д. Тепнадзе

Резюме

Использование новых чувствительных широкополосных сейсмографов, современной плотной сейсмической сети, современных методов обработки сигналов привело к прорыву в изучении таких явлений как триггерирование и синхронизация, и формированию новой важной области в сейсмологии землетрясений, связанной с динамическим триггерированием локальных землетрясений серий волновых пакетов, приходящих от удаленных землетрясений. В данной статье рассмотрены примеры триггируемой сейсмичности в Грузии на примере сильного землетрясения в Тохоку, Япония (11.03.2011, M=9) и среднего землетрясения в Восточной Греции (09.03.2011).

საქართველოში ლოკალური სეისმურობის დინამიკური ტრიგერირება დიდი 2011 წლის იაპონიის მიწისძვრით

თ. ჭელიძე, ნ. ჟუკოვა, ა. სბორშჩიკოვი, დ. ტეფნაძე

რეზიუმე

ახალი მაღალი გრძნობიარობის ფართოსიხშირული სეისმოგრაფებით აღჭურვილი მჭიდრო სეისმური ქსელების შექმნამ და სიგნალის დამუშავების ახალი მეთოდების შემოტანამ განაპირობა გარღვევა მიწისძვრების ტრიგერირების და სინქრონიზაციის კვლევაში. ფაქტობრივად შეიქმნა სეისმოლოგიის ახალი დარგი: ლოკალური სეისმურობის დინამიკური ტრიგერირება შორეული მიწისძვრების ტალღური პაკეტებით. სტატიაში განიხილება საქართველოში ტრიგერირებული სეისმურობის თავისებურობანი 11.03.2011 წლის დიდი ტოხოკუს (იაპონია) და 09.03.2011 აღმოსავლეთ საბერძნეთის საშუალო სიძლიერის მიწისძვრების მაგალითზე.

Stick-slip process and solitary waves

Nodar Varamashvili

M. Nodia Institute of Geophysics of I. Javakhishvili Tbilisi State University, 1 Alexidze str., Tbilisi, 0193, Georgia, ldvarama@gmail.com

Abstract

The mechanism of seismic and various engineering processes are explained well by the theory of stick-slip. We investigated stick-slip process in experimental spring-slider system by recording acoustic emission, accompanying the slip events. In the onset of expanded acoustic recordings can be seen a pulse, which is repeated in other records also. We think that its existence must be associated with solitary waves. Soliton wave arises in the process of stick-slip, propagates along the contact surface between the plates and produces a maximum effect on the upper plate at its end point in the direction of sliding. These impacts may affect triggering of new stick-slip events. It is important to generalize the above considered phenomenon for the earthquake event and to use it for explanation of triggering mechanism of the earthquake.

Keywords: friction, stick-slip, triggering, soliton, earthquake

Introduction

The problem of friction between two surfaces which are in moving contact is very important scientific problem. When the frictional force is nonzero, the friction generally displays two different regimes: a stick-slip motion at low driving velocities and smooth sliding at high velocities. Stick-slip is caused by the surfaces alternating between sticking to each other and sliding over each other, with a corresponding change in the force of friction. This type of sliding has been studied at different scale levels. It seems that the more we learn about friction the more complex it appears (Urbakh et al. 2004). Recent advances in friction reveal that it plays a major role in diverse systems and phenomena. A stick-slip with friction at the contact of blocks is considered by many researchers as one of the most simplified analogs of the earthquake source. Earthquakes occur due to an instability in the deformation of rocks in the earth's crust. The two sides of the fault are driven laterally, in opposite directions, characteristic of a strike-slip fault. Two directions by which we try to understand the physics and complexity of earthquakes are in laboratory studies of rock friction and mathematical dynamic rupture modeling (Scholz, 1998., Marone, 1998). In the last decades increased interest in stick-slip instabilities present in laboratory rock experiments as a means of understanding earthquake ruptures. It is known that, likewise in stick-slip experiments (Ohnaka and Kuwahara 1990, Sobolev 1993, Shibasaki and Matsu'ura 1998), the local deformation effects related to a lower friction on an irregular contact between blocks can cause solitary waves along the contact.

It is well-known that the major portion of earthquakes occurs in accordance with the scenario corresponding to the model of unstable stick-slip on regularly shaped ruptures with the asperities of different size and strength. However, the reported theoretical slider-block models, that is, simple

mechanical models of an earthquake fault, describe stick-slip as a motion of sliding blocks at a smooth stiff surface (Carlson and Langer 1989, Carlson 1991, Dieterich 1992, Hahner and Drossinos 1998).

The principal goals of the study are as follows: (i) modeling the mechanism generating solitary waves; (ii) modeling the observed stick-slip effects; (iii) attempt to explain the effect of stick-slip in the frame of solitary wave theory.

Models of stick-slip

The modern concept of seismic process relies mainly on the model of frictional instability, which develops on the preexisting tectonic fault (Brace and Byerlee, 1966) in contrast with the earlier assumptions on the brittle fracture of the crust material at attaining the critical stress. Modeling dynamic earthquake rupture at multiple scales requires combining many ingredients representing the physics at each scale. Traditionally, this is accomplished using a friction law. These relations, also known as constitutive laws, determine the shear stress on the fault, usually dependent on quantities such as the slip, slip rate, or other dynamic variables quantifying the internal state of the fault.

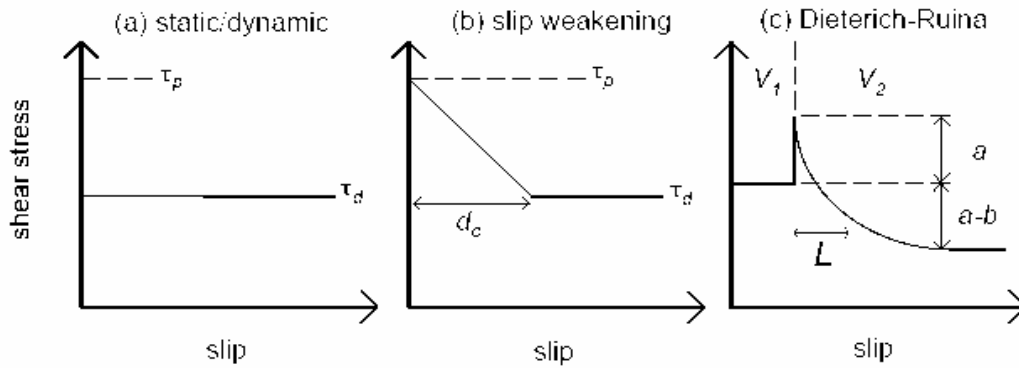


Fig.1. Friction laws for earthquake faults. (a) Static/dynamic friction. (b) linear slip weakening and (c) Dieterich-Ruina Rate and State law (Daub, 2009)

The simplest example of a friction law is the static/dynamic friction law from introductory physics. The shear stress is always proportional to the normal stress, and the proportionality constant μ (i.e. the coefficient of friction) takes on two different values. While the two sides of the fault are in stationary contact, the coefficient of friction is the static coefficient of friction $\mu = \mu_s$ and once the surfaces begin to slip the friction drops to the dynamic coefficient of friction $\mu = \mu_d$. Linear slip-weakening has been used extensively to study dynamic rupture (Ohnaka, Kuwahara, 1990). The slip-weakening law is intentionally simple, and serves as a first approximation for how stress weakens with slip.

Analysis of the experimental data, obtained by investigating of spring-slider system motion, has led to empirical law, named rate- and state-dependent friction law. The rate- and state dependent friction law assumes dependence on a single dynamic state variable in addition to the slip rate. This state variable captures the entire history dependence of friction through its evolution. The fundamental progress was made by experiments of Dieterich and theoretical analysis of Ruina, which show that the friction strength is rate-state dependent (Dieterich, 1979; Ruina, 1983):

$$\tau = \sigma_0 \left(\mu_0 + a \ln \left(\frac{V}{V_0} \right) + b \ln \left(\frac{V_0 \theta}{D_0} \right) \right), \quad (1)$$

where μ_0 is the initial coefficient of friction, V is the new sliding velocity, V_0 is the initial sliding velocity, θ is the state variable and D_0 is the critical slip distance, a and b are two experimentally determined constants.

The state variable varies according to:

$$\frac{d\theta}{dt} = 1 - \frac{V\theta}{D_0} \quad (2)$$

Experiments to study the inhomogeneous friction were carried out on a spring-block model, whose scheme is shown in Fig.1.

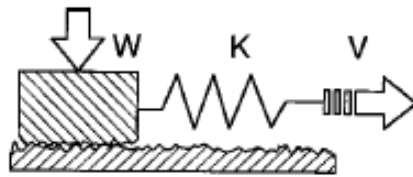


Fig.2. Schematic representation of spring-slider model. W is the weight of the sliding plate, K is the stiffness of spring and V is the velocity of the sliding plate

Depending on conditions (spring stiffness k , velocity of drag V , normal stress σ_n , slip surface state θ) three main types of friction are observed by displacement recording – stick-slip, inertial regime and stable regime, correspondingly, a, b and c in Fig.3.

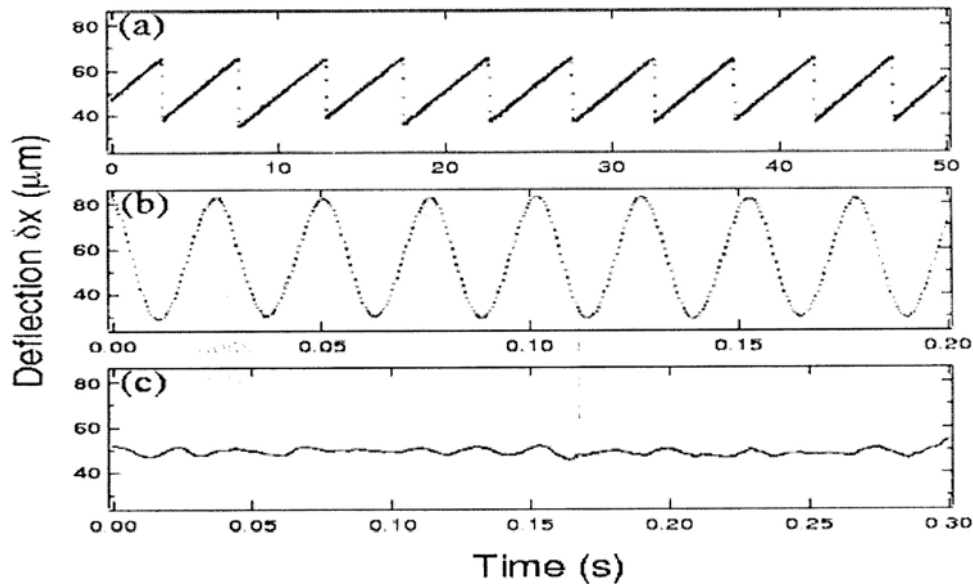


Fig. 3. (a) Stick-slip motion, (b) Inertia-dominated oscillation, (c) Steady sliding motion with fluctuations (Nasuno et al., 1998)

Fig.2 shows spring deflection δx , top plate position x and its instantaneous velocity V . Stick-slip regime is observed at relatively low velocities V and low stiffness. At higher V the transition to inertial periodic oscillations occurs; at still higher V we have the stable sliding with fluctuations.

Experimental setup

The dynamics of the sliding process in the spring-slider model depends on the dragging spring stiffness K and dragging velocity V (Boettcher and Marone, 2004). At low velocity, this process is of relaxation type, at intermediate velocity it is periodic, and at high velocity the sliding became relatively stable, with random deviations.

We investigated (mechanical) triggering and synchronization of instabilities in experimental spring-slider system by recording acoustic emission, accompanying the slip events; the setup is described in detail in Chelidze *et al.* (2006) and Varamashvili *et al.*,(2010). Experimental setup represents a system of two horizontally oriented plates (Fig. 4). The supporting and the slipping blocks were prepared from basalt; these samples were saw-cut and roughly finished. The height of surface protuberances was in the range of 0.1-0.2 mm.

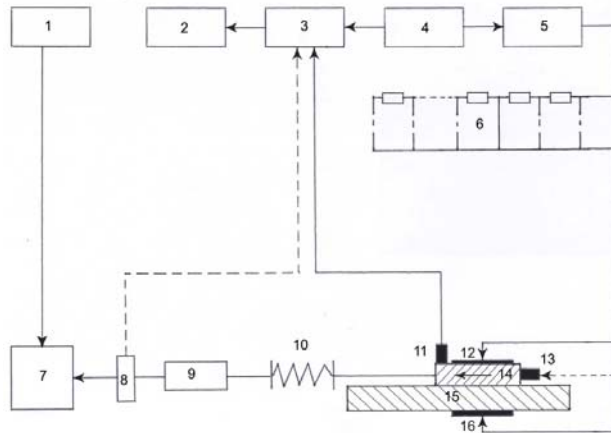


Fig. 4. Schematic representation of the experimental spring-slider model: 1 – Stabilized power source, 2 – personal computer, 3 – amplifier, 4 – forcing signal generator, 5 – external voltage generator, 6 – voltage divider, 7 – dragging device, 8 – tensometer, 9 – dynamometer, 10 – spring, 11 – piezoelectric sensor, 12 – electrode, 13 – vibrator, 14 – sliding block, 15 – fixed block, 16 – electrode.

A constant dragging force of the order of 4 N was applied to the upper (sliding) plate; In presented Figure (Fig.5a) is showing a recording of acoustic pulses of one experiment and in Fig.5b one acoustic pulse in expanded form.

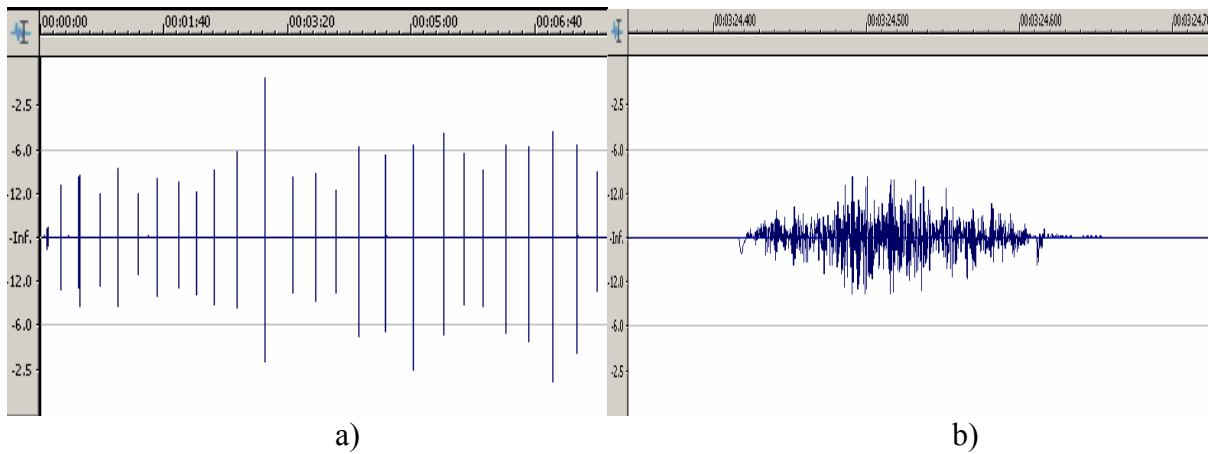


Fig. 5. The full record of AE pulses (a) and a separate acoustic pulse in expanded form (b)

In the beginning expanded acoustic recordings can be seen pulse, which is repeated in other records. Explanation of the nature of this pulse for us has always represented the great challenge.

The model

According to some authors (Bykov, 2006, 2008; Vikulin, 2006; Erickson et al., 2010) in the process of inhomogeneous friction can occur soliton wave that propagates along the friction surface. There are theories of soliton waves excitation in seismic processes (Vikulin, 2006; Lursmanashvili et al., 2010). It is noted from experiments that the strain waves propagating along the block contacts occur prior to the dynamic displacement which is the final stage of the stick-slip cycle. It is just at the boundary between the relatively displaced solid bodies where the generation of the strain waves of different type and scale occurs [Bykov, 2008].

According to Bykov (2008), the contacting surface of each of the interacting blocks is a homogeneous sinusoidal grained surface within asperity. The asperities of the contact surfaces of blocks stick to one another. A slip on the fault plane occurs when the stuck parts move apart.

Soliton-type solutions are also obtained by considering the Burridge-Knopoff model of earthquake. localized in space and oscillate in time however, are known as breathers. The significance of these types of solitary wave solutions was emphasized by Heaton [1990]. These types of soliton or breather solutions emerge for the nonlinear wave equation with Dieterich-Ruina friction, equation (1). These solutions can be understood as a proxy for the propagation of the rupture front across the fault surface during an earthquake and may determine a range for suitable parameter values to be used in dynamic modeling of earthquakes (Erickson et al., 2010).

Conclusion

We think that in Fig. 5 (b) expressed pulse at the beginning of acoustic burst, may be associated with a wave of soliton type. The results obtained by solving the equation sine-Gordon show that the velocity of the exciting soliton wave depends on various parameters, and may change from a few hundred microns/sec to several hundred m/sec (Bykov, 2006, 2008; Vikulin, 2006).

The generalized sine-Gordon equation can be applied for modeling peculiarities of fault dynamics. In fact, contribution of perturbation in the sine-Gordon equation in the form of friction and inhomogeneities leads to the solutions of the solitary-like waves that can be interpreted as the waves of friction activation. At definite values of friction and inhomogeneity parameters, the solitary wave

“acquires” the stationary regime with the values of $v \approx 10^{-4} - 10^{-1} \frac{m}{s}$ (Bykov, 2006, 2008). These waves, migrating along the friction surface, may trigger the stick-slip events.

Stick-slip is not a periodic phenomenon. One of the reasons can be that in each case the velocity profile of arisen soliton waves depends on the specific process parameters. In different cases of stick-slip events, soliton waves may be arisen which have different propagation velocity and respectively, which will trigger new stick-slip events at different time intervals.

The generalized sine-Gordon equation can be applied for modeling peculiarities of fault dynamics. Our goal is to develop a mathematical model of the mechanism of excitation of soliton waves in the process of friction and with its help, in the case of our experiments, to clarify the mechanism of stick-slip. The crustal fault zones are active, nonlinear, and unstable media. Therefore, it follows from the general physical regularities of the nonlinear processes that the solitary wave generation is inevitable in the faults. The solitary wave mechanism can lead to cyclic recurrence of the seismic displacements in the fault, as one of the possible mechanisms of tectonic stress migration in the Earth.

References

- [1] Boettcher, M. S., and C. Marone, Effects of normal stress variation on the strength and stability of creeping faults, *J. Geophys. Res.*, 109, B03406, doi:10.1029/2003JB002824, 2004
- [2] Bykov V.G., Stick-slip and strain waves in the physics of earthquake rupture: experiments and models, *acta geophysica*, v.56, no2, pp. 270-285, 2008, DOI: 10.2478/s11600-008-0002-5
- [3] Bykov, V. G., Solitary waves in crustal faults and their application to earthquakes, In: Teisseyre R, Takeo M, Majewski E (eds) *Earthquake source asymmetry, structural media and rotation effects*. Springer-Verlag Berlin Heidelberg, Chap. 18, 241-255, 2006.
- [4] Brace W.F., and Byerlee, J.D., Stick-slip as a mechanism for earthquakes. *Science.*, 153: 990–992, 1966.
- [5] Burridge, R., and L. Knopoff, Model and theoretical seismicity, *Bull. Seismol. Soc. Am.* **57**, 1967, 341-371.
- [6] Carlson, J.M., Time intervals between characteristic earthquakes and correlations with smaller events: An analysis based on a mechanical model of a fault, *J. Geophys. Res.* **96**, 1991, 4255-4267.
- [7] Carlson, J.M., and J.S. Langer, Properties of earthquakes generated by fault dynamics, *Phys. Rev. Lett.* **62**, 1989, 2632-2635
- [8] Chelidze, T., O. Lursmanashvili, T. Matcharashvili, and M. Devidze, Triggering and synchronization of stick slip: waiting times and frequency-energy distribution, *Tectonophysics* **424**, **2006**, 139-155.
- [9] Dieterich, J.H., Modeling of rock friction 1. Experimental results and constitutive equations, *J. Geophys. Res.* **84B**, **1979**, 2161-2168.
- [10] Dieterich, J.H., Earthquake nucleation on faults with rate- and state-dependent strength, *Tectonophysics* **211**, 1992, 115-134.
- [11] Erickson B., Birnir B, and Lavallee D, A model for aperiodicity in earthquakes, *Nonl. Proc. Geophys.*, 15, 2008, 1–12.
- [12] Erickson B., Birnir B., Lavallee D., Periodicity, Chaos and Localization in a Burridge-Knopoff Model of an Earthquake with Dieterich-Ruina Friction, Center for Complex and Nonlinear Science, UC Santa Barbara, 2010, <http://escholarship.org/uc/item/3r5811tp>
- [13] Frenkel', Ya.I., and T.A. Kontorova, On the theory of plastic deformation and twinning, *J. Exp. Theor. Phys.* **8**, 1938, 89-95
- [14] Hahner, P., and Y. Drossinos, Nonlinear dynamics of a continuous spring-block model of earthquake faults, *J. Phys. A.* **31**, 1998, 185-191.

- [15] Heaton, T.H., Evidence for and implications of self-healing pulses of slip in earthquake rupture, *Phys. Earth Planet Int.*, Vol 64, 1990, 1-20
- [16] Lursmanashvili, O., Paataashvili, T., and L. Gheonjian, Detecting quasi-harmonic factors synchronizing relaxation processes: application to seismology, in Valerio de Rubeis, Zbigniew Czechowski, Roman Teisseyre (Editors) *Synchronization and triggering: from fracture to Earthquake Processes*, Springer-verlag, DOI 10.1007/978-3-642-12300-9, 2010
- [17] Marone, C., Laboratory-derived friction laws and their application to seismic faulting. *Ann. Revs. Earth & Plan. Sci.*, 26, 643-696, 1998.
- [18] Nasuno, S., Kudrolli, A., Bak, A., and Gollub, J.P., Time-resolved studies of stick-slip friction in sheared granular layers, *Phys. Rev. E* 58, 1998, 2161–2171
- [19] Ohnaka, M., and Y. Kuwahara, Characteristic features of local breakdown near a cracktip in the transition zone from nucleation to unstable rupture during stick-slip shear failure, *Tectonophysics* **175**, 1990, 197-220.
- [20] Ruina, A., Slip instability and state variable friction laws, *J. Geophys. Res.* **88B**, 1983, 10359-10370.
- [21] Scholz, C.H., Earthquakes and friction laws. *Nature* **391**, 1998, 37–42
- [22] Shibazaki, B., and M. Matsu'ura, Transition process nucleation to high-speed rupture propagation: scaling from stick-slip experiments to natural earthquakes, *Geophys. J. Int.* **132**, 1998, 14-30.
- [23] Sobolev, G.A., *Fundamentals of Earthquake Prediction*, Nauka, Moscow, 1993 (in Russian).
- [24] Urbakh, m., J. Klafter., D. Gourdon and J. Israelashvili, The nonlinear nature of friction, *Nature*, 430, 2004, 525-528
- [25] Varamashvili, N., Chelidze, T., Lursmanashvili, O.: Phase synchronization of slips by periodical (tangential and normal) mechanical forcing in the spring-slider model. *Acta Geophys.* **56**, 2009, 357-371
- [26] Vikulin, A. V., Earth rotation, elasticity and geodynamics : earthquake wave rotary model, In: Teisseyre R, Takeo M, Majewski E (eds) *Earthquake source asymmetry, structural media and rotation effects*. Springer-Verlag Berlin Heidelberg, Chap. 20, 273-291, 2006.
- [27] Yuta Abe and Naoyuki Kato, Complex Earthquake Cycle Simulations Using a Two-Degree-of-Freedom Spring-Block Model with a Rate- and State-Friction Law , *Pure and Applied Geophysics*, 2012, DOI:10.1007/s00024-011-0450-8
- [28] Eric G. Daub, *Deformation and Localization in Earthquake Ruptures and Instabilities*, A dissertation submitted in partial satisfaction of the requirements for degree of Doctor of Philosophy in Physics, UCSB, 2009

(Received in final form 12 September 2012)

Процесс стик-слипа и солитонные волны

Нодар Варамашвили

Механизмы сейсмического и разных инженерных процессов хорошо объясняется в рамках теорий стик-слип. Мы исследовали процесс стик-слип: триггерирование и синхронизацию нелинейных явлений в лабораторной системе пружина-блок с помощью регистраций акустической эмиссии сопровождающей событий проскальзывания. В начале расширенной

акустической записи выден импульс, который повторяется в других записях. Мы считаем, что его присутствие связано с солитонными волнами. Солитонная волна появляется в процессе стик-слип, распространяется вдоль поверхности соприкосновения плиток и производит максимальное воздействие на верхнюю плиту, на крайнюю точку по направлению скольжения. Это может вызвать новые события стик-слипа. Важно обобщение рассмотренного выше явления для землетрясения и использование для объяснения механизма триггерирования землетрясения.

სტიკ–სლიპის პროცესი და სოლიტონური ტალღები

ნოდარ ვარამაშვილი

რეზიუმე

სეისმური და სხვადასხვა საინჟინრო პროცესების მექანიზმები კარგად აიხსნება სტიკ–სლიპის თეორიის ფარგლებში. ჩვენ ვიკვლევდით სტიკ–სლიპის პროცესს: ლაბორატორიულ ზამბარა–ბლოკის სისტემაში არამდგრადობების ტრიგერირებას და სინქრონიზაციას სრიალის შემთხვევის თანმხლები აკუსტიკური ემისიის რეგისტრაციით. გაშლილი აკუსტიკური ჩანაწერის დასაწყისში ჩანს იმპულსი, რომელიც მეორდება სხვა ჩანაწერებში. ჩვენ ვფიქრობთ, რომ მისი არსებობა უნდა ასოცირდებოდეს სოლიტარულ ტალღებთან. სოლიტონური ტალღა ჩნდება სტიკ–სლიპის პროცესში, ვრცელდება ფილების შემხები ზედაპირების გასწვრივ და აწარმოებს მაქსიმალურ ზემოქმედებას ზედა ფირფიტაზე, სრიალის მიმართულებით, მის ნაპირა წერტილზე. ამ ზემოქმედებამ შეიძლება გამოიწვიოს სტიკ–სლიპის ახალი მოვლენები. მნიშვნელოვანია ზემოთ განხილული მოვლენა განზოგადდეს მიწისძვრის მოვლენისათვის და გამოყენებული იქნას მიწისძვრის ტრიგერირების მექანიზმის ასახსნელად.

Complex geophysical Investigation of some characteristics of some strong local Guria (Georgia) magnetic anomalies

***G. Lominadze, **K. Kartvelishvili, **G. Berishvili, **N. Mebaghivili,
M. Nikolaishvili, **G.Tabagua, **A. Tarkhnishvili

**Georgian National Academy of Science, **M.Nodia Inst.of Geophysics of Iv.Javakhishvili State University*

Abstract

It should be mentioned, that the "man-made" magneto therapy has a wide application in the world, however the Ureki (Georgia) - Black sea-side health resort, is the only place of natural magneto therapy. In some case it will be a possibility of foundation of a new health resort of natural magneto therapy on the territory of the local magnetic anomaly within the Guria (Georgia) lowland. The local magnetic anomaly detected in the village of Atsana which, like the known Ureki seaside health resort, represents a natural laboratory" with the curative magneto therapeutically environment. The normal value characterizing the magnetic field in Georgia is $T_0 = 48800 \text{ nT}$. The full T component of the magnetic field in Atsana is liable to significant variations within a small area, maximum to 9000 gamma (Whereas the intensity of magnetic storm in our latitude is within 600-800 gamma). Special mention should be made of Atsana north-western slope, where the full T component of magnetic field varies from 45800 to 54800 gamma. Also, significant magnetic field gradients were registered in the river Atsaura basin (47900 - 55600 gamma) and in other places. Gradients in respect of the normal value have been fixed in Atsana, whose characteristic value is $\Delta T_0 = 1000 \text{ nT/m}$ (T-tesla, m-meter, pitch-10m). When moving on a preliminary fixed route path, or "magnetic terrain course" on such anomalous territory (300 m^2), one will find himself under the therapeutic effect of the magnetic field variations.

Key words: *Magneto therapy, environment, Ureki, Atsana.*

In the late 20th century, a basically new, so-called synergic approach was established to study a wide spectrum of natural phenomena. The basis of the synergic approach is the taking account of cooperative phenomena/events influencing a specific system. The advances of scientific research attained in various branches made it possible to analyze the processes ongoing in open, unbalanced, dynamic systems, such as the environment where man has to live.

Man represents an open, dynamic, unbalanced selforganized system exchanging substance and energy with the surrounding environment. The second half of the 20th century was characterized by a plethora of studies of the effects of different physical fields on human beings and on bio systems in general.

All physical fields where man had to function, may, by its nature, be divided into three principal groups: (1) Cosmic fields - generated principally by the Sun and possibly other space objects; (2) Geomagnetic and geological-geophysical fields - which are generated by geological bodies, the Earth and its nucleus; and (3) Technogenic fields - generated by technical objects: radio, television, communications systems, electrical devices, etc. The objective of the research is to determine quantitative parameters of the cooperative impact of the fields generated by different sources - from cell to man.

Special importance in our research is given to the study of the effects of the geomagnetic field

and of the fields generated by: lithospheric structures. As is well known, the Earth's geomagnetic field consists of internal and external components. The internal is conditioned by the Earth's structure as of a space body and these components give rise to slow and secular variations of the Earth's constant magnetic field. The external effect includes the ionosphere and the electrical fields related to it.

The Earth's magnetic field is the habitat of all living organisms. Man is especially responsive to any variations of the geomagnetic field.

The stationary effect of different geophysical anomalies caused by geological bodies also impacts geomagnetic fields and vital activity.

The curative properties of the seaside resort Ureki are well known in Georgia and abroad. Notwithstanding the research carried out in various directions of natural sciences - geology, geophysics, geomorphology, climatology, medicine, etc., the factors that condition the unique properties of the area have not been identified and established yet as a single and clear-cut scientific concept concerning the causes determining the curative properties and the scope of prevalence of this "magic" facility itself.

The Ureki medicinal facility is not pronouncedly distinguished from other Black Sea coastal areas for climatic conditions or for particular effects of cosmophysical fields within the area. In addition, the beach strip is also definitely uniform in terms of beach sands and the content of magnetite in them.

Then what is the cause, in what direction should the research be directed and what factors should be prioritized?

During the period of its existence, the M. Nodia Institute of Geophysics has carried out interesting researches in various directions of applied geophysics.

The first magnetic observations on the territory of Ureki resort were carried out by Prof. M. Nodia in the 1930s [1]. Similar research in the seaside area, land and sea was conducted by an expedition of the Georgian Geology Department [2]. Magnetic measurements on a local site were made by the Georgian Institute of Geophysics in the 1990s [3]. During the 1970s-1980s, an aeromagnetic regional surveying at three different elevations was carried out on almost the entire territory of Georgia, encompassing the areas adjoining Ureki as well [4].

The data of the above-mentioned magnetic research make it possible to characterize the magnetic field structure of the region, its spatial distribution, and the causes of abnormal zones.

The first electrometric work of investigatory nature in Ureki and in its adjacent zone was carried out by us in 2006-2007. The objective of the research was to study the geoelectrical, geological and hydrogeological peculiarities of the region and further to compare the obtained data with the neighboring areas, the curative properties of which still need detecting and reporting.

As seen from section I-Ia, an electrical layer with a 100-120 ohm resistance has been detected in Ureki and its adjacent zone (northward of the River Supsa and southward at a 2-2.5-km distance) section, at the depth of 40-45 m. In the northern part, according to the data of VES (vertical electric sounding) #13 and #26, a layer of high electric conduction, up to 50 m thickness ($p_m=5-16$ ohm) is detected in the depth. In the south, according to the data of YES #3 and #4 (electro drill), approximately after the 10m depth, a layer of high electric conduction and of up to 30 m thickness ($p_n= 5-10$ ohm) is also detected.

Thus, in the upper part of the cited section, between VES #2 and #8 a layer of increased resistance is recorded, being surrounded in the north and in the south by a low-ohmic environment. The layer below it, of 50- 80 ohm resistance, nearing the surface at sight #8, can't be regarded as the supporting electrical horizontal line.

Proceeding from the above, deposits represented within the section, at up to 50m depth, are characterized by abrupt facies changes. In the central part, in the resort Ureki and abutting areas, from the magnetite to the River Supsa, an $r= 100-120$ ohm resistance layer is detectable which, in some cases, is being overlapped by high-conductivity (1000 ohm series) lenses, hi the north and the south this layer is encircled by high-conductivity areas - at the magnetite in the south and in the River Supsa-Grigoleti section in the north.

Based on the above description, the geological section of the Resort Ureki and its adjoining areas may be represented electrically as a "peninsula" that is sea bound in the west, and by a high-

conductivity layer in the north and the south, the so-called “conventional sea”, as a result of mineralized water seepage into the land area. The existence of such a “peninsula” in the Black Sea coastal area shall be geologically considered as a rarity.

A question arises - what is the increased resistance layer of the “peninsular” that encompasses the Resort Ureki and its adjacent area, and in what does it differ from low-resistance areas, when the littoral area in the region gives the impression being of uniform in composition?

To this end, two issues, which represent problems of engineering geophysics and are successfully solved by electrometric methods, are to be considered. These are: 1. the sea water effect on the formation of the seaside area’s hydrological regime, and 2. the study of the paleobed of the river.

Let us consider these issues separately:

The sea water, due to high mineralization, is characterized by the value of one and tenth ohm resistance. As for the resistance of the water-saturated littoral area soil, it makes the unit and first tens of ohm.

The mineralized sea water effect on the seaside soil resistance was studied in different years in the areas of Bicjivinta, Gagra and Poti, as well as in the tributary regions of some big rivers [5], where the soil resistance values used to fall to one ohm. In the beach areas, low resistance was also recorded on the eastern littoral of the Mediterranean Sea, in the littoral part of the Syrian Arab Republic, Latakia region [6]. In this region, electrometric surveys detected a sea water and fresh ground water interface under the land, amounting to 100- 120 m.

On the territory of the Resort Ureki, in the northern and southern areas of the geoelectrical section I-I, low resistance of the soil, similar to the above, must have been caused by the sea water seepage into the coastal area.

On the other hand, the deposits in mountain river beds represented by grits, gravel or other form, due to low mineralization of ground waters, create an increased resistance of 100 ohm and over. Based on the above, increased resistance at the tributary of the river Supsa in section I-I is quite natural. However, as seen from the geoelectrical section, these deposits are widely spread in the south of the Supsa, up to magnetite (VES #3, #4) and significantly distanced from the present channel of the Supsa (2-2.5km).

Very likely, the said electrical layer in the area must be completely represented by fluvial deposits in the Supsa paleobed.

Geomorphologic surveys indicate that the southwestern rivers of Georgia were undergoing migration from the south to the north in the historical past [7], as well as the river Rioni, the old channel of which was located in the north and was known as “Narionali”.

The searching of river paleobeds by means of electric methods is fairly effective. We conducted such research in Syria [8] with a view to study the underground water resources and to establish the paleobed of the river Mashavera in Georgia [9].

Proceeding from the above, it is likely that in the lower part of the stream the Supsa riverbed was located 2.5km southward in the historical past, the deposits of which are known for increased electrical resistance in comparison with the lower layers.

Thus, it is evident from the geoelectrical section I- Ia that the Resort Ureki area is geologically different from the neighbor areas of the littoral due to the fact that a 40-45 m thick surface layer is represented here by the Supsa paleobed which, along the entire section, is impregnated with magnetic minerals (sands).

If this distinctive sign is one of the factors contributing to the curative properties of the area, then the study of the so-called “productive layer”, both in the littoral area and from shore to land, evokes interest.

For this purpose, field work continued in the southern direction, on the territory of the Natanebi and Choloki rivers (geoelectrical section II-IIa. The deposits represented here are geologically of the same origin as in the Ureki Resort area, while the so-called “productive layer” of 90-170 ohm resistance contains the same quantity of magnetic minerals. Based on the above, research of these areas with a view to determine their medico-biological property is of considerable interest.

Inside the land, with a view to study the geological situation, observations were held on the perpendicular section of the seaside strip (section III-IIIa). In this area too the electric parameters of

the rocks seem to be similar to those of other represented sections -resistance of the contour horizon is $\rho = 50-80$ ohm, the thickness of the so-called 'productive layer' is 30-80m, the resistance increasing to 170 ohm. This fact is quite natural given that abrupt facies changes are a characteristic feature of fluvial deposits.

As a result of the electrometric surveys conducted on the territory of Ureki Resort, the following conclusions and recommendations can be made:

1. The deposits represented within a 100 m section of the area under research are characterized by abrupt facies changes, both horizontally and vertically. The resistance of deposits in the section between Supsa and Magnetite, at a 45-50m depth, a horizon of 80-120 ohm resistance is detectable. In the river Supsa-Grigoleti area, the resistance of deposits falls to 5-16 ohm, the same being observable to the south of the magnetite, where a 30-35m thick low-ohm ($\rho_m = 5-10$ ohm) environment is observable under a 10m layer. The contour geoelectrical horizon is represented by a strong electrical layer $h > 50$ m, of 40-80 ohm resistance, being detectable along the entire area under study. The same is noted in the perpendicular section of the seaside, with the difference that the first layer's resistance increases to 150-170 ohm.

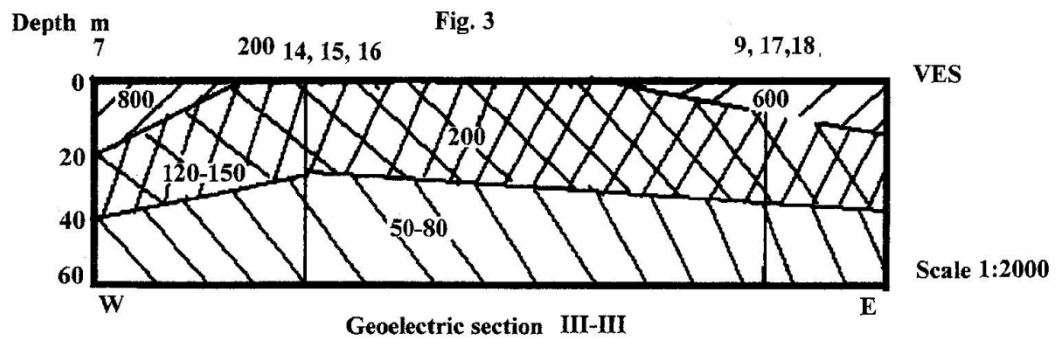
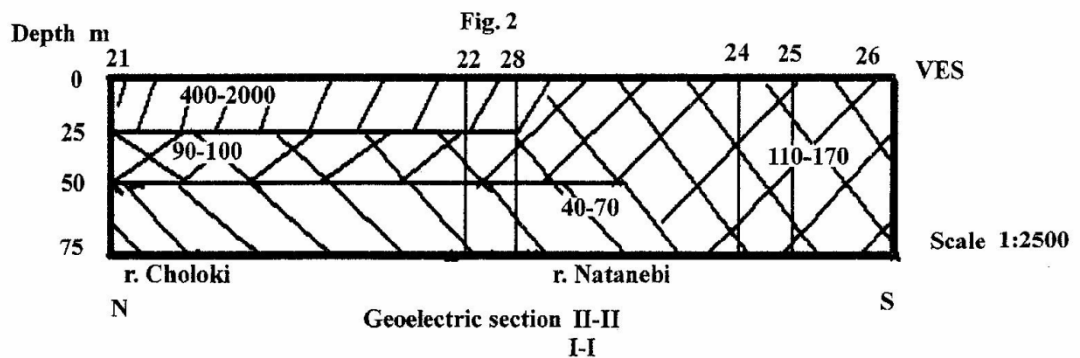
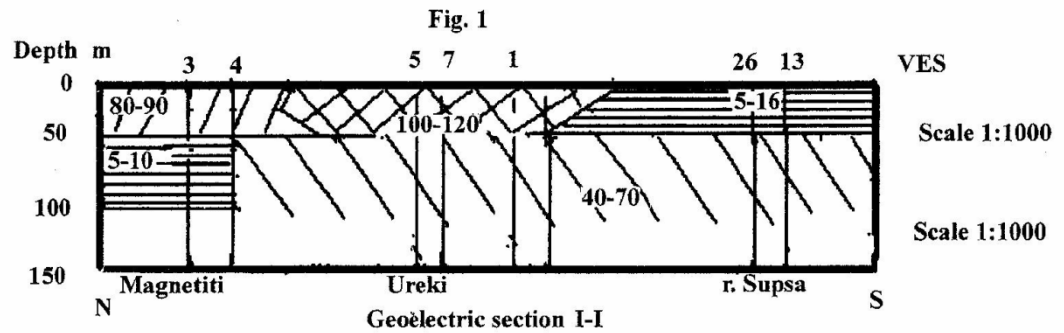
2. According to the geoelectrical surveys I-Ia and III-IIIa and the research conducted by us, the seawater- saturated areas are characterized by one, seldom first tens of resistance values, while the fluvial deposits with fresh groundwater filtrates - of first tens of ohm.

3. Based on point 2 above, the littoral of the Ureki area within section I-Ia may be represented electrically as a "peninsula" that is high-conductivity seawater bound in the west, and by a low-conductivity environment in the north and the south, the so-called "conventional sea". The said redistribution of deposits in the Ureki area, the so-called "peninsula" should be considered as a rarity in contrast to other areas of the littoral.

4. The geomorphologic and electrical surveys suggest that the increased resistance horizon in the Ureki area must have been represented only by fluvial deposits that used to be formed in the paleobed of the Supsa in the historical past.

5. The establishment of the Supsa paleobed is of practical importance because such deposits are associated with magnetic minerals which contribute to the commercial accumulation of iron. In the future, electrometric methods of study can be effectively applied to prospecting iron ore deposits in the riverbeds and the littoral of Ajara

6. If we assume that fluvial deposits of increased resistance (with high content of magnetic minerals) constitute one of the factors contributing to the curative properties of the area, then interest will attach to the study of the so-called "productive layer", both in the southern direction, where geologically it resembles the Supsa area deposits, as well as in land the littoral area, eastward.



120-150- Portion electric resistance for all Figures
 9, 17.18-Number and location of VES for all Figures

7. Deposits represented in geoelectrical section II- IIa, encompassing the Natanebi and Choloki river basins are, like in the Ureki Resort area, characterized by high content by magnetic minerals and the same electric parameters. Therefore, this area too deserves attention in terms of further investigation of its curative properties.

8. to future, in order to establish the causes of the unique medicinal properties of the Ureki Resort and to identify similar areas in the Black Sea littoral which are of great scientific and practical significance, we consider it necessary that detailed geophysical observations be continued involving the efforts of scientists of different directions, ranging from natural sciences to medical men.

Since the territory of Georgia is known for both regional and local magnetic anomalies, their research, identification of the ranges, recording the upper and lower levels of the magnetic field intensity growth is a vety urgent problem, especially as significant gradients of the magnetic fields

in various districts of the Guria regional anomaly have been detected as a result of repeated measurements of the magnetic field intensity by a complex field expeditionary team (the measurements were made by means of a proton magnetometer MMP- 2003). A large volume of literary material on magnetic prospecting has been studied. It has been found that under the South Caucasus conditions, namely in Georgia, taking into consideration its mountainous terrain, the tested aeromagnetic prospecting is adequately effective [10]. Accordingly, all magnetic anomalies need to be thoroughly studied by the earth surface magnetic research method, especially, given the contemporary scientific views that electromagnetic fields (including local magnetic anomalies) exert a significant impact on the health of living beings (both positive and negative) [11,12].

From this standpoint, special importance will be given to the study of Guria regional magnetic anomaly.

The expedition has studied in detail Ureki, Tsqaltminda, Mamati, Guliani, Atsana, and other local magnetic anomalies within the Ureki regional anomaly. The full T component of the magnetic field is liable to significant variations within a small area, maximum to 9000 gamma (whereas the maximum intensity of magnetic storm in our latitude is within 600-800 gamma). Special mention should be made of Atsana north-western slope, where the foil T component of magnetic field varies from 45800 to 54800 gamma. Measurements were made by a standard 10- meter step. In our opinion, the anomaly should be associated with the volcanic rocks containing ferromagnetic minerals, which are characterized by significant gradients. Also, significant magnetic field gradients were registered in the River Atsaura basin (47900-55600 gamma), as well as in (the North-Eastern) Serbeti area adjoining Atsana (46400- 51400 gamma) and in other places.

The volume of the work performed and of the results obtained by the expedition and the value of the obtained information make it possible to hope that, in cooperation with medical men and on condition the above organizational problems are settled, further research will yield results and conclusions that will prove useful not only for Georgian geophysics but also the future of this country.

References

- [1] М.З. Нодиа (1940), Сообщ. Груз. ФАН СССР, !, 6.
- [2] А.Н. Захаров (1948), Отчет о результатах магнитометрической съемки на море грузинской партией №5/47. Грузгеолфонд.
- [3] Z. KereseliZe, G.BeriSvili, V.Kircxalia (2000), geomagnituri velis bioefectuobis zogierTi faqtoris Sesaxeb. Tbilisi, 39 gv.
- [4] [Z.Kereselidze, G.Berishvili, V.Kirckhalia (2000). About Some Factors of Bioeffectivity of the Geomagnetic Field. Tbilisi, 39p.]
- [5] Г.А. Сехниаидзе (составитель) (1978). Карта аномального магнитного поля ΔТ Грузинской ССР.
- [6] Д.А.Цицишвили, Г.Г.Табагуа, Г.В.Татишвили (1985). Геоэлектрическая характеристика пляжевой полосы Черноморского побережья Грузии. Тбилиси.
- [7] Г.Г.Табагуа, Шамун Шамали (1986), Геофизические исследования в восточной части Сирийской Арабской Республики. Отчет: Фонды Ленгипроводхоза, Ленинград.
- [8] Д.Д. Табидзе (1985), Объемный анализ рельефа и проблемы морфологической систематики, Тбилиси.
- [9] Г.Г. Табагуа, Шамун Шамали (1977), Геофизические исследования в Сирийской Арабской Республике. Отчет по работам 1973-1976г.г. Фонды Мосгипроводхоза. Москва.
- [10] Г.Г.Табагуа, М.Л.Джухуташвили, Т.Л.Челидзе, А.Г.Тархнишвили. Эффективность археологических исследований в картировании молодых базальтовых лавовых покровов и некоторые соображения о дальнейшем направлении поисков останков гоминида в районе археологического объекта Дманиси. Труды Ин-та Геофизики.
- [11] А.А.Логачев, П.В.Захаров (1979), Магнитная разведка, Ленинград: 103-105.

- [12] С.И.Раппопорт, Т.К.Бреус, Н.Г.Клейменова, О.В.Козырева, Н.К. Малиновская (2006), Геомагнитные пульсации и инфаркты миокарда: Тер. Архив, т.78, № 4, С. 56-60.
- [13] Т.К. Бреус, С.М.Чибисов и др. (2002), Хроноструктура биоритмов сердца и факторы Внешней среды, М.: с. 231

(Received in final form 20 December 2011)

Комплексное геофизическое исследование некоторых строго локализованных Гурийских (Грузия) магнитных аномалий.

დ. ლომინაძე, კ. კარველიშვილი, გ. ბერიშვილი, ნ. მებაღიშვილი,

მ. ნიკოლაიშვილი, გ. ტაბაგუა, ა. თარხნიშვილი.

Резюме

«Искусственная» магнитотерапия широко используется во всем мире, тогда как единственным известным природным магнитотерапевтическим курортом, рекомендуемым при лечении заболеваний опорно-двигательного аппарата, ревматизма и пр., является уникальный черноморский курорт Уреки, расположенный в западной части Гурийского региона. Однако интенсивные локальные магнитные аномалии выявлены по всей территории Грузии. В данном случае исследуются геофизические характеристики территории локальных магнитных аномалий низкогорной Гурии (с. Ацана), что является первым этапом исследования возможности создания здесь природного магнитотерапевтического курорта. Особенно важными являются также комплексные исследования локальных аномалий Гурийской региональной аномалии с целью составления детальных магнитных карт. Нормальное значение, характеризующее магнитное поле в Грузии имеет величину $T=48800$ гамма. Максимальная величина полного вектора магнитного поля T в с.Ацана меняется на 9000 гамм (тогда как интенсивность магнитных бурь на данной широте не превышает 600-800 гамм). Следует особенно отметить северо-западной склон территории, где T меняется от 45800 до 54800 гамм. Значительные изменения T были зарегистрированы в бассейне реки Ацаура (47900-55600) и в других местах. Градиенты T относительно нормального поля для с. Ацана можно характеризовать величиной 1000 гамма/м (м-шаг 10м). Выявленная в с. Ацана на небольшой территории (около 300кв.м.) локальная магнитная аномалия позволяет наметить сеть «терренкуров», перемещаясь по которым на определенной скорости, можно создать определенные величины T . Таким образом, данная территория представляется природной «лабораторией», пригодной для многостороннего изучения воздействия магнитного поля на человека, а в дальнейшем - создания природного магнитотерапевтического курорта.

ზოგიერთი ძლიერი ლოკალური გურიის (საქართველო) მაგნიტური ანომალიების მახასიათებლის კომპლექსური გეოფიზიკური კვლევა

ჯ. ლომინაძე, კ. ქართველიშვილი, გ. ბერიშვილი, ნ. მებაღიშვილი,
მ. ნიკოლაიშვილი, გ. ტაბაგუა, ა. თარხნიშვილი

რეზიუმე

ადამიანი წარმოადგენს ღია, დინამიურ, არაწონასწორულ, თვითორგანიზებულ სისტემას; იგი ცვლის ნივთიერებასა და ენერგიას გარემოსთან, რომელიც მას გარს ერტყმის. სტატიის ავტორთა კვლევები შეეხება დედამიწის მაგნიტური ველის საქართველოში არსებული ძლიერი ლოკალური მაგნიტური ანომალიების

არეების გამოვლენას, მათი ფიზიკური მახასიათებლების დადგენასა და, მედიკოსებთან თანამშრომლობით, ადამიანზე მათი შესაძლო გავლენის შესწავლას, განსაკუთრებით, თუ გავითვალისწინებთ თანამედროვე მეცნიერულ შეხედულებებს, რომ ელექტრო- მაგნიტური ველები (მათ შორის ლოკალური მაგნიტური ანომალიები) მნიშვნელოვან გავლენას ახდენენ ცოცხალი არსებების ჯანმრთელობაზე, მათ განვითარებაზე (როგორც დადებითს, ასევე უარყოფითს). ავტორთა მიერ დაფიქსირებული ლოკალური ანომალიური მაგნიტური ველების გრადიენტები რამდენიმეჯერ აღემატება ჩვენს განედებზე მაგნიტური ქარიშხლების მაქსიმალურ მნიშვნელობებს. შესწავლილ ტერიტორიებზე მაგნიტური ველის სრული T მდგენელი მცირე ტერიტორიაზე განიცდის ძალზე მნიშვნელოვან ცვლილებებს - რამდენიმე ათასი გამის ფარგლებში (მაშინ, როდესაც ჩვენს განედებზე მაგნიტური ქარიშხლის მაქსიმალური ინტენსივობა არ აღემატება 600 - 800 გამას).

Gas Hydrates investigations in the Gurian Trough

¹E.Sakvarelidze, ²G. Tumanishvili

¹I.Javakchishvili Tbilisi State University

²Caucasian Institute of Mineral Resources of I.Javakchishvili Tbilisi State University

Abstract

The geological and geophysical conditions of gas hydrates formation in the Gurian Trough in the Black Sea are given in this work. The presented results of studies conducted in cooperation with German scientists from the University of Bremen during the sea cruises. It is shown that in the case of Gurian Trough intensive gassing (Batumi seep) observed is associated with the content of gas hydrates in marine sediments in the region.

The investigation of natural gas emission sites and gas hydrates within sediment deposits is of great scientific and practical interest. Methane is twenty times more effective as greenhouse than CO₂; however, its concentration within the atmosphere is much smaller. In contrast, methane generated by microbial decay and thermogenic breakdown of organic matter seems to be a large pool in geological reservoirs. Numerous features, such as shallow gas accumulations, pockmarks, seeps and mud volcanoes are present in a wide variety of oceanographic and geological environments. Release and uptake of methane by such sources may provide positive and negative feedback to global warming or cooling. Gas hydrates are of interest from the standpoint of energy resources, because their high methane density, when occurring close to the seafloor. Investigations have shown that hydrates generate extremely high and variable fluxes of methane to the overlying water column due to their exposed position close to the sediment/water interface.

Activity studies of gas hydrates are concentrated in the Black sea for various reasons. It is the largest anoxic basin with much higher methane concentrations than in any other marginal sea. Sediments of 10-19 km thickness reveal a potential reservoir for methane generation and hundreds of methane emission site are known from water column investigations of Russian, Ukraine and German researchers.

Oil - gas bearing province of Black Sea contains the coastal shelf, eastern, northeastern and southeastern part of the Black Sea. There are certain oil and gaseous reservoirs in this area, mainly along the eastern Black Sea shelf and Guria Trough.

The zone of oil-gas formation of Guria Trough (on land) belongs to the west part of Guria sector of Ajara-Trialeti folded system. Sea prolongation of Guria foothill deflection spatially is stretched on the prolongation of the middle of rivers Supsa- Kintrishi to the south-west into paleogenic series, in the zones of shelf and the continental slope. On the whole, sea part of Guria Trough is situated in the extreme south of Georgian sector of the Black Sea.

On the basis of complex geological, geophysical, geomorphologic and cosmogeologic data, it is established that tectonic faults (observed on land) extend in the zones of shelf and the continental slope; this is well reflected in thickness distribution of separate geocomplexes of sedimentary cover and formation of wide net of submerged canyons.

These weakened zones participate in lithogenetic processes of the eastern Black Sea depression with various intensity, which is well expressed in peculiarities of separate facies and sediment

accumulation velocity, spatial distribution of diapirism, mud volcanism and intensive gas streaming areas at the sea ground. The Sea prolongation of such weakened zones has deep faults of Supsa, Natanebi, Kobuleti Chorokhi. Existence of these fluid-conductive mobile faults conditioned the formation of diapiric structures in Oligocene-Miocene sediments of Guria Trough. At modern stage of geological development (land-the Black Sea) weakened zones are within sedimentary cover, as well as foundation; they are characterized by high values of thermal indices. Ajara -Trialeti zone and Guria foothill Trough are characterized by anomalously high heat flows ($80-84\text{mvt}/\text{m}^2$) and anomalously high depth temperatures: on the base of sedimentary cover $\sim 200^0\text{C}$, at the Conrad and the Moho discontinuities- ($550-600^0\text{C}$) and ($1000-1200^0\text{C}$) correspondingly.

High values of tectonically weakened zones and heat flows, as well as intensive submersions, especially in subsequent period of Eocene, condition the formation of elision fluidodynamical system of eastern Black Sea depression and Guria Trough as well. Biochemical, lithogenetic and depth genesis hydrocarbon fluids participate at certain stages of lithogenesis.

Powerful oil-gas manifestations in land of Guria deflection are connected with Middle Eocene, Middle Miocene, Sarmatian (Supsa) and Meotian (Shromisubani) collectors.

Hydrocarbon (oil, gas) resources can be revealed in anticlinal and diapiric structures of Cretaceous-Miocene geocomplexes. Deposits of biochemical gas can be revealed in geocomplexes of Mio-Pliocene-Quaternary, in the zone of deltaic sediments of paleorivers, in the form of lithologico-stratigraphic traps.

Highly perspective region of gas-hydrate formation is stretched in the zone of the continental slope, section of rivers Chorokhi-Supsa. Holocene-Quaternary sandy sediments are considered perspective. Gas-hydrate deposits can be revealed below sea ground till 500-800m depth.

In the last decade studies of gas hydrates in the Black Sea were conducted by German scientists from the University of Bremen which was coordinated by prof. Gerhard Bormann during cruises on the boards R/V Poseidon, R/V Meteor and R/V Mary S. Merian. The scientists from Georgia participated in this studies.

Shallow gas hydrates, potentially associated with free gas, are known from sediments in several areas and are of specific interest in the black Sea where a large number of active methane emission sites exist. In the territorial waters of Georgia gas flares, ascending methane gas bubbles recorded by echosounder were discovered at several sites offshore Suchumi and offshore Batumi (Guria Trough)

The area offshore Batumi (Batumi seeps area) was intensively studied by ELAC swath bathymetry, DTS side scan sonar, OFOS video sled and GC gravity corer, where gas bubbles were detected in about 800 m water depth. There in an area of about 1 km^2 , occur about 25 gas bubble streams in 10 distinguishable clusters. This is the area in the Black sea with the strongest within the gas hydrate stability zone.

Studies concentrated the seafloor observations and sediment sampling on Batumi Seep. It is placed on the ridge between the canyons and is placed on a local high that rises about 10m at 855 m water depth. This was also imaged by a high resolution 410 kHz side scan sonar survey. About six gas seeps recorded as acoustic anomalies by DTS. The gravity corer contained cm-size gas hydrates.

At the Batumi seep site, four temperature measurements were obtained using the ROV (remotely operated vehicle) temperature lance. The temperature value ranged between 8.94^0C and 9.17^0C . Compared to a bottom water temperature approximately 9.1^0C , this suggests a relatively low temperature anomaly, which may be related to gas ebullition associated with bottom water infiltration and circulation.

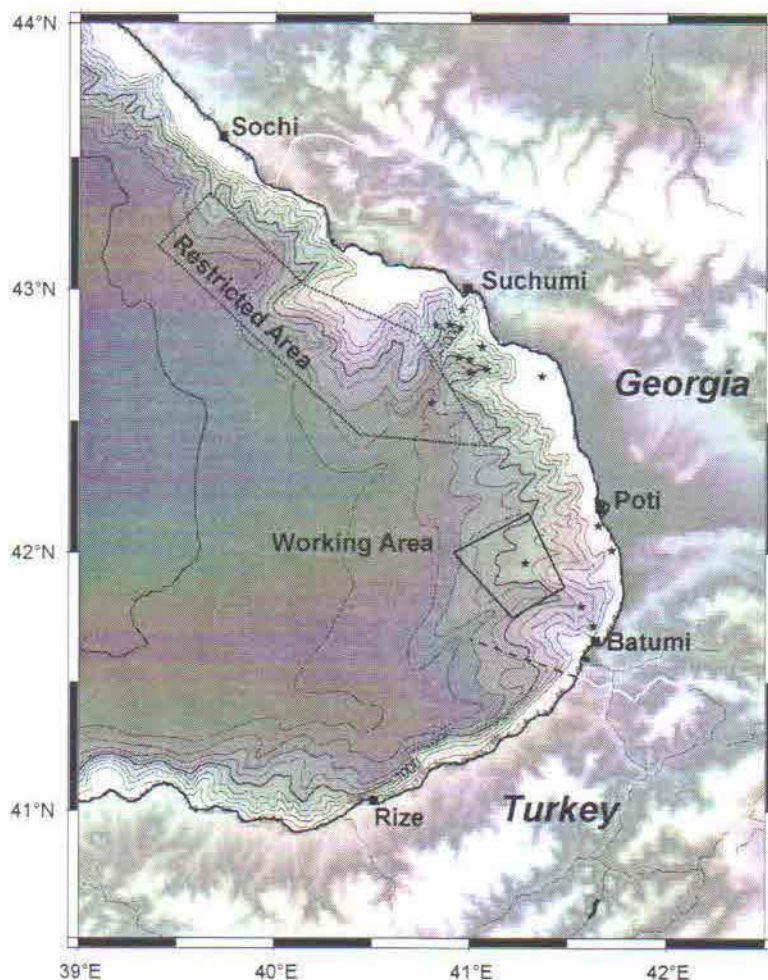


Fig.1 The working area of Georgia, stars – the location of gas flares.

References

- [1] E. Sakvarelidze, N. Mamulia. Some Results of the investigation the Heat Regim of the Crust for the Water Area of the Black Sea. Bull.of the Georg Acad.of Sciences, 161,1, 2000
- [2] E. Sakvarelidze, G. Tumanishvili, I.Amanatashvili, V Meskhia, Prospects of Revelling Gase Hydrates in Guria Depression. (Georgian Sector of the Black Sea) TTR-17 Post-Cruise Meeting end Intern. Conf. Granada 2-5 February 2009.
- [3] E. Sakvarelidze, I Amanatashvili, V.Meskhia, M. Otinashvili Heat Flow And Temperatures in the Sedimantari Complex in the Eastern Black sea Region And Adjacent Territory. Journal of the Georgian Geophysical Sositeti. Issu A. Physics of Solid Earth, vol 14A 2011.
- [4] G. Tumanishvili, T. Lasarashvili The Methane hydrate carrying perspectives of Georgian Sector of Black Sea. Second International Symposium on the petroleum Geology and Hydrocarbon potential of the Black Sea Area 22-24 September, Istanbul, Turkey, 1996
- [5] H. Sahling, V. Blinova, G. Cifci, N. Lursmanashvili e.o. Report and preliminary Results of R/V Poseidon Cruise P317/4, 2004
- [6] G. Bohrman, G. Pape and cruise participants. Report and preliminary Results of R/V Meteor Cruise M72/3, 2007
- [7] G. Bohrman, V. blinova, K. Dehning, E. Eakvarelidze e.o. Origin and Structure of Methane, Gas Hydrates and Fluid Flows in the Black Sea. Report and preliminary Results of R/V Maria S.Merian Cruise MSM 15/2.

(Received in final form 12 September 2012)

Исследование газовых гидратов в Гурийском Прогибе

Е. Сакварелидзе, Г. Туманишвили

Резюме

В работе рассмотрены геолого-геофизические предпосылки образования газовых гидратов в Гурийском прогибе на шельфе Черного моря. Приводятся результаты исследований, проведенных совместно с немецкими учеными из Бременского университета во время морских круизов. Показано, что в Гурийском прогибе имеет место интенсивное газовыделение (Батумское газовыделение), которое связано с содержанием газовых гидратов в морских осадках данного региона.

გაზური ჰიდრატების კვლევა გურიის როფში

ე. საყვარელიძე, გ. თუმანიშვილი

რეზიუმე

ნაშრომში განხილულია შავი ზღვის შეღვზე გურიის როფში გაზური ჰიდრატების წარმოქმნის გეოლოგიურ-გეოფიზიკური წინაპირობები. მოყვანილია ბრემენის უნივერსიტეტის მეცნიერებთან ერთობლივი საზღვაო ექსპედიციების დროს მიღებული კვლევების შედეგები. ნაჩვენებია, რომ გურიის როფში აღინიშნება გაზების ინტენსიური გამოყოფა (ბათუმის გაზგამოყოფა), რომელიც არის დაკავშირებული ზღვის ნალექებში გაზური ჰიდრატების არსებობასთან.

The geomagnetic variation in Dusheti observatory related with earthquake activity in East Georgia (January - July 1012)

**Tamar Jimsheladze, George Melikadze, Alexander Chankvetadze, Robert
Gagua, Tamaz Matiashvili**

Mikheil Nodia Institute of Geophysics of Ivane Javakhishvili Tbilisi State University

Abstract

Before strong earthquake magnetic precursors denoted by many authors, but must to say, that more of them don't satisfy stern criterions.

The method of earthquake's predictions are based on the correlation between geomagnetic quakes and the incoming minimum (or maximum) of tidal gravitational potential. The geomagnetic quake is defined as a jump of day mean value of geomagnetic field one minute standard deviation measured at least 2.5 times per second. The probability time window for the incoming earthquake or earthquakes is approximately ± 1 day for the tidal minimum and for the maximum- ± 2 days. The statistic evidence for reliability of the geomagnetic precursor is based on the distributions of the time difference between occurred and predicted earthquakes for the period January-June of 2012 for Dusheti region.

1. Introduction

The problem of "when, where and how" earthquake prediction cannot be solved only on the basis of seismic and geodetic data (1; 10; 6).

The possible tidal triggering of earthquakes has been investigated for a long period of time.

Including of additional information in the precursors monitoring, such as the analysis of the electromagnetic field variations under, on and above the Earth surface, can contribute towards defining a reliable earthquake precursor and estimating the most probable time of a forthcoming earthquake.

Simultaneous analysis of more accurate space and time measuring sets for the earth crust condition parameters, including the monitoring data of the electromagnetic field under and over the Earth surface, as well as the temperature distribution and other possible precursors, would be the basis of nonlinear inverse problem methods. It could be promising for studying and solving the „when, where and how" earthquake prediction problem.

Some progress for establishing the geomagnetic filed variations as regional earthquakes' precursors was presented in several papers (7; 9).

The approach is based on the understanding that earthquake processes have a complex origin. Without creating of adequate physical model of the Earth existence, the gravitational and electromagnetic interactions, which ensure the stability of the Sun system and its planets for a long time, the earthquake prediction problem cannot be solved in reliable way. The earthquake part of the model have to be repeated in the infinity way "theory- experiment- theory" using nonlinear inverse problem methods looking for the correlations between fields in dynamically changed space and time scales. Of course, every approximate model (16; 12; 13; 14; 3; 4; 5) which has some experimental evidence has to be included in the analysis. The adequate physical understanding of the correlations between electromagnetic precursors, tidal extremums and incoming earthquake is connected with the progress of the adequate Earth's magnetism theory as well as the quantum mechanical understanding of the processes in the earthquake source volume before and in the time of earthquake.

The achievement of the Earth's surface tidal potential modeling, which includes the ocean and atmosphere tidal influences, is an essential part of the research. In this sense the comparison of the Earth tides analysis programs (Dierks and Neumeyer, ws) for the ANALYZE from the ETERNA-package, version 3.30 (Wenzel, 1996 a, b), program BAYTAP-G in the version from 15.11.1999 (Tamura, 1991), Program VAV (17) is very useful.

The role of geomagnetic variations as precursor can be explained by the hypothesis that during the time before the earthquakes, with the strain, deformation or displacement changes in the crust there arise in some interval of density changing the chemical phase shift which leads to an electrical charge shift. The preliminary Fourier analysis of geomagnetic field gives the time period of alteration in minute scale. Such specific geomagnetic variation we call geomagnetic quake. The last years results from laboratory modelling of earthquake processes in increasing stress condition at least qualitatively support the quantum mechanic phase shift explanation for mechanism generating the electromagnetic effects before earthquake and others electromagnetic phenomena in the time of earthquake (2; 11; 15). The future epicentre coordinates have to be estimated from at least 3 points of measuring the geomagnetic vector, using the inverse problem methods, applied for the estimation the coordinates of the volume, where the phase shift arrived in the framework of its time window. For example the first work hypothesis can be that the main part of geomagnetic quake is generated from the vertical Earth Surface- Ionosphere electrical current. See also the results of papers (Vallianatos, Tzanis, 2003 ; Duma, Ruzhin, 2003, Duma, 2006) and citations there.

In the case of incoming big earthquake (magnitude > 5 - 6 the changes of vertical electropotential distribution, the Earth's temperature, the infrared Earth's radiation, the behaviour of debit, chemistry and radioactivity of water sources, the dynamics and temperature of under waters, the atmosphere conditions (earthquakes clouds, ionosphere radioemissions, and etc.), the charge density of the Earth radiation belt, have to be dramatically changed near the epicentre area- see for example papers .

The achievements of tidal potential modeling of the Earth's surface, including ocean and atmosphere tidal influences, multi- component correlation analysis and nonlinear inverse problem methods in fluids dynamics and electrodynamics are crucial for every single step of the constructing of the mathematical and physical models.

2. Method and data description

In the paper (Mavrodiev,2004) the geomagnetic quake was defined as a jump of the day mean value of the signal function Sig:

$$Sig = \sum_{m=1}^M \sigma_{Hm} / M, \quad \delta Sig = \sum_{m=1}^M \delta \sigma_{Hm} / M, \quad (1)$$

Here σ_{Hm} is the standard deviation of geomagnetic field component Hh , and $\delta \sigma_{Hm}$ is the corresponding error,

$$\sigma_{Hm} = \sqrt{\sum_{t=1, N} \frac{(H_t - H_m)^2}{N}}, \quad \delta \sigma_{Hm} = \sqrt{\sum_{t=1, N} \frac{(\delta H_t - \delta H_m)^2}{N}},$$

H_m is one-minute averaged value of geomagnetic vector projection H_i ,

$$H_m = \sum_{i=1}^N \frac{H_i}{N}, \quad \delta H_m = \sum_{i=1}^N \frac{\delta H_i}{N},$$

M=1440 minutes per day, and N=60 are the samples per minute.

The predicted earthquake is identified by the maximum of the function proportional to the density of the earthquake radiated energy in the monitoring point. The analytical size of this function is:

$$\text{SChtM} = 10M / (\text{D} + \text{Depth} + \text{Distance}^2), \quad (2)$$

Where the distances are in hundred km, fit parameter D = 40 km and M is the earthquake magnitude

Thus, if we have a jump of signal function Sig and its error δSig is such that satisfies numerically the next condition :

$$\text{SigToday} - \text{SigYesterday} > (\delta\text{SigToday} + \delta\text{SigYesterday}) / 2, \quad (3)$$

In the next tidal extreme time the function SChtM will has a local maximum value. The earthquake for which the function SChtM has a maximum can be interpreted as predicted earthquake.

The probability time window for the incoming earthquake or earthquakes is approximately ± 1 day for the tidal minimum and for the maximum- ± 2 days.

The analytical size of the function SChtM as well as one minute time period for calculating the unique signal for geomagnetic quake which is reliable earthquake precursor was established by *Dubna inverse problem method* (Dubna Papers).

In the case of vector geomagnetic monitoring, one has to calculate the minute standard deviation as a geodynamical sum of standard deviations of the tree geomagnetic vector components:

$$\delta_{H_m} = \sqrt{(\delta^2_{H_{mx}} + \delta^2_{H_{my}} + \delta^2_{H_{mz}})}$$

Dusheti Geomagnetic Observatory is located in Dusheti town (Georgia, Lat 42.052N, Lon44.42E), Alt900m). It is equipped with modern precise Fluxgate Magnetometer Model LGI and it accomplishes non-stop registration of X, Y, Z elements. The data includes minute and second records of the field elements. It is measured with 0,1nT accuracy daily.

3. Data

There was analyzed earthquakes data in region with Lat42.052N and Long44.42E for January-June of 2012, reported in EMSC: Earthquake research results, magnitude range from 3.5 to 9.0, data selection 62 earthquakes; Minute data of Geomagnetic fields elements received from Dusheti Geomagnetic observatory or 60 samples per hour, with 0,1nT accuracy; Coordinate of Dusheti Geomagnetic observatory: 42.052N, Lon44.42E Alt900m.

The distributions of earthquakes' magnitudes and depths, (Mgnitude >3.5) are presented in Fig.1 and Fig.2. (Epical distances up to 300km and magnitudes M>3.5).

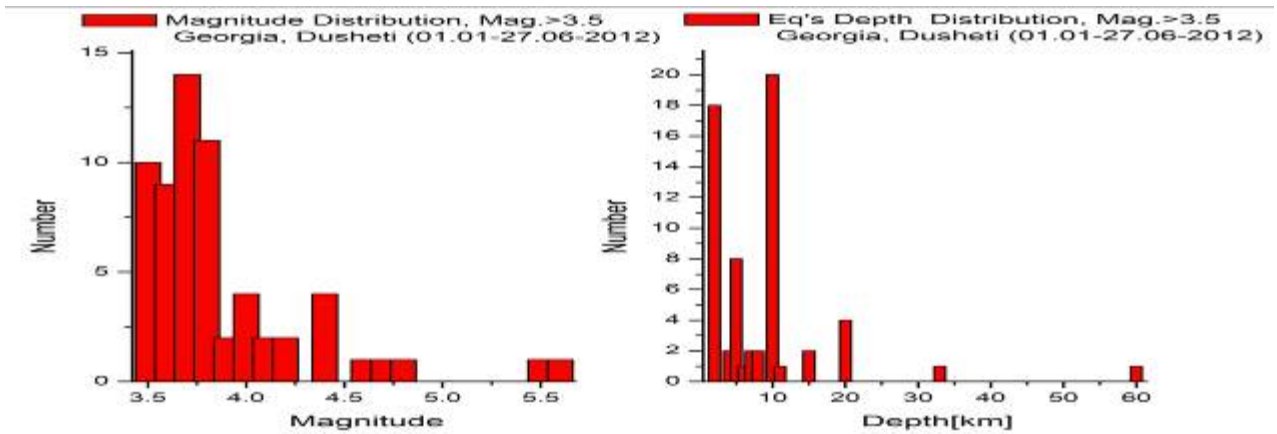


Fig.1. Magnitude distribution

Fig. 2 The earthquake's depth distribution

Fig3. Presents the SChtM and magnitude distribution for all occurred in the region earthquakes as function of distance from the monitoring point with magnitude>3.5.

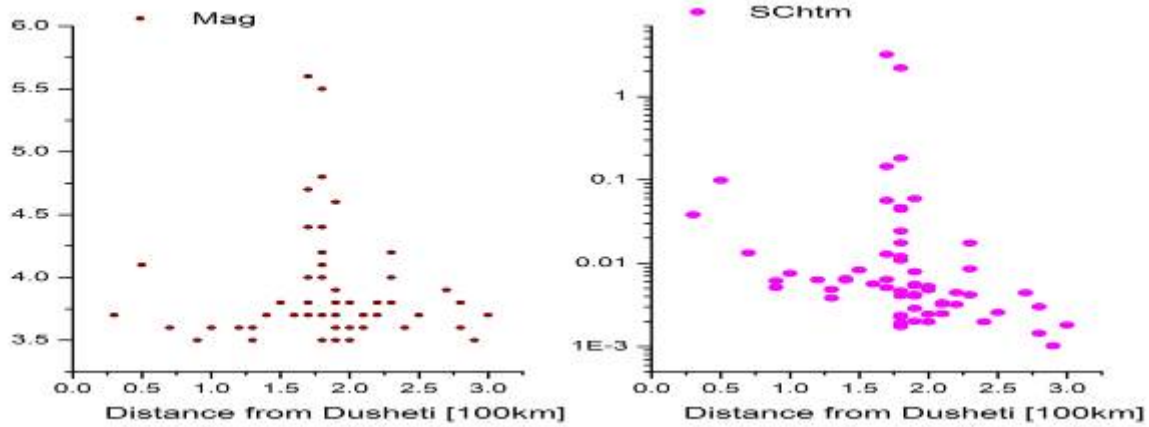


Fig. 3. The distribution of SChtM and Magnitude (>3.5) on distances for all occurred earthquakes in the region

The comparison of the distribution in the Fig3 and Fig.4 can give some presentation for distance and magnitude sensibility of the geomagnetic approach.

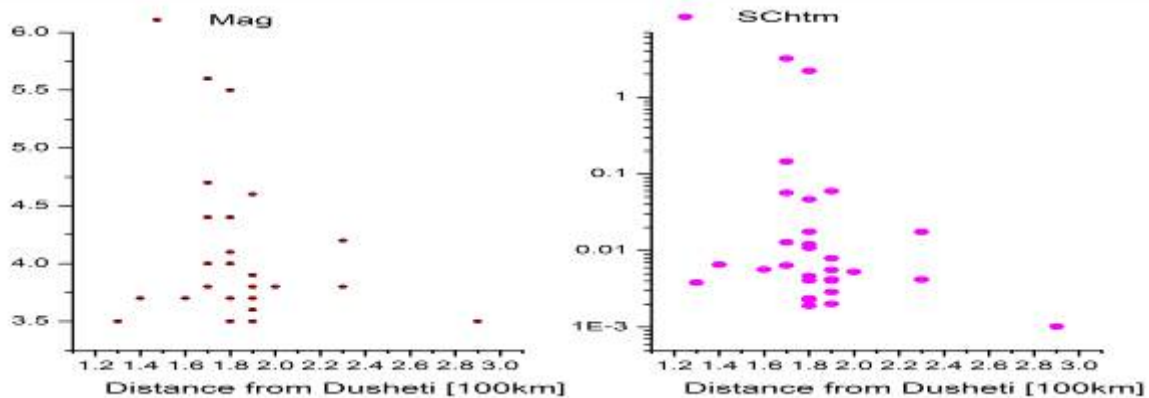


Fig. 4. The distribution of SChtM and Magnitude (>3.5) on distances for predicted earthquakes

4. Analysis

The next Table contains the monitoring data for Dusheti and its analysis, described above, which illustrate that the geomagnetic quake is regional reliable earthquake precursor. The columns present: the number of signals preceding the incoming tidal extreme data, information for the tidal minimum (1) or maximum (2), the time of tidal extreme, the time of occurred earthquake, latitude [degree], longitude [degree], depth [km], magnitude, distance from monitoring point [in 100 km], the value of function S_{ChtM} [J/km²], the difference between the time of tidal extreme and the time of occurred earthquake [in days]. The table consists a data for the earthquake with magnitude greater than 3.5

Number of Signals	Tidal min,max	Signal Time	Tidal Min,Max time	Eq Time	Lat	Long	Depth [km]	Mag	Dist[100km]	Schtm	Time difference(day)
	1	29.12.2011	12/31/2011 9:10	1/2/2012 1:08	42.7	43.41	10	3.6	1.3	0.005	2
		29.12.2011	12/31/2011 9:10	1/2/2012 5:49	44.42	45.74	10	3.6	2.8	0.001	2
	2	3.01.2012	1/8/2012 13:09	1/5/2012 9:01	42.46	43.82	20	3.5	0.9	0.005	-3
		3.01.2012	1/8/2012 13:09	1/5/2012 14:17	41.92	45.9	5	3.6	1	0.008	-3
		3.01.2012	1/8/2012 13:09	1/6/2012 3:13	40.81	42.6	7	3.8	2.2	0.004	-2
			1/15/2012 10:00	1/12/2012 3:37	43.19	46.76	10	3.7	2.1	0.003	-3
			1/15/2012 10:00	1/13/2012 14:10	39.97	42.42	15	3.7	3	0.002	-2
	1	12.01.2012	1/15/2012 10:00	1/15/2012 0:11	42.54	42.93	2	3.7	1.6	0.006	-0
			1/29/2012 9:25	2/1/2012 4:28	43.79	42.81	5	3.7	2.5	0.003	3
			2/6/2012 12:48	2/2/2012 12:37	42.86	46.79	2	3.5	2	0.002	-4
	2	30.01.2012	2/6/2012 12:48	2/3/2012 9:11	42.77	43.36	10	3.7	1.4	0.006	-3
3	2	24.02.2012	3/8/2012 11:27	3/11/2012 8:41	41.63	46.79	20	4.4	1.8	0.044	3
	2	27.02.2012	3/8/2012 11:27	3/11/2012 23:18	40.84	42.74	4	3.6	2.1	0.002	3
2	1	12.03.2012	3/16/2012 11:19	3/16/2012 13:25	43.64	43.44	10	3.7	2.1	0.003	0
	1	15.03.2012	3/16/2012 11:19	3/16/2012 19:55	42.66	46.87	10	3.8	1.9	0.005	0
			3/16/2012 11:19	3/18/2012 6:59	41.62	44.08	2	3.6	0.7	0.013	2
1	2	22.03.2012	3/22/2012 10:57	3/22/2012 9:11	42.67	41.91	2	3.6	2.4	0.002	-0
			3/22/2012 10:57	3/25/2012 10:03	43.4	46.34	10	3.6	2	0.002	3
			3/22/2012 10:57	3/25/2012 14:50	39.95	42.97	7	3.9	2.7	0.004	3
2	1	24.03.2012	3/31/2012 11:32	3/31/2012 16:49	43.42	45.92	5	3.7	1.9	0.004	0
			4/8/2012 10:40	4/5/2012 18:14	43.31	44.9	10	3.8	1.5	0.008	-3
1	2	5.04.2012	4/8/2012 10:40	4/8/2012 20:28	43.56	44.54	10	3.8	1.7	0.006	0
1	2	10.04.2012	4/15/2012 11:41	4/14/2012 3:13	39.47	43.95	2	3.5	2.9	0.001	-1
1	1	23.04.2012	4/22/2012 10:35	4/23/2012 15:50	42.3	45.21	2	4.1	0.5	0.099	1
2	2	3.05.2012	5/6/2012 10:36	5/7/2012 4:40	41.5	46.67	10	5.6	1.7	3.191	1
			5/6/2012 10:36	5/7/2012 5:08	41.5	46.75	10	4	1.8	0.012	1
			5/6/2012 10:36	5/7/2012 5:38	41.5	46.67	8	4.7	1.7	0.145	1
			5/6/2012 10:36	5/7/2012 5:40	41.37	46.52	4	4.4	1.7	0.056	1
			5/6/2012 10:36	5/7/2012 8:27	41.53	46.79	2	3.5	1.8	0.002	1
			5/6/2012 10:36	5/7/2012 8:36	41.54	46.82	2	4.1	1.8	0.018	1
			5/6/2012 10:36	5/7/2012 14:15	41.62	46.76	10	5.5	1.8	2.196	1
			5/6/2012 10:36	5/7/2012 14:36	41.51	46.69	8	4	1.7	0.013	1
			5/6/2012 10:36	5/7/2012 14:51	41.47	46.71	2	3.7	1.8	0.005	1
			5/6/2012 10:36	5/7/2012 16:58	41.51	46.8	10	4.4	1.8	0.046	1
			5/6/2012 10:36	5/7/2012 17:04	41.48	46.85	10	3.9	1.9	0.008	1
			5/6/2012 10:36	5/7/2012 17:08	41.46	46.81	10	3.7	1.9	0.004	1
			5/6/2012 10:36	5/7/2012 17:49	41.51	46.83	10	3.6	1.9	0.003	1
			5/6/2012 10:36	5/7/2012 18:49	41.54	46.88	10	3.8	1.9	0.006	1

			5/6/2012 10:36	5/8/2012 0:06	41.52	46.96	10	3.8	2	0.005	2
			5/6/2012 10:36	5/9/2012 6:24	39.87	42.97	5	3.8	2.8	0.003	3
1	1	8.05.2012	5/13/2012 13:06	5/12/2012 18:00	41.5	46.7	2	3.5	1.8	0.002	-1
			5/13/2012 13:06	5/12/2012 21:10	41.54	46.67	11	3.8	1.7	0.006	-1
1	1	9.05.2012	5/13/2012 13:06	5/14/2012 9:58	41.18	47.19	2	4.2	2.3	0.017	1
			5/13/2012 13:06	5/14/2012 15:50	41.19	47.23	6	3.8	2.3	0.004	1
			5/13/2012 13:06	5/15/2012 4:54	41.54	46.81	5	4.2	1.8	0.024	2
			5/13/2012 13:06	5/15/2012 5:17	41.56	46.63	2	3.7	1.7	0.005	2
			5/21/2012 10:38	5/18/2012 10:04	41.19	47.1	5	3.7	2.2	0.003	-3
			5/21/2012 10:38	5/18/2012 14:46	41.69	46.89	10	4.8	1.8	0.181	-3
1	2	16.05.2012	5/21/2012 10:38	5/19/2012 2:01	41.47	46.78	20	3.5	1.8	0.002	-2
			5/21/2012 10:38	5/20/2012 23:07	41	43.93	2	3.5	1.3	0.004	-0
1	2	18.05.2012	5/21/2012 10:38	5/23/2012 7:50	41.47	46.8	10	3.7	1.8	0.004	2
			5/21/2012 10:38	5/24/2012 2:22	42.83	46.6	33	3.5	1.8	0.002	3
1	1	22.05.2012	5/29/2012 13:29	5/28/2012 7:51	42.07	47.52	2	3.8	2.3	0.004	-1
1	1	23.05.2012	5/29/2012 13:29	5/29/2012 22:45	43.31	46.29	2	3.5	1.9	0.002	0
1	2	31.05.2012	6/4/2012 10:37	6/2/2012 0:32	43.32	46.2	60	4.6	1.9	0.059	-2
			6/4/2012 10:37	6/3/2012 9:07	42.82	46.01	5	3.7	1.4	0.007	-1
			6/4/2012 10:37	6/5/2012 16:29	41.45	46.75	20	4	1.8	0.011	1
			6/19/2012 10:33	6/16/2012 1:32	41.5	43.48	2	3.6	1.2	0.006	-3
			6/19/2012 10:33	6/16/2012 6:33	43.33	46.39	15	3.8	2	0.005	-3
			6/19/2012 10:33	6/16/2012 16:29	41.74	44.49	2	3.7	0.3	0.038	-3
			6/19/2012 10:33	6/22/2012 15:04	42.1	45.82	2	3.5	0.9	0.006	3
1	1	25.06.2012	6/26/2012 13:32	6/25/2012 20:05	41.21	47.21	5	4	2.3	0.009	-1

At the next figures are presented the samples of material work-up for 25.03-27.06_2012 Dusheti data. From up to down are presented the curve of tidal gravitational potential, density of earthquake energy (Schtm), earthquake's distribution at the same period, values of SigD and its standard deviation.

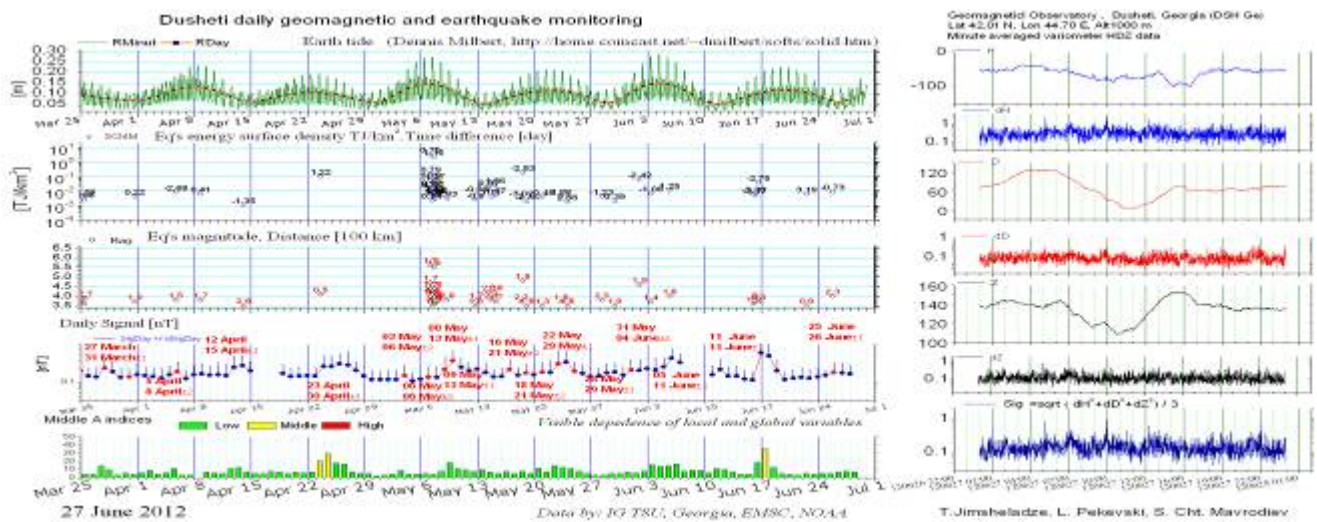


Fig.5. The reliability of the time window prediction for the incoming earthquake.

At Dusheti station, during the period of January-June 2012, there was revealed important disturbance before 7.05.2012 earthquake, Mag 7.5, epicenter Azerbaijan, which is located from Dusheti in 170km. The disturbance was detected 4 days earlier before earthquake. The disturbance was recorded as before earthquake in Azerbaijan as its aftershocks period.

Fig.6. Presents the comparison of the number of all occurred and predicted earthquakes For Dusheti. Fig6 Presents the map graphic for earthquakes with magnitude greater than 4 predicted simultaneously from Dusheti measurement.

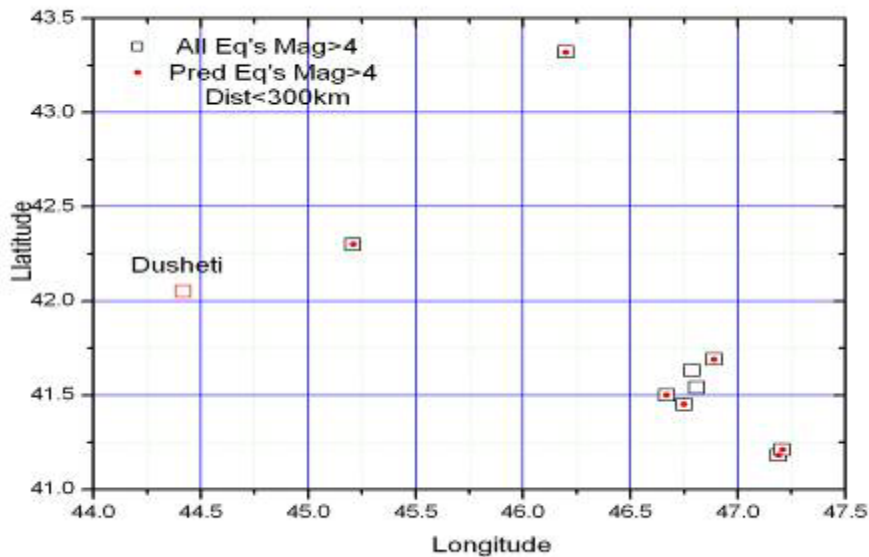


Fig.6 Map graphic for earthquakes with magnitude greater than 4 predicted simultaneously from Dusheti measurement.

It is clear from the picture that among 9 earthquakes for Mag>4; 7 of them were fixed by us.

It is obvious that the occurred in the predicted time period earthquake with maximum value of function S_{ChM} (proportional to the Richter energy density in the monitoring point) is the predicted earthquake. But sometimes there are more than one geomagnetic signals in one day or some in different days. It is not possible to perform unique interpretation and to choose the predicted earthquakes between some of them with less values of energy density. The solution of this problem can be given by the analysis of the vector geomagnetic monitoring data in at least 3 points, which will permit to start solving the inverse problem for estimation the coordinates of geomagnetic quake source as function of geomagnetic quake. The numbering of powers of freedom for estimation the epicenter, depth, magnitude and intensity (maximum values of accelerator vector and its dangerous frequencies) and the number of possible earthquake precursors show that the nonlinear system of inverse problem will be over determinate.

5. Conclusion

The correlations between the local geomagnetic quake and incoming earthquakes, which occur in the time window defined from tidal minimum (± 1 day) or maximum (± 2 days) of the Earth tidal gravitational potential are tested statistically. The distribution of the time difference between predicted and occurred events is going to be Gaussian with the increasing of the statistics.

The presented results can be interpreted as a first reliable approach for solving the “when” earthquakes prediction problem by using geomagnetic data.

References

- [1] Aki K., Earthquake prediction, societal implications, U.S. National Report to IUGG, 1991-1994, Rev. Geo-phys. Vol. 33 Suppl., © 1995 American Geophysical Union, <http://www.agu.org/revgeophys/aki00/aki00.html> , 1995.
- [2] Freund F.T., A.Takeuchi, B. W.S. Lau, Electric Currents Streaming out of Stressed Igneous Rocks – A Step Towards Understanding Pre-Earthquake Low Frequency EM Emissions, Special Issue “Recent Progress in Seismo Electromagnetics”, Guest Editors M. Hayakawa, S. Pulinets, M. Parrot, and O. A. Molchanov, Phys. Chem. Earth, 2006
- [3] Duma G., Modeling the impact of telluric currents on earthquake activity, EGU06-A-01730; NH4.01-1TH5P-0571, Vienna, 2006
- [4] Eftaxias K., P.Kapiris, J.Polygiannakis, N.Bogris, J.Kopanas, G.Antonopoulos, A.Peratzakis and V.Hadjicontis, Signature of pending earthquake from electro-magnetic anomalies, Geophysical Research Letters, Vol.28, No.17, pp.3321-3324, September 2001.
- [5] Eftaxias K., P.Kapiris, E.Dologlou, J.Kopanas, N.Bogris, G.Antonopoulos, A.Peratzakis and V.Hadjicontis, EM anomalies before the Kozani earthquake: A study of their behaviour through laboratory experiments, Geophysical Research Letters, Vol. 29, No.8 10.1029/ 2001 GL013786, 2002.
- [6] Ludwin, R.S., 2001, Earthquake Prediction, Washington Geology, Vol. 28, No. 3, May 2001, p. 27, 2001.
- [7] Mavrodiev S.Cht., Thanassoulas C., Possible correlation between electromagnetic earth fields and future earthquakes, INRNE-BAS, Seminar proceedings, 23- 27 July 2001, Sofia, Bulgaria, ISBN 954-9820-05-X, 2001, <http://arXiv.org/abs/physics/0110012>, 2001.
- [8] Mavrodiev S.Cht., On the Reliability of the Geomagnetic Quake Approach as Short Time Earthquake’s Precursor for Sofia Region, Natural Hazards and Earth System Science, Vol. 4, pp 433-447, 21-6-2004
- [9] Mavrodiev S.Cht., Pekevski, L., and Jimsheladze T., 2008, Geomagnetic-Quake as Imminent Reliable Earthquake’s Precursor: Starting point Future Complex Regional Network, Electromagnetic Phenomena related to earthquakes and volcanoes. Editor: Birbal Singh. Publ., Narosa Pub.House, new Delhi, pp. 116-134.
- [10] Pakiser L, Shedlock K.M., Predicting earthquakes, USGS, <http://earthquake.usgs.gov/hazards/prediction.html>, 1995.
- [11] St-Laurent F., J. S. Derr, Freund F. T. , Earthquake Lights and the Stress-Activation of Positive Hole Charge Carriers in Rocks, Special Issue “Recent Progress in Seismo Electromagnetics”, Guest Editors M. Hayakawa, S. Pulinets, M. Parrot, and O. A. Molchanov, Phys. Chem. Earth, 2006
- [12] Thanassoulas, C., Determination of the epicentral area of three earthquakes ($M_s > 6R$) in Greece, based on electrotelluric currents recorded by the VAN network., Acta Geophysica Polonica, Vol. XXXIX, no. 4, 373-387, 1991.
- [13] Thanassoulas, C., Tsatsaragos, J., Klentos, V., Determination of the most probable time of occurrence of a large earthquake., Open File Report A. 4338, IGME, Athens, Greece, 2001a.
- [14] Thanassoulas, C., Klentos, V., Very short-term (+/- 1 day, +/- 1 hour) time-prediction of a large imminent earthquake, The second paper, Institute of Geology and Mineral Exploration (IGME), Athens, Greece, Open File Report A. 4382, pp 1-24, 2001b.

- [15] Vallianatos F., Tzanis A., On the nature, scaling and spectral properties of pre-seismic ULF signals, Natural hazards and Earth System Science, Vol. 3, pp 237-242, 2003.
- [16] Varotsos P. A., N. V. Sarlis, E. S. Skordas, H. K. Tanaka, and M. S. Lazaridou1, Additional information for the paper 'Entropy of seismic electric signals: Analysis in natural time under time-reversal' after its initial submission, ftp://ftp.aip.org/epaps/phys_rev_e/E-PLLEE8-73-134603, 2006.
- [17] Venedikov A.P., Arnoso R., Vieira R., A program for tidal data processing, Computers & Geosciences, vol. 29, no.4, pp. 487-502, 2003.

(Received in final form 15 December 2012)

ВАРИАЦИИ ГЕОМАГНИТНОГО ПОЛЯ НА ДУШЕТСКОЙ ОБСЕРВАТОРИИ СВЯЗАНИЕ СЕЙСМОАКТИВНОСТЬЮ В ВОСТОЧНОЙ ГРУЗИИ

(Январь - Июнь 1012)

Тамар Джимшеладзе, Георгий Меликадзе, Александр Чанкветадзе, Роберт Гагуа, Тамаз Матиашвили

Резюме

Геомагнитные аномалий перед землетрясениями были зафиксированы многими авторами, но надо отметить что большинство из них не удовлетворяет строгие критерии. Этот метод прогноза землетрясений базируется на корреляции между землетрясениями, геомагнитными аномалиями и наступающими максимумами (или минимумами) приливными вариациями гравитационного поля. Геомагнитное отклонение определяется как отклонения в поле средних значений стандартного отклонения измеряемых минимум 2.5 раз в секунду. Окно вероятности совпадения во времени событий ровняется +- 1 дню для приливно -отливного минимума и +- 2 дня для приливно -отливного максимума. Статистическая достоверность геомагнитных предшественников, зафиксированные Душетской обсерваторий, еще раз подтверждаются данными распределение разницы между прошедшими и спрогнозированными землетрясениями для периода Январь- Июнь 2012

**აღმოსავლეთ საქართველოს ტერიტორიის
სეისმოაქტიურობასთან დაკავშირებული დუშეთის
ობსერვატორიაზე დაფიქსირებული გეომაგნიტური ველის
ვარიაციები**

(იანვარი - ივნისი 1012)

**თამარ ჯიმშელაძე, გიორგი მელიქაძე, ალექსანდრე ჩანკვეტაძე, რობერტ
გაგუა, თამაზ მათიაშვილი**

რეზიუმე

მიწისძვრის წინ გეომაგნიტური ანომალიები დაფიქსირებულია მრავალი ავტორის მიერ, თუმცა აღსანიშნავია რომ მათი უმეტესობა ვერ აკმაყოფილებს მკაცრ

კრიტერიუმებს. პროგნოზის ეს მეთოდი ეყრდნობა კორელაციას მიწისძვრებსა, გეომაგნიტურ ანომალიებს და მიზიდულობის ველის მიმოქცევითი ვარიაციების მოსალოდნელ მაქსიმუმს (ან მინიმუმს) შორის. გეომაგნიტური გადახრა განისაზღვრება როგორც სტანდარტული გადახრების საშუალო მნიშვნელობებიდან, რომლებიც განისაზღვრება მინიმუმ 2.5 ჯერ წამში. მოვლენების თანხვედრის ალბათობის ფანჯარა უდრის $+1$ დღეს, მიმოქცევითი ვარიაციების მინიმუმებისთვის და $+2$ დღეს - მაქსიმუმებისთვის. დუშეთის ობსერვატორიის მიერ დაფიქსირებული გეომაგნიტური წინამორბედების სტატისტიკური დამაჯერებლობა, კიდევ ერთხელ დასტურდება 2012 წლის იანვარ-ივნისის მონაცემებით

Radon and thoron measurements in West Georgia

¹ Janja Vaupotič, ¹ Mateja Bezek, ² Nino Kapanadze, ² George Melikadze, ² Teona Makharadze, ² Zurab Machaidze, ² Mariam Todadze

¹ Jožef Stefan Institute (JSI), Ljubljana, Slovenia (Mateja Bezek, Janja Vaupotič)

² M. Nodia Institute of Geophysics (GI MES), Ivane Javakhisvili Tbilisis State University, Tbilisi, Georgia (Nino Kapanadze, George Melikadze)

Abstract

The Jožef Stefan Institute, Slovenia and M. Nodia Institute of Geophysics, Ivane Javakhisvili Tbilisis State University, Georgia performed joint measurements of radon (^{222}Rn) and thoron (^{220}Rn) at selected places in Georgia using RTM1688-2 continuous radon/thoron monitor (Sarad, Germany) and a set of alpha scintillation cells with an alpha counter (SMM, Czech Republic). Radon in indoor air was measured in indoor air at some places in Tskaltubo, in cave air in the Sataplia Cave and Prometheus Cave, and in thermal waters in Tskaltubo areas. The highest radon concentrations in the air have been found in karst caves, up to 3100 Bq m^{-3} . In thermal waters, the highest radon concentration of 93.8 Bq dm^{-3} was found in thermal water in a health resort, measured from the pipe in bathroom.

Introduction

The Jožef Stefan Institute, Slovenia and M. Nodia Institute of Geophysics, Ivane Javakhisvili Tbilisis State University, Georgia performed joint measurements of radon in indoor air, karst caves and in thermal waters at different locations in Georgia, in the period from June 26 to July 16, 2012, within the international project entitled "Balkan, Black Sea, Caucasus, Caspian Network for Complex Research of Earthquake's Forecasting Possibilities, Seismicity and Climate Change Correlations" (BlackSeaHazNet).

1. Measurements performed by the Jožef Stefan Institute, Slovenia (IJS, SLO)

The research group of the Jožef Stefan Institute (PhD Student Mateja Bezek and Prof. Janja Vaupotič) performed measurements of radon (^{222}Rn) and thoron (^{220}Rn) using a portable RTM1688-2 Radon/Thoron Monitor (Sarad, Dresden, Germany) (Figure 1). Air is pumped at a flow rate of $0.3 \text{ dm}^3 \text{ min}^{-1}$ through the chamber in which the high voltage between the wall and a silicon detector causes the positively charged ^{218}Po and ^{216}Po ions, created by ^{222}Rn and ^{220}Rn alpha transformations, respectively, to deposit on the detector. Based on α -spectrometry, activity concentrations of ^{222}Rn and ^{220}Rn are calculated, stored in the internal memory and later transferred to a personal computer for data evaluation [1-3].



Figure 1. RTM1688-2 portable Radon/Thoron Monitor

1. 1. Radon and thoron measurements indoors

Indoor radon and thoron measurement have been carried out in Tbilisi and Tskaltubo. Average duration of measurement was 24 hours, with continuous recording of concentrations ones an hour. Results are summarised in Table 1 and graphically presented in Figures 2 to 5.

Table 1. Average radon (C_{Rn}) and thoron (C_{Tn}) concentrations in indoor air and C_{Tn}/C_{Rn} ratio

Place	Date in 2012	C_{Rn} in air $Bq\ m^{-3}$	C_{Tn} in air $Bq\ m^{-3}$	C_{Tn}/C_{Rn}
Tbilisi – Guest house (1 st floor)	24.6. 11:26 – 25.6. 20:26	12.9 ± 5.4	7.2 ± 5.5	0.56
Tbilisi – Tunnel (underground)	26.6. 11:42 – 27.6. 11:42	115 ± 20	28.7 ± 16.5	0.25
Tbilisi – Turkish bath (ground floor)	27.6. 12:55 – 28.6. 16:55	10.0 ± 5.5	6.6 ± 4.6	0.66
Tbilisi – Institute of Geophysics (basement)	29.6. 14:55 – 2.7. 14:55	101 ± 17	13.4 ± 10.1	0.13
Tbilisi – Private house Melikadze (basement)	2.7. 17:53 – 4.7. 10:53	190 ± 24	17.3 ± 11.8	0.09
Tskaltubo – Hotel Imereti (guest room, 1 st floor)	12.7. 00:01 – 12.7. 9:01	34 ± 10	6.3 ± 6.0	0.19
Tskaltubo Health Resort (room with swimming pool)	12.7. 11:39 – 12.7. 12:29	1110 ± 115	681 ± 475	0.08

Radon concentrations in indoor air of selected places range from 12.9 to 1110 $Bq\ m^{-3}$ and thoron concentrations from 6.3 to 681 $Bq\ m^{-3}$. In the guest house and in the Turkish bath in Tbilisi high Tn/Rn ratio was observed.

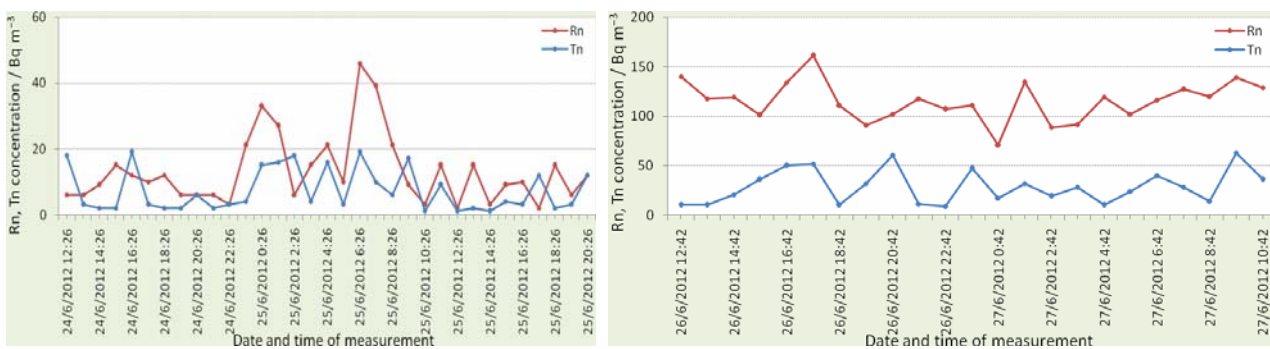


Figure 2. Radon and thoron concentrations in a guest house (1st floor) in Tbilisi and in an underground tunnel in Tbilisi

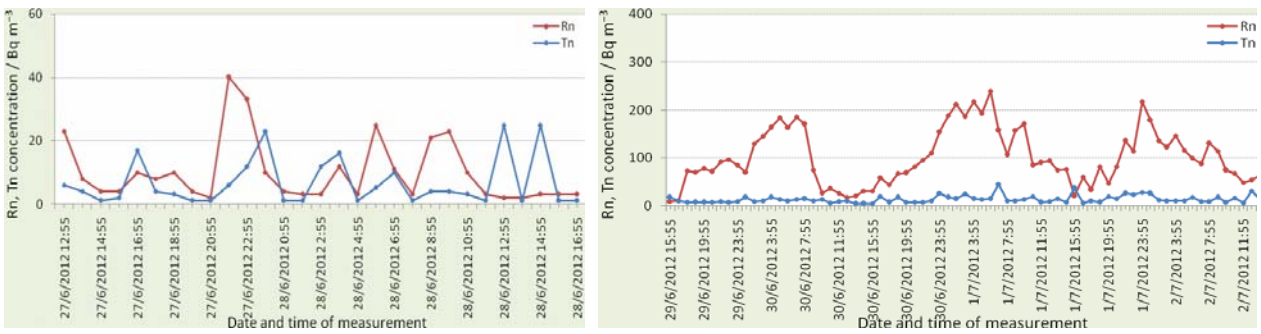


Figure 3. Radon and thoron concentrations in the Turkish bath (ground floor) in Tbilisi and in the basement of the Institute of Geophysics in Tbilisi

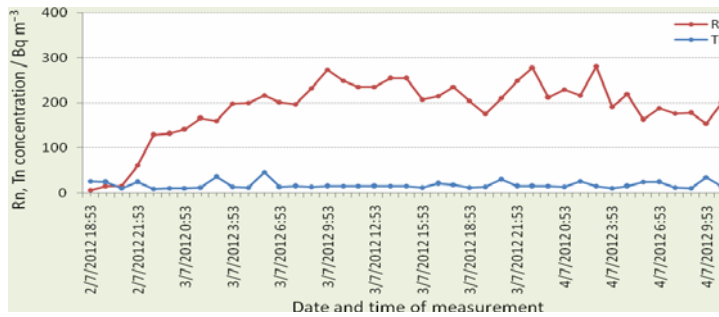


Figure 4. Radon and thoron concentrations in the basement of the private house Melikadze

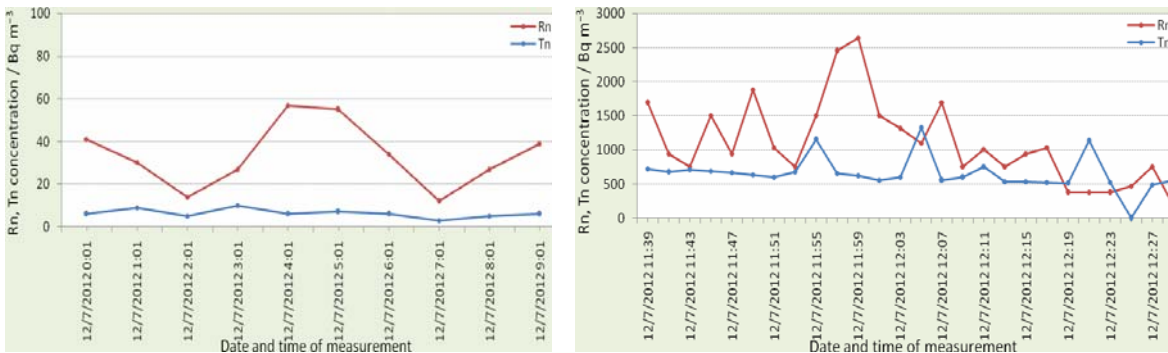


Figure 5. Radon and thoron concentrations in the first floor of the Hotel Imereti and in the room with swimming pool in the Health Resort 2 in Tskaltubo



Figure 6. Ground plan of the Sataplia Cave



Figure 7. Ground plan of the Prometheus Cave

1. 2. Radon and thoron measurements in karst caves

Radon and thoron measurements have been performed in two karst caves in Tskaltubo area: (i) Sataplia Cave and (ii) Prometheus Cave. Ground plans of both caves are presented in Figures 11 and 12. Results are summarised in Table 2 and graphically presented in Figures 6 and 7.

Table 2. Radon (C_{Rn}) in thoron (C_{Tn}) concentrations in the Sataplia Cave and Prometheus Cave

Place	Date in 2012	C_{Rn} in air $Bq\ m^{-3}$	C_{Tn} in air $Bq\ m^{-3}$	C_{Tn} / C_{Rn}
Sataplia Cave				
1. At the entrance, at the cave map	10.7.2012 14:53	1771 ± 266	69 ± 48	0.04
2'. At the end of left branch	10.7.2012 15:13	1995 ± 279	347 ± 239	0.17
2. At the point of left branch	10.7.2012 15:23	2428 ± 316	75 ± 52	0.03
3. Stony heart	10.7.2012 15:43	3094 ± 340	127 ± 88	0.04
3'. At the end of right branch	10.7.2012 15:53	3021 ± 332	85 ± 59	0.03
4. Exit (16 steps before the door)	10.7.2012 16:13	3075 ± 338	109 ± 75	0.04
Prometheus Cave				
1. Colchic Hall	11.7.2012 15:30	193 ± 87	27 ± 19	0.14
2. Medea's Hall	11.7.2012 16:00	880 ± 185	61 ± 42	0.07
3. Hall of Love	11.7.2012 16:20	988 ± 198	41 ± 28	0.04
4. Pass	11.7.2012 16:40	1472 ± 236	55 ± 38	0.04
5. Prometheus Hall	11.7.2012 17:00	1094 ± 208	53 ± 37	0.05
6. Iberia	11.7.2012 17:20	1297 ± 220	144 ± 88	0.11
7. By the Lake	11.7.2012 17:30	1444 ± 231	107 ± 74	0.07

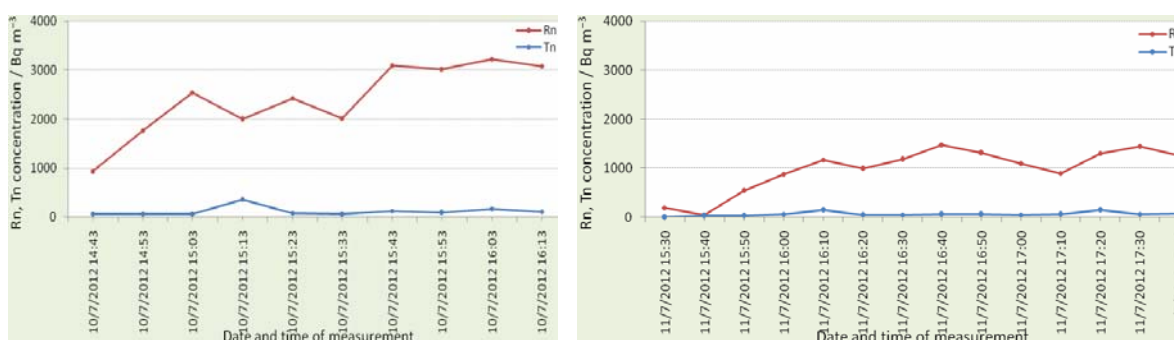


Figure 8. Radon and thoron concentrations in the Sataplia Cave and in the Prometheus Cave

Higher radon and thoron concentrations have been detected in the Sataplia Cave, ranging from about 1800 to 3100 $Bq\ m^{-3}$ and from 69 to 347 $Bq\ m^{-3}$, respectively. In the Prometheus Cave, radon concentration ranged from 193 to 1472 $Bq\ m^{-3}$ and thoron concentration, from 27 to 144 $Bq\ m^{-3}$. There is a relatively low thoron ratio in both caves.

1.3 Radon measurements in thermal waters

Radon has been measured in some selected thermal waters at the Tbilisi and Tskaltubo areas. For that purpose, about 1.5 dm^3 of water was sampled either directly from the borehole or from the bath (as in Health Resort 1 and Health Resort 2 in Tskaltubo) into a plastic vessel (volume 3.5 dm^3). Water sample was continuously bubbling in a closed loop with the RTM1688-2 monitor for about 20 to 30 minutes to expel the majority of radon from water into air [4]. On the basis of the final radon concentration detected in the air after bubbling was stopped, radon concentration in water was calculated. Results are summarised in Table 3.

Radon concentration in thermal waters ranged from 1.3 to 93.8 Bq dm⁻³. These values seem to be too low, especially in cases when radon in thermal water was measured directly from the borehole. Because the team was not able to use their sampling system specially designed for such measurement, a great portion of radon might have been escaped during sampling. Therefore, the results in Table 3 should be considered as preliminary and measurements should be repeated with the proper equipment.

Table 3. Radon (C_{Rn}) concentrations in thermal waters

Place	Comment	Date in 2012	C_{Rn} in water* Bq dm ⁻³	C_{Rn} in gas** Bq dm ⁻³
Tbilisi Spring water (cold)	Gas from borehole	4.7.2012 16:35		5.6 ± 2.8
	Water from borehole	4.7.2012 16:44	2.4 ± 1.2	
Tskaltubo 6 ($T = 43.7$ °C)	Water from borehole	10.7.2012 11:36	17.6 ± 3.9	
Tskaltubo Health Resort 1	Water from bathroom pipe	10.7.2012 12:09	93.8 ± 9.3	
Tskaltubo Health Resort 2	Water from swimming pool	12.7.2012 11:07	37.3 ± 2.2	

*Due to the difficulties with water sampling, most probably the majority of waters have significantly higher radon concentrations as reported

**Gas was sampled directly from the borehole

2. Measurements performed by the M. Nodia Institute of Geophysics, Georgia (GI MES, GE)

The research team from the Nodia Institute of Geophysics, Ivane Javakhishvili Tbilisi State University, Tbilisi, Georgia (Prof. George Melikadze, Dr. Teona Makharadze, PhD Student Nino Kapanadze) measured radon concentrations, gamma dose rate and the concentration of free ions in the air of karst caves [5, 6], and radon concentration in thermal waters [7, 8].

Radon concentration was measured by alpha scintillation technique. For that purpose, air is sampled directly into a scintillation cell (SC) using a pump or syringe, while from water samples radon is degassed and transferred into a scintillation cell. Most often, alpha activity is measured three hours after sampling when secular equilibrium between radon and its decay products has been reached. Commercially available scintillation cells are made of different materials, are of different size and have different efficiency. The system used was produced by SMM Company, Prague, Czech Republic (Figure 9 a).

Gamma dose rate has been measured with a Radiation Monitor (Atomtex, Belarus) (Figure 9 b) and free ions with an Air ion counter (AlphaLab Inc., USA) (Figure 9 c).

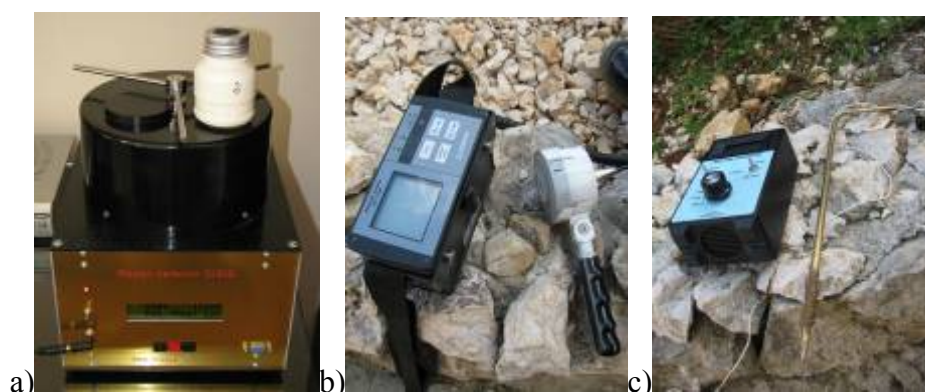


Figure 9. a) Alpha scintillation cell and counter, b) Gamma dose rate monitors and c) Air ion counter

2. 1. Radon measurements in karst caves

Radon was measured in the Sataplia and Prometheus Caves. At each location, air was sampled in parallel into two scintillation cells. Results are presented in Table 4. In the Sataplia Cave, radon concentrations, ranging from about 1100 to 2300 Bq m⁻³, are higher than in the Prometheus Cave. In the Prometheus Cave maximum radon concentration reached 1200 Bq m⁻³. At seven locations there is a good agreement between results of the parallel samples and in the remaining three, the difference is too high. Therefore, a new calibration of the scintillation cells is foreseen.

Table 4. Radon (C_{Rn}) concentrations in Sataplia Cave and Prometheus Cave

Place	Date in 2012	SC number	C_{Rn} in air Bq m ⁻³
Sataplia Cave			
1. At the entrance, at the cave map	10.7.2012 14:40	6	1284 ± 119
	10.7.2012 14:43	8	1446 ± 125
2. At the point of left branch	10.7.2012 15:01	5	1539 ± 129
	10.7.2012 15:02	4	1524 ± 129
3. Stony heart	10.7.2012 15:35	10	2285 ± 157
	10.7.2012 15:35	3	1039 ± 106
4. Exit (16 steps before the door)	10.7.2012 16:02	7	2274 ± 157
	10.7.2012 16:03	9	1582 ± 325
Prometheus Cave			
1. Colchic Hall	11.7.2012 15:30	10	472 ± 72
	11.7.2012 15:31	15	372 ± 63
2. Medea's Hall	11.7.2012 15:55	9	961 ± 102
	11.7.2012 15:59	11	764 ± 93
3. Hall of Love	11.7.2012 16:15	8	940 ± 101
	11.7.2012 16:16	5	1133 ± 111
4. Pass	11.7.2012 16:29	2	756 ± 91
	11.7.2012 16:30	6	1113 ± 110
5. Prometheus Hall	11.7.2012 16:50	3	700 ± 87
	11.7.2012 16:51	7	916 ± 100
6. Iberia	11.7.2012 17:10	14	1164 ± 112
	11.7.2012 17:11	1	1115 ± 110

The results of gamma dose rates and concentration of free ions are summarised in Table 5.

Table 5. Gamma dose rate (\dot{D}) and free ion number concentration (C^+ and C^-) in Sataplia Cave and Prometheus Cave

Place	\dot{D} nSv h ⁻¹	\dot{D} μR h ⁻¹	C^+ cm ⁻³	C^- cm ⁻³
Sataplia Cave				
1. At the entrance, at the cave map	22	0.043	27000	193000
2. At the point of left branch	70	0.250	29000	333000
3. Stony heart	130	0.062	20000	170000
4. Exit (16 steps before the door)	60		27000	21000
Prometheus Cave				
1. Colchic Hall	250	150	5000	3900
2. Medea's Hall	45	105	15000	16000

3. Hall of Love	49	17	18000	18500
4. Pass	600	99	15000	14000
5. Prometheus Hall	606	12	15000	17000
6. Iberia			24000	16000

2.2 Radon measurements in thermal waters

Radon was measured in twelve water samples, mostly thermal waters, sampled directly from boreholes, usually in parallel, using two scintillation cells. Results are presented in Table 6. Generally, there is a good agreement between results of the two parallel measurements. However, also results obtained with scintillation cells are most likely too low due to radon degassing during sampling.

Table 6. Radon (C_{Rn}) concentrations in thermal waters

Place	Comment	Date in 2012	SC number	C_{Rn} Bq dm ⁻³
Tskaltubo Health Resort 1	Indoor air	10.7.2012 12:07	1	1.1 ± 0.1
			2	0.4 ± 0.1
	Water from bathroom pipe	10.7.2012 17:34	14	9.1 ± 0.8
Tskaltubo 6 ($T = 43.7$ °C)	Water from borehole	10.7.2012 17:23	11	1.7 ± 0.3
Sataplia river	Water from river	10.7.2012 17:43	15	3.6 ± 0.5
Sataplia water under stalagmite	Water from under stalagmite	10.7.2012 17:50	16	1.3 ± 0.3
Prometheus Cave, lake	Water from lake	11.7.2012 19:13	17	0.9 ± 0.2

3. Comparison of radon results obtained by IJS, SLO and GI MES, GE

Intercomparison measurements of radon in air (karst caves) and radon in thermal waters (some boreholes) have been performed, comparing results obtained with radon/thoron monitor RTM1688-2 (IJS, SLO) and scintillation cells (SC) (GI MES, GE). Results are summarised in Table 7a for karst caves and in 7b for thermal waters.

Table 7a. Comparison of radon concentrations (C_{Rn}) obtained by RTM1688-2 (IJS, SLO) and SC (GI MES, GE) in the air of Sataplia Cave and Prometheus Cave

Place	RTM1688-2 C_{Rn} in air Bq m ⁻³	SC C_{Rn} in air Bq m ⁻³	SC / RTM1688-2	SCn1 / SCn2
Sataplia Cave				
1.	1771 ± 266	1284 ± 119 (SC6) 1446 ± 125 (SC8)	0.73 0.82	0.89
2.	2428 ± 316	1539 ± 129 (SC5) 1524 ± 129 (SC4)	0.63 0.63	1.01
3.	3094 ± 340	2285 ± 157 (SC10) 1039 ± 106 (SC3)	0.74 0.34	2.20
4.	3075 ± 338	2274 ± 157 (SC7) 1582 ± 325 (SC9)	0.74 0.51	1.44
Prometheus Cave				
1.	193 ± 87	472 ± 72 (SC10) 372 ± 63 (SC15)	2.45 1.93	1.27

2.	880 ± 185	961 ± 102 (SC9) 764 ± 93 (SC11)	1.09 0.90	1.21
3.	988 ± 198	940 ± 101 (SC8) 1133 ± 111 (SC5)	0.95 1.15	0.83
4.	1472 ± 236	756 ± 91 (SC2) 1113 ± 110 (SC6)	0.51 0.76	0.68
5.	1094 ± 208	700 ± 87 (SC3) 916 ± 100 (SC7)	0.64 0.84	0.76
6.	1297 ± 220	1164 ± 112 (SC14) 1115 ± 110 (SC1)	0.90 0.86	1.04

Table 7b. Comparison of radon (C_{Rn}) concentrations in thermal waters obtained by RTM1688-2 (IJS, SLO) and SC (GI MES, GE)

Place	Comment	RTM1688-2 C_{Rn} $Bq\ dm^{-3}$	SC C_{Rn} $Bq\ dm^{-3}$
Tskaltubo 6 ($T = 43.7\ ^\circ C$)	Water from borehole	17.6 ± 3.9	1.7 ± 0.3 (SC11)
Tskaltubo Health Resort 1	Water from bathroom pipe	93.8 ± 9.3	9.1 ± 0.8 (SC14)

As seen in Tables 7a and 7b, RTM1688-2 monitor shows significantly higher radon concentrations than SC at the majority of sampling points in air in karst caves and in thermal waters.

Conclusions

1. Radon concentrations in indoor air of selected places range from 12.9 to 1110 $Bq\ m^{-3}$ and thoron concentrations from 6.3 to 681 $Bq\ m^{-3}$. In the guest house and in the Turkish bath in Tbilisi high Tn/Rn ratio was observed.
2. Higher radon and thoron concentrations have been detected in the Sataplia Cave, ranging from about 1800 to 3100 $Bq\ m^{-3}$ and from 69 to 347 $Bq\ m^{-3}$, respectively. In the Prometheus Cave, radon concentration ranged from 193 to 1472 $Bq\ m^{-3}$ and thoron concentration, from 27 to 144 $Bq\ m^{-3}$. There is a relatively low thoron ratio in both caves.
3. Radon concentration in thermal waters ranged from 1.3 to 93.8 $Bq\ dm^{-3}$. These values seem to be too low, especially in cases when radon in thermal water was measured directly from the borehole. Because the team was not able to use their sampling system specially designed for such measurement, a great portion of radon might have been escaped during sampling. Therefore, the results in Table 3 should be considered as preliminary and measurements should be repeated with the proper equipment.
4. Intercomparison measurements of radon in air (karst caves) and radon in thermal waters (some boreholes) have been performed, comparing results obtained with radon/thoron monitor RTM1688-2 (IJS, SLO) and scintillation cells (SC) (GI MES, GE). Results are summarised in Table 7a for karst caves and in 7b for thermal waters. RTM1688-2 monitor shows significantly higher radon concentrations than SC at the majority of sampling points in air in karst caves and in thermal waters.

References

- [1] Saso Dzeroski, Ljupco Todorovski, Boris Zmazek, Janja Vaupotic, Ivan Kobal
Modelling Soil Radon Concentration for Earthquake Prediction. [Citation Graph (0, 0)][DBLP]
Discovery Science, 2003, pp:87-99 [Conf]

- [2] Janja Vaupotic “Levels of nanosize radon decay products in indoor air: a comparison for different environments” Radon Center, Department of Environmental Sciences, Jozef Stefan Institute, Ljubljana, Slovenia Coll Antropol 32:99-104. 2008
- [3] Janja Vaupotic “Nanosize radon short-lived decay products in the air of the Postojna Cave” Jozef Stefan Institute, Radon Center, P O Box 3000, 1001 Ljubljana, Slovenia Sci Total Environ 393:27-38. 2008
- [4] Kobal Ivan, Vaupotic J, Kozak K, Mazur J, Birovljev A, Janik M, Celikovic I, Ujic P, Demajo A, Krstic G, Jakupi B, Quarto M, Bochicchio F (2006): High natural radiation exposure in radon spa areas: a detailed field investigation in Niška Banja (Balkan region) (Article) Journal of Environmental Radioactivity, (2006) vol.89 (3) 249-260
- [5] Saakashvili N., Tabidze M., Tarkhan-Mouravi I., Khelashvili E., Amiranashvili A., Kirkitadze D., Melikadze G., Nodia A., Tarkhnishvili A., Chikhladze V., Lominadze G., Tsikarishvili K., Chelidze L. – Climatic, Aero – Ionizing and Radiological Characteristics of the Health Resort – Tourist Complex of Tskaltubo City, Papers of the Int. Conference International Year of the Planet Earth “Climate, Natural Resources, Disasters in the South Caucasus”, Trans. of the Institute of Hydrometeorology, vol. No 115, ISSN 1512-0902, Tbilisi, 18 – 19 November, 2008, pp. 31 – 40 (in Russian).
- [6] N. Saakashvili, M. Tabidze, I. Tarkhan-Mouravi, A. Amiranashvili, G. Melikadze, V. Chikhladze. “To a question about the organization of ionotherapy at the health resorts of Georgia”. Modern problems of using of health resources, Collection of scientific works of international conference Sairme-June 10-13, 2010, Collection of scientific works is refereed in abstract E-journal of “Tekhinform”.
- [7] Avtandil G. Amiranashvili, Tamaz L. Chelidze, George I. Melikadze, Igor Y. Trekov, Mariam Sh. Todadze, “Quantification of the radon distribution in various geographical areas of West Georgia”, Journal of Georgian Geophysical Association, №12, 2008.
- [8] George I. Melikadze, Avtandil G. Amiranashvili, Kahha G. Gvinianidze, David G. Tsereteli, Mariam Sh. Todadze “Correlation Between Radon Distribution and prevalence of lung Cancer in West Georgia”, “Environment and Recourses”, Association of Academics of Science in Asia Workshop, 25-27 September 2009, Izmir, Turkey, pp 176-180

(Received in final form 27 December 2012)

Измерение Радона и Торона в западной Грузии

Ианиа Вауротик, Матея Безек, Нино Капанадзе, Георгий Меликадзе, Теона Махарадзе, Зураб Мачаидзе, Мариам Тодадзе

Резюме

Словенским Институтом им. Иозефа Штефана и Институтом Геофизики им. Нодиа, Тбилисского Государственного Университета им. Иване Джавахишвили были проведены совместные измерения Радона (^{222}Rn) и Торона (^{220}Rn), с помощью прибора непрерывного мониторинга RTM1688-2 Радона/Торона (изготовления (Sarad Германия) и детекторов альфа датчиков с альфа счетчиком (SMM Чешская республика) Западной Грузии. Внутренние измерения радона были проведены в некоторых местах в Цкалтубо, в пещерах Сатаплия и Прометей и термальных водах Цкалтубо. Самые высокие концентрация радона в воздухе были зафиксированы в карстовых пещерах, до 3100 Беккерелей куб. мет. В термальный водах самые высокие значения радона- 93.8 Беккерелей куб. м, были зафиксированы сливной в трубе радоновых ванн.

რადონისა და თორონის გაზომვები დასავლეთ საქართველოში

იანია ვოროუტიკ, მატეა ბეზეკ, ნინო კაპანაძე, გიორგი მელიქაძე, თეონა მახარაძე, ზურაბ მაჩაიძე, მარიამ თოდაძე

რეზიუმე

სლოვენის ოსეფ შტეფანის სახ ინსტიტუტის და ივანე ჯავახიშვილის სახ. თბილისის სახელმწიფო უნივერსიტეტის, ნოდის გეოფიზიკის ინსტიტუტის მიერ ერთობლივად ჩატარდა რადონისა და თორონის გამოკვლევები დასავლეთ საქართველოში. კვლევების გამოყენებული იქნა რადონისა და თორონის სამონიტორინგო ხელსაწყო RTM1688-2 (Sarad, გერმანია) და ალფა სინტილიაციური დეტექტორები, ალფა მთვლელით (SMM ჩეხეთის რესპუბლიკა). რადონის შიდა გაზომვები განხორციელდა წყალტუბოს რაიონში, სათაფლიისა და პრომეთეს მღვიმეებში და წყალტუბოს თერმალურ წყლებში. რადონის ყველაზე მაღალი მნიშვნელობები დაფიქსირდა მღვიმეების ჰაერში, 3100 ბეკერელი კუბ. მეტრში. თერმალურ წყლებში ყველაზე მაღალი-93.8 ბეკერელი კუბ. მეტრში დაფიქსირდა ვანებიდან გამომავალ წყალსადენში.

Seismotectonic movements – one of the main receptors in exodynamic processes

Jashi G., Chelidze T., Chichinadze V.

Abstract

One of the most important tasks in the modern civilization is the study of the mechanism of exodynamic processes in nature, catastrophes caused by them and the problem of management of such processes. Defending society from natural disasters has become more actual problem nowadays, as disorganized and often irrational human interference in natural processes is often followed by sharp imbalance in the environment and development of vast natural catastrophes. The problem is especially acute in mountainous regions.

In Georgia the complicated geomorphologic and geotectonic conditions provoke activation of landslides, mudflows, erosions, which in their turn, in case of deterioration of harsh climate conditions cause activation of disastrous processes, damage of living environment and often human loss. Dimensions of landslide-gravitational processes in Georgia are conditioned by the fact that the bulk of the territory is situated within the VII-IX intensity earthquake belt. Georgia is characterized with complex geomorphologic and geotectonic structure and belongs to so called continental collision block, the tectonic processes in which are expressed by the seismicity in the region. As a global phenomenon it is observed as deformations caused by collision of lithospheric plates and movement of the Arabian continental block by several cm per annum in the northern direction.

According to catastrophe risk index Georgia belongs to the list of countries with medium and high risks.

Increase in occurrence and intensity of the natural catastrophes, high level of disasters risks have required adopting of international strategies and programs.

Exodynamic natural processes depend on multiple, different from one another, always active and time variation factors. These factors stipulate genesis, development and activation of exodynamic processes.

The main factors that cause disastrous processes may be divided in two parts: 1. the main, internal factors depending on the geotectonic structure of the region and 2. the external factors caused by natural phenomena – climate variation, human influence on the dynamic imbalance of the upper crust of the earth, etc [1,2,4].

The main factors determining the exodynamic processes are the engineering-geologic structures of the rocks in the region. Rocks are considered as a multicomponent dynamic system, the state (structure and properties) of which regularly changes from diagenesis to hypergenesis. Geomorphologic structure of the environment, relief shapes, its energy gradients that are tightly connected with the contemporary tectonic movements are very important for development of the above mentioned processes. Formation of morphogenesis is substantially influenced by the gravity force – a stress vector that is determined by tectonic movement gradient and energy potential of the relief [1,4].

Unity of endogeneous processes in soil and exodynamic processes on the day surface form the landscape shapes of the Earth crust and geomorphologic formations of the environment. Besides, activation of exodynamic processes mainly depends on contemporary seismotectonic vibrational processes.

The contemporary seismotectonic vibrational motions are very important for formation of geologic condition of a region. It may be admitted that contemporary tectonic movements and seismic phenomena are the main receptors for gravitational processes. In Georgia there is a great

deal of information on neotectonics and seismology as a result of numerous investigations. However, the qualitative and quantitative assessments of the contemporary movements and seismic hazard risks have not been completely done.

For assessment of the contemporary geomorphologic formation of the Earth's crust it is necessary to briefly review the history of its geological development.

The neotectonics of the regions of the Caucasus and Ponto refer to the fact that here new stage of geological cycle is developing that refer to certain cyclic nature of the late Alpine tectonic movements and consequently the innateness of the relief morphostructure.

The present shape of the Caucasus region was formed at the beginning of Miocene and Pliocene, the time when the Caucasian mega-anticlinorium was intensely and the Greater and Lesser Caucasus were formed. The rate of vertical movements especially increased in antropogen period when that main ridge of the Caucasus rose by 3-5 km (Hain), and the one in the Lesser Caucasus – by 2-3.5 km (Milanovsk). By this time in the sinking zones of the Transcaucasian territory the basins of the Caspian and the Black Sea were formed, and in the rising zones some crystal massifs appeared. The summarized movement amplitude in the region was 10-11 km. In the Pliocene-Miocene period the rise amplitude in the central segment of the Greater Caucasus was 4.75 km, in the then-time western and eastern regions – 2.5-3 km. Such a diapason of the neotectonic movement stipulated high energy potential of the relief. Consequently, the rising rate in the mountain system of the Caucasus increased and accumulation of coarse-granular continental sediments in the sinking zones was more massive as well. In the post-upper-Pleistocene period the rising rate of the Alpine orogenesis mountain system increases more intensely and reaches the maximum point in the Holocene.

The orogenic movements were accompanied by deep fault formation. Faults of seismic origin were especially observed in the cases of block compositions of geological structures where separate blocks moved by irregular speed. It was expressed in relief morphology, in slope inclinations by different angles, in the formation of low density sediments and development of hydrologic net in them.

In the middle of the twentieth century a new cycle of activation of seismic phenomena was recorded in the Caucasian region, examples of which are the earthquakes of Gegechkori in 1957, Madataph in 1959, Klukhori and Chkhalta in 1969, Zangezuri and Alaverdi in 1968, Dagestan in 1970, Dmanisi in 1976, Spitak in 1988, Racha-Imereti in 1991, Mtiuleti in 1998, Vani in 2010, etc. Some periods of earthquake recurrence were observed. The period of strong, intensity IX earthquake recurrence in the Caucasus lasted during 60-100 years, intensity VIII earthquakes – 10-15 years, intensity V earthquakes – 4 years, and intensity II earthquakes – 2 years. On slopes with tectonic stress the gravitational processes were manifested as intensity III-IV earthquakes; on the slopes with more than 40% inclination some landslide processes were activated and conditions for development of mudflows were prepared [1,3,4].

The geomorphologic and geodynamic investigations make it obvious that all the strong earthquakes in the Caucasus are caused by sign-changing movements of morphostructure blocks. The contemporary strong seismodislocations and gravitation phenomena are directly linked with seismotectonic zones.

The foci of all the strong earthquakes recorded in the Caucasus are situated in the granite layer. The earthquake foci on the Javakheti Highland are situated in the 5-10 km depth, on the Caucasus – in the 15-30 km depth, and on the Georgian block – 20 km depth.

The slope-gravitation processes caused by earthquakes are very quick-acting and do not depend on time factor. It mainly depends on slope stress, material constitution and water intrusion quality of the rocks.

There are two main cases of earthquake influence on gravitation processes: 1) the earthquake is manifested as force factor and reason for quick action (landslide, avalanche, vast collapse); 2) the earthquake is a mechanism that stimulates imbalance in gravitation slopes followed by development of landslides and mudflows, e.g. in the Adjara shore line the intensity IV-V

earthquake in 1968 caused activation of calmed earthquake foci in the Kobuleti and Khelvachauri regions.

Activation of exodynamic processes are mainly stipulated by endogenic processes in soil, in particular, earthquakes that may provoke landslides, mudflows, rock-avalanches and any microtectonic movements. A typical example for it was the Racha-Imereti earthquake that caused rock-avalanche and in its turn, it destructed the whole village of Khakhieti in Racha.

During the recent years the increased activation of exodynamic processes, high level of catastrophe risks stipulated working out international strategies and programs. Within the framework of the UNDP Development Program many of projects have been planned. The projects aim to eliminate probable risks and damages. These programs meet the priorities of the main working program and serve to the interests of the world development.

(Received in final form 20 December 2012)

References

- [1] Церетели Э.Д. – Природно-катастрофические явления и проблема устойчивого развития Грузии и приграничных территорий. Диссертация на соискание ученой степени докт. геогр. Наук, Тбилиси, 2003.
- [2] წერეთელი ე., გობეჯიშვილი ხ., ბოლაშვილი ნ., გაფრინდაშვილი გ., ნანობაშვილი თ. – ბუნებრივი ეგზოდინამიკური კატასტროფების მდგომარეობა და ანთროპოგენური დატვირთვის რისკი საქართველოში, მათი მართვის ოპტიმიზაციის ქმედებები, გეოგრ. ინსტ. შრომათა კრებული, ახალი სერია, №4(83), თბილისი, 2012.
- [3] Цицишвили Д.А. – Инженерная геофизика в условиях горной страны. Тбилиси, Мецниереба, 1980, с 216.
- [4] ჭელიძე თ. – გეოფიზიკური მეთოდები ბუნების დაცვაში, თბილისი, 2004, გვ. 267.

Сеймотектонические явления – основные рецепторы экзодинамических процессов

Джаши Г.Г., Челидзе Т. Л., Чичинадзе В.К.

Резюме

Экзодинамические процессы зависимы от многих, отличающих друг от друга постоянных и меняющихся во времени факторов. Они определяют возникновение, развитие и активизацию экзодинамических процессов. Современные тектонические движения и сейсмические явления представляют собой основные рецепторы гравитационных процессов. На Кавказе все сильные землетрясения обусловлены знакопеременными движениями морфоструктурных блоков.

სეისმოტექტონიკური მოძრაობები – ეგზოლინამიკური პროცესების ერთ-ერთი ძირითადი რეცეპტორები

გ. ჯაში, თ. ჭელიძე, ვ. ჭიჭინაძე

რეზიუმე

ბუნებაში მიმდინარე ეგზოლინამიკური პროცესები მრავალ, ერთმანეთისაგან განსხვავებულ მუდმივ მოქმედ და დროში ცვალებად ფაქტორებზეა დამოკიდებული. ისინი განაპირობებენ ეგზოლინამიკური პროცესების წარმოშობას, განვითარებას და აქტივიზაციას. თანამედროვე ტექტონიკური მოძრაობები და სეისმური მოვლენები არის გრავიტაციული პროცესების ერთ-ერთი ძირითადი რეცეპტორები. კავკასიაში ყველა ძლიერი მიწისძვრა განპირობებულია მორფოსტრუქტურული ბლოკების ნიშანცვლადი მოძრაობებით.

The anomalous magnetic field and its relation to the deep structure of the territory of Georgia

Mindeli P.Sh., Ghonghadze S.A., Ghlonti N.I., Kiria J.K

Abstract

One of the important properties of the Earth is that it is characterized with its intrinsic magnetism – magnetic field. The observed magnetic field reflects summarized effects of anomalous masses. Analyses of geophysical fields, whatever purpose they have, require to be divided into main components. It is one of the important conditions for revealing physical-geological nature of an observed field. Besides, the anomaly parameters are in direct correlative dependence with the attitude positions of anomalous bodies.

Multi-aspect self-descriptiveness of the magnetic field has stipulated multiple and multibranch mapping of the magnetic field of the Earth by the aeromagnetic method.

It is very difficult and labour-consuming to map the territory of Georgia with the aeromagnetic method in appropriate scale and precision. The bulk of the territory is occupied with high mountain chains being an obstacle for flying around the area in necessary direction and at required height. It influences on the quality of surveys and accuracy of cartographic images of the anomalous magnetic field. However, certain studies of the geomagnetic field of Georgia may be considered completed and before passing to the following phase, higher in quality, its materials are undergoing detailed analyses, construction of unified summarized maps, reinterpretation and generalization.

This work involves a survey of works for mapping the anomalous magnetic field ΔT_a in 1:200000 scale.

The study of the territory of Georgia by aeromagnetic method began with surveying by *West Geophysical Trust* (Leningrad) in 1960 in the North Caucasus. The survey involved the southern slope of the Greater Caucasus and the part of the Black Sea to the north from the Poti latitude in the 1:20000 scale. However, those surveys do not meet nowadays requirements due to the low quality of techniques and methods of that time.

Modern technical progress in absolute measurement of the magnetic field module ΔT_a by means of nuclear precession and nuclear quantum equipments, also by technically and methodically improved aeromagnetic surveys begun in 1960ies have stipulated for resurvey of the territory of Georgia by aeromagnetic method in 1:50000 and 1:200000 scales.

In 1973 the second phase of the investigation of the territory of Georgia by the higher standard aeromagnetic methods began. Besides, in geological-geophysical investigations the most prioritized were the prospect trends in order to discover new deposit minerals by means of equipment АЯМП-7 in ore areas of different genetic type and formation structure.

In 1973-74, after aeromagnetic surveys in Bolnisi Region, aeromagnetic investigations of the whole territory of Georgia in the 1:50000 and 1:200000 were carried out.

The main goal of the investigations was to study constant constituents of the magnetic field of the region at different heights in detail and accurately and in appropriate specified scales. More precisely they involved constructing of maps and schemes describing the anomalous magnetic field ΔT_a with optimal precision that would favour the solution of the following geological tasks:

- a) Mapping of magnetoactive, magmatogene and volcanogenic-sedimentary formations and determining boundaries between them;

- b) Studying deep geologic structure as a whole and determining the structural elements and material constitution to the extent of possibility.
- c) Determining magnetic distinctions of different mineral deposits with assessment of their prospects.

Nevertheless, according to the authors of the report [G.Sekhniaidze, N.Sagharadze] precision of the survey by control observations is $m_T = \pm 5nTl$, and in high gradient fields it is $m_T = \pm 10nTl$.

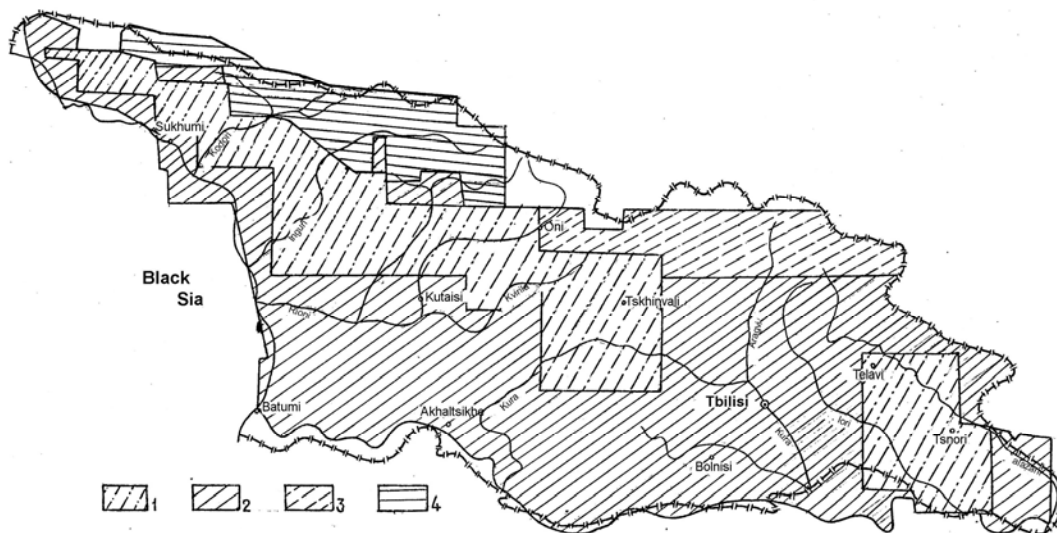


Figure 1. Scheme of aeromagnetic study of the territory of Georgia, scale: 1:2500000

Areas of aeromagnetic surveys

- 1 - scale: 1:50000, equipment KAM-28, photo connection.
- 2 - scale: 1:50000, equipment AMII-7 photo and visual connection.
- 3 - scale: 1:50000, equipment ACF-45.
- 4 - scale: 1:50000, horizontal survey, equipment M-13, visual connection.

The materials of aeromagnetic surveys are different in quality and information value due to complicated geologic-geophysical conditions of the region and different technical-methodological standards of works. Nevertheless, the level of study of the territory on the basis of scale taxonomy is assessed and presented as a cartogram (Figure 1). As shown by the cartogram the territory is not completely covered in any scale of aeromagnetic survey. Besides, there are some areas left without surveying: the high mountainous (ridge) part of the Greater Caucasus, the water area of the Black Sea in the scales 1:200000 and 1:50000, the southern part of the Lesser Caucasus (Adjara, Trialeti) in the scale 1:2500000 and other small, border areas.

Complete description of the structure of the magnetic field and its effective interpretation for solving the tasks of the deep structure and substantive composition of the Earth's deep heterogeneity requires mapping of the anomalous magnetic field at different heights. Such maps are also important for carrying out exploratory-prospecting works. Heights and scales of such maps are determined by taking into account geological tasks and geological-geophysical condition of an investigated area. In this respect there is too limited choice as the scales and heights of surveys of the magnetic field of the territory of Georgia are conditioned and

determined mainly in accordance to abilities of air transport (airplanes, helicopters) in difficult relief conditions. Consequently, the aeromagnetic surveys carried out on the whole territory of Georgia are done in three different scales: 1:2500000, 1:200000 and 1:50000.

As a result of revision of the primary aeromagnetic materials a map (on 14 sheets) of the anomalous magnetic field of Georgia in the scale 1:200000 with the section in 0.5 mega-erg was constructed. The map is constructed on the bases of normal field in 1975 by Institute of Terrestrial Magnetism Ionosphere and Radio Wave Propagation. Precision of the cartographic image of the anomalous magnetic field taking into account precision of measurements is $m(\Delta T) = \pm 15-20 \text{ nTl}$.

As the bulk of the archives materials of the aeromagnetic investigations of the past century are in paper form and the modern methods of analysis and interpretation of geophysical data require computer technologies, it is necessary to digitize those data that will be acceptable for up-to-date digital geophysical cartography.

As a whole, processing of the archives materials is to be divided in three phases: digitization of paper data, conversion of the digitized results into the required data format and mathematical procession of data in order to eliminate probable errors. Magnetic data of different surveys were converted into 2*2 grid by the *Kriging* method, a geostatic method for grid constructing, by which a map in the scale 1:200000 was constructed by means of the *Surfer* software.

In addition, in order to verify the accuracy of the constructed map and determine spatial regulations of the anomalous magnetic field of the region of the Caucasus isthmus similar magnetic maps of the adjoining countries have been digitized. The data on the Black Sea water area obtained from the available maps in the 1:000000 were digitized in order to be involved in the map construction.

By means of the GIS technology (*MapInfo*, *Surfer*, *Vextractor*) the obtained data were included into a unite system and the task of construction of the magnetic map was newly solved (*Figure 2*). On the basis of the drawn maps some digital maps of isolines were constructed by the method of linear interpolation. The length of the calculated isodynamic line is 20 nTl.

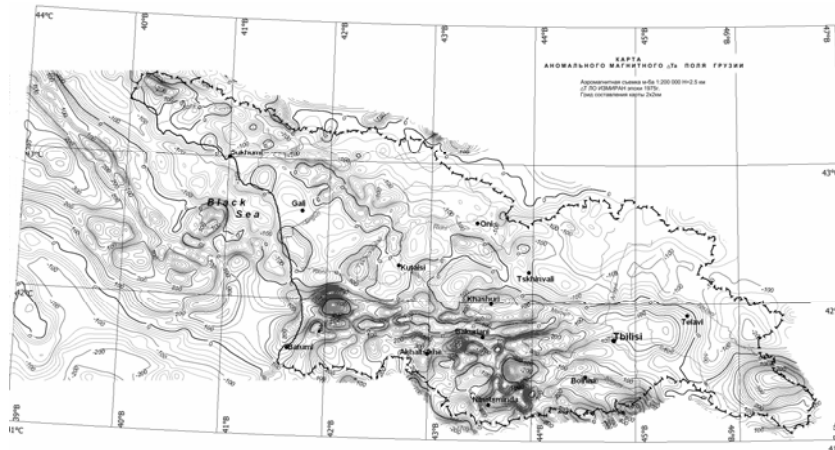


Figure 2.

Usually, a qualitative analysis of potential geophysical fields considers only solution of direct and reverse tasks. However, on the basis of the quantitative analysis, it is also possible to carry out the study of field structure and substance-formation interpretation of anomalies supposed for obtaining more geological information from them, formerly named as “Qualitative interpretation”.

One of the primary phases in the analysis of the geophysical field in respect of solution geological, partially regional tasks is their zoning that has been used so far. At the stage of so called qualitative interpretation the method of visual zoning of fields is a source for different subjective conclusions. Formalized zoning by means of corresponding programmed-

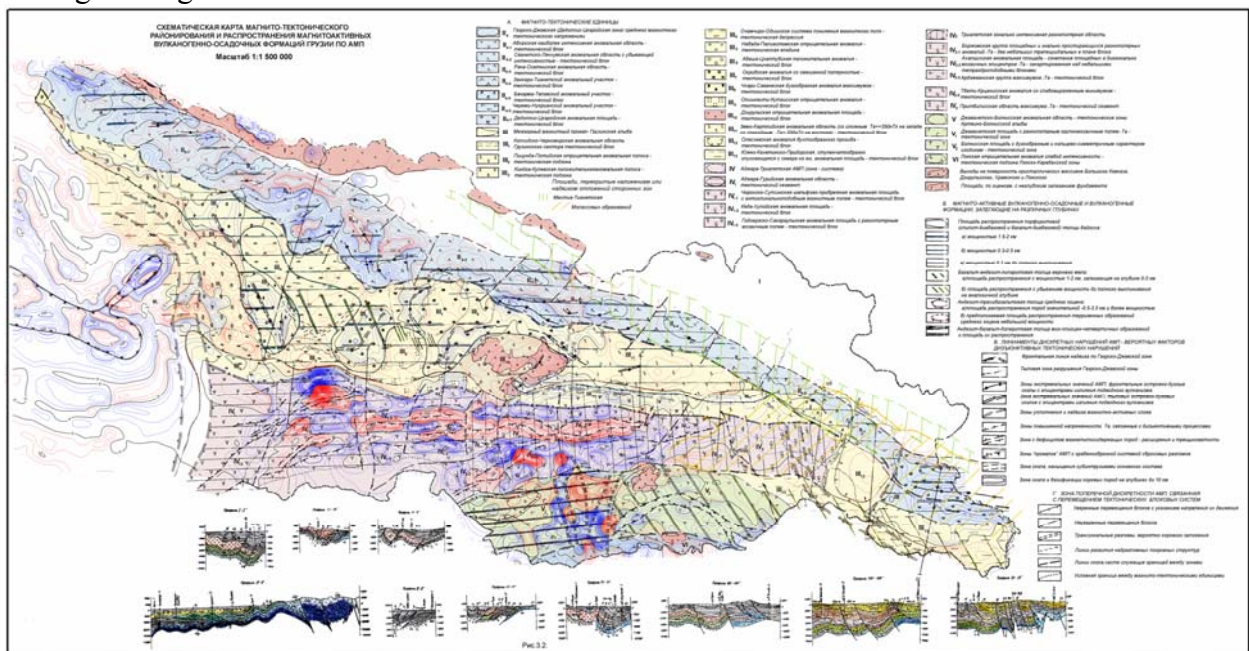
mathematical equipment with the consequent geological interpretation and connection to the real geological situation of the received formal result is able to use the information obtained from geological fields more completely.

For magnetic-tectonic zoning of a studied territory a transformed magnetic field is used. Transformation is the most wide-spread method for transformation and formal division of fields and filtration of the observed fields in order to distinguish useful information and suppress interference.

The theoretical basis for transformation of potentially useful fields is the Poisson integral, which is a solution for the outer Dirichlet problem for plane.

The transformation of the magnetic field was carried out by *Oasis Montaj* software.

For the zoning of the magnetic field we used two methods: the method of smoothing of fields and the method of analytic continuation in the upper direction. The method of smoothing is used to suppress interference connected with random errors. The method of analytic continuation in the upper direction makes it possible to smooth interference, suppress local anomalies and distinguish regional ones.



We recalculated the magnetic field of Georgia in the upper semi-space at heights of 6, 9 and 12 km. The optimal height for recalculation in order to receive maximal effect in the summarized field is determined in a practiced way – gradual increase in the height of recalculation.

At less height the intensity of the residual field rapidly decreases and mainly reflects local anomalies. As we have observed the interval of slow variation of the anomalous field takes place after 10 km and the configuration of anomalous areas is conserved in smoothed form. Magnetic anomaly of any sign is stipulated by surplus or shortage of rock magnetization. This is the consequence of mineral accumulation of deposits.

A map of magnetic-tectonic zoning of the territory of Georgia was constructed (*Figure 3*) on the basis of the geological-formational map.

As a whole, magnetic-tectonic zoning is adaptation of the same action carried out with geological background. However, when considering this process from the viewpoint of deep structure received by magnetic prospecting the former substantially specifies the latter. Besides, the interzonal tectonic boundaries and zone structures inside the blocks are specified, their continuation in immersion under young and molasse sediments is determined.

The schematic map of magnetic-tectonic zoning and distribution of magnetoactive volcanogenic formations in the depth is interesting for paleogeotectonic (geodynamic) study of the territory. Substantive properties distinguished during zoning of different areas of the

magnetic field may be geologically considered in further works on interpretation of the anomalous magnetic field of Georgia.

References

- [1] Aleksidze M.A., Kartvelishvili K.M., etc. – Investigation of several problems of transformation of potential fields. Tbilisi, publishing house *Metsniereba*, 1972, p-282.
 - [2] Bloch Y.I., Interpretation of gravitational and magnetic anomalies, 2009.
 - [3] Computational mathematics and tectonics in prospecting Geophysics, Moscow, publishing house *Nedra*, 1990, p.437.
 - [4] The geological-formational map of the Caucasus in 1:500000, edited by Gogishvili T.Sh.
 - [5] Davis D.J., Statistics and analysis of geological data, Moscow, Publishing house *Mir*, 1977.
 - [6] Sander V.N. Method of connection of anomalous field with rectilinear profiles and horizontal relieves. Prospecting and preservation of soil, №110, 1975.
 - [7] 50-th anniversary of Institute of Geophysics (a booklet), 1983.
 - [8] Litvinova G.P., Characteristic properties of cartographic image of the complex differentiated field, in the book *The Principles of magnetic cartography and methodology for constructing maps*, Works, VCEGEL.
 - [9] Nodia M.Z., The magnetic field of the Caucasian isthmus, The works of Institute of Geophysics of Academy of Sciences of GSSR, V, 1939.
 - [10] Sekhniadze G.A., The magnetic field of Georgia and its geological interpretation, Author's abstract on dissertation, Tbilisi, Publishing house *Metsniereba*, 1976, p.20.
 - [11] Logachev A.A., Zakharov V.P., Magnetic exploration, Publishing house *Nedra*, Leningrad, 1973.
 - [12] Cheishvili M., Anomaly of the vertical stress components of the magnetic field of the Transcaucasia.
- Archives Materials
- [1] Gamkrelidze N.P. etc., Study of physical occupancy of the territory of Georgia for 1*1 in 1980. Georgian Fund for Department of Geology, 1982.
 - [2] Gamkrelidze N.P., Basiladze G.S., Report on “Study, generalization of physical properties of rocks and ores for regional geophysical works in 1974-78.

(Received in final form 20 December 2012)

Аномальное магнитное поле территории Грузии и ее связь с глубинным строением

Миндели П.Ш., Гонгадзе С. А., Глonti Н.Я., Кирия Д. К

Резюме

В статье проанализированы данные аеромагнитной съемки территории Грузии и представлена схема его распределения.

На основе полученного материала составлена карта аномального магнитного поля территории Грузии. Карта пересечена в верхнее полупространство на высотах 6, 9 и 12 км. и приведен анализ полученного материала.

Составлена схематическая карта магнитно-тектонического районирования территории Грузии.

საქართველოს ტერიტორიის ანომალური მაგნიტური ველი და მისი კავშირი სიღრმულ აგებულებასთან

მინდელი პ., ღონღაძე ს., ღლონტი ნ., ქირია ჯ.

რეზიუმე

სტატიაში გაანალიზებულია საქართველოს ტერიტორიის აერომაგნიტური აგეგმვის მასალები და წარმოდგენილია მისი განაწილების სქემა.

არსებული მასალა მოყვანილია ერთიან სისტემაში. შედგენილია საქართველოს ტერიტორიის ანომალური მაგნიტური რუკა, რომელიც გადათვლილია ზედა ნახევარსივრცეში 6, 9 და 12 კმ. სიმაღლეებზე და ჩატარებულია მიღებული შედეგების ანალიზი.

შედგენილია საქართველოს ტერიტორიის მაგნიტო-ტექტონიკური დარაიონების სქემატური რუკა.

Preliminary Results of Electrometric Search on the territory of the Svetitskhoveli complex

**G.Tabagua, N.Gogvadze, T. Gorgiashvili, M. Jakhutashvili, O.Seskuria,
S.Vepkhvadze, S.Matiashvili, K.Tabatadze**

Abstract

*On the territory of Svetitskhoveli resistivity was conducted el. profiling different Spacing ($AB=3\delta; 6\delta; 9\delta$ and 18δ). Two of the main was profile of temple spent at in the north, and one – east and Vertical Electrical Sensing (VES) twenty-one point, the maximum $AB/2=25\delta$. Geoelectric section excreted next horizons: 1. Bulk; 2. Loamy; 3. Riqnari clay composition ; 4. Basic rock -clay shale.
The electric profiles seven archaeological plot anomalies of nature.
In the study area range from height ground-water 4,2-4,2 m.*

Applied Geophysics, one of significant fields of Natural Sciences, is often very important for the study of cultural development of our civilization and is used as an effective instrument for verification and reconstruction of the history of culture.

In Archaeology of geophysical methods is that they enable to study a monument before its excavation.

Geophysical data make it possible to conduct geological-archaeological explorations as these data contain information not only about the cultural layer, but about the upper part of the geological section as well. This makes simpler to find links between old buildings and territories of exploration [1,2].

Sveti-Tskhoveli is one of the greatest ecclesiastic buildings survived so far in Georgia. It has been a religious center of Christian Georgia for centuries. In spite of the monastery has undergone many changes – the most part of the frescoes has disappeared, and whitening of the walls has resulted in the lack of other organic elements necessary for its artistic integration, it makes a great impression even in our days [3].

Sveti-Tskhoveli Monastery, as one of oldest buildings, keeps many secrets in itself. Georgian catholicos-patriarchs, kings and people have always been reconstructing and taking care of it.

It is well known that the monastery of Sveti-Tskhoveli is situated on the territory of the “Royal Garden”. Since the oldest times the monastery has kept many Christian sacred things, but we are aware of the location of just some part of them. It also keeps the graves of many Georgian kings and patriots that are to be studied and verified by Georgian people. It is supposed that there must be the remains of King Mirian’s palace in the yard of the monastery [4].

The Geophysical investigations have been conducted in two directions:

1. Study of hydro-geological particularity of the territory around the monastery;
2. Search of unknown (hidden) archaeological monuments on the territory of the monastery and around it.

We used two modifications of electric resistance – electrical profiling and Vertical Electrical Sounding (VES). The placement of the profiles and the points VES are shown in the scheme (Chart. 1).

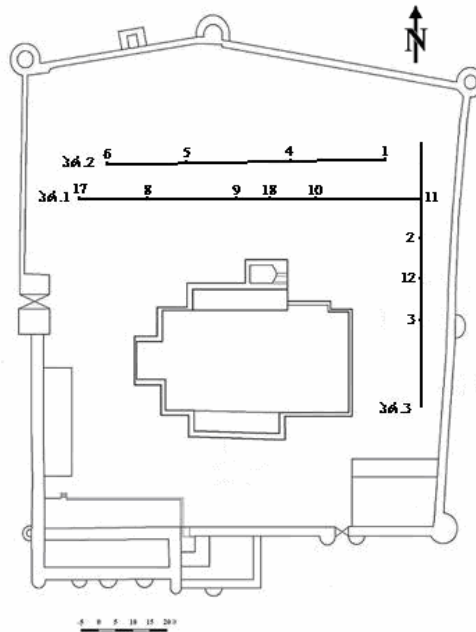


Chart.1. Electrical profiles and vez - specific deployment scheme

On the territory of Sveti-Tskhoveli the profiling was made by resistance method with four spans ($AB=3\text{m}$; 6m ; 9m and 18m) that enabled the current distribution and the study of the geological section in the depth of $3\text{-}4\text{ m}$ and $1,5\text{m}$ step. Vertical Electrical Sounding was conducted with a maximal span of $AB/2=25\text{m}$ that makes possible to describe the geological environment till $8\text{-}10\text{ m}$ depth.

Two main profiles were made in the North of the monastery, and one – in its East. We also conducted VES in the northern, eastern and southern parts. (Fig.1)



Fig1. Electrical profiles

We studied the sections of the above mentioned profiles till 12 m depth and distinguished four main horizons.

Profile 1

The capacity of the first horizon along the profile fluctuates between 0,5-0,9 m and is characterized by 50-140 ohm resistance (Chart 2).

In the first horizon (layer) along the profile in approximately 35 m the resistance is 40-60 ohm, in the 40 meters during it is 90-110 ohm, and to the east at the end of the profile it rises up to 140 ohm.

In 9-11 m along the profile the capacity of the horizon varies, and the resistance fluctuates between 12-30 ohm.

Along 40 m from the beginning of the profile the resistance equal to the first layer in the depth is approximately 7 m capacity. In the №10 VES area the layer with 25-30 ohm resistance approaches the day surface. To the East, at the end of the profile the resistance fluctuates again between 12-18 ohm. After 8-11 m from the depth the resistance becomes less than 8 ohm.

From the archaeological viewpoint the interesting areas are: I area – in the 22-58 m line and II are – in the 78-83 m line.

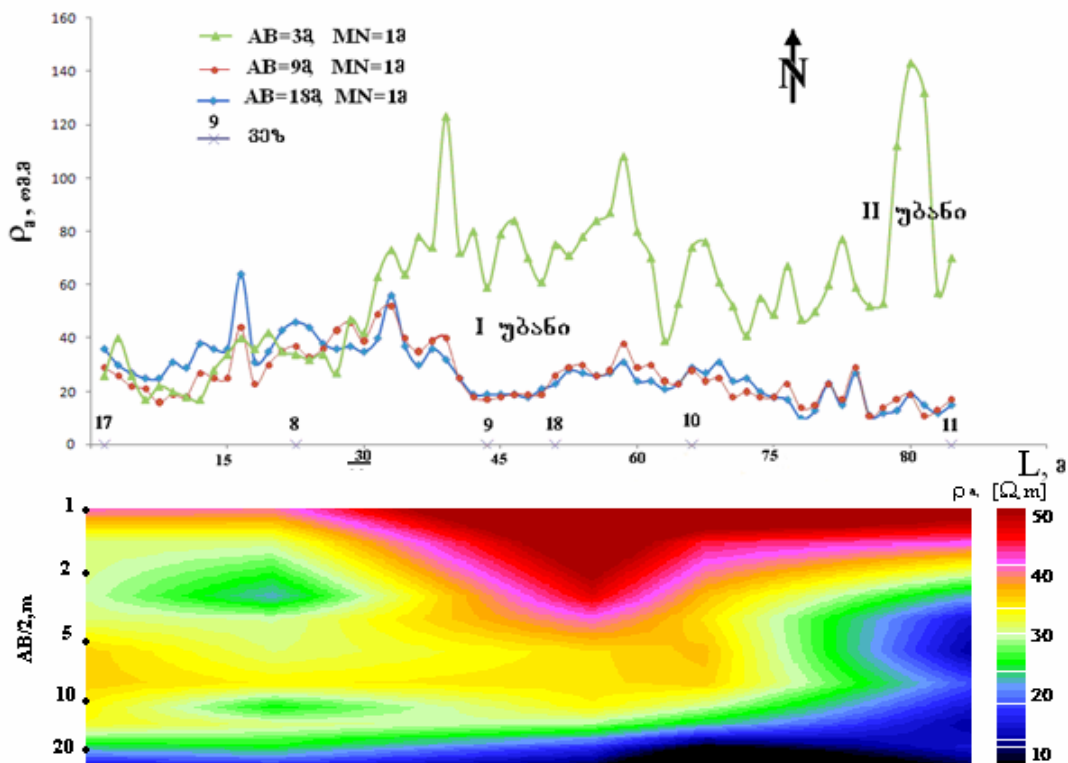


Chart 2. Distribution of phantom electrical resistance Pr .1 - he along.

Profile 2 is situated in the 10 m North from the profile 1 (Chart 3). In this profile the resistance distribution is analogical in depth to the one in the profile 1 with three distinguished layers: the resistance of the first layer fluctuates between 20-90 ohm, and the capacity is 0,4-0,8 m. The capacity of the second layer varies between 8-12 m.

At the beginning of the profile, by the data of the №6 VES, the first layer is continued in nearly 2,5 m by a layer with less resistance that slightly increases in the depth. Along the profile it approaches the surface approximately in 20 m, and in the depth it extends to 12 m. At the end of the profile the resistance decreases.

The third layer also decreases here and is less than 8 ohm.

We distinguished two interesting areas in the archaeological viewpoint in the second profile: III area – from the beginning till 12 m of the profile, and IV area – from 36 m to 42 m.

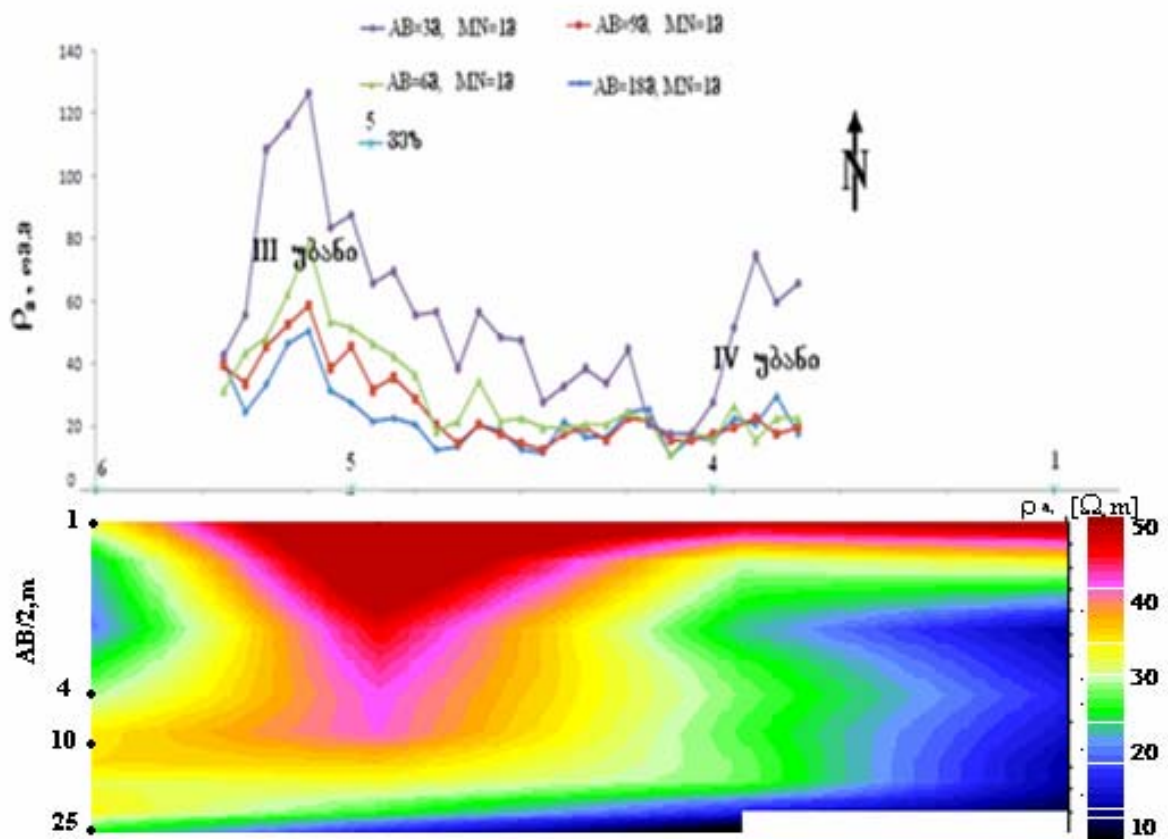


Chart 3. Distribution of phantom electrical resistance Pr .2 - he along.

In the **profile 3** the capacity of the first horizon fluctuates between 0,6-1,0 m and is characterized by 40-120 ohm, at some places – by 150-200 ohm resistance (Chart 4).

The areas with their resistance values up to 50 ohm correspond to dump layer, that is presented by clay and gravel fragments. The areas with increased resistance as 70 ohm and more must also correspond to dump layer with building materials and ruins of buildings.

In all geo-electrical segments the third geo-electrical horizon is obviously distinguished and widely spread. As a matter of fact its resistance is of first unit ohm order. Such a value of resistance must correspond to sediments on the terrace of the river Mtkvari, in particular – clay and cobble soil with ground water observed in it.

The third geo-electrical horizon is situated in 5-9 m depth from the horizon. If its little resistance values are caused by ground waters, then any sharp changes of the surface of this horizon in the limits of the profile is quite doubtful. This is also corroborated by existence of ground water surface in 4-4,5 m depth in the prospect holes cut in the monastery corners.

There are three archaeologically interesting areas along the profile 3: V area covering 0-15 m, VI area – in 26-30 m, and VII area – from 58 m to 72 m.

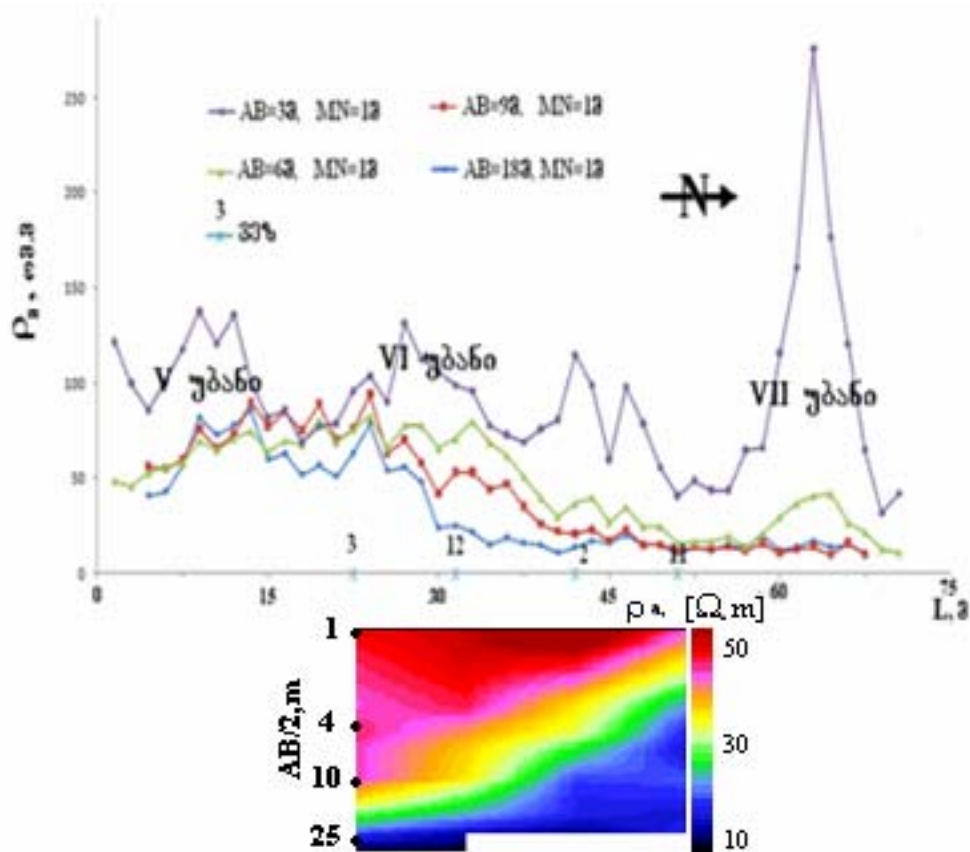


Chart 4. Distribution of phantom electrical resistance Pr .3 - he along.

The second geo-electrical horizon prevents attractions too. Here abrupt changes of resistance values take place in the horizontal direction. The horizon capacity along the profile is mainly 5-8 m, in some areas – 10-11 m. The zones with little resistance that are widely spread and characterized mainly by 12-18 ohm must correspond to clay or river sediments containing clay. Increased resistance of 30-40 ohm values are distinguished in separate areas of the first and second profiles, and 90 ohm is observed in the third profile to the East of the monastery. Taking into consideration the geological data on prospect holes cut in the monastery corners and the boreholes on the territory the zones with increased resistance must have originated due to cobble soil- round stone containing sand and clay.

On the basis of the data of the conducted Vertical Electrical Sounding on the territory we revealed the following situation in the constructed geo-electrical sections: the first layer is represented by dump with the resistance of 50-120 ohm, and its capacity varies between 1,2-2,9 m. Under it an environment with little resistance (2-10 ohm) is observed that is represented by argillaceous soil and its capacity varies as 0,5-3,2 m. The resistance of the third layer changes between 40-180 ohm. It is represented by cobbles and round stone of small size. Its capacity is 1,0-2,5 m. The section in its depth is continued by the main layer – argillaceous slates. The level of the ground water here varies between 4,2-4,5 m (Chart 5).

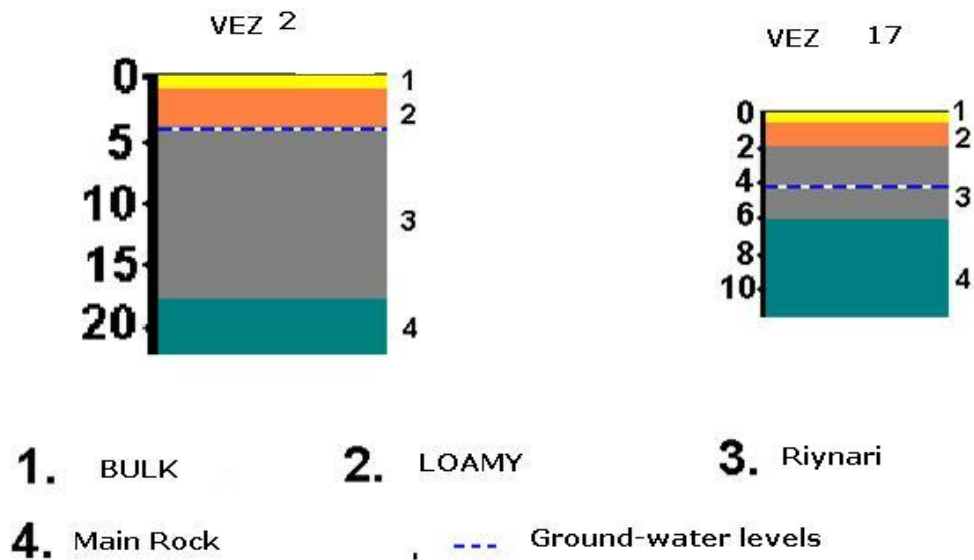


Chart.5

Conclusion:

The profiling works showed, that in all the geo-electrical sections there is a distinguished and widely distributed Riynari, this area contains ground water.

Some separate areas of the first and second profiles have great values of resistance. The third profile in the East of the monastery is especially distinguished by high resistance.

Capacity of individual layers of the sharp variation of the horizontal in the river sediments is quite reasonable. But it is also acceptable that the zones with high resistance might have originated due to ruins of the building or the fence. Thus, they might be interesting in archaeological viewpoint.

It is quite obvious that further detailed investigations with small size parametric prospect holes will make clear many above mentioned issues.

References:

[1] **M.Jakhutashvili**- Search the effectiveness of geophysical methods for detection of Georgia archaeological sites in the. Abstract. 2006 year

[2] Журбин И, В. Геофизика в археологии: методы, технология и результаты применения. Ижевск. 2004.

[3] **V. Beridze**- The Georgian architecture of the old . Tb. 1974 Year

[4] Svetitskhoveli complex (Georgian description of the historical and cultural monuments) T.5. Tb. 1990 year

(Received in final form 20 December 2012)

Предварительные результаты поиска Электрометрические на территории комплекса Светицховели

Г. Табагуа, Н. Гогоуадзе, Т. Горгиашвили, М. Дзахуташвили, О. Сескуриа
С. Вепхвадзе, С. Матиашвили, К. Табатадзе

Резюме

На территории Светицховели методом сопротивления было проведено эл. профилирование разными разностями и ВЭЗ в дватеть одной точке, максимальный $AB/2=25\text{м}$.

Геoeлектрическом разрезе выделяются следующие горизонты: 1. насыпь; 2. глинозем; 3. галичник с глинозем; 4. глинистые сланцы-основные породы.

На эл. профилях выделяются семь участков аномалии археологической природы.

На изучаемой территории уровень грунтовой воды 4,2-4,4 м.

ელექტრომეტრული კვლევის წინასწარი შედეგები სვეტიცხოვლის ტაძრის ტერიტორიაზე

გ. ტაბაგუა, ნ. გოგუაძე, თ. გორგიაშვილი, მ. ჯახუტაშვილი, ო. სესკურია,
ს. ვეფხვაძე, ს. მათიაშვილი, კ. ტაბატაძე

რეზიუმე

სვეტიცხოვლის ტაძრის ტერიტორიაზე წინააღმდეგობის მეთოდით განხორციელებულ იქნა ელ. პროფილირება ოთხი გაშლით ($AB=3\text{მ}$; 6მ ; 9მ და 18მ). გატარებული იქნა ორი მაგისტრალური პროფილი ტაძრის ჩრდილოეთით, ერთი კი – აღმოსავლეთით და ვერტიკალური ელექტრული ზონდირება (ვეზ) ოცდაერთ წერტილში, მაქსიმალური $AB/2=25\text{მ}$.

გეoeლექტრულ ჭრილებში მკაფიოდ გამოიყოფა შემდეგი ჰორიზონტები: 1. ნაყარი; 2. თიხნარი; 3. რიყნარი თიხნარის შემავსებლით; 4. ძირითადი ქანი-თიხა ფიქლებრივი.

ელ. პროფილებზე, საერთო ჯამში გამოიყო არქეოლოგიურად საინტერესო შვიდი ანომალური უბანი.

ტერიტორიაზე გრუნტის წყლის დონე მერყეობს 4,2-4,4 მ-ის ფარგლებში.

Methodology creation numerical model of alluvial deposit aquifer for implement heat pump system of Kutaisi international airport

G. Melikadze, G. Kobzev, N. Kapanadze, Kh. Bedineishvili

Mikheil Nodia Institute of Geophysics of Ivane Javakhishvili Tbilisi State University, 1, M. Alexidze str., 0171, Tbilisi, Georgia melikadze@gmail.com

Abstract

In order to implement heat pump system of Kopitnary International Airport (Kutaisi), had been organized the hydrogeological testing of two existing and six new drilled drinking water boreholes on the territory of in order to determine the boreholes' properties and to create a model of aquifer. The digital modelling represents the main steps of calibration and simulation process, which gives the possibility to estimate and study the different scenarios of exploitation and development of precesses.

Introduction

Study area is located close to Kopitnary airport, between Rioni and Gubis-tskali rivers and represents the wide flat area. The territory is 340 m² and it is flat and is tilted from the North-East to the south-west direction with 0.004⁰. The most elevated place of the area is 120-130 m from sea level (to the north) and the lowest place is 20 m to the south-west.

River Rioni, which bounds the territory by two sides, is the biggest river of the west Georgia. The second river Gubis-Tskali bounds the area from the west.



Fig.1 Map of study area

The climate of the area is the type of subtropical, with high temperature regime. The mean annual temperature is 15-16⁰C. The annual precipitation is 1800-2000 mm or 18-20 thousand tones / hectare.

Due to nigh population there functions few water-pumping stations on the above mentioned territory (Phartskhanakanebi, Kopitnari, Mukhiani and etc) for Kutaisi, Tskaltubo and other populated places water supply. There are also passing the main highway and the railway nearby.

Hydrogeological conditions

Study area belongs to the east part of Tskaltubo artesian basin. (1). There are located deep and less deep circulation waters here. Less deep circulation waters are from quaternary and modern alluvial period and the deep (with pressure) circulation waters are cretaceous karstic waters that are located under the above mentioned Quaternary waters. The karstic waters come out on the surface only on the northernmost part of

territory, where they are fresh and without pressure. Deeping to the south the temperature and pressure as well as the mineralization is increasing. But this water bearing horizon still is not opened with boreholes.

Thus, only alluvial and quaternary period horizons are subject of our interest. (2)

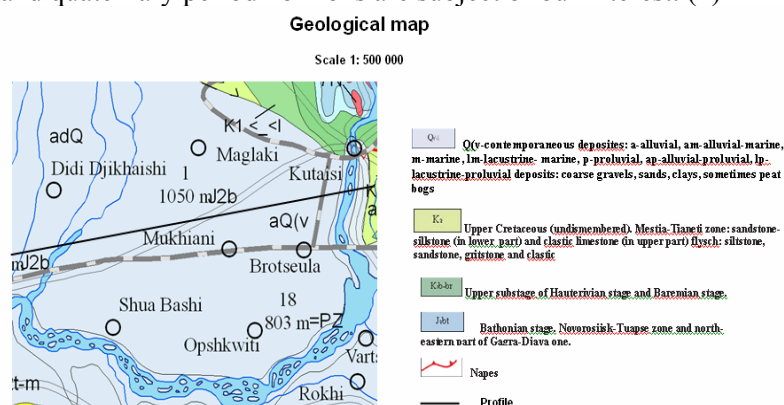


Fig.2 Geological map of the area

Modern alluvial aquifer

Modern alluvial water aquifer strata is developed between the valleys and terraces of rivers Rioni and Gubis-tskali and in the breadth of it at some places reaches 2.5-3 km. the widest part we observe at the end of river valleys. The lithology of sedimentary rocks is conditioned by the diversity of the main rocks: among the volcanic and intrusive rocks we meet sandstones and limestones. The water abundant in water bearing horizons depends on the granule composition of the rocks. The water content of sands, sandstones and gravel is 10 l/sec, the specific debit of boreholes varies from 5 till 30 l/sec, the coefficient of filtration is 100-300 l/day and for sands it increase till 30-50 l/day and sometimes till 100 l/day. The mineralization of water bearing horizon is low 0.3 g/l. As to chemical composition it is hydrocarbonate-calcium and hydrocarbonate-calcium-sodium, with moderate rigidity. Underground water level at river valleys is 0.5-1 m, in some cases 2-2.5 m. which decreases along the flowing direction. The water bearing horizon is fed mainly by rivers, less by the precipitation. Those underground waters have the close hydrodynamic connection with underlying Quaternary water bearing horizon – aquifer.

Previous Studies

Few years ago, in order to organize water supply system for Kopitnari airport two boreholes (we could not determine the drilling company) were drilled: # 1 (located closer to the Kutaisi-Samtredia highway) and # 2 (located further from Kutaisi-Samtredia highway). The coordinates you can see below:

Table 1. Coordinates of existing boreholes

#	X coordinate	Y coordinate	Altitude
Borehole #1	4673204	290854	42.85
Borehole #2	4673186	290861	42.52

Table 2. Borehole parameters

Bor.#	Deepness	Diameter (mm)	Borehole spacing (m)	Interval of a filters spacing in boreholes (m)	Stoical level (m)	Dynamic level (m)	Debit (l/sec)
1	40	300	0-40	12-40	-2	-3	15
2	40	300	0-40	12-40	-2	-3	15

According to the done chemical analysis water is of moderate mineralization and rigidity and possible exploitation debit was 130 m³/hour.

Hydrodynamic Research Methods

In order to determine the hydrodynamical parameters (coefficient of filtration, permeability, conductivity, debit, temperature, static and dynamic pressure and etc) of main quaternary water bearing horizon should be done field pump tests of the boreholes that have been done according to the standard method (Domenico and Schwartz, 1998; Middlemis, 2000) using licensed softwares.

There were already existed two ## 1 and 2 boreholes on the territory of airport from which water was pumped out. For those boreholes was selected the slug testing “pump out” method. In order to reinject water into the aquifer has been drilled six ## 3, 4, 5, 6, 7, and 8 boreholes of different depth. And for their hydrodynamic testing we decided to use “pump in” – reinjection method.

Between the slug-testing methods (“pump in” and “pump out”) we used “pump out” method. Before testing the head of boreholes were constructed. On the both boreholes were installed registration equipments. Recorded data gave us possibility to study the background processes.

Data were recorded daily and processed at the laboratory by the specific Exel programme, which formats hex file into text, sorts out data column according to sensors quantity and etc.

The next step was to make time series of microtemperature and hydrodynamical data and analyzing.

Based on recived material we determined the hydrodynamical parameters (coefficient of filtration, permeability , conductivity, debit, temperature, static and dynamic pressure and etc).

Determination of hydrodynamic parameters

One day before starting the pump test, in order to find out the background condition, the pump testing on #1 borehole had been stopped. After we continued pumping process on # 1 borehole using the pump with capacity of 50 m³/hour. Water level variations had been monitored in both (#1 and #2) boreholes using the “Diver”, survey frequency 1 min. (Fig 3, 4)

Hydrodynamic parameters had been calculated based on data from #2 borehole.

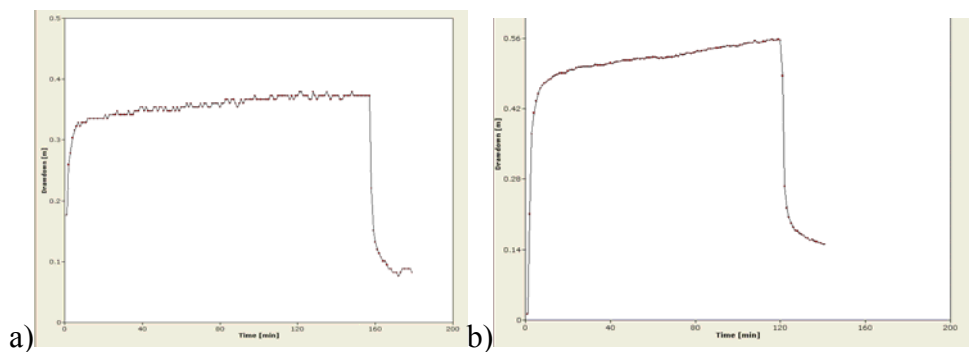


Fig. 3 water level variation diagram during pumping out process on a) #1 and b) #2 borehole

Recorded row data during pump test had been processed by the specific programme Aquifertest pro 4.2.

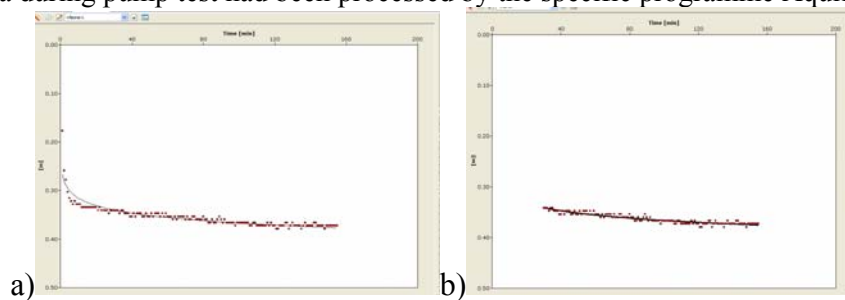


Fig. 4 The logarithmic curve of water level variation for 1 (a) and 2 (b) boreholes

In order to calculate the parameters of our interest we used Taisy-Jacob ‘ s method. For this purpose on the curve of water level drop we choose straight sections.

In order to verify the results, data had been processed also manually using Borevsky's method (4) , which is also based on Taisy-Jacob's equation. By inputting in the equation the data of water level dropping during pumping up making a plot $x=\lg t$ and $y= D$ and $D=k*\lg(t)+b$, where the unit of t is day and for water dropping – meter.

On the dropping curve we can see the straight section, where the equation $Y=k*x+b$ works. We can calculate also the transmissivity $T=0.183*Q/k$, where Q is water discharge m^3/day . We can also calculate logarithmic data of conductivity $\lg(a)=2\lg(r)-0.35+b/k$, where r is the distance between the boreholes and at the end we calculate coefficient of specific yield using equation $\lg(S)=\lg T - \lg(a)$

As a result we got following values:

Table 3 . Calculated parameters

Parameters (bore 1)	Data	Parameters (bore. 2)	Data
k (coefficient)	0.0456	k	0.1442
b (coefficient)	0.4183	b	0.7139
r (distance,meters)	20	r (distance,meters)	20
Q (extract m^3/day)	1200	Q (extract m^3/day)	2400
Transmissivity (m^2/day)	4815	Transmissivity (m^2/day)	3045
Storativity S	$1.8*E-08$	Storativity S	$1.9093E-4$

As a result there is an entire consentaneity between manually and using software package calculated data.

Table 5. 1st step, pump out , # 1 borehole

	Transmissivity (m^2/day)	Storativity	Coefficient of filtration (m/day)
AquiferTestPro (method Theis with Jacob corrections)	4340	$1.07*E-7$	330
Borovsly's method	4815	$1.8*E-08$	370

Table 6 . 2nd step, pump out, # 2 borehole

	Transmissivity (m^2/day)	Storativity	Coefficient of filtration (m/day)
AquiferTestPro (method Theis with Jacob corrections)	3550	$5.04*E-5$	275
Borovsly's method	3045	$0.191*E-5$	250

As we can see, the permeability of # 1 borehole is much more than # 2 one. Mentioned borehole has not been under exploitation for a long period of time and most likely it is polluted with sand and clay. Thus, its important the further detailed studies and the borehole should be cleaned (washed) to avoid the problems of its functioning.

In order to verify the existing data in the both boreholes had been done synchronous pump tests during two weeks (1-15 april). On #1 and #2 boreholes with the pumps of capacity correspondingly 50 and 80 $m^3/hour$ (Fig. 5). The process has been under the technical control.

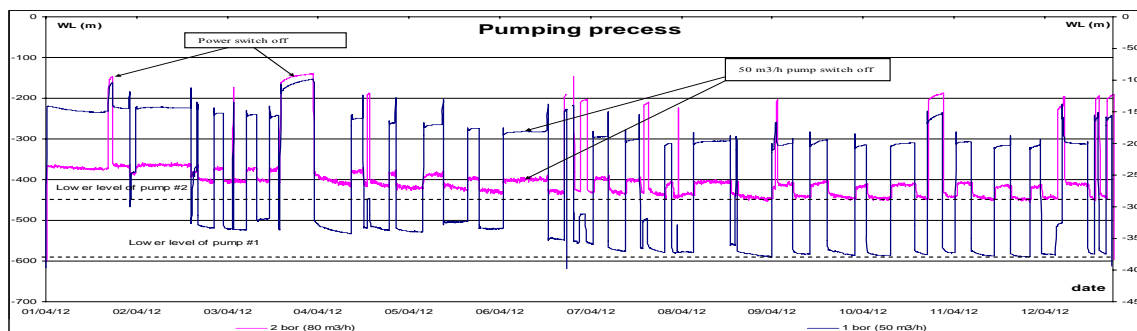


Fig. 5 Water level variation diagrams for #1 and # 2 boreholes

Slag testing by injecting into new drilled ## 3, 4, 5, 6, 7, and 8 boreholes

In order to reinject water pumped out from ## 1 and 2 boreholes after removing heat, on the territory of airport had been drilled 6 boreholes. Before testing the head of boreholes were constructed. On all boreholes were installed registration equipments (water level, temperature, conductivity, discharge). Recorded data gave us possibility to study the background processes. ## 1 and 2 boreholes were connected with a special pipeline with ne drilled boreholes.

In order to determine the value of permeability injection process was done with several steps. The first step was to pump out water from # 1 borehole and reinject into one of the new well with different discharge. Before starting of testing process one day earlier, in order to get real background value, the pumping out of water from ## 1 and 2 boreholes had been stopped.

In contrast to calculations done for ## 1 and 2 boreholes, for “injection”- pump in “ the hydrodynamic parameters were calculated by Nesterove’s method, where the coefficient of filtration is calculated by the equation:

$$K=0.123 Q/h^2 \lg 2h/r$$

Where K is coefficient of filtration, Q- discharge, h- water level increase during injection, r- radius of borehole.

Statistical analysis of determinant factors of water level variation

As it was mentioned above, after slug-test all boreholes had been under monitoring. Data of water level, atmospheric pressure and temperature variation had been recorded. For better understanding of all factors that may influence the aquifer “living” conditions, also data from meteorological service (precipitation and discharge of main river Rioni) had been inquired.

After review all data we determined all factors which have and influence on aquifer: atmospheric pressure and precipitation. The last one plays the main role. Fig. #6.

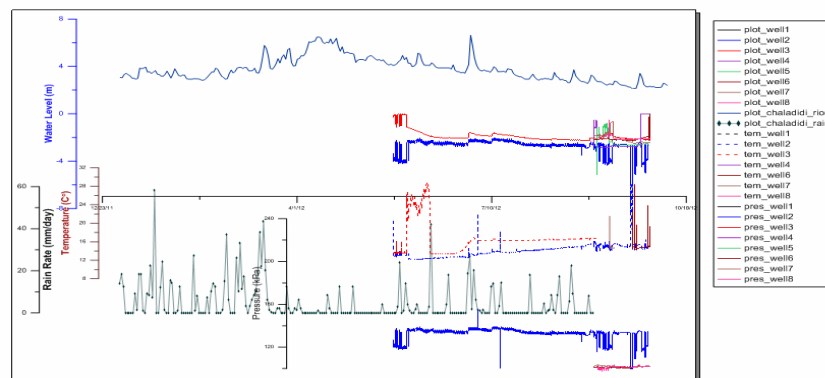


Fig. 6 Multiparametral variations in borehole

Fig. 6 shows the good correlation between amount of precipitation, discharge of river Rioni and water level variation in boreholes. Almost for all boreholes it is more visible the correlation between river discharge and water level variation in boreholes. This is caused by the accumulation of precipitation by river which feeds aquifer by its side.

For each borehole had been carried out the statistical analysis in order to determine the relation between variations of Rioi discharge, precipitation and water level as well as the character of those variations.

Exapmle of analysis of correlated ratio of water level variation, r. Rioni and precipitation Borehole # 3

In order to compare data from borehole # 3 with precipitation, data had been normalized in diapason [0: 1]. For precipitation data the weighted average method was used (blue line, fig. 7)

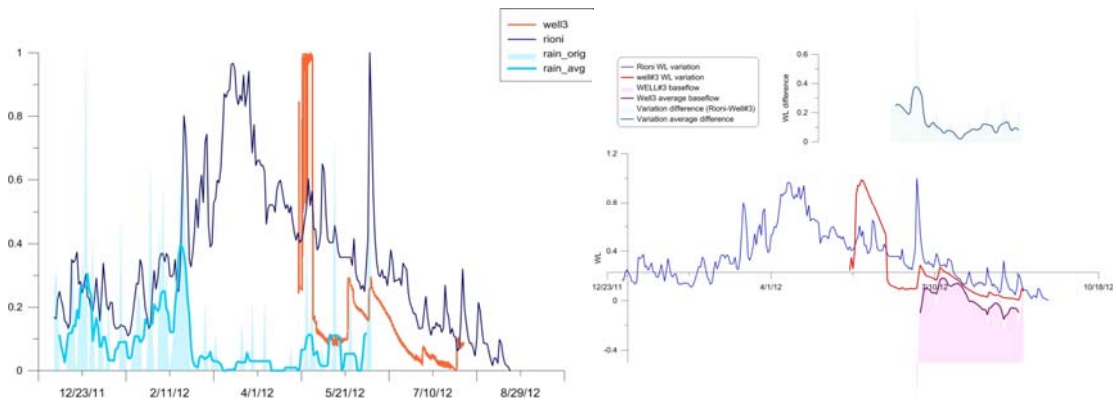


Fig. 7 Borehole 3; water level, Rioni river and precipitation variations

Borehole #3 minute data were averaged to daily series (red line in Fig. 7). Rate of variation difference between water level in Rioni and Borehole #3 is shown on upper plot in Fig. 7. Borehole #3 baseflow is calculated as difference between well#3 variation and rate difference.

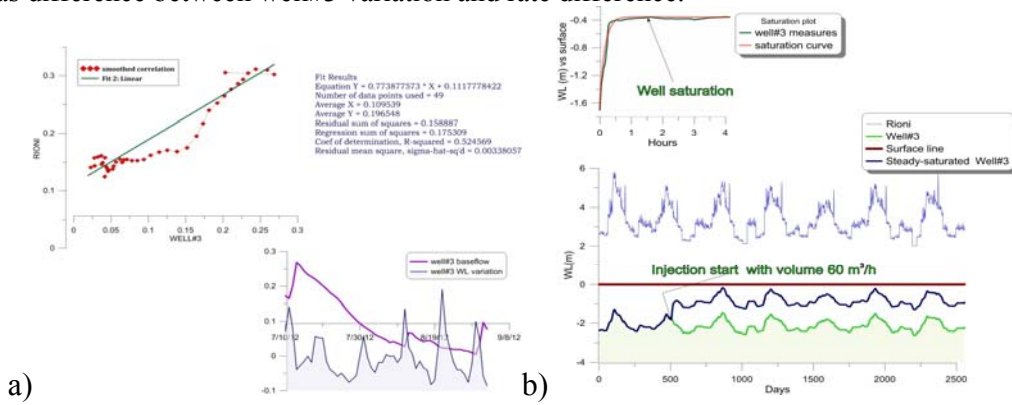


Fig. 8 Borehole # 3, a) water level variation background series plot b) Plot of potential water level variations. Correlation plot of Rioni and borehole #3 water level variations is shown in Fig. 8. Statistics shows that data are correlated. Borehole # 3 baseflow on lower plot is calculated by extraction linear trend (correlation line) from water level variation.

Based on correlated ration and slag-test data, we have calculated the potential water level variations in boreholes for the next 25 years.

After starting water injection into borehole #3 with volume 60 m³/h water levels rises to saturation within 2 hours. Water increase with such a volume is about 1.3 meter. The further water level variations are conditioned by the background variation.

Example of Statistical analysis of data - Borehole # 2

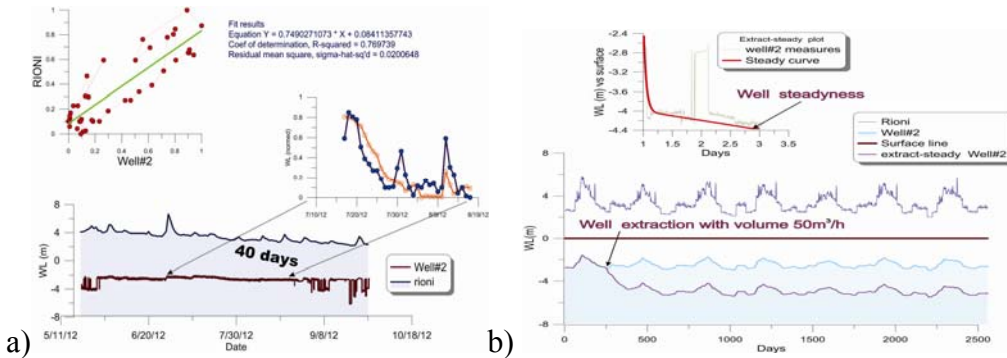


Fig. 9 a) Correlated ratio of water level variation in Borehole # 2 and rioni river discharge b) Borehole 2- Prognostic curve of water level potential variations

For regressive analysis was selected water level variation of period of 40 days. Calculated coefficient of filtration equals 0.77. The results show that the water level variations in Rioni River and in borehole # 2 are correlated. After pumping out of water with volume 50m³/hour from borehole #2 the water level stabilaized during 3 days on the level of 2.25 m. This regime will be kept in future.

Table 13 Summary hydrodynamic parameters of borehles

Name	Screen, m	K m/day	Max discharge m ³ /h +out from boreholes; - into boreholes.	Injections, m ³ /hour	Water level increasing, m	Amount of discharge for 1 m	for 1.5 m	for 2.4 m	Injection in Bor. #5 and influence on the #7, 8, 6	Injection in bor. #7 and influence on the #3, 8,5	Injection in bor. #6 and influence on the #3
Borehole #1	15	350	+70-80								
Borehole #2	15	350	+70-80								
Borehole #3	13	423	-70-80	60	1.05	57.14	85.71	137.13		11.43	28.57
Borehole #4	14	69	-25-30	27	2.1	12.86	19.29	30.86			
Borehole #5	15	470	-80-100	48	1.1	43.64	65.45	104.74	48.00		
Borehole #6	13	156	-40-50	50	2.34	21.37	32.05	51.29	4.27	4.27	34.19
Borehole #7	15	368	-70-80	51	1.3	39.23	58.85	94.15	11.77	51.00	
Borehole #8	15	159	-25-30	25	1.7	14.71	22.06	35.30	4.41	2.94	
Total						188.94	283.41	453.47	68.45	69.64	62.76

As we can see the amount of water that the boreholes are able to receive varies with seasons. For instance, for low water level, 2-4 m (summer), boreholes can receive the maximum total volume of water 453 m³/hour, and for high level, 1.5 m (spring) – less- 283 m³/hour.

Also, coefficient of interrelation varies between 1.4-1.8, which means that in case of simultaneously reinjection in several boreholes the maximum value of injection will decreas and accordingly equals 177 m³/hour and 283 m³/hour.

Conceptual Model

The modeling has been done by the software Feflow 5.3, which gives possibility to calculate 3D model of study area. First of all the digital map of a surface has been done (ArcMap 9.2 and ArcView 3.2a). For study area the boundary conditions were defined. The recharge area at its North border is fed by precipitation. As to east and west borders, the source of feeding is Rivers rioni and Gubis Tskali. The discharge area is the River Rioni bed, which is located to the south as well as boreholes # 1 and # 2 on the territory of the airport. The study site has an area of 314 square kilometers- the length of the east part is 10.5 km, the west part – 23 km and south part- 31 km.

Callibration

As it was mentioned, the main source of recharge area is precipitation which is plenty because of subtropical climate. In the table bellow is represented some data from Kutaisi meteorological station of precipitation for last 7 years

Tab. # 14 precipitation mm/year

Years	2005	2006	2007	2008	2009	2010	2011
mm/year	1668	1363	1555	1252	1420	1387	1459

In order to calculate the amount of precipitation which reach the aquifer, the modeling had been done as well as some initial conditions were set. For water level value in rivers was considered the geographic

elevation of points. According to measurements in the borehole # 1 the water level is 1 meter below from the surface (45 m). Afterwards the modeling was done.

According to model to reach the mentioned water level it is necessary $12.23 \cdot 10^{-4}$ m/day of precipitation for per square meter of study area, which is 446 mm/sec, water penetration is $(446/1459) \cdot 100 = 30\%$.

Hydrodynamic head

The digital map of study area was designed based on satellite data. The next step was the calculation of static hydrodynamic pressure distribution in aquifer. In program were inserted absolute value of boreholes and water level data, as well as water level value in rivers for recharge and discharge areas, which varies from 125 m (to the north-west, recharge area) till 24 m (to the south-west, discharge area).

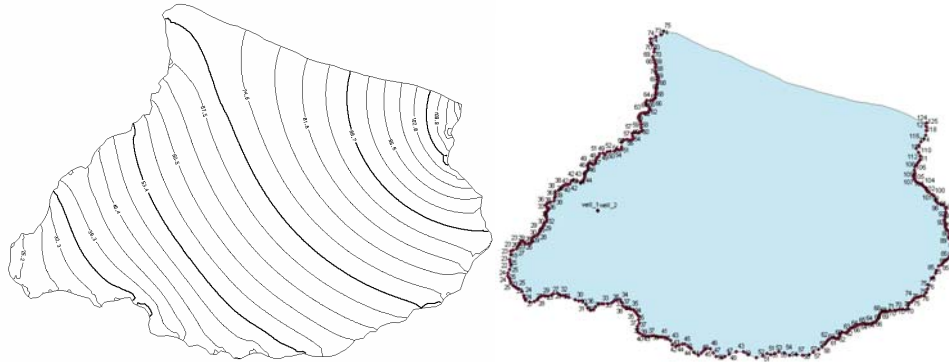


Fig. #10 Isoplines of hydrodynamic head Fig. 67 Outline of hydrolic head of recharge and discharge areas

The next step was the calculation of season variation of hydrodynamic head based on water level variation data in Rioni river from meteorological stations

According to those data, the season water level season variations in Rioni river vary from 2.1 m (minimum October) till 5.8 m (maximum March-April). The mean value of water level is 3.8 m. accordingly above mentioned data was used for whole recharge and discharge areas and the variable of hydrodynamic head of aquifer had been calculated. There were also defined 8 waterprof and permable layers, with total thickness 40 m.

Table # 15 Thickness of defined horisonz

. N layer	1	2	3	4	5	6	7	8
Thickness,m	3	4	2	1	8	2	10	10

Based on all those data the 3D model had been created

Hydrodynamic parameters

After slag testing of boreholes we determined the hydrodynamic parameters of aquifer they open. Mentioned gave us possibility to assess the coefficient of filtration for each borehole as well as of aquifer.

After inserting data into model, program calibrated model and corrected some parameters. For instance, by the program was recalculated the coefficient of filtration according to observed water level variation data during reinjection in ## 3,4,5,6,7 and 8 boreholes.

We conceded that in the model the coefficient of filtration is $K_x = K_y$ and $K_z = 0.1 \cdot K_x$

For each borehole was calculated the coefficient of filtration. For all boreholes for upper clay layer we got common coefficient (blue color) $K_x = 0.02 \cdot 10^{-4}$ m/sec

Borehole #1 and #2 - $K_x = 35 \cdot 10^{-4}$ m/sec ;Borehole #3 $K_x = 4.2 \cdot 10^{-3}$ m/sec.;Borehole #4 $K_x = 7 \cdot 10^{-4}$ m/sec ;Borehole #5 $K_x = 4.7 \cdot 10^{-3}$ m/sec ;Borehole #6 $K_x = 1.6 \cdot 10^{-3}$ m/sec.;Borehole #7 $K_x = 3.7 \cdot 10^{-3}$ m/sec ;Borehole #8 $K_x = 1.6 \cdot 10^{-3}$ m/sec ;

Programme also gives possibility to estimate the distribution of coefficient of filtration for whole aquifer by the interpolation.

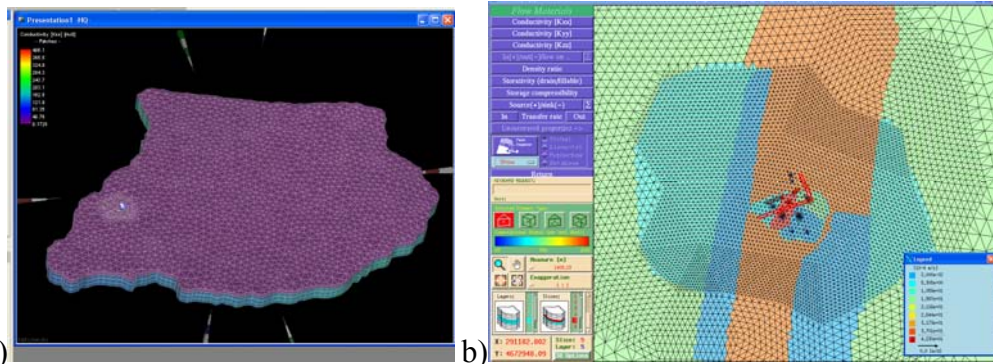


Fig. # 11 a) distribution coefficient of conductivity on all the territory and b) Distribution coefficient of conductivity

Modeling

After all calculations we were ready to make some model simulations in order to determine the required scenarios of event developing. For instance, the case of pumping out maximum $70 \text{ m}^3/\text{hour}$ water from ## 1 and 2 boreholes and reinjecting in ## 3 and 7 boreholes with $50 \text{ m}^3/\text{hour}$, and into # 5 with $40 \text{ m}^3/\text{hour}$. Figures show the flow directions in boreholes.

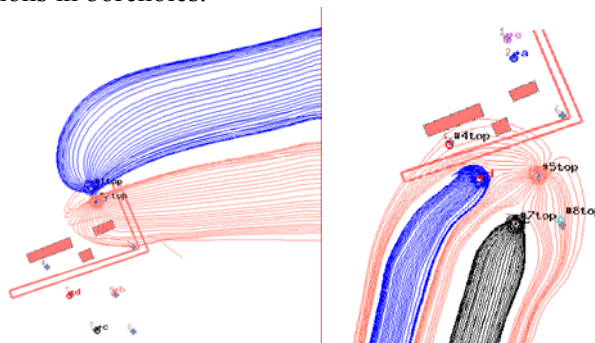


Fig. 12 flow directions in ## 1 and 2 boreholes (left) and ## 3, 5 and 7 boreholes (right)

As we can see, that recharge area for ## 1 and 2 boreholes, as it was expected, is located to the North-east direction, as to ## 3, 5 and 7 boreholes, flow direction is to the south-wes to the discharge area.

Model calculated the system functioning perspective under above mentioned regime for the next 25 years.

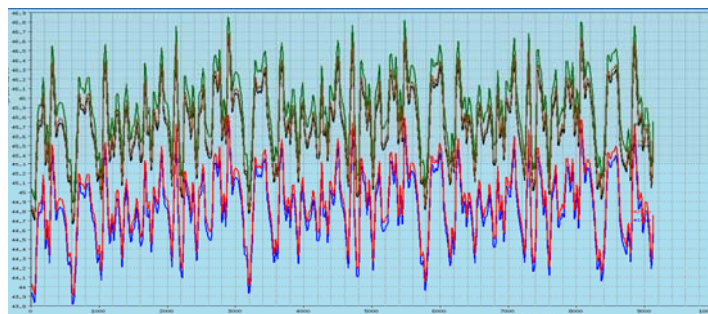


Fig. 13 water level potential variations in boreholes

As we can see on the figures, water level variations in boreholes are of seasonal nature – by the amount of precipitation and river discharge seasonal variations. Water levels in boreholes vary in parallel regime. The other kind of influence we cannot observe, and in fact the system is able to operate under this regime.

Therefore there should be calculated the acceptable regimes for productive and reinjection boreholes. In case of needs for more volume of water, we recommend to use #6 borehole as a productive one together with #1 and #2 boreholes. Exploitation of those three boreholes is possible under the regimes given below in the table 16. In this case the flow direction and exploitation conditions should not change.

In these calculations the maximum volume of pumped out water is $140 \text{ m}^3/\text{hour}$, but probably it is also possible to increase the volume. In this case the the slag testing with increased discharge must be done as well as new calculations. It is also possible to decrease the discharge upon request of course.

Tab. 16 the different cases of productive boreholes exploitation regimes

Version #		Boreholes #		
		#1	#2	#6
1	Pumping (m ³ /h)	70	70	-
2		60	60	20
3		50	50	40
4		60	50	30

As to reinjecting boreholes, we can review many cases of borehole exploitation. We have chosen characterizing figures of borehole exploitation with different discharge and flow direction always following the main flow direction as well as the ineligible regime case, when “new” flow crosses the main flow and reinjected water flows back to the productive boreholes.

For instance, under the same regime we pumped out 50 m³/hour volume water from ## 1 and 2 and from # 6 borehole 40 m³/hour and reinjected 50 m³/hour volume water into ## 3 and 7 and into # 5 40 m³/hour volume water (fig. 14). This is the most acceptable version because of its simplicity.

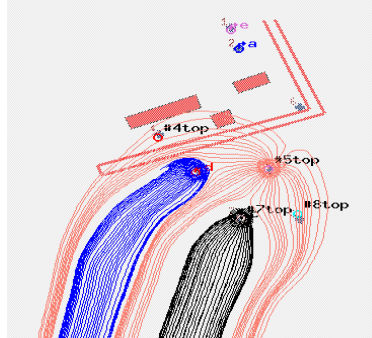


Fig. 14 water flow directions from ## 3, 4, 5, and 7 (right) boreholes

As we can see the main flow direction does not change, It neither changes if we pump out 60 m³/hour volume water from ## 1 and 2 boreholes and 20 m³/hour volume water from # 6 borehole and reinject into # 3 - 50 m³/hour, # 4 - 10 m³/hour, # 5 - 20 m³/hour, #7 - 40 m³/hour and # 8 - 20 m³/hour.

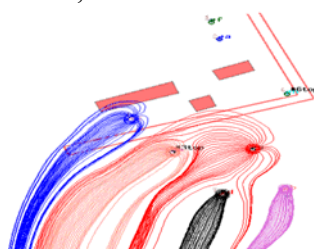


Fig. 15 water flow directions for ## 3,4,5,7 and 8 boreholes

As it was expected, the main flow direction does not change if we decrease pumping out volume.

In the table below are given few version of acceptable exploitation regimes for operating n boreholes

#	Injection (m ³ /h)	Boreholes					Sum
		#3	#4	#5	#7	#8	
1	50	50		40	50		140
2		50	10	20	40	20	160
3		50		40	50		140
4		50		30	40	20	140
5		50			20	50	20

Thus, the most acceptable version for regime is to pump out 50 m³/hour volume water from operating ## 1 and 2 boreholes and reinject into ## 3 and 7 ones with appropriate discharge and in case of needs of additional 40 m³/hour discharge, to pump out needed volume of water from # 6 borehole and reinject it into # 5 borehole or use the given into table other variations.

Main results

- In order to create the aquifer hydrodynamic model had were studied the geological, hydrogeological, geophysical and meteorological data of study area.
- During long term pumping out for each borehole was determined value of permeability and use to new methodology statistical analysis for calculate maximum value of hydrodynamic parameters.
- Created the aquifer conceptual model and during modeling determined the water flow directions, the expectable borehole exploitation regimes for the next 25 years;

References

- [1] Buachidze I. M at all, "Hydrogeology of USSR" Book X, Georgia, "Hedra", Moscow, 1970.
- [2] Buachidze I. M at all, "Distribution of artesian basins on the territory of Georgia", Geologic Institute of Academi Science of Georgia, Book XII, 1953.
- [3] Kharatishvili L. A. "Report of geological Department of Kolkheti 1966-68", Geological Department of Georgia, 1967.
- [4] Zedgenidze S., Beselia V. at all, "Investigation drinking water resource in alluvial deposits of Quaternary age in the catchment Rioni-Gubistskali for organization supply system for Kutaisi", Geological Department of Georgia, 1972-73.
- [5] Боровский Б.В., Самсонов Б.Г., Язвин Л.Г. Методика определения параметров водоносных горизонтов по данным откачек. Изд 2-е, М. "Недра", 1979, 326 стр.

(Received in final form 15 December 2012)

Методика создания цифровой модели современного аллювиального водоносного горизонта

გიორგი ი. მელიქაძე, გერადი ნ. კობზევი, ნინო ა. კაპანაძე, ხატუნა გ. ბედიანიშვილი

Резюме

Для внедрения системы отопления Кутаисского Международного Аэропорта с помощью теплового насоса, было организовано тестирование уже существующих двух и вновь пробуренных шести скважин, что дало возможность выяснить их фильтрационные свойства и создать цифровую модель водоносного горизонта. Моделирование включало в себя ступеньки калибровки и симуляции, что позволило изучить возможные сценарии эксплуатации водоносного горизонта и развития процессов во времени.

ალუვიური წყალშემცველი ჰორიზონტის ციფრული მოდელის შექმნის მეთოდოლოგია

გიორგი ი. მელიქაძე, გენადი ნ. კობზევი, ნინო ა. კაპანაძე, ხატუნა გ. ბედიანიშვილი

რეზიუმე

ქუთაისის საერთაშორისო აეროპორტის თბური ტუმბოს მეშვეობით გათბობის სისტემის დანერგვისთვის ორგანიზება გაუკეთდა უკვე არსებულ ორ და ახლად გაბურღულ ექვსი ჭაბურღილების ტესტირებას, რამაც საშუალება მოგვცა დაგვედგინა მათი ფილტრაციული თვისებები და შეგვექმნა წყალშემცველი ჰორიზონტის ციფრული მოდელი. ციფრული მოდელირება მოიცავდა კალიბრაციის და სიმულაციის რამოდენიმე საფეხურს, რამაც საშუალება მოგვცა შეგვესწავლა ჰორიზონტის ექსპლოატაციის სხვადასხვა სცენარები და პროცესების დროში განვითარება.

Obituaries:

Grigol Tabaghua
(1932-2012)



Grigol (Griel) Tabaghua died on October 11, 2012 at the age of 80. He was an Academic Doctor of Geological and Mineralogical Sciences and a senior scientist at the Department of Earth Physics and Geomagnetism at Institute of Geophysics, Grigol's merits for which is too great.

Grigol Tabaghua graduated with honours from the faculty of Geography-Geology with the specialization of Geophysical Methods for Prospecting Mineral Deposits of Tbilisi State University in 1956. Since then he worked at Institute of Geophysics during his whole life. First he was a postgraduate student at Department of Geoelectrics and Electrometry, then - a senior scientist, and later - the Head of Laboratory for Engineering Geophysical Investigation for reservoirs. Grigol Tabaghua participated in developing of geophysical methods for prospecting the mineral deposits in Georgia. In order to study electricity of complex geophysical methods he carried out investigations for iron, copper, manganese and complex ores in Georgia. In 1965 he defended Candidate Dissertation on "Results of Complex Geophysical Investigations for Iron Ores in Georgia".

In 1974-78 Grigol Tabaghua was in official mission in Syrian Arab Republic. There he headed geophysical investigations in order to study hydro-geologic properties of some regions in the republic.

For decades Grigol Tabaghua participated in complex geophysical investigations for debris dams in order to study their resistance. He also investigated exodynamic processes in reservoirs, established prospecting geophysical criteria for archaeogeophysical explorations to reveal material cultural monuments belonging to different periods.

Grigol Tabaghua was a great teacher as well. He delivered lectures at Ivane Javakhishvili Tbilisi State University. He has published more than 60 scientific works, 2 monographs among them.

Grigol Tabaghua was a high rank geophysicist, a good person and a very gifted man.

Zaza Injia
(1964-2011)



Zaza Injia was born in 1964 in Gori. In 1985 he graduated from Tbilisi State University, after which for several years he worked as an engineer-interpreter at geophysical prospecting companies in Russia. Zaza was very efficient and gifted. In addition to his main speciality he had good knowledge at seismic prospecting equipment and interpretation methods. He invented a portable seismic prospecting equipment MARK-24-1 and its interpretation software quite compatible to similar foreign products.

Zaza was a highly qualified programming specialist. He designed softwares for financial, industrial spheres, etc. With his participation an electronic Georgian-English Dictionary has been published. He worked only three years at Institute of Geophysics. However he was a very active scientist and carried out lots of works during this short period. He was one of the main participants of the NATO project *Seismic Hazard of South Caucasus-Turkey Energy Corridor*. Besides his gift and great knowledge Zaza Injia was distinguished with his personal qualities. He was hardworking, modest and scrupulous. Zaza untimely passed away after an incurable disease. His death was a great loss for our Institute.

Information for contributors

Papers intended for the Journal should be submitted in two copies to the Editor-in-Chief. Papers from countries that have a member on the Editorial Board should normally be submitted through that member. The address will be found on the inside front cover.

1. Papers should be written in the concise form. Occasionally long papers, particularly those of a review nature (not exceeding 16 printed pages), will be accepted. Short reports should be written in the most concise form not exceeding 6 printed pages. It is desirable to submit a copy of paper on a diskette.
2. A brief, concise abstract in English is required at the beginning of all papers in Russian and in Georgian at the end of them.
3. Line drawings should include all relevant details. All lettering, graph lines and points on graphs should be sufficiently large and bold to permit reproduction when the diagram has been reduced to a size suitable for inclusion in the Journal.
4. Each figure must be provided with an adequate caption.
5. Figure Captions and table headings should be provided on a separate sheet.
6. Page should be 20 x 28 cm. Large or long tables should be typed on continuing sheets.
7. References should be given in the standard form to be found in this Journal.
8. All copy (including tables, references and figure captions) must be double spaced with wide margins, and all pages must be numbered consecutively.
9. Both System of units in GGS and SI are permitted in manuscript
10. Each manuscript should include the components, which should be presented in the order following as follows:
Title, name, affiliation and complete postal address of each author and dateline.
The text should be divided into sections, each with a separate heading or numbered consecutively.
Acknowledgements. Appendix. Reference.
11. The editors will supply the date of receipt of the manuscript.

CONTENTS

<i>Tamaz Chelidze</i> Pitfalls and Reality in Global and Regional Hazard and Disaster Risk Assessments	3
<i>Tsereteli E., Gaprindashvili M., Gaprindashvili G., Chelidze T., Varazanashvili O., Tsereteli N.</i> Problems of natural and anthropogenic disasters in Georgia	14
<i>T. Chelidze, D. Odilavadze, K. Pitskhelauri, J. Kiria, R. Gogua</i> Archaeogeophysics in Georgia – New Results, New Prospects.	24
<i>T. Chelidze , N. Varamashvili , Z. Chelidze</i> Acoustic Early Warning Telemetric System of Catastrophic Debris Flows in Mountainous Areas.	35
T. Chelidze, N. Zhukova, T. Matcharashvili SEISMOTOOL – easy way to see, listen, analyze seismograms	42
<i>T. Chelidze, T. Matcharashvili, V. Abashidze, M. Kalabegishvili, N. Zhukova, E. Meparidze</i> Real time telemetric monitoring system of large dams and new methods for analysis of dam dynamics.	49
<i>A. Amiranashvili , T. Matcharashvili , T. Chelidze</i> Climate Change in Georgia; statistical and nonlinear dynamics predictions . . .	67
<i>T. Chelidze, N. Zhukova, A. Sborshchikov, D. Tepnadze</i> Dynamic triggering of local seismic activity in Georgia by the great 2011 Japan earthquake.	88
<i>Nodar Varamashvili</i> Stick-slip process and solitary waves.	98
<i>G. Lominadze, K. Kartvelishvili, G. Berishvili, N. Mebaghivili, M. Nikolaishvili, G.Tabagua, A. Tarkhnishvili</i> Complex Geophysical Investigation of some Characteristics of some Strong Local Guria (Georgia) Magnetic Anomalies.	138
<i>E.Sakvarelidze, G. Tumanishvili</i> Gas Hydrates Investigations in the Gurian Trough.	114
<i>Tamar Jimsheladze, George Melikadze, Alexander Chankvetadze, Robert Gagaa, Tamaz Matiashvili</i> The geomagnetic variation in Dusheti observatory related with earthquake activity in East Georgia (January - July 1012)	118
<i>Janja Vaupotič, Mateja Bezek, Nino Kapanadze, George Melikadze, Teona Makharadze, Zurab Machaidze, Mariam Todadze</i> Radon and thoron measurements in West Georgia.	128

<i>Jashi G., Chelidze T., Chichinadze V.</i> Seismotectonic movements – one of the main receptors in exodynamic processes.	138
<i>Mindeli P.Sh., Ghonghadze S.A., Ghlonti N.I., Kiria J.K</i> The anomalous magnetic field and its relation to the deep structure of the territory of Georgia.	142
<i>G.Tabagua, N.Gogvadze, T. Gorgiashvili, M. Jakhutashvili, O.Seskuria, S.Vepkhvadze, S.Matiashvili, K.Tabatadze</i> Preliminary Results of Electrometric Search on the territory of the Svetitskhoveli complex.	148
<i>G. Melikadze, G. Kobzev, N. Kapanadze, Kh. Bedineishvili</i> Methodology creation numerical model of alluvial deposit aquifer for implement heat pump system of Kutaisi international airport.	155
Obituaries.	166
Information for contributors.	167

სარჩევი

<p><i>თამაზ ჭელიძე</i> შეცდომები და სინამდვილე კატასტროფების რისკების გლობალურ და რეგიონულ შეფასებებში</p>	3
<p><i>ემილ წერეთელი, მერაბ გაფრინდაშვილი, გიორგი გაფრინდაშვილი, თამაზ ჭელიძე, ოთარ ვარაზანაშვილი, ნინო წერეთელი</i> ბუნებრივ-ანთროპოგენური კატასტროფების მდგომარეობის პრობლემა საქართველოში.</p>	14
<p><i>თ. ჭელიძე, Dდ. ოდილავაძე, კ. ფიცხელაური ჯ. ქირია, რ. გოგუა</i> არქეოგეოფიზიკა – ახალი პერსპექტივები</p>	24
<p><i>თამაზ ჭელიძე, ნოდარ ვარამაშვილი, ზურაბ ჭელიძე</i> მთიან რეგიონებში კატასტროფული ღვარცოფების აკუსტიკური ტელემეტრული წინასწარი შეტყობინების სისტემა</p>	35
<p><i>თ. ჭელიძე, ნ. ჟუკოვა, თ. მაჭარაშვილი</i> სეისმო-ტული - ადვილი გზა სეისმოგრამების ვიზუალიზაციისათვის, მათი მოსმენისა და ანალიზისათვის.</p>	42
<p><i>თამაზ ჭელიძე, თეიმურაზ მაჭარაშვილი, ვახტანგ აბაშიძე, მირიან ყალაბეგაშვილი, ნატალია ჟუკოვა, ეკატერინე მეფარიძე</i> დიდი კაშხლების რეალურ დროში ტელემეტრული მონიტორინგის სისტემა და კაშხლების დინამიკის ანალიზის ახალი მეთოდი</p>	49
<p><i>ა. ამირანაშვილი, თ. მაჭარაშვილი, თ. ჭელიძე</i> კლიმატის ცვლილება საქართველოში: სტატისტიკური და არაწრფივ-დინამიკური პროგნოზირება</p>	67
<p><i>თ. ჭელიძე, ნ. ჟუკოვა, ა. სბორშჩიკოვი, დ. ტეფნაძე</i> საქართველოში ლოკალური სეისმურობის დინამიკური ტრიგერირება დიდი 2011 წლის იაპონიის მიწისძვრით.</p>	88
<p><i>ნოდარ ვარამაშვილი</i> სტიკ-სლიპის პროცესი და სოლიტონური ტალღები.</p>	98
<p><i>ჯ.ლომინაძე, კ.ქართველიშვილი, გ.ბერიშვილი, ნ.მებადიშვილი, მ.ნიკოლაიშვილი, გ.ტაბაღუა, ა.თარხნიშვილი</i> ზოგიერთი ძლიერი ლოკალური გურიის (საქართველო) მაგნიტური ანომალიების მახასიათებლის კომპლექსური გეოფიზიკური კვლევა.</p>	106
<p><i>ე. საყვარელიძე, გ. თუმანიშვილი</i> გაზური ჰიდრატების კვლევა გურიის როფში</p>	114

თამარ ჯიმშელაძე, გიორგი მელიქაძე, ალექსანდრე ჩანკვეტაძე, რობერტ გაგუა, თამაზ მათიაშვილი აღმოსავლეთ საქართველოს ტერიტორიის სეისმოაქტიურობასთან დაკავშირებული დუშეთის ობსერვატორიაზე დაფიქსირებული გეომაგნიტური ველის ვარიაციები (იანვარი - ივნისი 1012)	118
<i>იანია ვოროუტიკ, მატეა ბეზეკ, ნინო კაპანაძე, გიორგი მელიქაძე, თეონა მახარაძე, ზურაბ მაჩაიძე, მარიამ თოღაძე</i> რადონისა და თორონის გაზომვები დასავლეთ საქართველოში	128
<i>გ. ჯაში, თ. ჭელიძე, ვ. ჭიჭინაძე</i> სეისმოტექტონიკური მოძრაობები – ეგზოდინამიკური პროცესების ერთ-ერთი ძირითადი რეცეპტორები.	106
<i>მინდელი პ., ღონღაძე ს., ღლონტი ნ., ქირია ჯ.</i> საქართველოს ტერიტორიის ანომალური მაგნიტური ველი და მისი კავშირი სიღრმულ აგებულებასთან	142
გ. ტაბაღუა, <i>ნ. გოგუაძე, თ. გორგიაშვილი, მ. ჯახუტაშვილი, ო. სესკურია, ს. კეფხვაძე, ს. მათიაშვილი, კ. ტაბატაძე</i> ელექტრომეტრული კვლევის წინასწარი შედეგები სვეტიცხოვლის ტაძრის ტერიტორიაზე.	148
<i>გიორგი ი. მელიქაძე, გენადი ნ. კობზევი, ნინო ა. კაპანაძე, ხათუნა გ. ბედიანიშვილი</i> ალუვიური წყალშემცველი ჰორიზონტის ციფრული მოდელის შექმნის მეთოდოლოგია	155
ნეკროლოგები.	166
ავტორთა საყურადღებოდ	167

საქართველოს გეოფიზიკური საზოგადოების
ჟურნალი

სერია ა. დედამიწის ფიზიკა

ჟურნალი იბეჭდება საქართველოს გეოფიზიკური საზოგადოების პრეზიდიუმის
დადგენილების საფუძველზე

ტირაჟი 200 ცალი

ЖУРНАЛ ГРУЗИНСКОГО ГЕОФИЗИЧЕСКОГО ОБЩЕСТВА

Серия А. Физика твердой Земли

Журнал печатается по постановлению президиума Грузинского геофизического общества

Тираж 200 экз

JOURNAL OF THE GEORGIAN GEOPHYSICAL SOCIETY

Issue A. Physics of Solid Earth

Printed by the decision of the Georgian Geophysical Society Board

Circulation 200 copies